Extreme weather and climate in Europe

ETC/CCA Technical Paper N. 2/2015

10 November 2015

Authors: Paul van der Linden[1], Peter Dempsey[1], Robert Dunn[1], John Caesar[1], Blaz Kurnik[2]

Reviewers: Rutger Dankers[1], Blaz Kurnik[2], Andre Jol[2], Michael Kunz[3], Henny van Lanen[4], Rasmus Benestad[5], Simon Parry[6], Mikael Hilden[7], Andreas Marx[8], Jaroslav Mysiak[9], Lizzie Kendon[1]

European Environment Agency

European Topic Centre on Climate Change Impacts, Vulnerability and Adaptation

The European Topic Centre on Climate Change Impacts, Vulnerability and Adaptation (ETC CCA) is a consortium of European institutes under contract of the European Environment Agency:
CMCC Alterra AU-NERI CUNI FFCUL MetOffice SYKE THETIS UFZ UPM

Cover photo: © Karlsruher Institute of Technology

Layout/editing: Met Office (MO)

Authors affiliation

[1]Met Office, [2]EEA ,[3]Karlsruhe Institute of Technology, [4]Wageningen University,[5] The Norwegian Meteorological Institute, [6]CEH Wallingford, [7]SYKE, [8]Helmholtz Centre for Environmental Research (UFZ), [9]CMCC

EEA Project manager

Blaz Kurnik, European Environment Agency, Copenhagen, Denmark

European Topic Centre on Climate Change impacts, vulnerability and Adaptation (ETC/CCA)

Website: http://cca.eionet.europa.eu/.

European Topic Centre on Climate Change impacts, vulnerability and Adaptation (ETC/CCA)
C/o Fondazione Centro Euro-Mediterraneo sui Cambiamenti Climatici (CMCC)
Via M. Franceschini 31, 40128 Bologna, Italy
Phone: +39 051 4151411, int. 277
E-mail: silvia.medri@cmcc.it
Website: http://www.cmcc.it/.

Contents

Summary **4**

1 Introduction **6**

1.1 Setting the Scene 6

1.2 Climate context of extreme weather events 6

1.3 Features of recent extreme events in Europe 8

1.4 Intended readership and scope of report 14

2 Data **16**

2.1 Observations **16**

2.1.1 Data types 16

2.1.2 European datasets 19

2.1.3 Data gaps, homogeneity and time series 21

2.1.4 Gridded data 22

2.1.5 Climate indices and interrelations 23

2.1.6 Extreme Value Analysis 24

2.2 Climate modelling and scenarios 24

2.2.1 Climate models and bias correction 24

2.2.2 Emissions scenarios 26

2.2.3 Socio-economic & policy scenarios 27

3 Extremes **29**

Introduction 29

3.1 Temperature (Heat waves) 29

Key Messages 29

3.1.1 Observations and data - temperature 30

3.1.2 Observed trends - temperature 32

3.1.3 Attribution - temperature 38

3.1.4 Projections - temperature 39

3.1.5 Links to drought 45

3.2 Precipitation 46

Key Messages 46

3.2.1 Observations and data - precipitation 46

3.2.2 Observed trends – precipitation 47

3.2.3 Projections – precipitation 54

3.3 Hail 59

Key Messages 59

3.3.1 Observations and data – hail 60

3.3.2 Observed trends and variability - hail 65

3.3.3 Projections 67
3.4 Drought 69
Key Messages 69
3.4.1 Meteorological Drought 72
3.4.1.1 Observations - meteorological drought 72
3.4.1.2 Projections – meteorological drought 78
3.4.2 Hydrological drought 80
3.4.2.1 Observations - Hydrological drought 80
3.4.2.2 Projections - hydrological drought 83
3.4.3 Soil moisture drought 85
3.4.3.1 Observations - soil moisture drought 85
3.4.3.2 Projections - soil moisture drought 88
Appendices 89
A.1 Temperature, precipitation, drought and excess heat indices 89
A.2 Case studies 93
A2.1 Case study: 2010 Russia heat wave 93
A3.2 Case study: 2002 and 2013 extreme precipitation 96
A2.3 Case study: Drought in 2011 in Europe 97
A2.4 Case Study Hail 101
References 104

Summary

This report describes the current scientific knowledge of extreme weather and climate events in Europe for the following variables: temperature, precipitation, hail, and drought (with the following types of drought: meteorological, hydrological and soil moisture). The content summarises key literature drawn from peer reviewed journals and other sources (business and government reports), and builds upon the synthesised results presented in international assessments such as IPCC reports. It describes the recorded observations and modelled projections for extreme events including definitions, frequency, trends, spatial and temporal distribution. The report also presents an overview of the indices used to characterise extreme events as well as their main uses, before going on to describe the datasets where they are recorded, and provides information on the strengths and weaknesses of the indices and the datasets. Extra consideration is given to indices that are relevant to socio-economic impacts resulting from climate change and relevant statistical techniques for analysing extreme events. Observed changes in global climate and extreme events provide the context to the changes in extreme events observed in Europe, which are described for much of the 20th century. Modelled projections of extreme events are also given, under different emissions scenarios and time horizons, including results from regional models covering the European domain, such as EURO-CORDEX. The report is written for climate scientists, climate researchers and experts who use climate information in a professional role. There are four case studies (Appendix 2) which provide an anatomy of different recent European extreme weather/climate events including meteorological impacts and synoptic context.

Observed global temperature trends show the number of warm extremes has increased and number of cool extremes has decreased over the last 100 years, and the length and frequency of summer heat waves has increased during the last century. In Europe these trends are most pronounced in the last 40 years although regional variations exist. For Europe, 2014 was the warmest year on record, although it had fewer hot days than recent years. Under future climate change with continued warming, the number of heat waves is projected to increase, along with their duration and intensity. Under all emissions scenarios, summers like the hot summer experienced in 2003 will become commonplace by the 2040s.

The global trend in precipitation is generally for wetter conditions over the 20th century although changes are less temporally and spatially coherent than those observed for temperature. The general trend in precipitation for Europe in the 20th century is of increases over northern Europe and decreases over southern Europe. Extreme precipitation is becoming more intense and more frequent in Europe, especially in central and eastern Europe in winter, often resulting in greater and more frequent flooding. Since 1950 winter wet spells increased in duration in northern Europe and reduced in southern Europe, while summer wet spells became shorter in northern and eastern Europe. An increasing proportion of total rainfall is observed to fall on heavy rainfall days. Extreme precipitation (including short intense convective or longer duration frontal types) demonstrates complex variability and lacks a robust spatial pattern. Climate models project that events currently considered extreme are expected to occur more frequently in the future. For example a 1-in-20 year annual maximum daily precipitation amount is likely to become a 1-in-5 to 1-in-15 year event by the end of the 21st century in many parts of Europe.

There are few ground based hail observation networks, so satellite measurements and weather models are used to identify hail forming conditions. In Europe most extreme hail events occur in the summer over Central Europe and the Alps where convective energy is greatest. Intense hail events are linked to increases in convective energy in the atmosphere observed over the last 30 years. Hailstorm projection studies, although limited to France, northern Italy and Germany, show increases in the convective conditions that lead to hail and some areas show a rise in damage days although this is not statistically significant.

Recent severe droughts include Italy (1997-2002), the Baltic countries 2005-2009, the European heatwave of summer 2003, and the widespread European drought of 2011. The 1950s were prone to long, intense, Europe-wide meteorological and hydrological droughts. In northern and eastern Europe the highest drought frequency and severity was from the early 1950s to the mid-1970s. Southern and Western Europe (especially the Mediterranean) show the highest drought frequency and severity since 1990. There has been a small but continuous increase of the European areas prone to drought from the 1980s to the early 2010s. Regional climate models project a decrease in summer precipitation until 2100 of 17%. Dry periods are expected to occur 3 times more often at the end of this century and to last longer by 1 to 3 days compared to the period of 1971-2000. There is significant uncertainty associated with future projections of drought, with climate variability being the dominant source of uncertainty in observed and projected soil moisture drought.

1 Introduction

1.1 Setting the Scene

The IPCC AR5 (2013) states that 'warming of the climate system is unequivocal' and it is 'virtually certain' that human activity is the main cause. In Europe the effects of climate change on climate indicators are well documented, although the magnitude of future climate change depends on past and current as well as future human activity. Extreme weather events will change as the climate changes and the changes are not necessarily direct or easily predicted. The rarity of extreme weather (heat waves, extreme rainfall, droughts, etc) makes them more difficult to understand scientifically, or to analyse and project compared with 'average' weather. However they often have the highest impact on and cause the greatest damage to human wellbeing and both natural and managed systems.

Extremes of climate are of increasing interest to European policy makers because of their severe impacts on individuals, communities and the wider European economy. An understanding of extreme weather and climate change is an essential input to European policy making in key areas of Climate Change Adaptation (CDA) and Disaster Risk Reduction (DRR). EU adaptation strategy acknowledges that Europe is warming faster than many other parts of the world. The European land temperature over the past decade has been on average 1.3°C higher than in the pre-industrial era, compared with a global average rise of 0.8°C (European Environment Agency, 2012). Impacts vary across the EU, but the Mediterranean basin, mountain areas, densely populated floodplains, coastal zones, outermost regions and the Arctic are particularly vulnerable to climate change impacts. Extreme weather events have increased, with southern and central Europe seeing more frequent heat waves, forest fires and droughts. Heavier precipitation and flooding is projected in northern and north-eastern Europe, with a heightened risk of coastal flooding and erosion. An increase in such events is likely to enlarge the magnitude of disasters, leading to significant economic losses, public health problems and deaths (EU Strategy on adaptation to climate change[1] and the European Environment Agency's key observed and projected climate change and impacts for the main regions in Europe[2]). The European Commission's office for Humanitarian Aid and Civil Protection[3] (ECHO) develops DRR (Disaster Risk Reduction) policy guidelines which make disaster preparedness a central principle in, for example, the European Civil Protection Forum[4]. Improved knowledge of extremes will support its key aim of reducing the vulnerability of the European and global communities to extreme climate events and climate change (European Commission, 2013). The Copernicus Climate Change Service[5] (C3S) provides an operational service and knowledge base to support these initiatives. It provides reliable information about the current and past state of the climate, seasonal forecasts, and future projections in the coming decades for various scenarios of greenhouse gas emissions and other Climate Change contributors.

1.2 Climate context of extreme weather events

Accurate measurements of the global surface temperature go back to the mid 19th century (e.g. HadCRUT4 (Morice et al., 2012), MLOST (Vose et al., 2012, Smith et al., 2008), GISS (Hansen et

[1] http://ec.europa.eu/clima/policies/adaptation/what/documentation_en.htm
[2] http://www.eea.europa.eu/data-and-maps/figures/key-past-and-projected-impacts-and-effects-on-sectors-for-the-main-biogeographic-regions-of-europe-3
[3] http://ec.europa.eu/echo/where/europe-and-the-caucasus_en
[4] http://ec.europa.eu/echo/partnerships/civil-protection-partners/civil-protection-forum_en
[5] http://climate.copernicus.eu/

al., 2010), Berkeley (Rohde et al., 2013) and show an increase in the global surface temperature over this time period. The datasets capture the changes in the mean surface temperature, but are less good at capturing extreme events which usually occur on timescales shorter than monthly averages, and over relatively small regions. A natural extrapolation of the observed increase in global average surface temperatures is that the extreme values would also increase by a similar amount (Figure 1). Therefore, compared to an earlier baseline, there would be more extreme events, and also events that are outside what would normally be expected in the un-warmed climate (also called "the world that might have been").

As Figure 1 makes clear, this view underlies the assumption that the distribution of temperatures does not change significantly as the average climate warms. Using daily maximum and minimum temperatures, Donat et al. (2012) showed that there have been changes in the shape of distributions as well as a mean shift, and these changes manifest as skews towards the hotter parts. Also, the changes in the minimum temperatures have been stronger than the maximum temperatures (e.g. Karl et al., 1993, Easterling et al., 1997, Donat et al., 2013a), indicating that the distribution of temperatures measured at sub-daily resolutions have also changed in the last decades. Changes in extreme temperatures are discussed in Section 3.1.

Figure 1: How a change in the distribution of the mean (a), the variance (b), the mean and variance (c) in temperature affect the frequency of both hot and cold extreme events. Panel (d) illustrates how an increase in the variance in precipitation leads to an increase in heavy precipitation events (Source: Figure 1 from Zwiers et al., 2013).

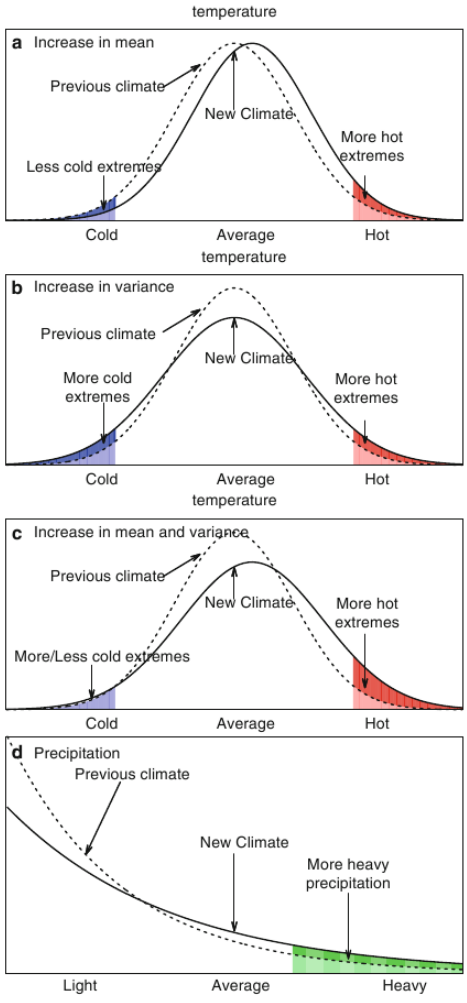

Global and regional trend analysis suggest that European winters are getting warmer and wetter, summers are getting warmer and drier, and that northern Europe is getting wetter, southern Europe is getting drier. This has been generalised by some to suggest intensification, i.e. dry areas are getting drier, wet areas are getting wetter (Durack (2012) quoted in Greve and Seneviratne, 2015). There has also been an increase in the number of very wet days, the proportion of total from heavy precipitation events, and increases in the frequency of rare events. However, precipitation data are more variable than temperature data, trends are less clear to distinguish and extreme values are subject to significant uncertainty. Trends in extreme precipitation are explored in section 3.2.

Hail records are limited compared with temperature and rainfall, being collected from limited hail-pad networks and physical observations. Records are currently insufficient to identify trends in time with confidence, although research is active in the areas of dynamic (hail-producing) meteorology and remote sensing using, for example, radar reflectivity and satellite temperature data. This will contribute to improved forecasting and warning models and a better understanding of hail producing mechanisms. Longer term it will contribute to the European spatial and temporal database of hail frequency and magnitude, a baseline for future trend analysis. Extreme hail events are reviewed in Section 3.3.

Severe recent droughts in eastern Europe have generated increased interest in their social, economic and environmental impacts (e.g. a 1 in 200 year drought event in 2015 reduced shipping by 75% on the Danube[6]). Over the period 1950-2009, the duration of dry spells increased in summer and reduced winter in northern and eastern Europe. Dry spells and wet spells both reduced in duration all year round in southern Europe. This implies a lengthening of wets spells at the expense of dry spells, and grouping of dry and wet days rather than a changing number of wet days (Zolina, 2012). The area affected by droughts has increased in many regions since 1970, as has the intensity (Klein Tank et al., 2009). Drought extremes are explored further in Section 3.4.

1.3 Features of recent extreme events in Europe

A summary of recent extreme events in Europe is shown on Table 1. The characterising features of extreme temperature, precipitation and drought are discussed below. A comprehensive study of heat waves, their characteristics, drivers and projected future changes on a global scale can be found in Perkins (2015). In this report we focus on recent studies and analyses, concentrating on the European region. Before 2000, the extreme summer temperatures experienced during heat wave events were on the whole within 2-3 standard deviations of the climatologically expected values (Figure 1). Some events had occurred within the relatively recent past, but these were restricted to relatively small regions. Within the following ten years, large swathes of the continent had experienced heat waves that were outside of what had previously occurred. Heat waves in Turkey (2001), south-western central Europe (2003, 2006), the Balkans (2007) and eastern Europe (2010) had caused up to 500-year long records to be broken over about 65% of Europe (Figure 2, Barriopedro et al., 2011). Also the areas which experienced maximum temperatures over 3 standard deviations above the climatology had doubled within this decade.

[6] http://www.telegraph.co.uk/news/worldnews/europe/hungary/8936080/Worst-drought-in-200-years-paralyses-Danube-river-shipping.html

Table 1: Extreme Events in Europe since 1999 (Adapted from NAS & NMI, 2013)

December 1999	Winter storms in western and central Europe. Heavy precipitation and extremely high windspeed.
August 2002	Heavy precipitation and floods along central European rivers. Economic losses exceeded €15 billion.
Summer 2003	Heat wave in central and western Europe. Extremely high temperatures for weeks led to more than 30 000 deaths and extreme drought across Europe. More than 25 000 fires burnt 650 000 hectares.
Summer 2005	Heat and drought in southern Europe. Extremely high temperature. Significantly less precipitation than average.
Winter 2006	Extreme cold in eastern and central Europe. Minimum temperature was 4–12° C colder than the 1961–1990 mean.
Mild winter 2007	Winter of 2007 ranked among the warmest ever recorded in a large part of Europe. Average temperature anomalies were more than 4° C.
May 2008	Flash floods in central Europe.
Summer 2008	Floods across eastern European river. Nearly 50 000 homes were submerged; more than 30 000 hectares of farmland was destroyed.
Winter 2009	The winter of 2009 was colder than usual in central and western Europe.
Spring 2010	Flooding in Poland and eastern Europe. In May 2009 the precipitation amount was 100 mm above the long-term mean across vast regions of eastern Europe. Total flood damage exceeded € 2.5 billion.
Winter 2010	Unusually cold, snowy winter in Europe. Most areas of Europe saw between 10 and 20 additional ice days than normal from December through February. Due to the prolonged cold temperatures and the frequency of snow storms, the number of days with more than 1 cm of snow on the ground was significantly greater than normal across Europe.
February 2010	Severe winter storms in Europe. Tropical storm Xynthia passed through Portugal, Spain, France, Belgium, the Netherlands and Germany, causing heavy rainfall and high wind speed.
Summer 2010	Heat and drought in eastern Europe. This region was hit by record temperatures; very low rainfall amounts resulted in crop losses, peat and forest fires. Mean temperature was between 4 and 8° C higher than the long-term average during July and August. For many regions there were at least 10 and up to 30 more summer days than normal during July 2010.
Summer 2011	Widespread drought in Europe
Winter 2013	Extreme rainfall and flooding in Europe
Summer 2014	Extreme rainfall and flooding in Europe affecting Bosnia-Herzegovina
Summer 2015	Drought in Europe 'extreme weather belt' linked to worst drought since 2003. Severe droughts that stretched across a central European band this summer are consistent with climate models for a warming continent
Summer 2015	Flooding in southern France (French Riviera) caused by heavy rain killed at least 15 people and left 12 missing near France's Mediterranean coast. More than 350 mm (14 inches) of rain fell on the Var department in southern France in a few hours, triggering flooding that surged in some places to two metres over normal water levels
Autumn 2015	Heavy rain and flooding Italy (Pisa, Florence), Croatia, Serbia, Bosnia (5-deaths)

Figure 2: Spatial distribution of the hottest European summers. The height and the colour of the bars indicate the best-guess maximum anomaly (degrees Celsius, relative to the 1970–1999 period) and the decade of the corresponding summer, respectively, for the periods (A) 1500–2000 and (B) 1500–2010. For better readability, each bar is subdivided with 1°C intervals. The embedded plot shows the corresponding percentage of European areas with summer maxima above the given temperature (in SDs) for the 1500–2000 (dashed line) and 1500–2010 (dotted line) periods. (Source: Figure 3 from Barriopedro et al., 2011)

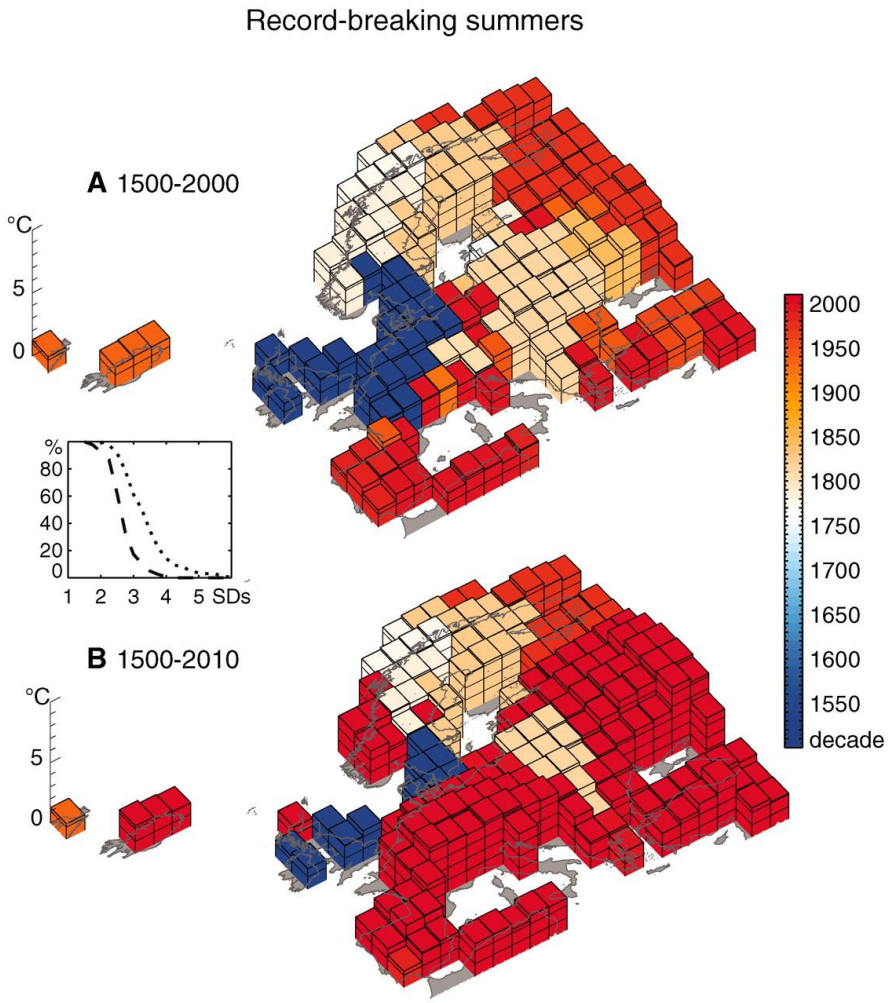

Although now over a decade ago, the heat wave in France and surrounding countries in 2003 was classified as the warmest summer in Europe in the last 500 years (Luterbacher et al., 2004, Beniston 2004). The average temperatures exceeded all historical measurements on both monthly and seasonal timescales (Figure 3, Schaer et al., 2004, Fouillet et al., 2006). The most severe impacts on human health were experienced in France, with over 14,000 excess deaths recorded from 1st to 20th August 2003 (e.g. Vandentorren et al., 2004, Foulliet et al., 2006). The vast majority of these excess deaths occurred in the elderly population. Other countries affected by the event also recorded excess deaths: e.g. around 6,500 in Spain (e.g. Martinez et al., 2004), 2,100 in England and Wales (Johnson et al., 2004) and 1,400-2,200 in the Netherlands (e.g. Garssen et al., 2005); further information is available in Garcia-Herrara et al., (2010). The event also contributed to severe forest fires in Portugal (Trigo et al., 2006), low vegetation productivity (because of low soil moisture Ciais et al., 2005) with knock on

effects for agriculture. The magnitude of this heat wave was the result of persistent anticyclonic conditions from late spring through into the late summer with particularly clear skies (Black et al., 2004). This resulted in a strong deficit in the soil moisture, which reduced the buffering effect of evaporation on the high temperatures (Fischer et al., 2007).

Figure 3: Extent of 2003 heat wave event. TERRA MODIS derived land surface temperature data of 1km spatial resolution. The difference in land surface temperature is calculated by subtracting the average of all cloud free data during 2000, 2001, 2002 and 2004 from the ones in measured in 2003, covering the date range of July 20 to August 20. (Source: NASA MODIS[7]).

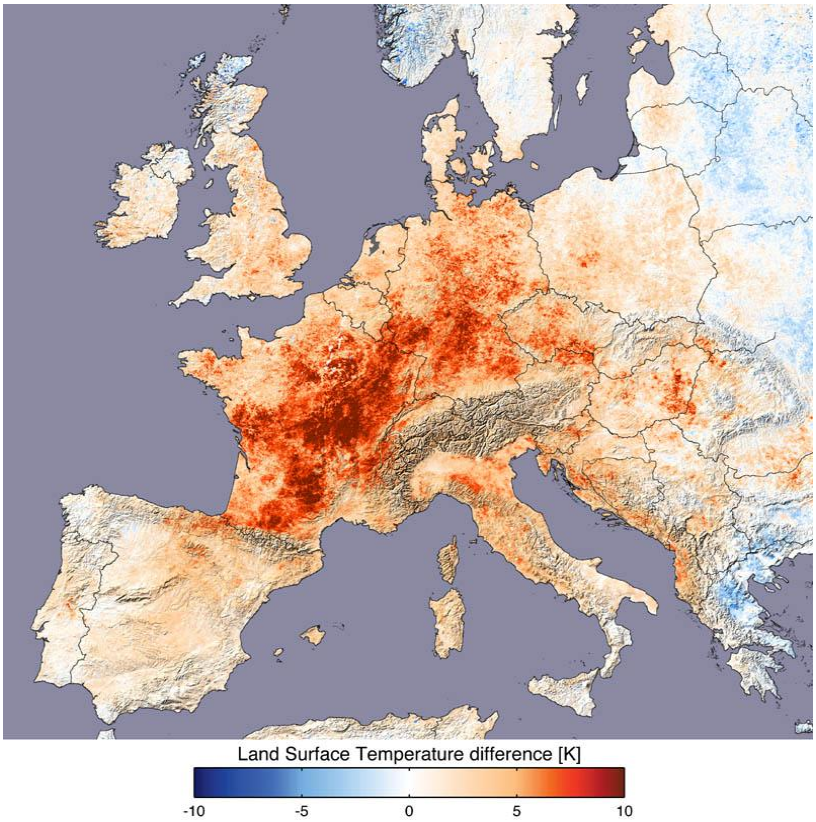

A few years later, in 2006, another warm summer occurred in a very similar region. The health impacts of this event in France were lower than those of 2003, in some cases because of lessons learnt during the previous event (Fouillet et al., 2006). In 2007, a heat wave occurred in the eastern Mediterranean, the Balkan peninsula and parts of Asia Minor (Founda & Giannakopoulos 2009, Busuioc et al., 2007). Many stations in this region broke records that had been set in the 1940s (Tolika et al., 2009), and major forest fires occurred in the Peloponnese as a result of the dry vegetation.

There have been three notable events in recent years; the large heat wave in eastern Europe in 2010 and smaller events in the Balkan peninsula in 2012 and central Europe during 2013. The extended and severe event in western Russia and eastern Europe in 2010 was by far the worst such event of the past 33 years (Nature News 2014), based on the Heat Wave Magnitude Index (Russo et al., 2014). An estimated 55,000 people died as a result of the high temperatures. This event is discussed in more detail in (Appendix A.2 Case Studies). There have been no published studies of the 2012 event thus far. The heat wave in 2013 resulted in unprecedented temperatures in parts of Austria, contributing to the fifth warmest summer over Europe since 1951. Three individual warm periods occurred, one each

[7] *http://earthobservatory.nasa.gov/IOTD/view.php?id=3714*

in June, July and August, driven by blocking pressure patterns and a preceding precipitation deficit (Lhotka & Kyselý, 2015).

During July and August 2015, western Europe experienced a significant heat wave (NOAA 2015). Austria experienced its "most extreme summer on record"[8], and the second warmest (after 2003) since 1767, 2.5°C above average. In Germany, a new national record of 40.3°C was set on the 7th, and August as a whole was 2.8°C warmer than normal[9]. The Netherlands came with 0.4°C of a new temperature record with a maximum of 38.2°C on 2nd July[10]. In France, three stations set all time records (Boulogne-sur-mer, Dieppe, and Melun with temperatures of 35.4°C, 38.3°C, and 39.4°C respectively), and Paris measured 39.7°C, the second highest maximum on record[11]. Madrid managed 40°C for the first time since 1943[12].

Despite the focus that heat waves have in the picture of a warming climate, the opposite events, cold snaps, can still occur – albeit they are expected to become rarer as time passes. During 2010, northern-Atlantic Europe experienced a cold December (Cattiaux et al., 2010). Although this had impacts on the health of vulnerable people, and also on transport and infrastructure, it was not as cold as extreme winters of the previous six decades nor as cold as the atmospheric patterns would have lead to in the absence of warming (Cattiaux et al., 2010).

From a climatological perspective, heat wave-like events can also occur in the shoulder seasons (spring and autumn) as well as in winter. Although temperatures elevated above the average in these seasons will not reach the levels where they have impacts on human health, they can still have widespread impacts on agriculture and forestry.

Extreme precipitation includes short term high intensity rainfall, resulting from strong convergence of atmospheric vapour with convection or other dynamics triggering precipitation in localised areas, and flooding in urbanised catchments. Lower intensity rainfall over longer duration, sufficient to cause significant river flooding, may also be classified as extreme. For example in England and Wales, 2000 was the wettest autumn on record since 1766 with €1.8 billion in damages, and 2007 saw the wettest July on record with damages of €4.2 billion. In 2011-12 and 2013-14, relatively low intensity but exceptionally prolonged winter rainfall caused extensive pluvial and fluvial flooding.

There have been several high profile examples of intense flooding caused by intense and prolonged rainfall and disruption to infrastructure in Europe over the last few years. The European Commission is set to grant an aid package worth €16.2 million to Greece and Bulgaria following predominantly flood disasters that occurred in the winter of 2015. Extreme flooding in Central Europe occurred after heavy rain in late May and early June 2013 when flooding affected south and East Germany, western regions of the Czech Republic, and Austria. Switzerland, Slovakia, Belarus, Poland, Hungary and Serbia were affected to a lesser extent. Parts of central Europe received more than 100 lm^{-2} in 72 hours in June 2013 and severe flooding occurred in the Elbe and Danube catchments (Figure 4).

[8] https://www.zamg.ac.at/cms/de/klima/news/sommer-2015-neue-rekorde-bei-temperatur-trockenheit-und-sonnenscheindauer Retrieved 19th October 2015

[9] http://www.dwd.de/DE/presse/pressemitteilungen/DE/2015/20150828_deutschlandwetter_august_2015.html?nn=495064 Retrieved 19th October 2015

[10] http://www.knmi.nl/over-het-knmi/nieuws/zomer-vol-uitersten Retrieved 19th October 2015

[11] http://www.meteofrance.fr/actualites/26520660-vague-de-chaleur-des-temperatures-record Retrieved 19th October 2015

[12] https://www.climate.gov/news-features/event-tracker/summer-heat-wave-arrives-europe Retrieved 19th October 2015

Figure 4: (a) Rainfall (lm^{-2}) over 72 hours in June 2013 and (b) Flooding in Passau, Bavaria, 2013[13].

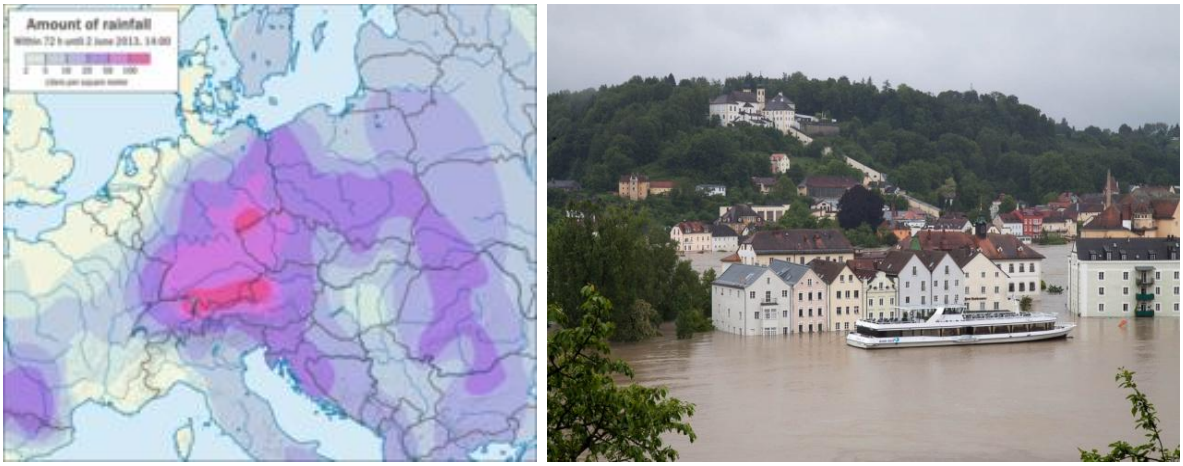

In 2014, the heaviest rain in 120 years was recorded in Serbia and in Bosnia and Herzegovina, with flooding affecting 1.6 million people, including the loss of 62 lives, and over 2000 landsides across the Balkan region[14]. Record daily totals were recorded in Belgrade (107.9 mm), Valjevo (108.2 mm) and Loznica (110 mm) on 15 May, and the highest monthly total of 205mm in Belgrade the highest since 1897. Damages were estimated to be €1.55 billion, and it is estimated that it will take 5 years for agriculture in the affected regions to recover and up to a year for coal mines at Tamnava and Veliki Crljeni to be recommissioned.

Droughts remain a persistent and damaging phenomenon affecting vital life support systems of water availability, food production and both land and water based habitats. They are complex to measure, comprising interacting meteorological, hydrological and soil moisture components. They are therefore assessed using indices, for example the standardized precipitation index (SPI), the standardized precipitation evapotranspiration index (SPEI), and the Palmer Drought Severity Index (PDSI). Other indices include for example the crop moisture index, drought magnitude and surface water supply index (Bradford, 2000). See Section 3.4 for further details. There is limited evidence that they are intensifying in terms of their magnitude or duration, (see later sections), but there are several recent examples which highlight their importance to European social and economic communities. Recent European droughts occurred in Russia (2010), in France, England and Central Europe (2011), and Europe wide in 2012 affecting southern and eastern Europe (Romania, Slovenia and the Carpathians). Figure 5 shows soil moisture in Iberia at the end of 2013 from the European Drought Observatory (EDO) by the Joint Research Centre (EC-JRC).

[13] https://en.wikipedia.org/wiki/2013_European_floods
[14] https://en.wikipedia.org/wiki/2014_Southeast_Europe_floods

Figure 5: Monthly soil moisture anomaly in Iberia, 2013-2014, Source EDO Drought Report August 2014.

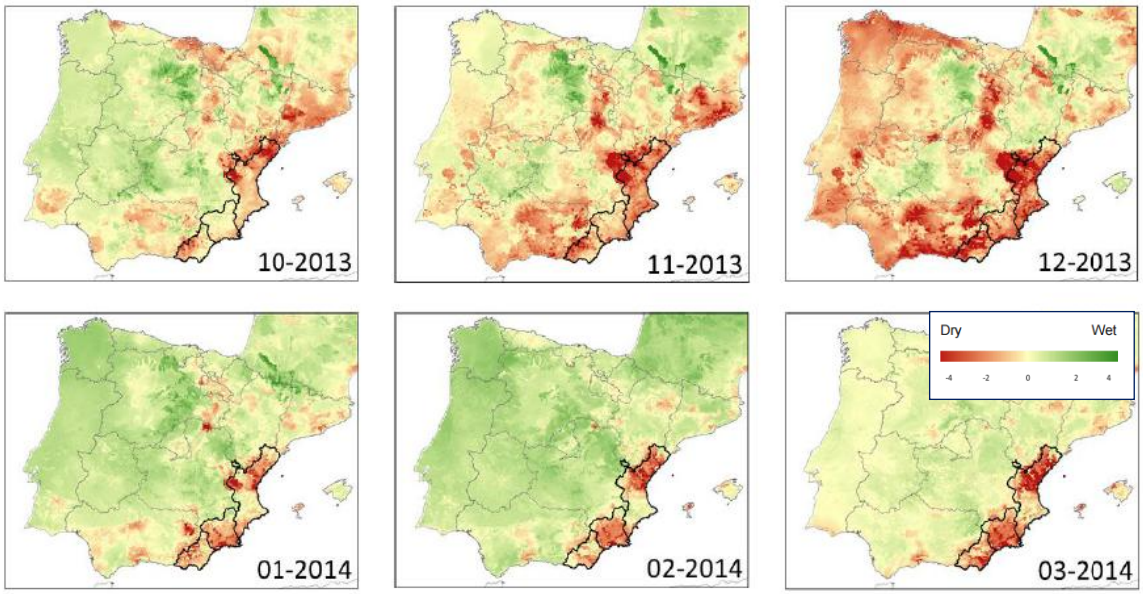

Hail extremes are less well understood due to the technical challenges of measuring hail magnitude directly, hence fewer data records are available. The incidence of extreme hail is more often characterised in terms of the size of hail physically measured at ground level, and economic (insurance loss) data for significant events e.g. Germany 2013, (refer case study 3.4). Indirect measurement by remote sensed (radar reflectivity and satellite temperature) data is increasingly used to identify hail in combination with temperature and modelled CAPE (convective available potential energy). Other extreme hail events have been recorded in southern Germany in July 1984, June 2006, July 2013, several events occurring in States of Baden-Württemberg and Bavaria; south-west France in 2013 (Berthet et al., 2013); Spain in 2013 (Merino et al., 2013), and Sofia Bulgaria in 2013 (Papagianuki 2013) and 2014. These events were caused by summer supercell thunderstorms and caused significant economic damage. Two supercells moving over central and southern Germany on 27 and 28 July 2013 caused economic losses of €2.8 billion, which represent the highest insured loss by natural hazard in Germany to date.

1.4 Intended readership and scope of report

Thus report is aimed at readers who are familiar with climate and/or weather science and who use this knowledge in their professional activities. It will be of value to policy makers in the areas of European Climate Change Adaptation (CCA) and Disaster Risk Reduction (DRR) for prioritising responses to climate related risk and reducing the vulnerability of European communities to climate extremes.

This report assesses recent scientific literature on extreme events in Europe, the level of understanding of the meteorological and climate components, and provides information on the metrics used to quantify extreme events. It presents the current scientific understanding of past, current and future extreme events for Europe and updates the European results of the IPCC AR5 (2013) and IPCC SREX (2012). It also updates information on extremes in the European Environment Agency's report on Climate Change Impacts and vulnerability report (EEA, 2012) and, like that report, emphasises the use of indices to characterise extreme events.

This report considers extremes of temperature (heat and cold), hail, precipitation (excess in terms of intensity or duration), and drought, (meteorological, soil moisture, and hydrological (river flow)). These were identified as climate variables of particular interest due to the impacts of recent European extreme events and perceptions of their changing magnitude and frequency. It examines trends in time based on available observational data (i.e. physically measured with ground based sensors or remote sensed from radar or satellite instruments) and model reanalysis (the analysis of model data run historically in time). It also examines future projections of these extremes from climate models.

Case studies of a heat wave, drought, extreme precipitation and hail event are provided in Appendix A.2 which describe the 'anatomy' of specific European events in the context of climate, weather patterns, indices and, where relevant, interactions with other systems (e.g. health, agriculture). This report excludes extremes in the following variables and events: wild fires; sea surface temperatures; storms, windstorms and storm surges; coastal and river flooding; severe convection and lightning; and snow and ice.

The impacts of extreme weather and climate events are not dealt with in this report, although emphasis is given to where aspects of the research can be carried through for use in impact studies. No analysis of attributing climate change (to anthropogenic causes or natural climate variability) is attempted, although the role of emissions (and their uncertainty) in affecting future climate change, and therefore extreme events, is described. Indices and other analytical techniques are used in this report to describe and understand extreme events, except for those based purely in the realm of statistics.

2 Data

2.1 Observations

2.1.1 Data types

Climate data are gathered and managed by national meteorological and hydrological services (NMHS). Data are produced from extensive ground based networks of temperature and rain gauges and weather radars. These are supplemented with satellite data from provided by international satellite data programmes. There are also some limited hail-pad networks in some countries. Hydrological data includes river and stream flow gauge data at strategic locations, as well as soil water and groundwater measurements. The availability of these data varies by country and by region, due their physical density and because data licensing policies also vary (Figure 8a lower panel).

Land surface temperature data are gathered from a dense network of ground base temperature gauges, some with very long records, supplemented with data from aircraft.

Precipitation data are collected from rain gauges, weather radar, and satellites. Rain gauge networks, provide a direct measurement of rainfall at a point location, at daily, hourly, and sub-hourly temporal resolutions. Long records of quality-controlled daily rain gauge data, sometimes as far back as the start of the 20th century, are available in many European locations, as well as good sub-daily (hourly) records in specific locations. However, the spatial density of rain gauges varies by country with less good coverage in eastern and southern Europe. Spatial density is generally insufficient to capture all storms, or full storm extent. The length of record also varies between stations and there may be data gaps and outages affecting data quality. Some of these discrepancies can be addressed by blending data from different sources, for example rain gauge data are combined with radar rainfall data by the UK Met Office into a single product (Nanding et al., 2015; Jewell, 2013).

A key source for ground based synoptic data is WMO's Global Climate Observing System (GCOS), a global synoptic network of automatic weather stations sending data to national meteorological services, WMO's World Weather Watch, and weather and climate organizations such as the European Centre for Medium-Range Weather Forecasts (ECMWF) and EUMETSAT. Record lengths vary but in some cases extend back to the beginning of 20th century or earlier. Rain gauge data are supplemented with, and sometimes merged with radar and satellite data.

Monthly and daily precipitation datasets are essential for characterising annual and seasonal climatologies. Higher resolution data (spatial and temporal) are necessary to identify localised and sub-daily extremes, in particular those associated with convective rainfall. In support of very high (1.5km) resolution modelling studies, the CONVEX project has produced a high resolution hourly precipitation dataset for the UK based on 1,300 rain gauges (Blenkinsop et al., 2015). Kendon et al., (2014) used 5km gridded hourly UK radar data which is available from 2003 to present day, as well as 5km gridded daily rain gauge data for UK (Perry et al., 2009) for model validation. A global hourly precipitation dataset is being produced under the FP7 INTENSE (INTElligent use of climate models for adaptatioN to non-Stationary climate Extremes) project (Fowler, 2015).

Radar and satellite remote sensing data

Radar is an indirect measurement technique by which rainfall rates are derived from raindrop reflectivity above ground, and converted to provide an estimate of ground level rainfall. They

supplement rain gauge data with spatial and relative intensity information. Radars measure rainfall intensity indirectly at high spatial (up to 0.5 km) and temporal (typically 5 or 15 minute) resolution. Radar rainfall complements rain gauge data providing improved spatial coverage in near real-time so are especially useful for operational applications (e.g. flood forecasting) but can underestimate very heavy rainfall. Radar rainfall data are calibrated using rain gauge data, and the two data types can be combined to make a composite dataset (Sideris et al., 2014).

Satellites are an important source of precipitation data where rain gauges scarce. Satellite radiometers are used to estimate rainfall from cloud top temperatures and overshooting tops, a zone of elevated temperature indicating convective activity beneath. They have the shortest records (up to approximately 30 years) and, like radar, records are updated at intervals for new instruments and algorithms. Satellite data are subject to greater uncertainty, and processed at lower temporal resolutions (2-day accumulations or lower).

Two key satellite rainfall products are GPCP and TRMM/GPM, providing data at daily, 10-day and monthly intervals. GPCP (Global Precipitation Climatology Project) merges data from over 6,000 rain gauge stations with geostationary and low-orbit satellite data to estimate monthly rainfall on a 2.5-degree global grid since 1979. TRMM (The Tropical Rainfall Measuring Mission) monitored tropical rainfall from 1998 until its retirement last year. It provided 3-hourly and 7-day rainfall totals. TRMM products have been shown to overestimate rainfall over continental Europe compared with NOAA's very high resolution CPC Morphing Method, CMORPH (Stampoulis et al., 2012). Both techniques underestimate rainfall over higher elevations, especially during the cold season.

PERSIANN is another satellite derived global precipitation product at 3-hourly and 0.04 degree resolution but was found to capture convective rainfall less well than CMORPH in a study over northern Italy and southern France (Stampoulis et al., 2013). Merged satellite and gauge-data products (e.g. GPCP-Int, CMAP, CAMS-OPI) combine the satellite's advantages of superior sampling in space and time, and the accuracy of direct rain gauge measurement.

Integrated and combined data (including reanalyses)

The representation of rainfall on the local scale, and in particular at spatial and temporal scales sufficient to represent convective extremes, requires high resolution datasets. The following climatological datasets are compiled from the observations networks above as well as additional data from regional observations networks.

The European Climate Assessment & Dataset[15] is gridded dataset for daily precipitation, temperature and sea level pressure in Europe based on ECA&D information published by KNMI. The full dataset covers the period 1950-2014. EURO4M (European Reanalysis and Observations for Monitoring) provides high resolution precipitation data for Austria, Croatia, France, Germany, Slovenia, Switzerland, and Italy. STAMMEX is a high-resolution (0.05-0.2 degree) gridded long-term precipitation dataset based on DWD's daily-observing precipitation network for the period 1880-2007 (Zolina et al., 2014a). CLIMDEX provides a suite of in-situ and gridded land-based global datasets of indices representing in particular climate extremes. ACRE (Atmospheric Circulation Reconstructions over the Earth) is a large regional to global historical weather and climate observational databases. The HadISD dataset (Dunn et al., 2012) includes precipitation data as well as other ground-based climate variables for the period 1973-2014, although to date, the precipitation data have not been quality controlled.

[15] ECA&D/E-OBS http://www.ecad.eu/download/ensembles/ensembles.php

Other global climate datasets include NCAR's Global Land Precipitation and Temperature dataset[16], a gridded monthly time series for the period 1900-2010, which incorporates long-term monthly and annual station averages (Legates and Willmott, 1990). Monthly data provide information on unusually prolonged wet or dry spells but will not capture shorter duration extremes. The Water and Global Change (WATCH) project combined ERA-14 reanalysis with a soil moisture indicator to produce a gridded dataset to assess crop evapotranspiration overland (Weedon et al., 2011). A new high-resolution (0.05-0.2 degree) precipitation dataset STAMMEX (Spatial and Temporal Scales and Mechanisms of Extreme Precipitation Events over Central Europe) enables regional analysis of precipitation extremes, and includes a number of supplementary datasets. These datasets include monthly and seasonal precipitation totals, intensities, number of wet days, characteristics of heavy (95th percentile) and very heavy (99th percentile) precipitation, as well as the distribution of fractional contribution (DFC), and statistics of wet- and dry-spell durations. Model reanalysis datasets such as ERA-Int[17] and ERA-CLIM[18] provide climate data for multi-decadal periods.

Hail data

Hail data are not collected routinely by any NMS (National Meteorological Service). There are some limited hail pad networks, mainly in hail prone areas of Germany, comprising styrofoam pads from which hail size is derived from dent size (after Schleusener et al., 1960). Hermida et al., (2013) used hail data from 2335 hail pads at 386 stations to quantify spatial, altitudinal and temporal hail variability for two regions (Atlantic and Midi-Pyrénées) in France. More specialist meteorological equipment is operated by European universities and researchers, for example, one recent device derives the kinetic energy and momentum of hailstones from sound waves measured with piezo-microphones from which hail size and the size spectrum can be inferred (Figure 6). However, because hail pads networks are generally scarce, with large areas without coverage, researchers generally depend on voluntary observations and model data. Standards for hail measurement and classification are described in section 3.3.

Figure 6: Prof. Martin Löffler-Mang and Dr. Michael Kunz with hail sensor at the Baden-Württemberg Office for the Environment, Measurements and Nature Conservation (LUBW) in Wiesloch, Germany (image: IMK-TRO).

[16] The Climate Data Guide: Global (land) precipitation and temperature: Willmott & Matsuura, University of Delaware. https://climatedataguide.ucar.edu/climate-data/global-land-precipitation-and-temperature-willmott-matsuura-university-delaware

[17] http://apps.ecmwf.int/datasets/data/interim-full-daily/

[18] http://www.era-clim.eu/

Hydrological data

Hydrological data are compiled from a European network of river flow gauging stations. Figure 7 shows the availability of river flow data from the WMO Global Runoff Data Base (GRDB) since the early 1980s. The database includes monthly discharge data from more than 9,000 gauging stations (open and historic) compiled from UNESCO, FRIEND-Water and the European Water Archive (EWA). Relatively dense coverage of flow gauges can be seen in France, Germany, UK and Italy, while much sparser coverage can be seen in eastern Europe, Sweden, and southern Spain.

Figure 7: Location of more than 4000 open river flow gauging stations from which data are collated by the WMO Global Runoff Data Centre, Koblenz (source: personal correspondence with Ulrich Looser).

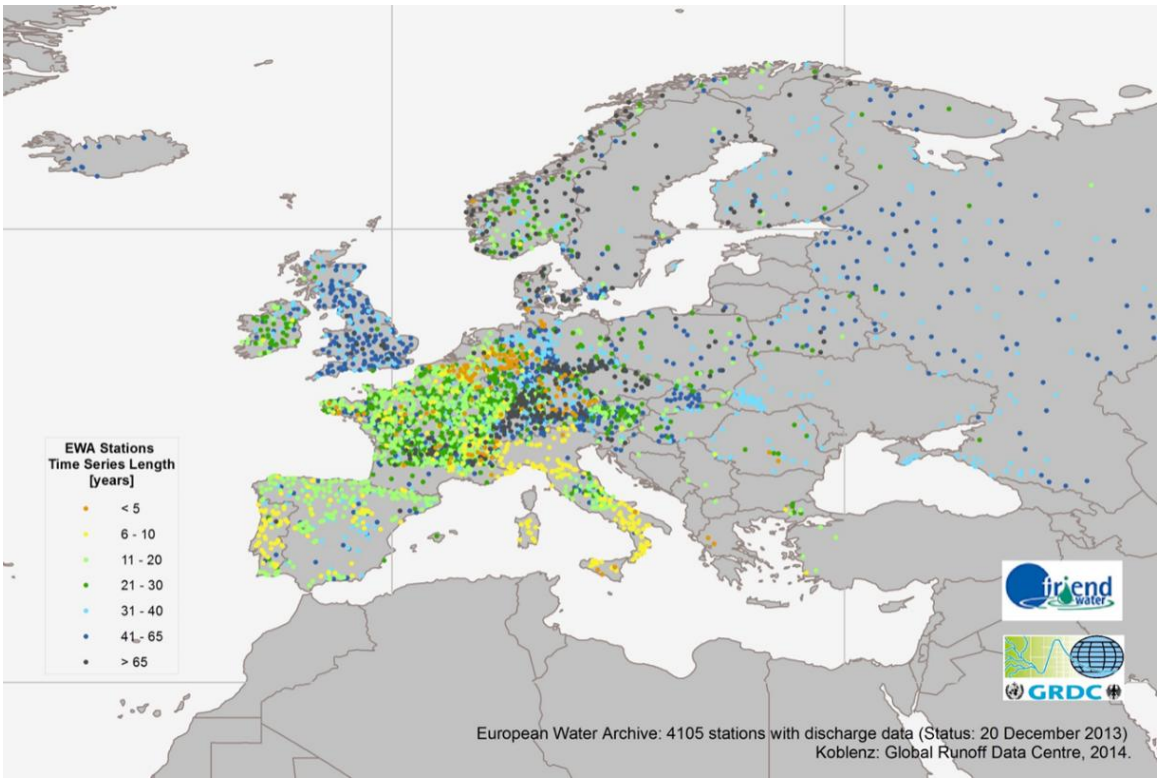

River flow data are derived from measured river levels and rely on gauge calibration against in-stream flow gauging, itself subject to high uncertainty for large river flows (Hannah et al., 2011). High and extreme flows are generally out-of-bank, and may bypass the river gauge altogether, and are therefore subject to far greater uncertainty.

Groundwater levels are continuously monitored as an indicator of available water resources and baseflows in rivers, an important indicator of streamflow drought as well as available groundwater resources. Soil moisture is sometimes monitored, but it is more commonly modelled from evapotranspiration as an indicator of surface water runoff, and soil moisture drought.

2.1.2 European datasets

Rainfall data, especially daily data, are available as a gridded rainfall dataset, e.g. ECA&D/E-OBS[19] in Europe , and UK daily rainfall data at 5km resolution since 2003 (Perry et al., 2009). The quality of

[19] http://eca.knmi.nl/download/ensembles/ensembles.php

the gridded data is influenced by that of individual gauges and the choice of interpolation scheme. Furthermore, National Hydro-meteorological Services may prioritise quality control for some long term gauges, and gauges used operationally.

At the level of individual countries, climate data is managed by the National Meteorological Service. There are relatively few large international data holdings that are easily interrogated. One of these is E-OBS/ECAD, hosted by the KNMI (Haylock et al., 2008). The raw station data (ECAD) has been created from over 10,000 station records from 62 countries, for surface temperature and precipitation as shown in Figure 8a, with the period of record shown in Figure 8b. This raw data has been gridded to create the E-OBS daily dataset.

Figure 8a: Locations of stations where data is freely available (green) and where it is only available for use in the EOBS gridded product (red) for temperature (top) and precipitation (bottom)[20].

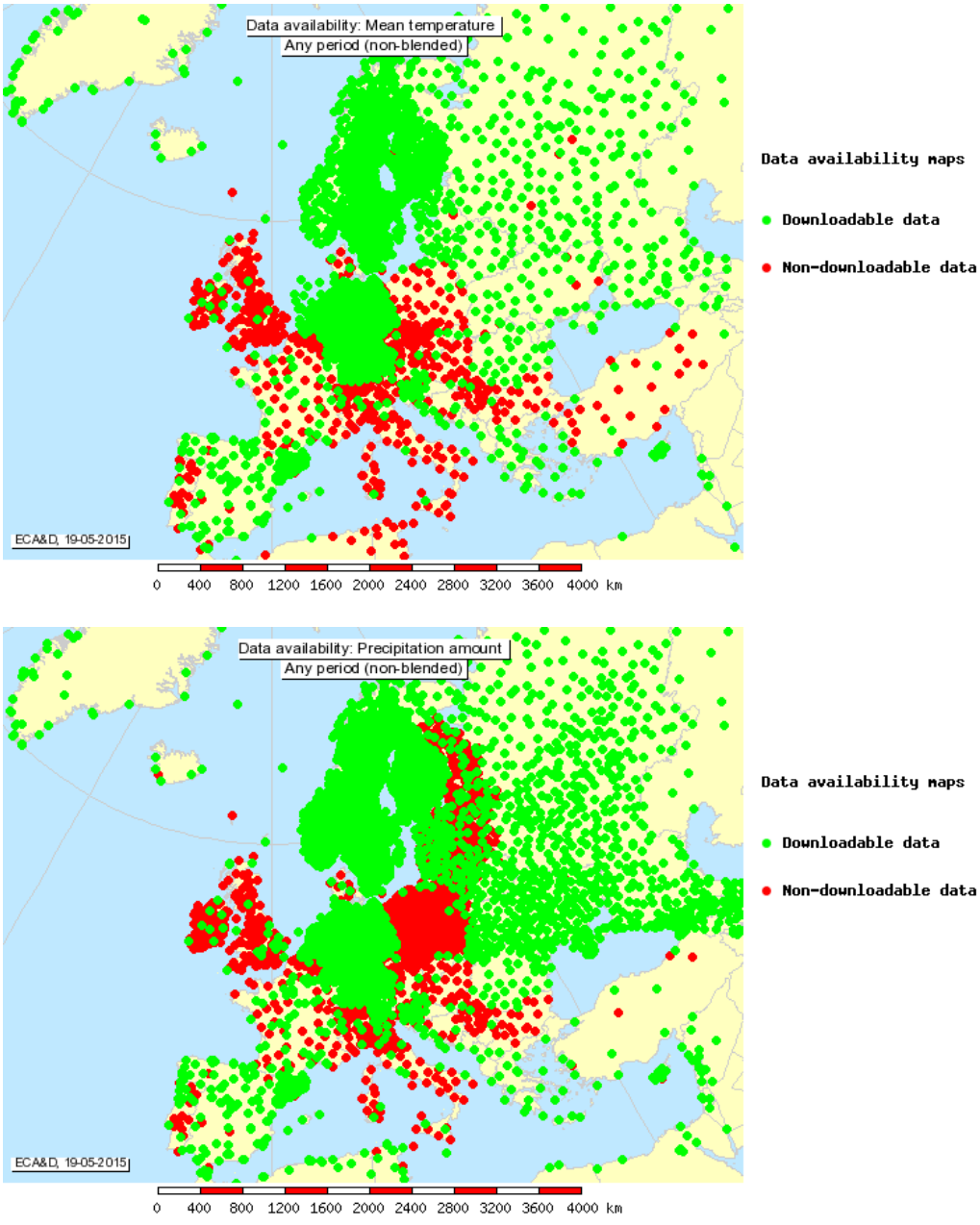

[20] http://www.ecad.eu/utils/mapserver/stations.php

Figure 8b: Length of station record available in the EOBS dataset for temperature (top) and precipitation (bottom)[21].

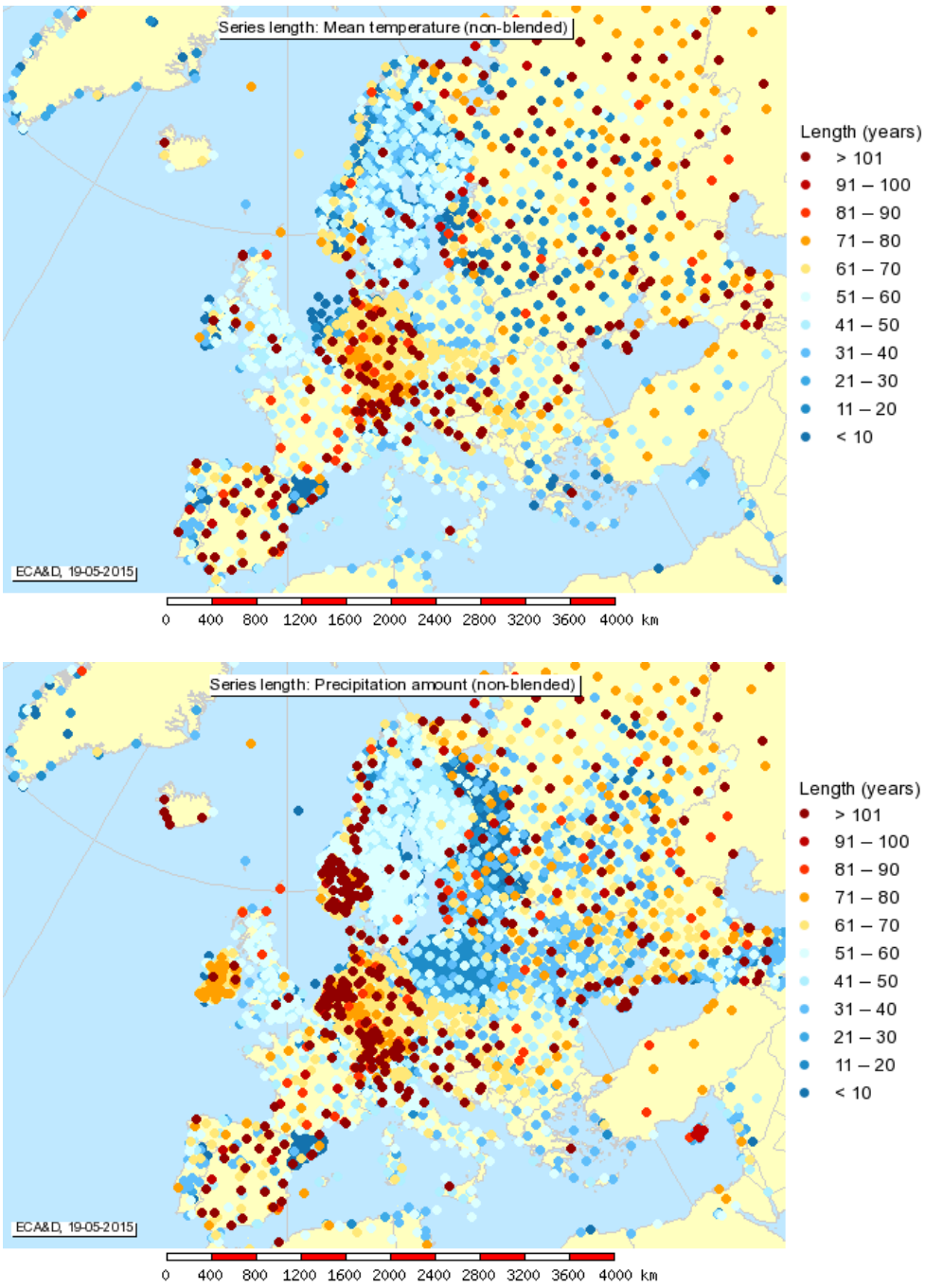

2.1.3 Data gaps, homogeneity and time series

The WMO provides international guidelines stipulating the time when minimum and maximum thermometers should be read, and rainfall accumulation times. Standardisation of these factors is important for consistency and comparability for long term climatological studies. However there are differences in the way the data are gathered. Haylock et al., (2008) showed that NMHSs in Europe use

[21] http://www.ecad.eu/utils/mapserver/stations.php

a variety of measuring intervals and methods to construct daily mean temperatures, creating uncertainty in the inputs to the E-OBS dataset (van der Schrier et al., 2013).

Station data themselves are subject to different levels of quality control. Raw data are usually archived (e.g. the Integrated Surface Dataset, Lott et al., 2008) usually with none or limited quality control applied. NMHSs then perform various quality assurance techniques, but the final data products are not always shared. Some more recent products (e.g. HadISD, Dunn et al., 2012) have received intensive quality control, but there are few standard tests that have been applied consistently and automatically across all station data.

As can be seen in Figure 8, there are significant areas which have no or very sparse measurements. Some regions also have much shorter data records than others, which limit what can be inferred from any long-term trends. Also, although some station data are shared freely, not all countries provide or share similar numbers of stations. In Germany, where many stations with long records are provided and made available to all users, more detailed analyses would be possible than in other countries within Europe. This problem increases when attempting to study climatological extreme events across the globe, with large data gaps even in interpolated products (Donat et al., 2013b, Zwiers et al., 2013). Increased data sharing by NMHSs would improve the accuracy of conclusions drawn about the region.

Not all the individual daily station data has been authorised for release by the data owners. This is a common problem for meteorological data at the current time, and becomes a greater issue as the time resolution of the data increases. By gridding the data, derived information has been permitted for release, to be used by the scientific community. These data have been quality controlled but not homogenised[22].

Homogenisation is the process by which the effects of (undocumented) station moves, instrument changes and changes in observing practices are removed from the data. For monthly data this is a common practice as the methods used have been assessed and benchmarked (Venema et al., 2012, Williams et al., 2012), but for daily and higher time resolution data (which are required for the study of extreme events) there have been few large scale applications thus far. However, even for monthly data, there remain uncertainties in the times of changes and the level of adjustment required to undo the non-climatic change.

The E-OBS dataset starts on 1st January 1950, but not all stations will report for the entire span of the data. Many will start later or finish earlier. This creates data gaps, and also has implications for the homogeneity of the gridded product; as stations become active or inactive the average value within a grid box can change (van den Besselaar et al., 2012). The length of record available is regionally dependent, and breaks can occur aligned with political changes within a country or region.

2.1.4 Gridded data

Point data from land surface weather station observations are converted to gridded format to enable direct comparison with model or reanalysis output. Various other interpolation methods exist (e.g. Voronoi Tessellation), but these will not be discussed in this paper.

The HadEX2 dataset (Donat et al., 2013a) uses a version of the Angular Distance Weighting scheme from (Shepard, 1968) to calculate the values for each grid box. This uses a search radius around the

[22] www.ecad.eu/documents/atbd.pdf retrieved 8 April 2015

grid box centre to find stations that could contribute. The search radius is determined by analysing the correlations between every station pair, and fitting the resulting decay curve. In some instances, especially in areas with poor data coverage, this can result in grid boxes having values but which themselves contain no stations. Dunn et al., (2014) assessed the effect of four different gridding schemes on the behaviour of the HadEX2 dataset, and found that this, along with changes to the station network, had the largest influence on the global and regional characteristics. Similar results have also been found by (Gervais et al., 2014, Avila et al., 2015). For globally averaged, and even regionally averaged trends, the actual method used has a relatively small effect on the behaviour of the trends; areas showing increases in the numbers of warm extremes are consistent between versions. But at local scales, then the choice of method used can affect the magnitude of the trend (Dunn et al., 2014, Avila et al., 2015). HadEX2 is a static dataset, covering 1901-2010, however, the same processing is run on the Global Historical Climate Network – Daily data (GHCND, Menne et al., 2012) creating the GHCNDEX dataset (Donat et al., 2013b), which is updated in near-real-time.

For the ECA&D/EOBS dataset, a technique similar to universal kriging was used in a three-step process to interpolate the daily data (van der Schrier et al., 2013). Gridding was carried out first, then aggregated to monthly scales, which requires a denser station network than if the aggregation preceded gridding. Haylock et al., (2008) described the method for producing the high resolution European precipitation grid for the period 1950–2006. The data were gridded at four spatial resolutions to match the grids used in current (rotated pole) RCMs. They used the same three-step process of interpolation, by first interpolating the monthly precipitation totals, then interpolating the daily anomalies using indicator and universal kriging for precipitation, then combining the monthly and daily estimates. The contributing gauges are shown in Figure 8a lower panel.

Gridding introduces some uncertainty depending on station density and homogeneity as well as the interpolation scheme (van der Schrier et al., 2013). Some grid boxes will represent a single station, elsewhere uncertainty increases with distance from the contributing station, which may be hundreds of kilometres distant, and which may represent significantly different climatological conditions.

2.1.5 Climate indices and interrelations

In many situations it is not easy to compare the observation records from individual stations. This may be because the data are not easily available (see Section 2.1.3 on data gaps) or because what constitutes an extreme event in one place (e.g. the northern coast of Norway) is very different to another (e.g. central Iberia). Even between different National Meteorological Services there are differences in how a heat wave for example is defined. For some extreme events, calculating indices derived from the meteorological and other observations is a useful way of capturing the impact of these events as these can be standardised across national borders. Indices are also more stable and less variable than raw data.

Single climate variables (e.g. maximum daily temperature or rainfall) may be insufficient to characterise climatological extremes. Indices can be tailored for specific impacts of interest, e.g. temperature thresholds which affect human health and water demand; rainfall thresholds at which flooding occurs; thresholds associated with drought impacts on crops and water resources; and indices at which hail of a magnitude or intensity likely to cause significant damage. Temperature indices

include heat, humidity and heat wave indices. Rainfall indices include the standardised precipitation index (SPI), rainfall accumulations (Rx5d), or exceedances above a threshold (e.g. T99%ile, T95%ile). The CCI/CLIVAR/JCOMM Expert Team on Climate Change Detection and Indices (ETCCDI) recommend a core set of 27 indices[23], including some which are relevant to extremes. The full list is included in Appendix A.1.

The use of indices also allows additional influencing variables to be included in a single combined indicator. For example, indicators like the Standardized Precipitation Evapotranspiration index (SPEI) and the Palmer Drought Severity Index (PDSI) take potential evapotranspiration into account, so provide a better indication of soil moisture drought, other examples being the crop moisture index and the surface water supply index (Bradford, 2000). A probabilistic hail index (PHI) combines measured hail data with a model mini-ensemble to genetrate a hail prediction indicator. Specific indices are discussed under the following sections.

2.1.6 Extreme Value Analysis

The definition of extreme is affected by the choice of statistical distribution, the baseline period and significance test. The choice and application of EVA method (Mann-Kendall, GEV, Gumbel, Tweedie) will affect the frequency (rarity) estimates, as will other factors affecting EVA like the length of record (avoiding excessive extrapolation), the assumption of stationarity, and variability. EVA is not discussed in detail in this paper.

2.2 Climate modelling and scenarios

2.2.1 Climate models and bias correction

Global general circulation models (GCMs) resolve the climate system at relatively coarse spatial resolutions, though with improvements in computing resources the resolutions are increasing. The IPCC assessment reports rely heavily on GCM projections delivered as part of the Coupled Model Intercomparison Project (CMIP), with results from CMIP3 being used in IPCC AR4, and the more recent CMIP5 (Taylor et al., 2012) in IPCC AR5. CMIP5 improves on previous assessments as it includes more comprehensive climate models, and uses a broader set of experiments that address a wider range of scientific questions. It also uses generally higher spatial resolution models and a more comprehensive set of output variables. More than 20 modelling centres from around the world have contributed results to CMIP5 with over 50 climate models. The simulations are based on two types of model experiments, one being long-term (century time scale) simulations, and the other on near term (10-30 year) decadal prediction experiments. The future scenario experiments are based upon the Representative Concentration Pathways (RCPs, see next section), an improvement over previously used scenarios which account for a wider range of outcomes. One benefit of multi-model ensembles is that they have been found to give clearer signals of change than the individual models which make up this ensemble for extremes indices (Kiktev et al. 2009, Sillmann et al., 2013a).

The World Climate Research Program Coordinate Regional Downscaling Experiment (CORDEX) is producing high resolution (at least 50km) downscaled climate data based upon the CMIP5

[23] http://etccdi.pacificclimate.org/list_27_indices.shtml

experiments (Jones et al., 2011) with various domains for different regions of the world including Europe. The EURO-CORDEX study (Jacob et al., 2013) uses 12 different GCMs and 10 different RCMs over the approximate region 27°N-72°N, 22°W-45°E, at 12.5km (EUR-11: 0.11°) and 50km (EUR-44: 0.44°) horizontal resolutions, and representing the time periods from 1951 to 2100 using the RCP4.5, 8.5 and 2.6 forcing scenarios.

A significant recent development is the move towards very high resolution climate model simulations, which are particularly beneficial for the study of precipitation changes on daily and sub-daily timescales. Kendon et al., (2014) have performed the first climate change experiments at 1.5km grid spacing, using a model more typically used for weather forecasts with explicit convection. The modelling results, with a particular focus on CORDEX and very high resolution model simulations, are described later in the report.

Bias correction is often applied to climate model data in order to account for biases in the models, usually with respect to an observational baseline, but also to account for differences between climate models. The main assumptions underlying bias correction are that the quality of the bias correction is limited by the quality of the observations used, that the bias behaviour of the model is stationary in time, and that a key limitation is that temporal errors of major circulation systems (e.g. the monsoon onset) cannot be corrected for. A variety of methods are in use which should be chosen carefully since they can affect the physical consistency of different variables, and also affect different parts of the probability distribution in different ways. Ideally a bias correction should correct more than one aspect (e.g. mean or variability) in order to capture future change across the whole distribution (Hagemann et al., 2011).

Many previous studies of hydrological changes have used the delta change approach (e.g. Hay et al., 2000) which involves calculating the projected change relative to present day, and adding this on to present day observations. However, this only considers changes in the mean and not variability, and therefore future extremes in climate may not be represented well. Several different bias correction methods have been compared for daily precipitation over the Alps and found that quantile mapping showed the best performance in reducing biases, particularly at high quantiles, and therefore might be better suited to representing extremes (Themessl et al., 2011).

A key issue with statistical bias correction techniques is the assumption of stationarity, which implies that the transfer function relating the observations to the model simulations remains the same in a future climate (Rojas et al., 2011). However, some techniques may be more suitable than others to address this problem. Borloy and Burlando (2013) presented a method to correct RCM output in a region of complex topography (the Rhone catchment) and found an improvement in the accuracy of, not just mean daily temperature and precipitation, but across the probability distribution. The authors suggest that the technique is suitable for correcting RCM biases regardless of the stationarity of the climate. It has been found that the projected regional precipitation changes in GCMs are significantly correlated with the respective regional biases for about 30% of the seasonal/regional cases investigated. For temperature, only a negligible effect of the regional bias on the projected change was noticed (Giorgi and Coppola, 2010). This suggests, at least for precipitation, that an impact of the bias correction on the climate change signal may be reasonable.

Bias-corrected results show a general reduction in the summer temperature climate change signal compared to the uncorrected simulations, especially over parts of central and southern Europe, and also has been found to influence the probability of extreme events over Europe, such as extremely hot

days or frost days (Dosio et al., 2012). Percentile extremes indices can also be affected by bias correction (Sillmann et al., 2014) since they tend to be defined relative to each model's own climatology.

Whilst bias correction is able to improve the mean and variance of model simulated temperature and precipitation in many regions of the world, there are issues with other variables particularly where observational datasets may not be adequate to provide a robust baseline against which to adjust model output. Uncertainties can also arise due to differences in the observational datasets which may be chosen to bias correct climate model data.

Bias correction methods which adjust each variable independently run the risk of removing the physical consistency between variables, and this can be a particular problem if, for example, an impacts model requires multiple climate model variables as input (e.g. temperature, precipitation, humidity, and soil moisture). It has been argued that bias correction can hide, rather than reduce, uncertainty (Ehret et al., 2012). Research into comparison of bias correction methods is currently underway (e.g. Nikulin et al., EGU 2015). Bias corrected results should be applied with caution, and users should ensure that they understand how the particular methods used might impact the change signal, the variability and distributions of the data, and the inter-relationships between variables.

2.2.2 Emissions scenarios

The potential future impacts of increasing greenhouse gas emissions are represented by scenarios which represent plausible future trajectories of emissions and associated atmospheric concentrations of greenhouse gases (GHGs). GHG emissions represent one of the components of uncertainty in climate change projections. Prior to the IPCC AR5, many assessments used the scenarios described in the IPCC Special Report on Emissions Scenarios (SRES) (Nakicenovic et al., 2000). The SRES scenarios were based upon socio-economic storylines as a starting point to develop the emissions pathways used to model the impacts upon the climate systems.

Table 2: Overview of representative concentration pathways (RCPs) (Van Vuuren et al., 2011). Radiative forcing values include the net effect of all anthropogenic greenhouse gases and other forcing agents. (CO_2 equivalent in parts per million) From Wanders et al., 2015.

RCP	Scenario	CO_2 equivalent
2.6	Peak in radiative forcing at ~ 3.1 W m^2 before 2100 and then decline (the selected pathway declines to 2.6 W/m^2 by 2100)	~490 ppm
4.5	Stabilization without overshoot pathway to 4.5 W/m^2 at stabilization after 2100.	~650 ppm
6.0	Stabilization without overshoot pathway to 6 W/m^2 at stabilization after 2100	~850 ppm
8.5	Rising radiative forcing pathway leading to 8.5 W/m^2 by 2100.	~1370 ppm

The IPCC AR5 uses a new set of scenarios called Representative Concentration Pathways (RCPs) (Moss et al., 2010), Table 2. Unlike the SRES scenarios, RCPs are based upon the level of radiative forcing (at a global level) by the year 2100 from which atmospheric concentrations and emissions pathways can be determined. The RCPs represent a wider range of warming for the twenty-first century compared to SRES, a low emissions RCPs scenario being used to represent explicit climate change mitigation and a radiative forcing of 2.6 Wm^{-2} by 2100. The other RCPs are RCP 4.5, RCP 6.0, and RCP 8.5. However, this should not be taken to imply a wider range of uncertainty, it is simply

a choice of emissions scenarios (Knutti and Sedlacek, 2013). Rogelj et al., (2012) provide a useful indication of the analogues between the SRES scenarios and the RCPs. Knutti and Sedlacek (2013) also provide a comparison of SRES and RCP warming in climate models and found that projected global temperature change in the new AR5 GCMs is very similar to that found in the AR4 report when scenario differences are accounted for, and spatial patterns of both temperature and precipitation are very consistent (Figure 9). Beyond the year 2100, RCP extension scenarios are also available which a more limited number of modelling centres have used to produce climate projections towards 2300.

Figure 9: Global temperature change and uncertainty (Knutti and Sedlacek, 2013). Global temperature change (mean and uncertainty) relative to 1986-2005 for the SRES scenarios run by CMIP3 and the RCP scenarios run by CMIP5. The number of models is given in brackets. The box plots (mean, one standard deviation, and minimum to maximum range) are given for 2080-2099 for CMIP5 (colours) and for the MAGICC model calibrated to 19 CMIP3 models (black), both running the RCP scenarios.

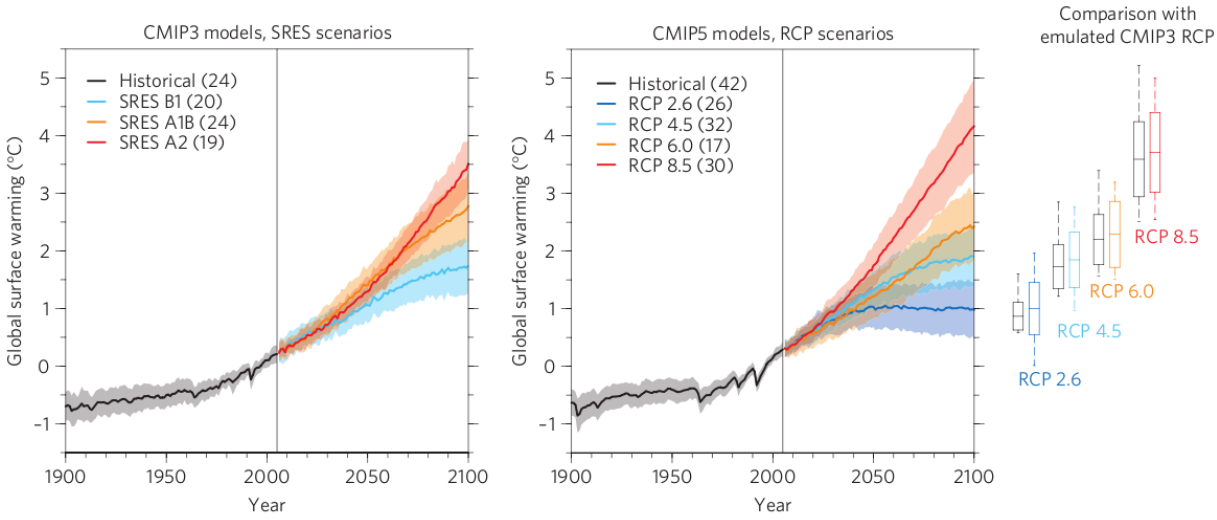

2.2.3 Socio-economic & policy scenarios

In the IPCC AR5, the climate and socio-economic scenarios have effectively been decoupled. Unlike the SRES scenarios, where a GHG emissions scenario was developed from an associated socio-economic storyline, the climate change component of the scenarios are now represented by RCPs, and the socio-economic component by the Shared Socioeconomic Pathways (SSPs) (Figure 10, O'Neill et al., 2014). SSPs represent 'alternative pathways describing plausible alternative trends in the evolution of society and ecosystems over a century timescale, in the absence of climate change or climate policies'. The SSPs are designed to work in a framework with the RCPs to provide alternative pathways of socioeconomic development which can be used in conjunction with the different climate pathways represented by the RCPs. Kriegler et al. (2012) set out a range of scenarios that should be spanned by the SSPs, which is divided into five with one SSP in each domain.

Figure 10: O'Neill et al., 2015, SSP 'challenges space'. Five shared socioeconomic pathways (SSPs) representing different combinations of challenges to mitigation and to adaptation.

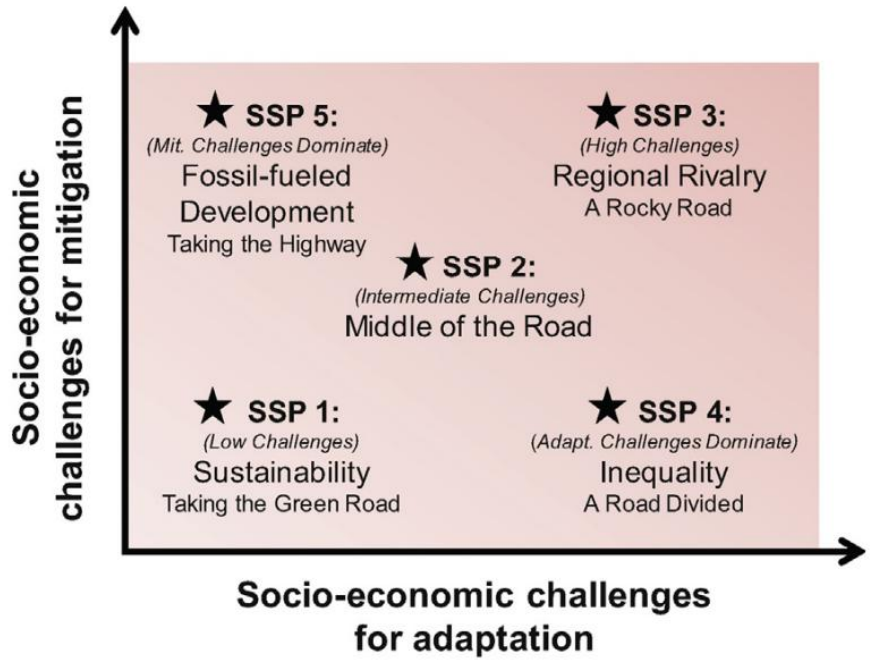

An example of key drivers of changes captured by the SSPs include population and gross domestic product (GDP). The development of the SSPs is in two stages with the first being a 'basic' set that includes broad-scale narratives and global quantifications. This provides a platform for developing an 'extended' set of SSPs which expand on the detail for specific sectors and regions (van Ruijven et al., 2014). The ability to combine SSPs with RCPs allows researchers to ask questions such as "what could be the impacts of a given amount of climate change in worlds characterized by different development pathways?" (i.e. combining a single RCP with multiple SSPs), or "what could be the impacts of different levels of climate change under one possible future world?" (i.e. combining a single SSP with multiple RCPs). This separation of climate from socioeconomics provides more options for investigating policy relevant issues than was possible with the previous scenarios.

Additionally, when SSPs are combined with the RCP pathways or climate change outcomes in integrated scenarios, there will be associated policy assumptions in order to produce emissions pathways that would result in the desired climate outcomes (O'Neill et al., 2014). Shared climate Policy Assumptions (SPAs) therefore define climate related policies , particularly aspects relating to mitigation and adaptation measures, and form an important additional dimension to the scenario matrix (Kriegler et al., 2014).

3 Extremes

Introduction

This section examines extremes of temperature, precipitation and hail in terms of their rarity in time and /or the severity of their impact. Extremes are considered in relation to climate change, to identify increasing frequency and severity of extreme events in a warming climate. The number of warm extremes is expected to increase in a warming climate (Figure 1). Even with a decrease in the number of cold extremes, the total number of extremes will increase, as what is considered an extreme is based on past experience (Coumou & Rahmstorf 2012). Increases in the average atmospheric temperature will lead to greater evaporation over the oceans and on land (Rahmstorf & Coumou, 2011) which will increase the intensity and duration of drought (Trenberth et al., 2011). Warmer air can carry a greater quantity of water (7% increase for each 1°C from the Clausius Clapeyron equation) so increases in the magnitude and frequency of rainfall can also be expected (Kendon et al., 2014), a warmer climate generating more convective events which are associated with very intense rainfall and thunderstorm activity. This may also generate a greater incidence, and magnitude of severe hail events, as recently observed in several European regions.

3.1 Temperature (Heat waves)

Key Messages

- Heat waves can be characterised in a number of ways including intensity, duration, and frequency of occurrence. A number of indices have been developed to allow the comparison of individual events and changes over time.
- Prolonged high, or extreme summer temperatures lead to increased mortality and morbidityRecent past heat wave events have resulted in reduced crop (grain) yields
- On a global scale, the number of warm extremes has increased and number of cool extremes has decreased over the last 100 years. Cold extremes or those based on minimum temperatures are changing faster than warm extremes or those based on maximum temperatures.
- For Europe, 2014 was the warmest year on record, and resulted from nearly every month being warmer than normal, rather than extreme events or days. In fact there were fewer hot days than recent years.
- The length and frequency of summer heat waves has increased during the last century.
- Under future climate change with continued warming, the number of heat waves is expected to increase, along with their duration and intensity.
- Under all emissions scenarios, summers like that experienced in 2003 will become commonplace by the 2040s, and with unabated greenhouse gas emissions, would be regarded as cool by the end of the century.
- There are contradicting studies as to where the greatest human impacts will be, dependent on topography, land-use and population dynamics.

3.1.1 Observations and data - temperature

To capture the severity of a heat wave there are a number of factors that can be accounted for, including the duration, the intensity (how much hotter than normal) and when the event occurred during the year. Perkins & Alexander (2013) assessed a variety of heat wave metrics that could be determined from temperature measurements alone. They found that CTX90p, CTN90p and Excess Heat Factor (EHF, see Appendix A.1 for a definition) were more suited than others for following the changes in heat wave number, duration intensity and frequency. The first two use the threshold of the 90^{th} percentile of the maximum and minimum temperature respectively to find the onset of the heat wave, which must last at least three days. The EHF (Nairn et al., 2009) is based on two other indices and measures the high temperatures encountered during a heat wave against both a climatological value and also an acclimatisation factor of the last month.

Using these three indices Perkins & Alexander (2013) measured the yearly number of heat waves, the length of the longest heat wave event, the yearly sum of heat wave days, the hottest day of the hottest event and the average magnitude of all the heat waves within a year. These quantities were suggested by Fischer & Schaer (2010) to study the multiple elements of a heat wave. Other extremes which were considered by Perkins & Alexander (2013) included those from the WMO/CLIVAR ETCCDI. There are eight possible indices that could be used for heat wave studies (summer nights (SU), tropical nights (TR), numbers days with maximum and minimum temperatures over the 90^{th} percentile (TX90p, TN90p), highest maximum and minimum temperatures (TXx, TNx) and warm spell duration index (WSDI). These indices fall into a number of categories – those which are absolute quantities, frequencies of exceedance above/below fixed thresholds, and frequencies of exceedance above/below relative thresholds, each with their own limitations. For example, these indices are calculated for years, seasons and months individually, so spanning events are split into two and appear to have a reduced impact (Russo et al., 2014). Further issues with the use of the ETCCDI and other indices are discussed in Zwiers et al. (2013), including the lack of availability of the source data and geographical coverage. However, these ETCCDI indices have become widely used both in observational analyses and also in combination with climate projections. Table 3 shows a list of heat wave indices discussed in this section.

Other indices have also been suggested over the past decade, each with their merits and problems (see Perkins 2015). Some also include humidity information, for example the apparent temperature, T_a (Steadman, 1979), Heat Index (Rothfusz 1990, Steadman 1984) and humidex (also called humiture, Masterton & Richardson, 1979). As the level of moisture in the atmosphere determines the rate at which sweat can evaporate from the skin, these indices are important for studies of the impact of hot weather on human health. The Wet Bulb Globe Temperature (WBGT, Yaglou & Minard, 1957) was developed by the US military with the impact of elevated temperature and humidity on the human body in mind.. This allows the mapping of meteorological variables onto a model of the response of the human body. However, as not all information required for these indices has been routinely recorded at meteorological stations, it is difficult to assess past heat wave events using these indices. The Universal Thermal Climate Index (UTCI, Jendritzky et al., 2012) takes the impact on human comfort further by including the effect of clothing on a person.

Table 3: List of heat wave indices discussed in Section 3.2.1.

Index Name	Reference	Notes
CTX90p/CTN90p	Perkins & Alexander, 2013	Number of days when T_{max}/T_{min} is above the 90th percentile as calculated for each calendar day. Adapted from ETCCDI TX90p/TN90p.
Excess Heat Factor (EHF)	Perkins & Alexander, 2013, Nairn et al., 2009	Includes acclimatisation period. See Section 5.a for full definition.
TX90p, TN90p	Frich et al., Alexander et al., 2006	Number of days when T_{max}/T_{min} is above the 90th percentile as calculated for each month or year. From ETCCDI list (see Appendix A.1)
SU, TR	Frich et al., Alexander et al., 2006	Summer days/Tropical nights – when maximum/minimum temperature is above 25C/20C. From ETCCDI list (see Appendix A.1)
TXx, TNx	Frich et al., Alexander et al., 2006	Maximum T_{max}, maximum T_{min}. From ETCCDI list (see Appendix A.1)
WSDI	Frich et al., Alexander et al., 2006	Warm Spell Duration Index – count of days where T_{max} > 90th percentile. From ETCCDI list (see AppendixA.1)
Apparent Temperature (T_a)	Steadman 1979	$T_a = T + 0.33e – 0.7w -4$, where e is vapour pressure and w is wind speed.
Heat Index (HI)	Rothfusz, 1990, Steadman, 1984	See Rothfusz, 1990 for full calculation.
Humidex	Masterton & Richardson, 1979	$h = T + 0.5555(e-10)$, where e is vapour pressure
Wet Bulb Globe Temperature (WBGT)	Yaglou & Minard, 1957	pseudo-$WBGT = 0.567T +0.393e + 3.94$, where e is vapour pressure. Includes effect of solar radiation on black globe thermometer.
Universal Thermal Climate Index	Jendritzky et al., 2012	Includes effect of clothing, movement, and activity. See www.utci.org
Heat Wave Magnitude Index	Russo et al., 2014	See Appendix A.1 for full definition.

Recently another index has been suggested by Russo et al. (2014), the Heat Wave Magnitude Index (HWMI – see Section 5.1 for definition). This index has the advantage of combining both the duration and the intensity of an event into a single quantity which not many other indices are able capture. Assessments of recent events with this index have been carried out using reanalyses (see Section 2.4.1). However, as this is a relatively new index, few studies have used this to compare recent heat wave events. And also, Schoetter et al. (2014) define an index from the 98th percentile of the maximum temperature to determine individual and cumulative heat wave severity. Using indices to study heat waves is not without its problems. Some indices have fixed thresholds, and so are of little relevance in large parts of the world. Some of the ETCCDI indices do not require that all warm days belong to the same event, an effect that is even more problematic when converting between station records and the space-filling gridded representation. Some also cannot account for the intensity of any event, and only give its duration. And as all these are calculated for each observation station, none presented here can easily capture the extent of a heat wave. When comparing two heat wave events, then the time range over which the index is calculated is also important when assessing which event was the more severe; in Barriopedro et al. (2011) the 2003 and 2010 events were compared, and when using very long averages, the 2010 event appeared less severe than the 2003 event. Thus, when selecting indices to assess individual heat waves it is important to bear in mind what the index used is able to capture – no single index (so far) can account for the heat wave duration, intensity, absolute

level and also allow easy combination and comparison between regions. Depending which impacts are of interest, different indices at different scales may be the most appropriate to use.

3.1.2 Observed trends - temperature

For Europe (35N-75N, 10W-30E), 2014 was the warmest year on record (Blunden & Arndt, 2015, with nearly every month being 2-3 standard deviations warmer than normal. However it was not exceptional in terms of extreme temperatures; it even had a lower number of summer days (where the maximum temperature > 25C) then usual (EURO4M Climate Indicator Bulletin (CIB)[24] - accessed 21 May 2015), Figure 11.

Figure 11: TOP: the European yearly average temperature with respect to the 1981-2010 climatology. Years with temperatures below this climatology are in blue, above in red, and 2014 is highlighted in green. BOTTOM: the anomaly in the number of summer days (Tmax > 25C) for 2014. (Source: CIB[5])

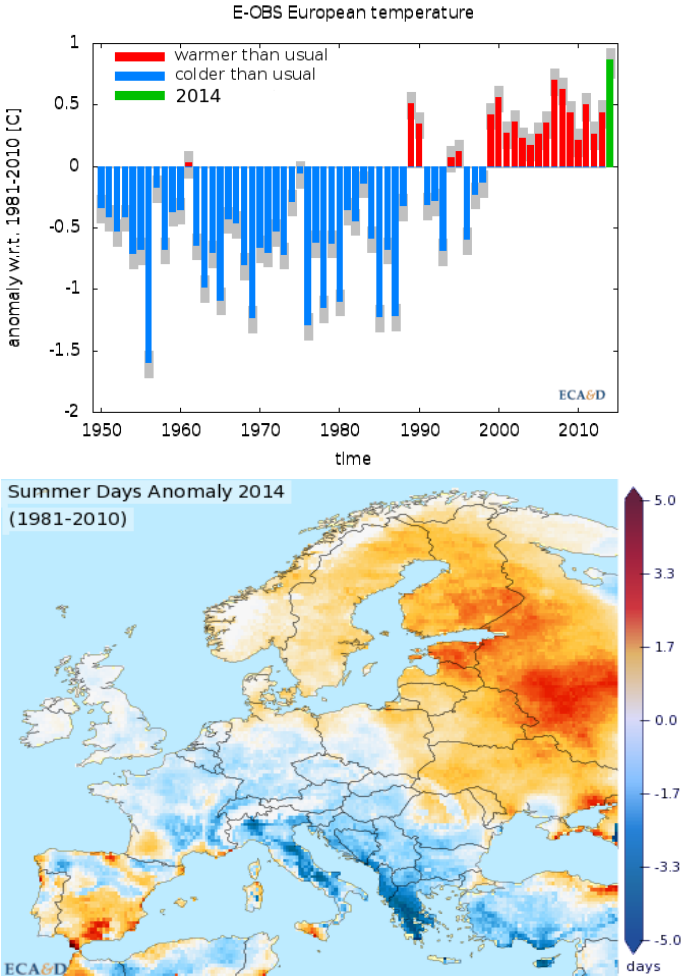

Over the recent decades, changes in extreme temperatures over Europe show a significant upward trend (see Donat et al., 2013a), and for specific indices (e.g. TXx) Europe is one of the few regions in the world which show significant upward trends, Figure 12. This gridded dataset also shows that the minimum temperatures are exhibiting as stronger warming signal than the maximum temperatures, both in the percentile (TX90p vs TN90p) and in the absolute indices (TXx vs TNx) (also pointed out

[24] http://cib.knmi.nl/mediawiki/index.php/2014_warmest_year_on_record_in_Europe *(CIB accessed 19 May 2015)*

by Karl et al., 1993, Easterling et al., 1997). Hanlon et al., (2013) using the E-OBS data found increases in the magnitude in both moderate and 1-5 day extremes. In contrast, Fischer & Knutti (2014) found the wide spread significant increases in moderate extremes (e.g. TX90p) are not mirrored by similarly wide spread significant increases in hot extremes (e.g. TXx), resulting from the high internal variability on small scales of these intensity measures. Just the same, if spatially aggregated, a shift in their distribution is observed.

Figure 12a: (TOP) The trend maps and global average time series for the annual percentile temperature indices from HadEX2 (Donat et al,. 2013a). (BOTTOM) Trend maps and regional time series for two representative areas in Europe for annual percentile temperature indices calculated from GHCNDEX (Donat et al, 2013b). Boxes with outlines contain more than three observing stations, and those with a dot in the centre have a trend which is significantly different to zero.

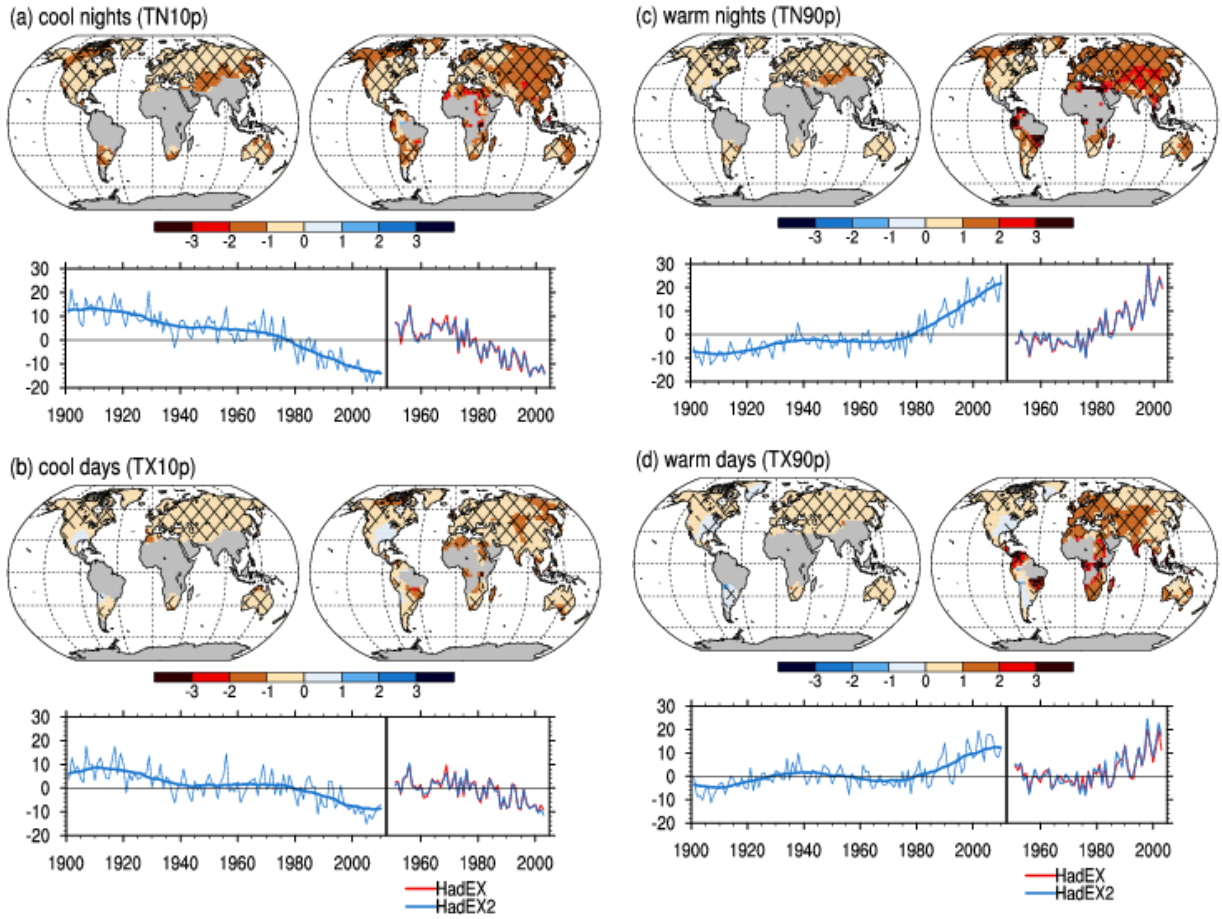

Figure continues on next page.

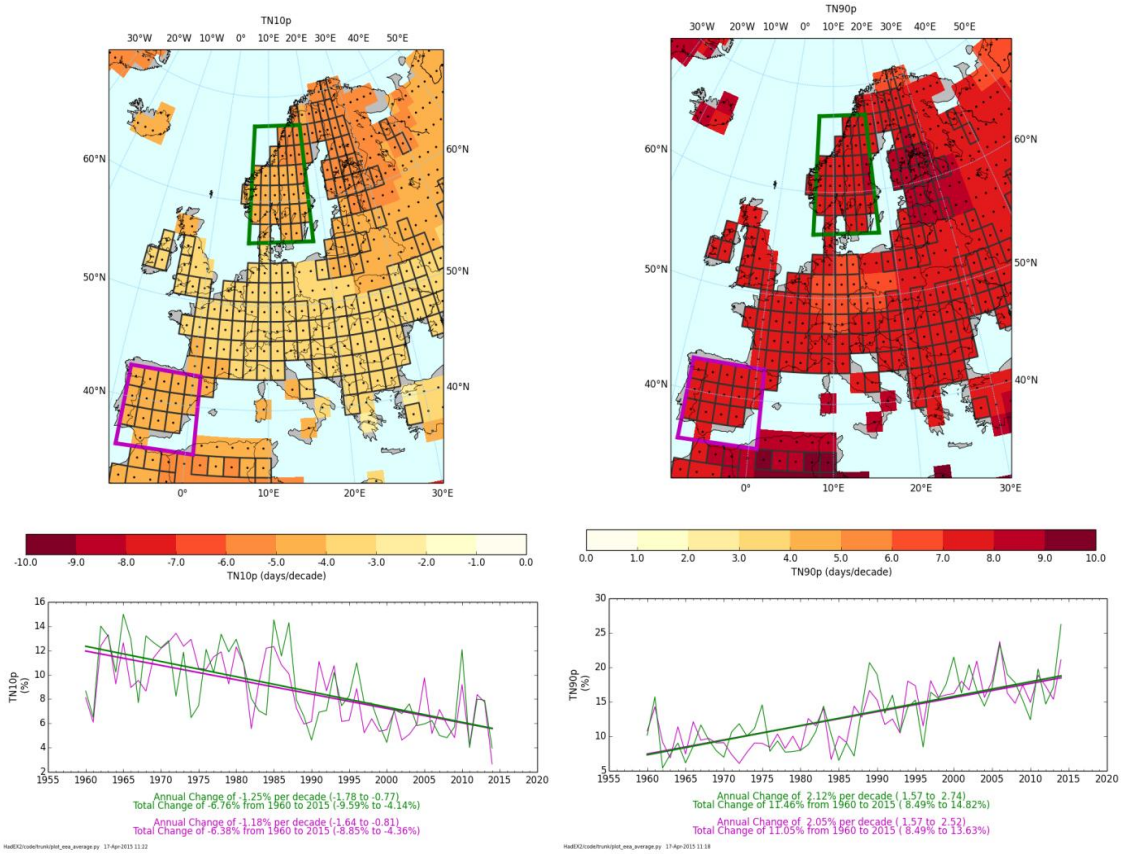
TN10p
TN10p (days/decade)
TN10p (%)
Annual Change of -1.25% per decade (-1.78 to -0.77)
Total Change of -6.76% from 1960 to 2015 (-9.59% to -4.14%)
Annual Change of -1.18% per decade (-1.64 to -0.81)
Total Change of -6.38% from 1960 to 2015 (-8.85% to -4.36%)
TN90p
TN90p (days/decade)
TN90p (%)
Annual Change of 2.12% per decade (1.57 to 2.74)
Total Change of 11.46% from 1960 to 2015 (8.49% to 14.82%)
Annual Change of 2.05% per decade (1.57 to 2.52)
Total Change of 11.05% from 1960 to 2015 (8.49% to 13.63%)

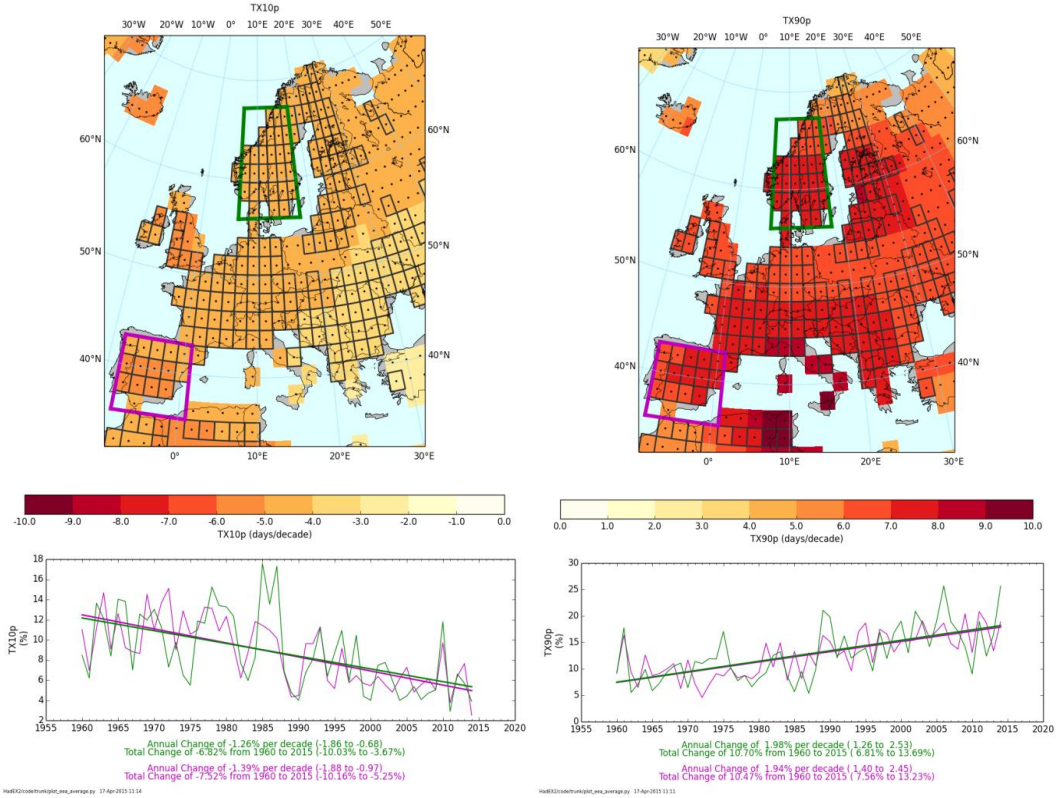
TX10p
TX10p (days/decade)
TX10p (%)
Annual Change of -1.26% per decade (-1.86 to -0.68)
Total Change of -6.82% from 1960 to 2015 (-10.03% to -3.67%)
Annual Change of -1.39% per decade (-1.88 to -0.97)
Total Change of -7.52% from 1960 to 2015 (-10.16% to -5.25%)
TX90p
TX90p (days/decade)
TX90p (%)
Annual Change of 1.98% per decade (1.26 to 2.53)
Total Change of 10.70% from 1960 to 2015 (6.81% to 13.69%)
Annual Change of 1.94% per decade (1.40 to 2.45)
Total Change of 10.47% from 1960 to 2015 (7.56% to 13.23%)

Figure 12b: (TOP) The trend maps and global average time series for the annual block maxima/minima temperature indices from HadEX2 (Donat et al., 2013) (BOTTOM) Trend maps and regional time series for two representative areas in Europe for annual percentile temperature indices calculated from GHCNDEX (Donat et al., 2013b). Boxes with outlines contain more than three observing stations, and those with a dot in the centre have a trend which is significantly different to zero.

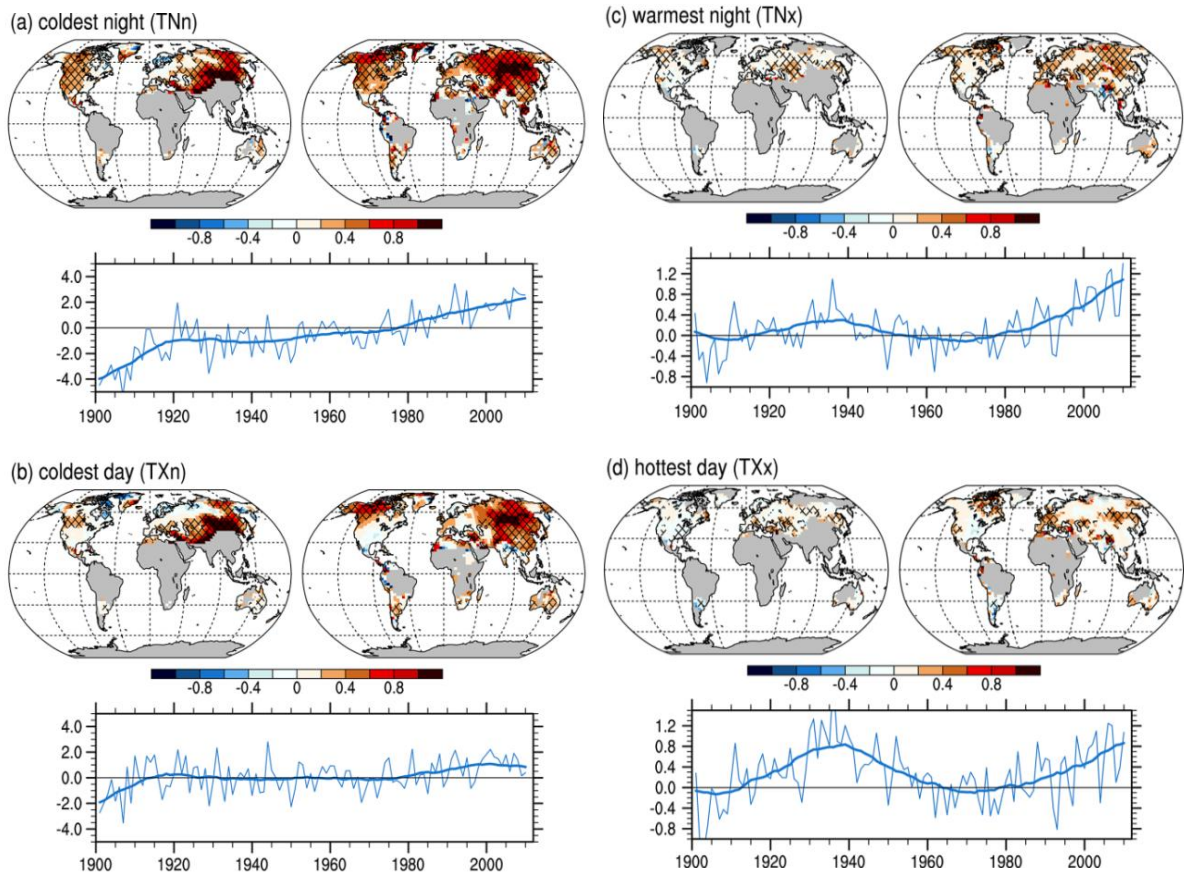

Figure continues on next page.

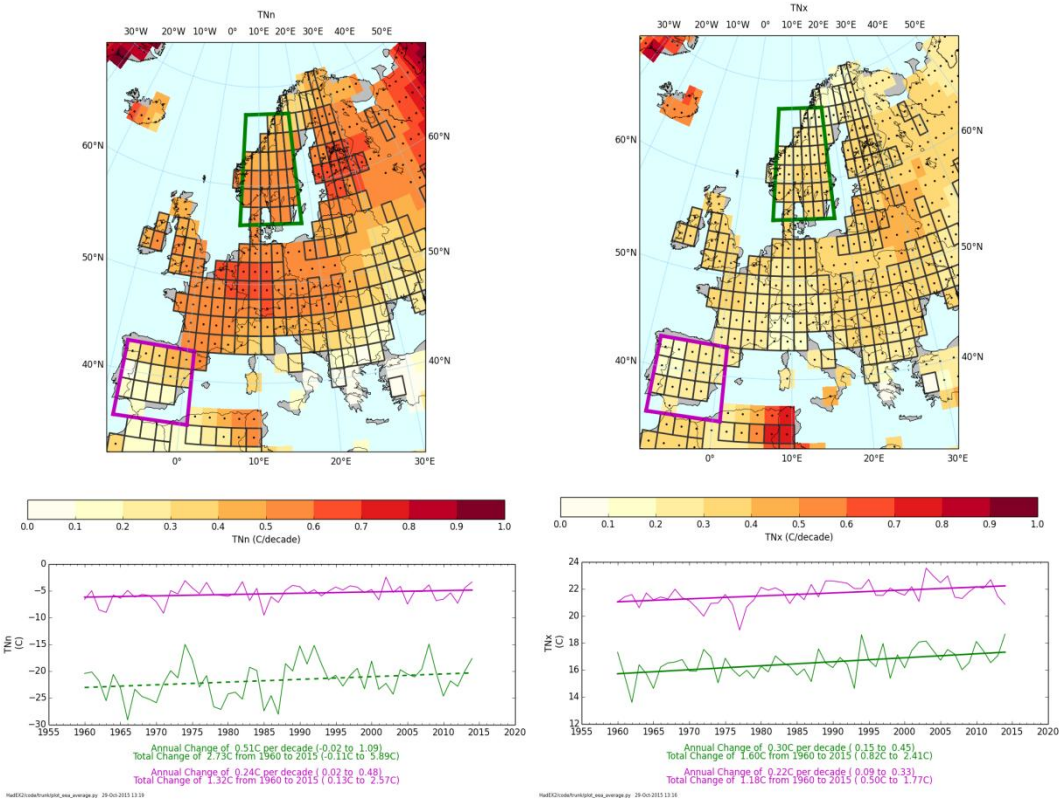

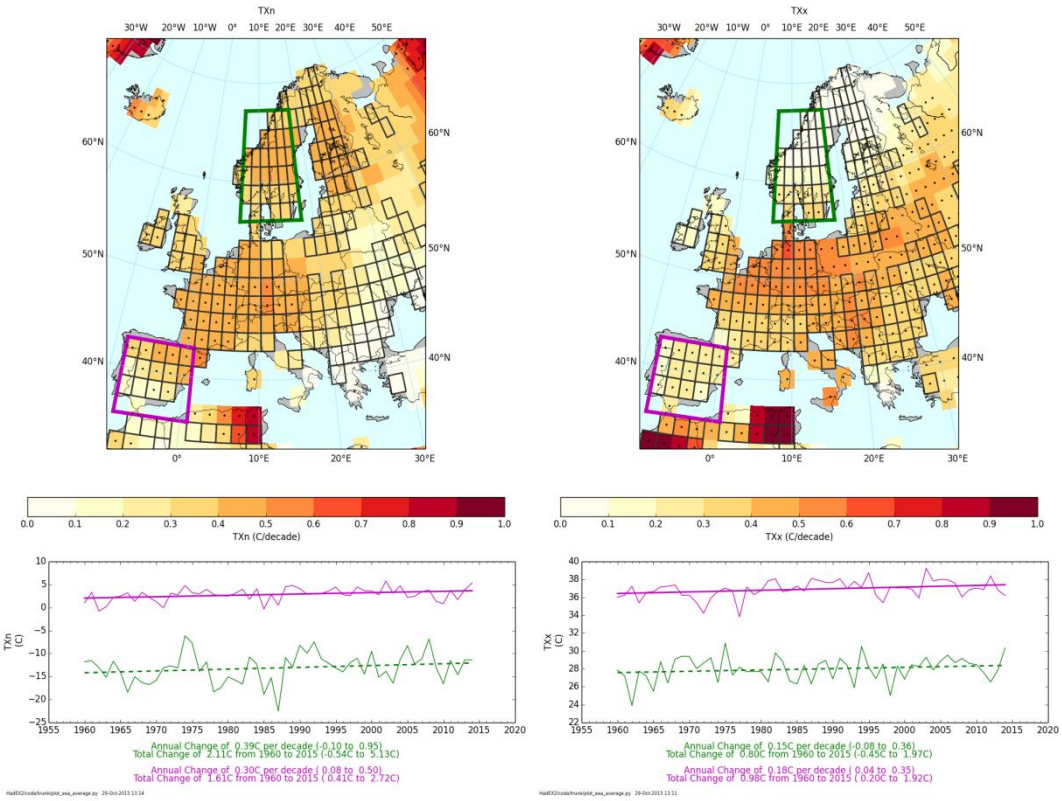

In a study on the variability of the daily maximum temperatures over summer in western Europe prior to 2005, Della-Marta et al. (2007) showed that the climate in Europe over the last century has become more extreme with an increase in variance of the summer temperatures. They also found that the length of summer heat waves has doubled, and the frequency of hot days almost tripled. In the eastern

Mediterranean the intensity, length and number of heat waves have increased by factors around 6 to 8 since the 1960s (Kuglitsch et al., 2010). In the Carpathian mountains, heat waves have been most common in the 2000s, whereas cold wave occurrences peaked in the 1960s and 80s (Spinoni et al., 2015), with the largest changes observed in maximum temperature values (Micu et al., 2015).

During the last decade or so, there have been a number of studies into the apparent stalling of global average temperatures (also known as the "pause" or "hiatus"). This has been most apparent in the global average (land and sea-surface) datasets, but less so for purely land based data. The most recent studies using the latest datasets do not support this stalling in the increase of global surface temperature (e.g. Cowtan & Way 2014, Simmons & Poli, 2014, Karl et al., 2015). Moreover, there has been no pause in the increase in hot temperature extremes (Seneviratne et al., 2014).

The climate system has a level of internal variability – one year can be warmer/cooler wetter/drier than the previous. It can take many years to sample the full distribution of a constant climate. As the global average surface temperature has already risen by almost 1°C, it is likely that few regions have experienced all possible conditions of our current climate can produce.

Heat waves are usually associated with high pressure (blocking) patterns (e.g. Pfahl & Wernli, 2012), but can be exacerbated by rainfall deficits in previous months (e.g. Mueller & Seneviratne, 2012, Clarke et al., 2006, Hirschi et al., 2010, Quesada et al., 2012 – see Section 3.4 on Drought). These high pressure systems are can be particularly stationary, and also have higher than usual central pressures. Although not always directly over the region affected by a heat wave, they work in the same way, by advecting warm dry air to the affected region. These patterns occurred in many recent European heat waves (2003 – Black et al., 2004, Fischer et al., 2007; 2006 – Rebetez et al., 2009; 2007 - Founda & Giannakopoulos 2009; 2010, Barriopedro et al., 2011). There are indications that a weakening in large scale circulation patterns may have contributed to more persistent heat waves in recent summers (Coumou et al., 2015). Also, as well as their persistence, changes in the frequency and duration of regional circulation patterns have changed the risk of extreme temperatures over some regions in recent decades (Horton et al., 2015).

Links between heat waves and large-scale modes of variability exist for heat waves across the globe. The influence of the El Niño/Southern Oscillation (ENSO) is strong, especially in those regions surrounding the Pacific, but also further afield (Kenyon & Hegerl, 2008, Arblaster & Alexander, 2012). For Europe, the North Atlantic Oscillation (NAO) is the most important mode, driving the occurrence of the blocking highs outlined above, but the Atlantic Multidecadal Oscillation (AMO) may also have an effect from the sea-surface temperatures and connections to high pressure over Scandinavia (Della-Marta et al., 2007).

Urban heat islands are a result of the physical properties of buildings and other structures, and the emission of heat by human activities. Hence urban areas experience higher temperatures than corresponding rural areas (see e.g. Parker 2009 for more details). For Europe, Chrysanthou et al., (2014) have calculated the effect of urbanisation on the daily mean temperature for the region, and show that contributes 0.0026°C/decade of the 0.179°C/decade trend. Stone (2007) showed that for 50 large US metropolitan areas, the urban heat island intensity increased by 0.05°C/decade between 1951 and 2000, which is likely due to the urban development during that time. Some old city centres no longer show warming trends relative to rural sites as the urbanisation has stabilised (Parker 2009). However, over the last four decades, there is little evidence for a strong disparity in the rate of increase in the number of hot days between urban and non-urban sites, although non-urban sites did show slightly lower increases (Mishra et al., 2015).

3.1.3 Attribution - temperature

Attribution is a process by which changes in the climate are shown to be the result of specific influences on the climate. Usually the influences are split into natural (e.g. volcanic eruptions and variations in the solar output) and anthropogenic (e.g. greenhouse gas emissions, land-use change, aerosol changes), although alternative framings have been suggested (Trenberth et al., 2015). This procedure has been used to support the IPCC statement that "It is extremely likely that human influence has been the dominant cause of the observed warming since the mid-20th century" (IPCC, 2013). The results of comparing climate model simulations of past conditions using only natural or also including anthropogenic influences to observations are shown in Figure 13. Observed global average temperatures do not match climate model simulations when only natural conditions are included. However, when including anthropogenic effects the match is much better. The improvement in the match between models and observations allows the change in probability of an event occurring or its intensity as a result of climate change to be calculated.

Figure 13: Observed time series (red line) and the range of temperature anomalies from simulations with the seven CMIP5 models used in the analysis that include all forcings (red area, a), and from simulations that include natural forcings alone (blue area, b). The black line represents the time series of the mean of the model simulations. The observed mean anomalies in decades 1990–1999 (0.77 K) and 2003–2012 (1.58 K) are marked by the green horizontal lines. (Source: Figure 17 from Christidis et al., 2015.)

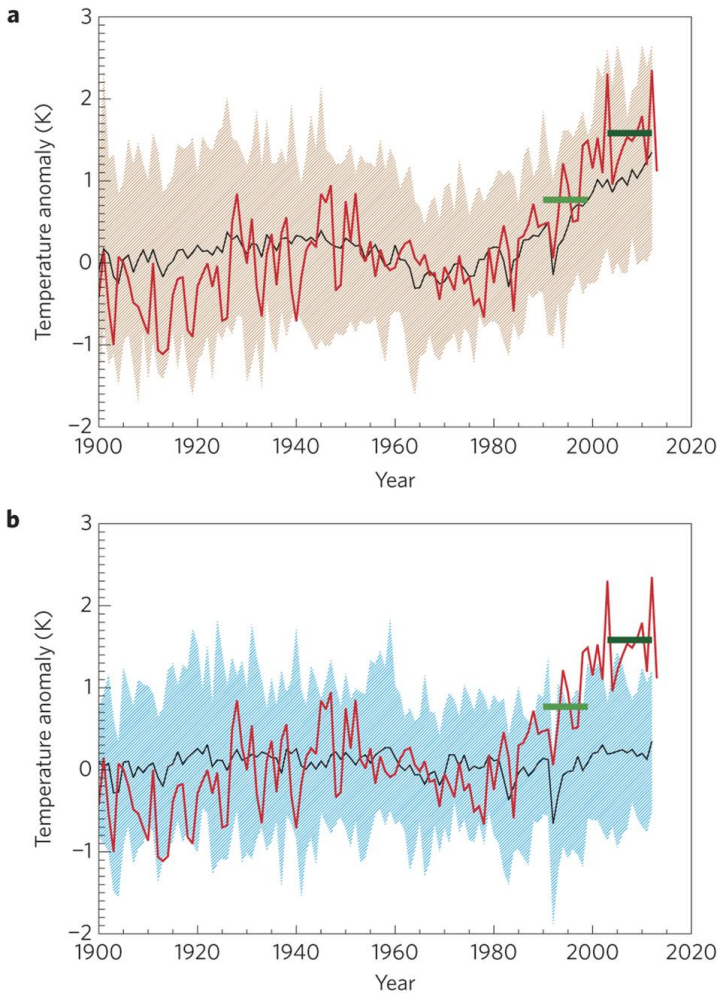

The number of extreme events can be assessed using attribution methods, to determine if changes are (partially) the result of human influences. These studies require comparable types of extremes, selected by a priori criteria from a sufficiently long and high-quality data set (Coumou & Rahmstorf 2012). Wergen & Krug (2010) found that around 30% of the observed daily high temperature records over Europe can be attributed to a warming climate. Zwiers et al. (2011) use the attribution framework to show that anthropogenic emissions have reduced the return period of hot extremes from 20 years in the 1960s to 10-15 years today, and similarly increased for cold extremes to around 30-35 years.

However individual extreme events can also be studied using the attribution framework, either to show how the chances of an event occurring have changed, or that the magnitude has. Christidis et al. (2005, 2011) found a significant human influence in the increasing severity of warm nights and decreasing severity of cold days and nights. This influence is combined with studies (e.g. Morak et al., 2011) which show that there are changes in the frequency of moderate extremes, e.g. warm nights (TN90p). More recently Fischer & Knutti [(2015]) showed that about 75% of the present day moderate daily hot extremes over land are attributable to human influence and that this fraction increases non-linearly with further warming. The rarest and most extreme events have the largest anthropogenic fraction. Furthermore, those locations where the current climate has low internal variability (the tropics and many island states) also have high vulnerability (Mahlstein et al., 2011, Stott 2015).

3.1.4 Projections - temperature

When using climate model projections (regional or global) then differences can arise because of the internal variability versus any long term trend. At times, although any individual model run will be dominated by internal variability in the short term, the results over century scales will be very similar. Also the multi-model mean can sometimes give clearer results than any individual ensemble run.

Using updated global GCMs from CMIP5 for the IPCC AR5, projected temperature changes were found to be very similar to those used in the IPCC AR4, once differences in the underlying scenarios were accounted for (Knutti and Sedlacek, 2013), and also the spatial patterns remained consistent. Despite the development of climate models, the local model spread has not changed much,

A number of assessments of the recent suite of CMIP5 models show that they can accurately reproduce heat waves which match the historical record, in terms of their evolution over time, and the areas affected (Coumou & Robinson, 2013; Kharin et al., 2013, Hanlon et al., 2013.) and also for extremes indices (Sillmann et al., 2013a). This is especially true when considering the atmospheric and circulatory mechanisms associated with extreme temperatures (Krueger et al., 2015). Often, the multi-model-mean values match the observations better than individual model runs (Kiktev et al., 2009; Sillmann et al., 2013a). A recent assessment by Fischer & Knutti (2014) shows that the land fraction showing positive trends in hot extremes (e.g. TXx) in models from the CMIP5 archive is larger than expected from internal variability, and similarly for cold extremes, despite trends in extremes not being significant in many individual grid points. However, the level of intensification of hot extremes is over estimated, and under estimated for cold extremes.

Generally, future projections also show that there will be more frequent and intense summer temperature extremes (Collins et al., 2013). In common with observational studies, they also show that cold extremes are changing faster than warm extremes or that indices based on minimum temperatures warm faster than those from maximum temperatures (e.g. Kharin et al., 2013, Sillmann et al., 2013b), linked to snow and ice retreat, but in dry and tropical areas, the converse is sometimes true. Overall, the number of record breaking events is expected to increase (Rahmstorf & Coumou, 2011), in proportion to the ratio of the warming trend and the short-term variability. Hence the total number of

extremes increases with any climate change (warming or cooling). The increase in temperature variability is also projected to increase in some areas, up to 20-40% over a zone between the Mediterranean and Baltic Seas, arising from increases in interannual, seasonal and intraseasonal variability (Fischer & Schär, 2009). This leads to an enhanced warming during the summer, leading to a higher intensity of extremes and a lengthening of the summer period.

In one assessment of the CMIP5 model ensemble, focussing specifically on heat waves that could impact the stability of the electricity supply in Europe, Schoetter et al., (2014) found that no model when forced by historical emissions simulates a heat wave as severe as 2003. Future conditions from the RCPs do result in more heat waves, with greater duration, extent and intensity. Although the distribution of temperatures does broaden in their analysis, it is the shift of the mean that has the greatest effect on the extremes. Furthermore, the diurnal and interdiurnal variations of European summer temperatures are also projected to increase (Cattiaux et al., 2015).

As outlined in previous sections, changes in the shape of the distribution of temperatures are implied by the more rapid increase in the minimum versus the maximum temperatures. However, changes in distributions in future projections are also borne out. Using the 25 models from the CMIP5 archive, Fischer (2014) showed changes in the hottest days per year under a 2°C global mean temperature rise. Over large parts of continental Europe, this resulted in the hottest days in a year being over 4°C warmer with southern Europe having the strongest signal for large increases worldwide. This implies a change in the distribution of the temperatures under such a warmed climate (Figure 14).

Figure 14: The change in mean summer temperatures (top) and hottest daily maximum temperature (bottom) for 25 models of the Coupled Model Intercomparison Project Phase 5 (CMIP5) averaged across the 20-year period in which their respective global mean temperatures are 2°C warmer than in 1986–2005. Redder colours indicate temperature increases exceeding the global mean warming. (Fig 14 from Fischer 2014.)

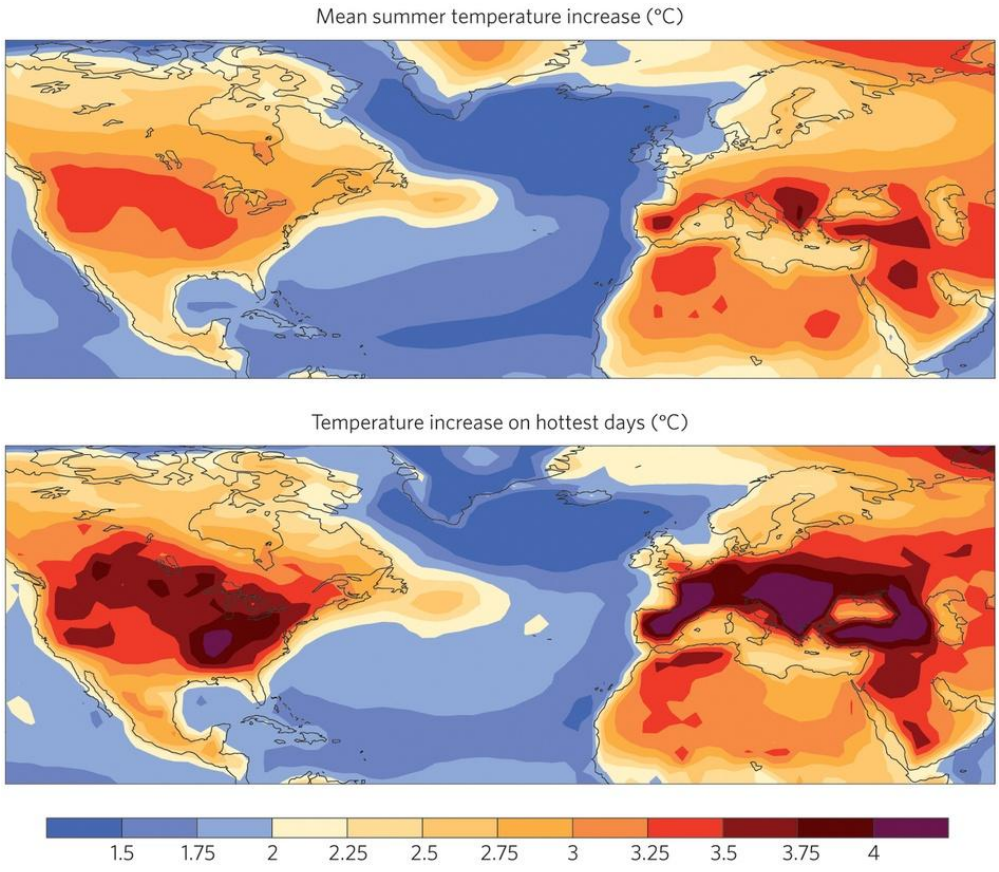

As some heat waves are associated with large scale weather patterns, changes in the occurrence and persistence of these patterns in a changing climate is likely to affect the number of heat waves. For example, Meehl & Tebaldi (2004) show that the intensification of blocking highs affected increases in the frequency of heat waves. However Cattiaux et al., (2012) show using the CMIP3 ensemble that no major future changes in pressure patterns are found over Europe. Hence future extremes are likely to be associated with weather patterns similar to the ones experienced in the present.

Russo et al., (2014) calculated the Heat Wave Magnitude Index (HWMI) for 16 GCM simulations from the CMIP5 archive over the period from 2006 to 2100, under RCP2.6, RCP4.5 and RCP8.5 (Figure 15). The HWMI takes account of both the event duration and the intensity. All models project increases in the global median HWMI for all scenarios for 2020-2052. From 2068-2100, the trend remained positive under RCP4.5 and RCP8.5 but decreases slightly under RCP2.6. The probability of extreme events increases, and heat waves that are rare in the present day (e.g. Europe 2003) could become the norm around 2070 under RCP8.5. The 2010 Russian heat wave was detected as the strongest event in the present climate, and this is projected to become the norm by the end of the century under RCP8.5, but remain rare under the other two scenarios.

Figure 15: The top maps show the median of the number of heat waves in a multi-model ensemble of the near future (2020–2052) and the latter half of the century (2068–2100) under the RCP4.5 scenario, and the lower maps are for the same time periods but under RCP8.5.[25]

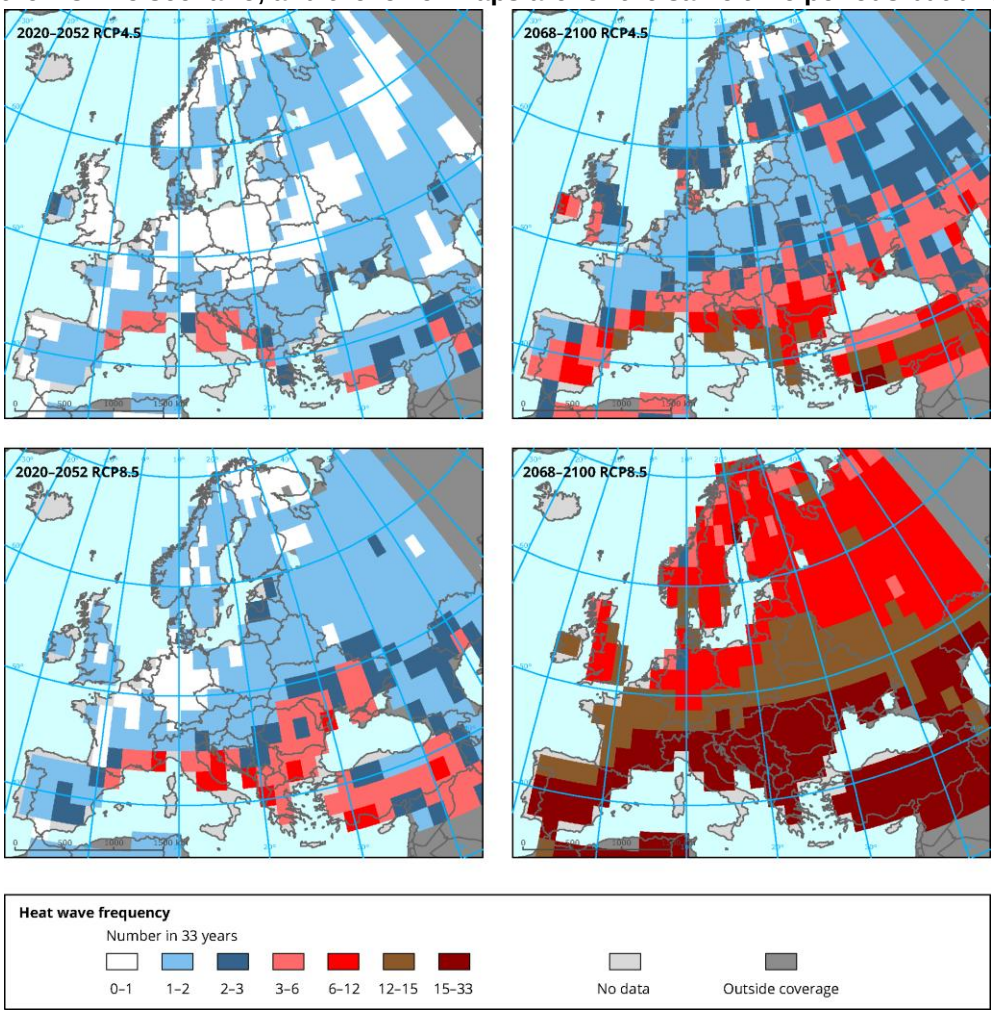

[25] Source: http://www.eea.europa.eu/data-and-maps/figures/number-of-extreme-heat-waves

Note that models are not able to fully represent the number and spatial pattern of heat waves as found in the reanalysis datasets, especially over Europe and the US (Russo et al., 2014). They found that under RCP8.5, southern Europe could experience very severe heat waves (HWMI > 8, comparable to the maximum value of the 2010 Russian heat wave) will occur at the same frequency as current extreme heat waves (HWMI>4) i.e. once every 2 years. Mitigation, as represented by RCP2.6, results in the probability of extreme heat waves being almost unchanged at the end of the century compared with 2020-2052.

A separate study by Coumou & Robinson (2013) showed that the current rate of warming will result in a several fold increase in the frequency of heat waves by mid-century (~2040), regardless of the emissions scenario. After this point, then the paths diverge ranging between strong mitigation leading to a reduction in the number of heat extremes for the last half of the century; and totally unmitigated leading to even the coldest summer months by the end of the century being substantially hotter than the hottest experienced today. Similarly Nikulin et al., (2011) found that what were 1-in-20 year heat wave events in 1961-90 reduce to 1-in-2 to 1-in-5 year events by the end of the century, and cold extremes almost disappear by the same time.

Despite the issues with using individual models, ensembles and multi-model ensembles, in some cases it has been shown that the patterns of change are very similar, even if the magnitudes of the changes differ between models (Fischer & Schär, 2010). High resolution (25km) RCM projections from the ENSEMBLES project using the SRES A1B scenario showed that European summer heat waves could become more frequent and severe during this century (Fischer and Schar, 2010), with the most severe impacts from multi-day events coupled with high night temperatures and relative humidity (Figure 16 top). Southernmost Europe experienced the strongest increases in the frequency and duration of heat waves, but low-altitude southern Europe was strongest for health-related measures. These river basins and coastal areas also are projected to experience the largest increases in the number of warm days and nights by the end of the century and correspond to areas of high population densities. For the Iberian peninsula and the Mediterranean region, the frequency of heat wave days increases from an average of 2 days per summer (1961-1990), to around 13 days (2021-2050) and up to 40 days by the end of the century (2071-2100). Changes in heat wave frequency and duration were stronger in southern Europe, but further north changes in amplitude were more pronounced. In contrast with previous studies, Lung et al., (2013) found that the risks of increases in heat could be greatest in central Europe, as a result of the ageing population of the region.

Figure 16: TOP From Fischer & Schär, 2010 - projected ensemble mean of average number of summer days exceeding the apparent temperature (heat index) threshold of 40.6 °C (105 °F). BOTTOM European population density from IIASA[26].

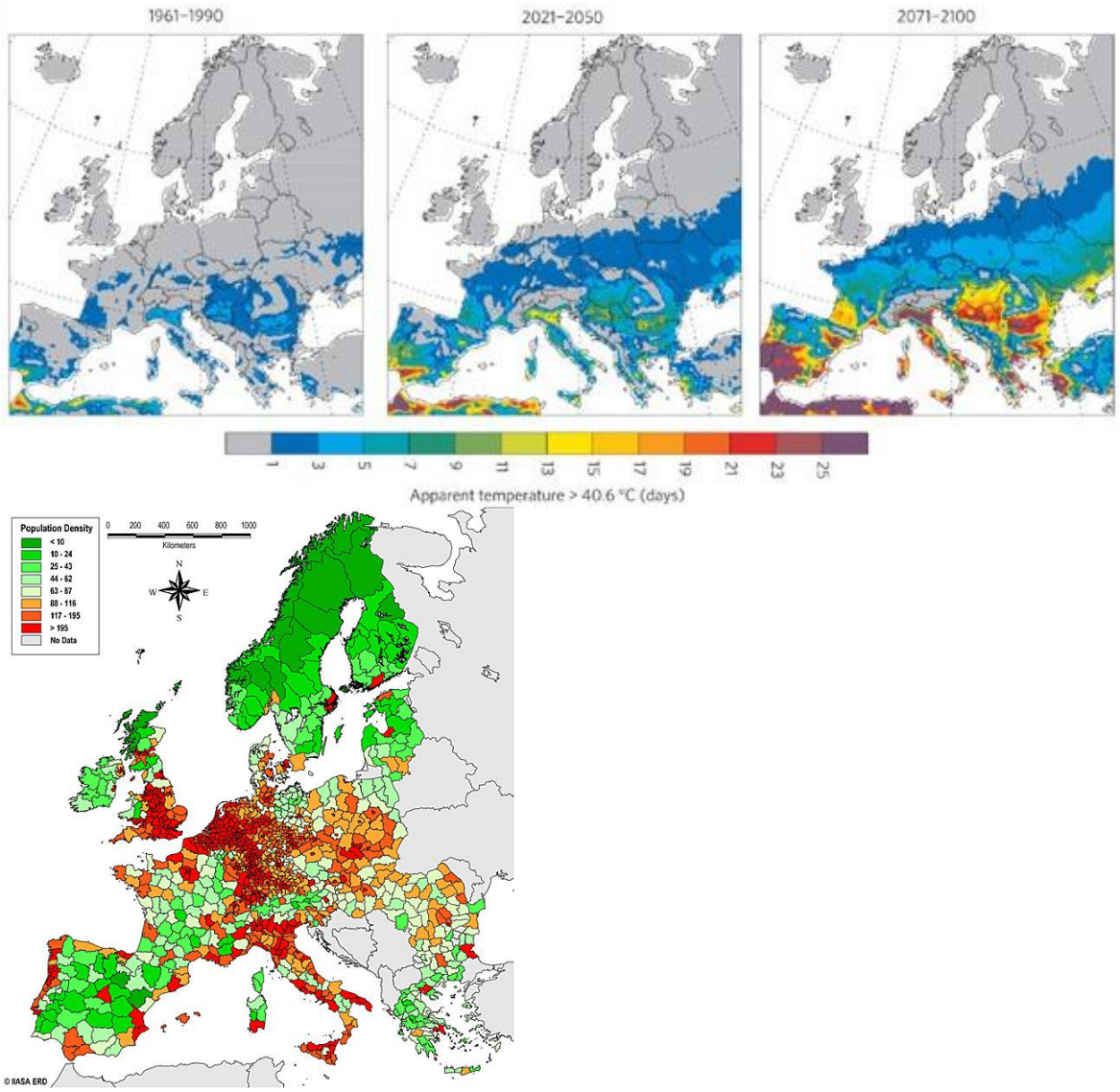

The development of higher resolution regional climate models allows an assessment of potential improvements in the simulation of mean and extreme temperatures. Initial simulations in EURO-CORDEX (Jacob et al., 2014) used RCMs at a 12.5km horizontal resolution using the RCP4.5 and RCP8.5 emissions scenarios, (Figure 17). These results were compared with the SRES A1B scenarios used in the EU FP6 ENSEMBLES project (van der Linden and Mitchell, 2009) and found that the three scenarios show similar large-scale patterns of change in mean temperature. Projections using RCP8.5 show larger changes in temperature compared with RCP4.5. Also validating the EURO-CORDEX models, from the point of view of heat waves, Vautard et al., (2013) found no clear improvements in the representation of heat wave magnitude in higher spatial resolution models. However, the simulated heat waves were found to be too persistent, even after bias removal, but a higher resolution simulation reduced this deficiency. The differences seen between individual models are larger than the differences between model simulations at different spatial resolution.

[26] IIASA, 2010, http://webarchive.iiasa.ac.at/Research/ERD/DB/mapdb/map_9.htm

Figure 17: Projected changes in the mean number of heat waves (defined as periods of more than 3 consecutive days exceeding the 99th percentile of the daily maximum temperature) occurring in the months May–September for 2021–2050 (a,b) and 2071-2100 (c,d) compared to 1971–2000. Left column (a,c) is a 'medium' emissions scenario, right column (b,d) is a 'high' emissions scenario. (Source: Figure 8 in Jacob et al., 2014.)

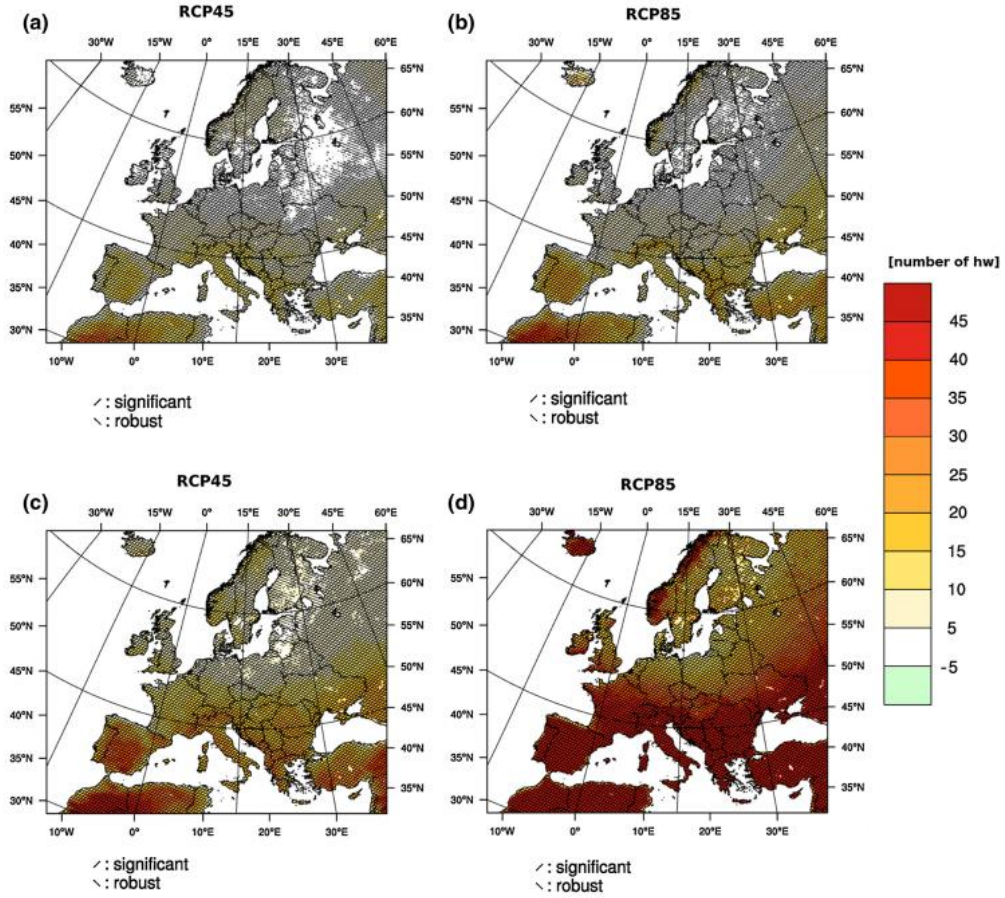

Christidis et al. (2015) updated the analysis of the 2003 heat wave by Stott et al. (2004) to account for the observed 0.81°C rise in summer temperatures since then. The return period for hot summers, as defined using an anomaly of 1.6K, has reduced from 50 years for 1990-99 to 5 years in 2003-12. For a summer as anomalously hot as 2003 (an anomaly of 2.3K) the return time reduced from over 1000 years to around 100 years (though both of these changes have a large spread). Therefore events that would occur twice per century during the climate around the turn of the century now are expected to occur twice per decade – a tenfold increase. Figure 18 shows the projected change in the probability distribution functions of summer temperatures with time during the 21st century under four emissions scenarios. With large and rapid reductions in emissions there is little change in the distribution over the century (RCP2.6) but with no change or even increasing emissions, warmer temperatures become more likely (RCP8.5). Under all emissions scenarios, summers like that of 2003 will become commonplace by the 2040s, and with unabated greenhouse gas emissions, would be regarded as cool by the end of the century.

Figure 18: Distributions constructed with data from CMIP5 models with different RCPs. The RCP scenario is shown at the top of each vertical column of panels. Each distribution corresponds to the decade marked on its panel. Temperature anomalies are relative to period 1961–1990. The vertical line marks the temperature anomaly in summer 2003. (Source: Figure 3 from Christidis et al. 2015.)

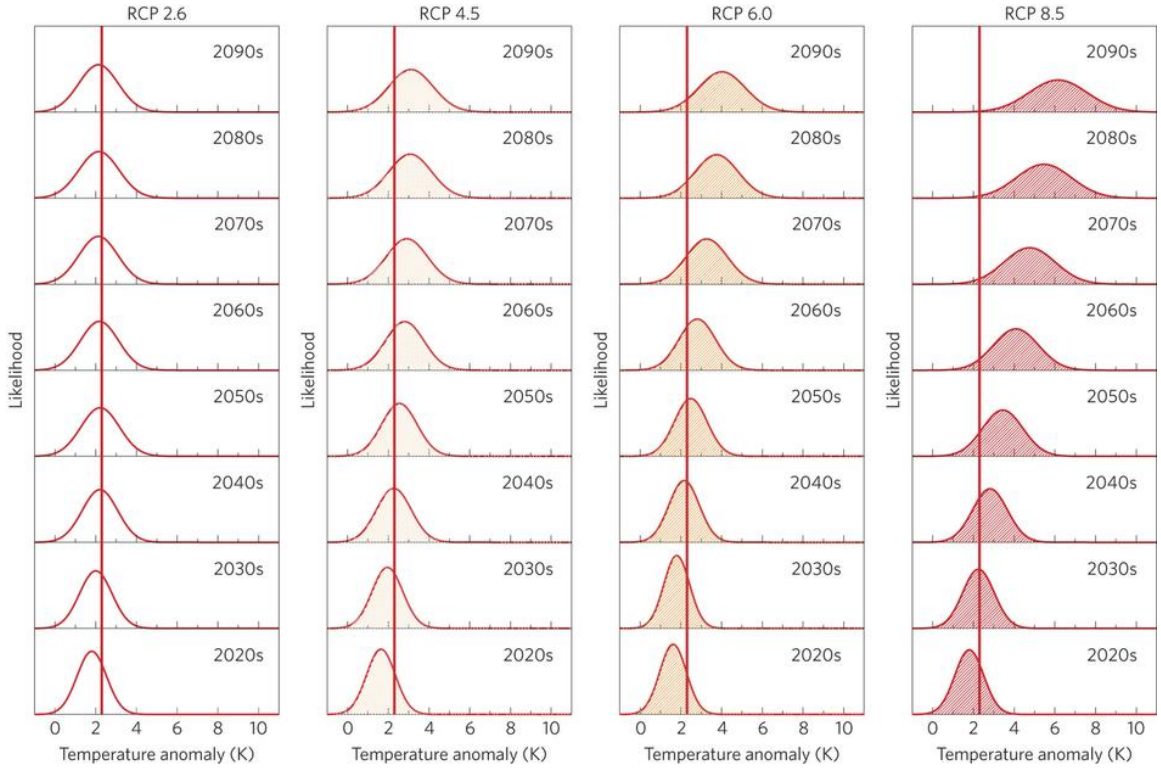

3.1.5 Links to drought

Heat waves are linked to meteorological drought events, and hence also to soil moisture droughts. In the months after reduced precipitation amounts, the lack of water in the upper layers of the soil reduces the buffer to high temperatures. The probability for an above-average number of hot days within a month is higher after months with precipitation deficits than after wet conditions (Mueller & Seneviratne, 2012, Clarke et al., 2006, Hirschi et al., 2010, Quesada et al., 2012). Therefore, if the winter and spring has been dry, then extreme summer temperatures are more likely given the right weather pattern (anti-cyclonic/blocking). However, if the summer weather patterns are not conducive to high temperatures (cyclonic) or the winter and spring have been wet, then extreme temperatures are less likely (Quesada et al., 2012). Heat waves are also more persistent when there are soil moisture deficits (Lorenz et al., 2010). The 2003 heat wave in Europe was amplified by the lack of soil moisture during that summer (Fischer et al., 2007). By combining the conditions that occurred in a particularly dry year (2011) with the weather patterns of a European heat wave (2003) (Whan et al., submitted Weather and Climate Extremes) showed that the resulting heat wave would have been 1°C warmer. Similar links have been found for the 1930s US "Dust Bowl", with indications that a hot drought more severe than 2011-12 would be possible with ocean temperature anomalies at the level they were during the 1930s (Donat et al., 2015). The soil moisture variability on intraseasonal and interannual scales can account for 5-30% and 10-40% of the heat wave anomaly respectively (Jaeger & Seneviratne, 2011). The effects of low soil moisture along with a multi-day memory of the land surface and atmospheric boundary layer resulted in the extreme temperatures during the heat waves of 2003 and 2010 (Miralles et al., 2014).

3.2 Precipitation

Key Messages

- Extreme precipitation includes high intensity short durations events and extended duration low intensity events (wet spells), both capable of generating flooding and other impacts.
- Global trends show generally wetter conditions between 1901-1953 and 1979-2003 but the changes are less spatially coherent than those for temperature. There are now more areas getting more extreme precipitation than those getting less, consistent with a warming atmosphere and an increasing trend in daily rainfall intensity.
- In Europe increases in precipitation have been observed over northern Europe and decreases over southern Europe in the 20th century. Since 1950 winter wet spells increased in duration in northern Europe but reduced in southern Europe. Summer wet spells have become shorter in northern and eastern Europe. There is evidence of lengthening wet spells at the expense of dry spells in some areas (such as the Swiss Alps).
- Extreme precipitation is becoming more intense and more frequent in Europe, especially in central and Eastern Europe in winter, often resulting in greater magnitude and frequency of flooding.
- An increasing proportion of total rainfall falls on heavy rainfall days.
- Correlation analysis shows that the most extreme events could be changing at a faster absolute rate in relation to the mean than more moderate events.
- Modelled projections of extreme precipitation events show an increase in frequency, intensity and/or amount under climate change in Europe.
- Events currently considered extreme are expected to occur more frequently in the future. For example, globally, a 1-in-20 year annual maximum daily precipitation amount is likely to become a 1-in-5 to 1-in-15 year event by the end of the 21st century.
- Extreme precipitation (including short intense convective or longer duration frontal types) demonstrates complex variability and lacks a robust spatial pattern.

3.2.1 Observations and data - precipitation

The representation of rainfall on the local scale, and in particular at spatial and temporal scales sufficient to represent convective extremes, requires high resolution datasets including ground based and remote sensed observations. From these are derived precipitation indices (e.g. the Standardized Precipitation Index, Standardised Precipitation Evapotranspiration Index) which are used in preference to absolute rainfall measures because they are spatially and temporally invariant, necessary for identifying anomalies, underlying trends, and continuous monitoring. They are also comparable across various regions and terrain. Indices used for monitoring European rainfall are listed in Appendix A.1.

The CLIMDEX website (www.climdex.org) provides access to indices calculated from datasets such as the Global Historical Climatology Network (GHCN-Daily, Menne et al., 2009; called GHCNDEX, Donat et al., 2013b) and the European Climate Assessment & Dataset (ECA&D). It also provides access to global gridded datasets such as HadEX (Alexander et al., 2006), HadEX2 (Donat et al.,

2013a and HadGHCND (Caesar et al., 2006). ETCCDI CLIMDEX precipitation indices are described in Appendix A.1.

A number of other indices have been developed for precipitation extremes, including the circulation extremity index (CEI), the modified circulation extremity index (mCEI) and the European Precipitation Index (EPIC). EPIC is a proposed index based on climatology to monitor the European domain for upcoming severe storms potentially leading to flash floods (Alfieri et al. 2012). The index is run once a day from COSMO-LEPS forecasts for each grid point of a river network at 1 km resolution. The south-western European Precipitation index (SWEP) is a measure of average precipitation for the region covering Iberia, France, and Italy, and could be useful for studies of precipitation baseline or drought.

3.2.2 Observed trends – precipitation

Global trends

Alexander et al. (2006) produced an overview of global observed changes in daily climate extremes of temperature and precipitation. Precipitation indices such as the monthly maximum 1-day precipitation (RX1d), the monthly maximum consecutive 5-day precipitation (Rx5d), the maximum number of consecutive days (CWD), or the simple day (precipitation) intensity index (SDII) were derived for the period 1951–2003 based on HadEX data for the Northern Hemisphere's mid-latitudes for the periods 1901–1950, 1951–1978 and 1979–2003. In addition to significant warming throughout the 20th century, the study showed evidence of a tendency toward wetter conditions, the 1979-2003 period significantly different from the 1901-1950 period, but the changes were less spatially coherent compared with temperature change. The SDII showed the most significant changes in precipitation indices over land compared with other indices such as Heavy Rainfall Days. A seasonal analysis detected increases in Europe for the Sep-Nov period.

Donat et al. (2013a) updated the analysis for the extended period 1901–2010 in HadEX2 (Figure 19). Results from 12 precipitation indices (R10mm, R95pTOT) indicated more areas, including eastern Europe, with increasing trends in extreme precipitation amounts, intensity, and frequency than areas with decreasing trends, e.g. the Mediterranean. However, changes in precipitation were spatially heterogeneous. A seasonal analysis of Rx1d, Rx5d indicated significant tendency towards stronger extremes over Europe across all seasons, but most significant in winter (DJF) and autumn (SON).

Westra et al. (2014) investigated global trends in annual maximum daily precipitation from 1900 to 2009 and found a statistically significant increasing global trend, and an association between globally averaged near-surface temperature and the median intensity of extreme precipitation changing in proportion with changes in global mean temperature at a rate of between 5.9% and 7.7%/°C.

Min et al. (2011), showed that anthropogenic increases in greenhouse gases have contributed to the observed intensification of heavy precipitation events found over approximately two-thirds of land areas parts of Northern Hemisphere. In 2012 the IPCC report Managing the Risks of Extreme Events and Disasters to Advance Climate Change Adaptation (SREX) summarized global studies on extreme indices. The report confirmed with medium confidence that anthropogenic influences have contributed to the intensification of extreme precipitation at the global scale (Seneviratne et al., 2012). Increases in the number of heavy precipitation events (e.g. 95th percentile) over the second half of the 20th century over land were observed, even where there had been a reduction in total precipitation amount. A late 20th-century 1-in-20 year annual maximum daily precipitation amount is likely to become a 1-in-5 to 1-in-15 year event by the end of the 21st century in many regions. However, the rainfall statistics are dominated by inter-annual to inter-decadal variability.

Figure 19: Decadal trends and global average time series for annual indices. (a) Number of heavy precipitation days (R10) in days, (b) contribution from very wet days (R95pTOT) in %, (c) consecutive dry days (CDD) in days, and (d) simple daily intensity index (SDII) in mm per day. Source: Donat et al., 2013b

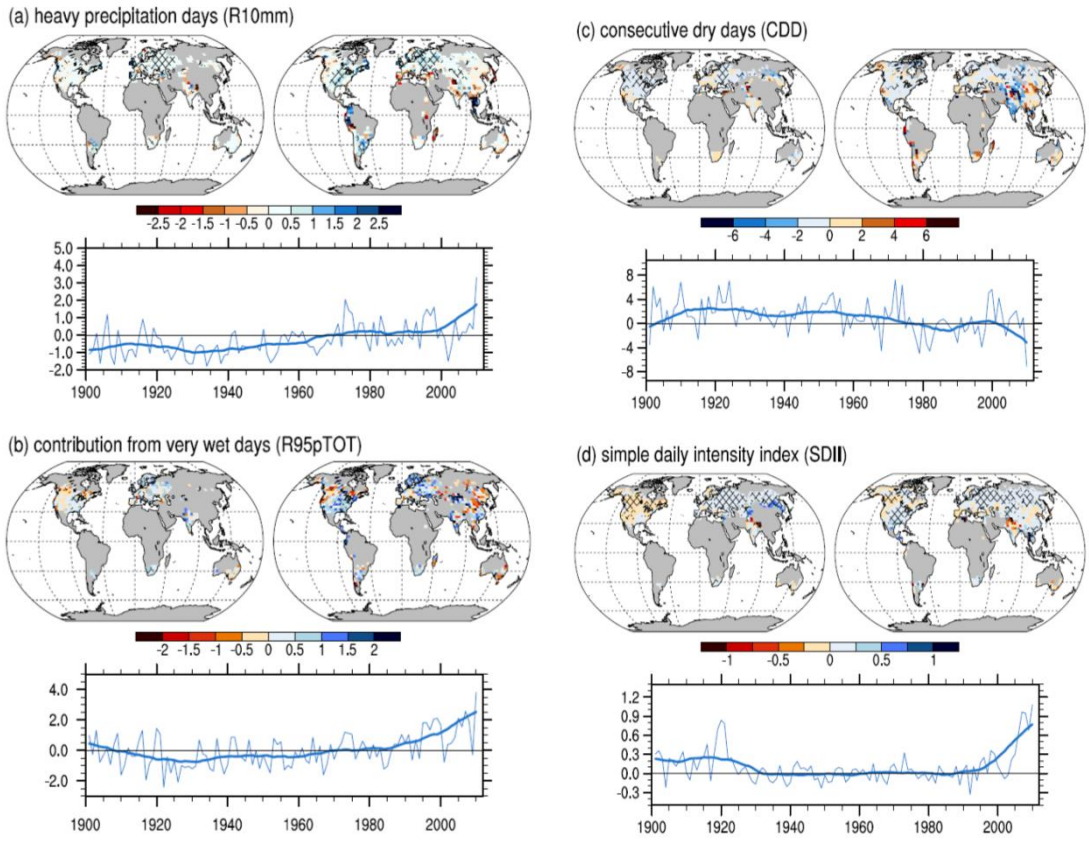

European trends

Most precipitation studies show a tendency toward wetter conditions, in the Northern Hemisphere throughout the 20th century, but the changes are less spatially coherent compared with temperature change. According to a recent European report (NAS & NMI, 2013), intense precipitation has become more severe and more frequent in Europe, especially in central and eastern Europe in winter, but with complex variability and a non-uniform spatial pattern. There is a lack of a clear large-scale pattern associated with extremes because the number of events is small and they take place at irregular intervals and with irregular intensity. Winter precipitation has decreased over southern Europe, and has increased in land north of 30°N (1901-2005) and decreased over land between 10°S and 30°N after the 1970s. The latter increase was caused by a poleward shift of the North Atlantic storm track and a weakening of the Mediterranean storm track. Short and isolated rain events have been regrouped into prolonged wet spells (NAS & NMI, 2013).

Trend analyses show increases in precipitation over northern Europe and decreases over southern Europe (Trenberth, 2011). However, trends in wet and dry spells differ regionally and by season (Zolina et al., 2012). Over the period 1950-2009, winter wet spells increased in duration by 15-20% in northern Europe and reduced in southern Europe, while summer wet spells were shorter in northern and eastern Europe. Dry spells reduced in duration in summer and winter in Scandinavia and southern Europe although opposite tendencies were observed in France and central southern Europe in summer.

The study indicates a rearrangement or grouping of dry and wet days rather than a changing number of wet days. Regional studies confirm lengthening of wet spells in winter and summer in the Netherlands, over the Swiss Alps (Schmidli & Frei, 2005), and in Poland (Wibig, 2009).

Data from Germany showed that the mean length of winter (October–March) wet periods increased by about 2-3% while that of extreme wet periods increased by up to 6% for extremely long wet periods. In eastern Germany, an increase in the intensity of precipitation of up to 10% per decade during long wet periods (more than 5 days), and a weakening of precipitation events associated with short and moderately long wet periods were observed (Zolina 2014a).

Extreme regional precipitation events are frequently associated with specific circulation conditions in central Europe. Kaspar and Mueller (2014) used the Circulation Extremity Index (CEI) correlated with ERA40 extreme precipitation to describe, for the Czech Republic, the large scale circulation conditions associated with extreme precipitation. Gallant et al. (2014) used the modified CEI on a daily timescale to show that extremes in many areas of Europe are changing mainly because of a shift of temperature and daily rainfall distributions. Applying the CEI in Europe revealed significant increases in the spatial prevalence of extremes from 1950 to 2012. All regions showed increasing areas where the proportion of annual total precipitation falls on heavy-rain days. Wet and dry periods became more frequent after 1970 according to the IPCC AR5 and Kaspar and Meuller (2014).

The trend in R95pTOT has been widely used to indicate a positive trend in precipitation extremes in northern latitudes (Klein Tank and Können 2003). R95pTOT is also considered to be an indicator of the amplified response of extreme precipitation events to climate change (Turco and Llasat, 2011; Ducic et al., 2012; Sillmann et al., 2013; Donat et al., 2013a, all quoted in Leander et al., 2014). In their seasonal assessment of very wet days (daily rainfall exceeding 95%ile) to total precipitation over Europe (1961-2010), Leander et al., 2014 introduced a new index S95pTOT better suited to characterising extremes which contradicted the increasing trend in extreme precipitation in northern Europe based on R95pTOT.

European Trends for the Rx5d, R99pTOT and SDII indices have been compiled by the Met Office from 1960 to 2015 using CLIMDEX data. CLIMDEX[27] is a project to produce gridded land-based global datasets of indices representing climate extremes (Donat et al. 2013a). Three indices were assessed. Rx5d is the monthly maximum consecutive 5-day rainfall total; R99pTOT is the annual sum of precipitation in days when daily precipitation exceeds the 99th percentile of daily precipitation in the base period; the simple day intensity index (SDII) is the ratio of annual or seasonal total rainfall to the number of days during the year or season when rainfall occurred.

Figure 20 shows a decreasing trend of -2.1 mm per decade in Rx5d across southern and central Europe over Iberia, and an increase over the Scandinavian region, with a positive trend of 1.74mm per decade. There is a decrease in R99pTOT over Iberia and an increase of 0.4mm per decade over the rest of Europe although not statistically significant. SDII shows a decrease over central Europe and Iberia, with a falling trend in the latter of -0.11mm per decade, while the rest of Europe shows an increase with a trend of 0.08mm per decade defined over Scandinavia.

There is medium confidence in European trends in heavy precipitation, especially in winter. Winter extremes have increased in central-western Europe and European Russia, but the trend in summer precipitation has been weak or spatially varying. Increasing trends in 90th, 95th, and 98th percentiles of daily winter precipitation over 1901-2000 were found in Europe, and in a country-based study for

[27] http://www.climdex.org/

the United Kingdom, Germany, and central and eastern Europe, while decreasing trends have been found in some regions such as northern Italy, Poland, and some Mediterranean coastal sites. Uncertainties are overall larger in southern Europe and the Mediterranean region, where there is low confidence in the trends (Seneviratne et al., 2012 (SREX Chapter 3)). A recent study has indicated that there has been an increase of about 15 to 20% in the persistence of wet spells over most of Europe over the last 60 years, which was not associated with an increase of the total number of wet days (Zolina et al., 2010, quoted in Seneviratne et al., 2012).

Zolina et al. (2014a) used the STAMMEX data (section 2.1.2) over the period 1950-2009 to show wet spells lengthening by about 2-3% during the winter season (October-March), and up to 6% for extremely long wet periods. This tendency is associated with an increase of up to 10% per decade in precipitation intensity in eastern Germany during long wet periods (more than 5 days) and the weakening of precipitation events associated with short and moderately long wet periods. There was no similar trend in the warm season (April-September). These changes in winter precipitation increase winter ground water recharge as well as the risk of winter flash and river flooding (Zolina et al., 2014b).

Figure 20: Spatial distribution (upper panel) and trend in time (lower panel) for precipitation indices including (a) Rx5d (b) R99pTOT & (c) SDII. Units are mm/decade. Source: GHCNDEX data from CLIMDEX (www.climdex.com). Wetting trends are shown in green, drying trends in pink.

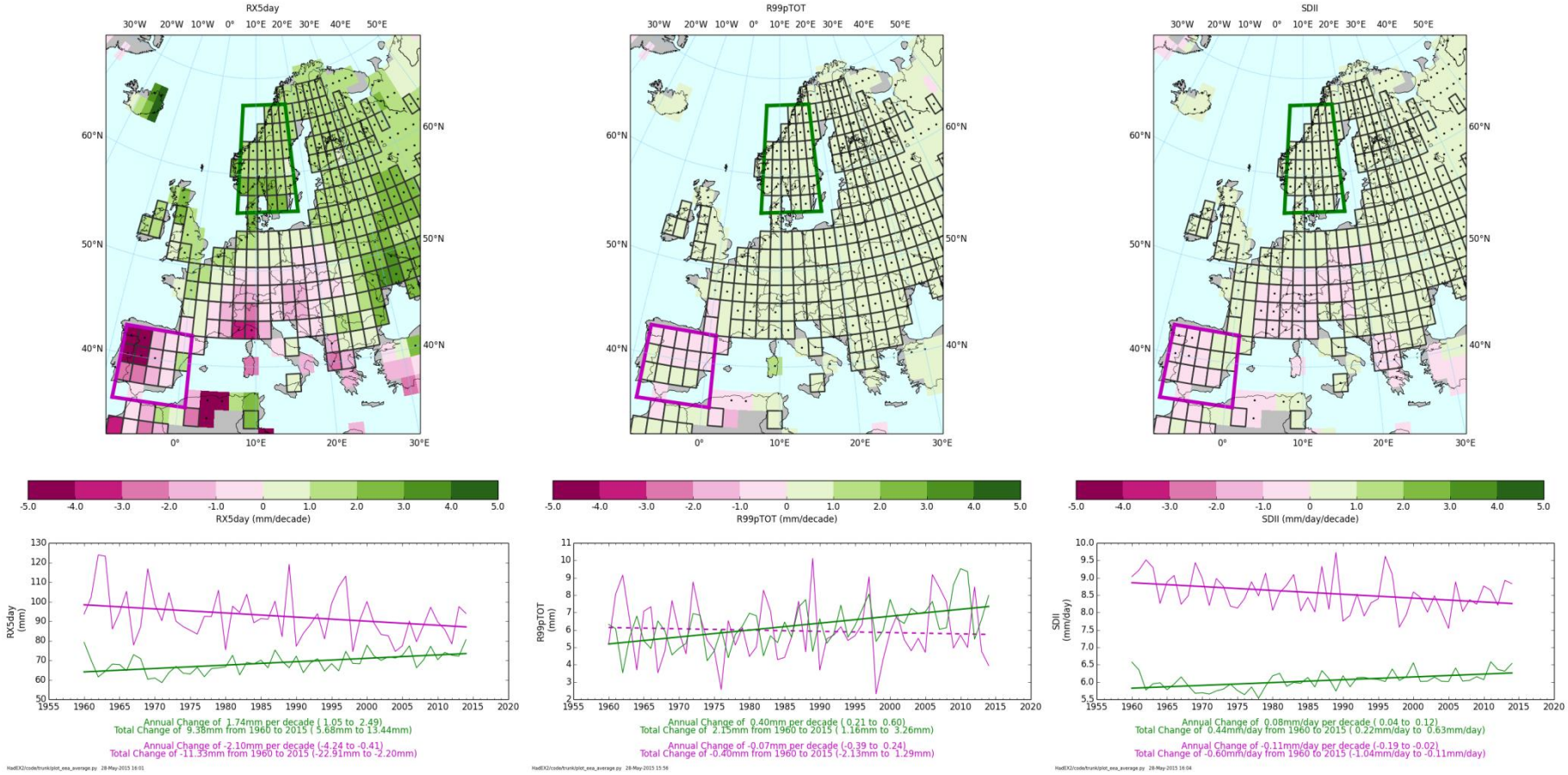

(a) (b) (c)

Van den Besselaar et al. (2013) analyzed up to 20-year extremes of maximum 1-d and 5-d precipitation amounts over the period 1951–2010 in all four seasons for northern and southern Europe. In northern Europe, the picture for the changes in extreme precipitation is approximately the same as that for the trend in total precipitation amount. In southern Europe the 20-year Rx1day and Rx5day events stay about the same in winter, but become slightly wetter in other seasons, although the regional trend in total precipitation amount in winter and summer indicates drying. Results for northern Europe showed that 20-year events in 1951–1970 have a probability of occurring more often in later periods. This is in line with work in annual 5-d and 10-d precipitation amounts in the UK (Fowler and Kilsby, 2003) which found that the 50- year event during 1961–1990 has become an 8, 11 and 25 year event in East, South and North Scotland, respectively, during the 1990s. In northern England the average recurrence interval has also halved.

An examination of historic ECA&D data for 1951-2012 did not indicate any significant trend in extreme precipitation (Hirabayashi et al., 2013). Figure 21 suggests a trend towards more heavy precipitation (>20mm) days in May, and the opposite in June, but the differences are generally not significant (green circles). A seasonal analysis indicates a significant shift towards wetter winters.

Figure 21: Trend in very heavy (>20mm) precipitation days 1951-2012 for May (left) and June (right) (source: E-OBS).

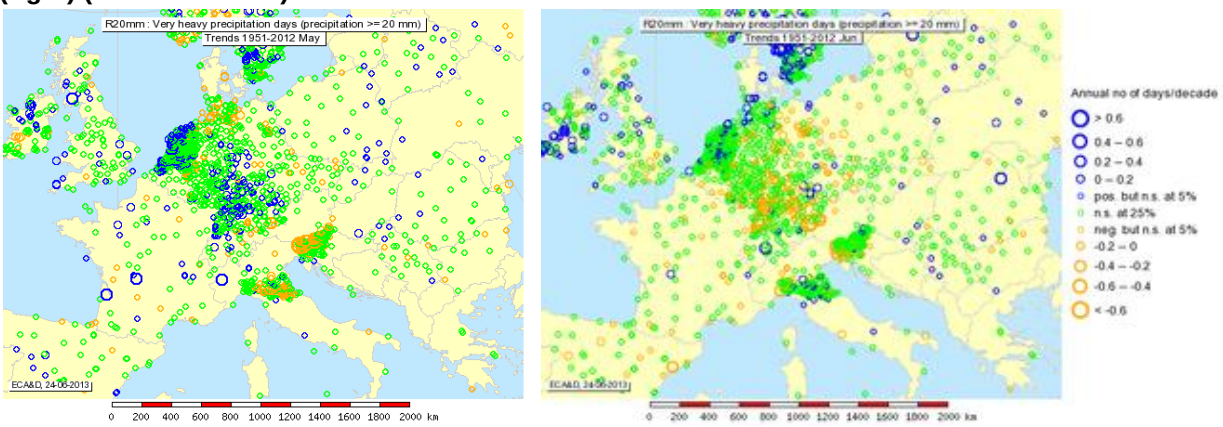

The study concluded that there is no convincing evidence of a tendency towards more extreme precipitation events in this region in summer. However, the frequency of weather patterns associated with heavy rainfall event has increased, and heavy precipitation events are projected to increase in frequency, intensity and/or amount under global warming (Hirabayashi et al., 2013).

Standardised precipitation indices (SPI & SPEI) show a tendency toward wetter conditions throughout the 20th century, while seasonal analyses show an increase in mean precipitation in winter, and decreases over much of Europe in summer (IPCC, 2014). European studies indicate an increase in heavy precipitation, especially in summer and winter extremes in central-western Europe and European Russia. Increasing trends in 90th, 95th, and 98th percentiles of daily winter precipitation over 1901-2000 have been shown in northern, central and eastern Europe, while decreasing trends have been found in southern regions especially some Mediterranean coastal sites, although at lower confidence. There has been an increase (of about 15 to 20%) in the persistence of wet spells over most of Europe over the last 60 years, which was not associated with an increase of the total number of wet days, and a lengthening of wet spells by 2-3%, and 6% for long wet periods (more than 5 days), in German winters over the period 1950-2008.

Other indices e.g. the Circulation Extremity Index (CEI) and the modified CEI showed that (daily) extremes are increasing because of a shift of temperature and daily rainfall distributions toward warm extremes and heavy-rainfall extremes. European data for 1950 to 2012 shows increasing areas where the proportion of annual total precipitation falls on heavy-rain days (Gallant et al., 2014). Correlating the Circulation Extremity Index (CEI) with ERA40 reveals large scale circulation conditions associated with extreme precipitation for central Europe.

Teleconnections between precipitation and large scale climatic features

There are known teleconnections between severe precipitation events and large scale climate patterns including North Atlantic Oscillation (NAO), the Atlantic Multi-decadal Oscillation and the El Niño/Southern Oscillation. Several papers suggest a warmer Atlantic Ocean has a positive (increasing) effect on European precipitation extremes. Associations have been identified between extreme rainfall indices (e.g. 90 and 95percentiles) and the Atlantic Multi-decadal Oscillation, an inverse association with the North Atlantic Oscillation in winter and summer, and with El Niño/Southern Oscillation events in spring and autumn in western Europe. One index (the South West European Precipitation) Index demonstrated ENSO variability affects on rainfall over Iberia, southern France and Italy by altering low-level westerly winds and onshore moisture advection from the Atlantic. However, it is less clear how the teleconnections affect *trends* in precipitation extremes.

2004 study by Haylock & Goodess identified a strong winter correlation between R90N (the number of wet days above the 90th percentile) and consecutive dry days (CDD) in Europe with NAO for the period 1958–2000. They also showed an increase in R90N for northern Europe, and a reduction in the South for the period 1958–2000. Casanueva et al. (2014) also found a significant positive relationship between the Atlantic Multi-decadal Oscillation and R95pTOT although it was more closely associated with localised convective activity. Trends in extremes were found to be more significant than those for mean precipitation, especially for R95pTOT which showed a close agreement with the positive Clausius–Clapeyron relation relating warmer air temperature and water vapour. Interannual variability of autumn and early winter precipitation over south western Europe is linked to ENSO variability in the eastern Pacific via an eastward-propagating Rossby wave.

De Lima et al.'s 2015 study of precipitation extremes in Portugal for the period 1941-2007 used a combination of 13 indices including wet and dry spell indices, thresholds, percentiles and standardised indices (e.g. R95pTOT) to show an inverse relationship between daily precipitation intensity index and NAO. A decreasing trend in the simple daily precipitation intensity index is related to the predominance of the positive phase of the NAO. For the period 1976-2007, the proportion of the total precipitation attributed to heavy and very heavy precipitation events increased and, daily precipitation events show a tendency to become more intense. Correlation analysis showed that the most extreme events could be changing at a faster absolute rate in relation to the mean than more moderate events.

KNMI used ECA&D data to analyse for two noteworthy Central European heavy precipitation events in 2002 and 2013 (case study Appendix A.2). In late May/early June 2013 between 100 and 200mm occurred over Switzerland, Austria, southern and eastern Germany and Czech Republic. The 2002 event was a high intensity short duration event concentrated over the Elbe basin.. Elevated sea surface temperatures in the eastern Mediterranean and especially the Black Sea, and the persistence of the low pressure system due to meanders in the Northern Hemisphere jet stream[28] were deemed to be significant

[28] The jet stream is a narrow band of fast flowing air at high altitude generally flowing from the west to east over the mid-latitudes, caused by a combination of the Earth's rotation and atmospheric heating (solar radiation).

influencing factors. Another assessment attributed the extreme winter rainfall of 2013 to the prevailing cyclonic conditions (NAO and Atlantic Ridge) and the warm north east Atlantic Ocean which intensifies precipitation extremes (Yiou et al. 2014).

Extreme precipitation may be enhanced by the presence of 'atmospheric rivers', narrow filaments that convey the majority of poleward water vapour within extra-tropical cyclones. Lavers and Villarini (2013) showed that ARs are responsible for up to eight out of ten annual maximum daily rainfalls in some parts of Europe. Their effect is especially strong along the western European seaboard, but is observed as far inland as Germany and Poland. They are associated with negative North Atlantic Oscillation (NAO) conditions in southern Europe, and positive NAO in the north. ARs are a critical factor in explaining the distribution of extreme precipitation western Europe.

3.2.3 Projections – precipitation

Increases in the spatial and temporal resolution of climate models are potentially of particular benefit to the simulation of precipitation, which tends to be associated with smaller spatial scales than temperature. New regional climate model simulations have been made available over recent years as part of co-ordinated projects, but there have also been significant developments in the use of very high resolution models which explicitly represent convection, as opposed to using the traditional approach of parameterizing convection. A number of observation-based analyses have indicated that sub-daily extreme rainfall is intensifying more rapidly than daily rainfall (Westra et al., 2014) and the use of higher spatial resolution models has resulted in improvements in aspects of the simulation of sub-daily precipitation on hourly timescales.

On a global scale, CMIP5 GCMs have shown quite a wide range of uncertainty in extreme precipitation projections (Rx5day) during the 21st century despite a general tendency towards heavier precipitation intensity and longer dry spells. This raises the question of how robust they are for projecting future changes. Fischer et al. (2013) assessed the impact of internal model variability and found that whilst models may disagree on the exact location of precipitation changes, at a more aggregated scale they actually provide robust evidence for heavier precipitation events even over the timescales of just two or three decades.

Using higher resolution versions of global scale GCMs has been found to improve the representation of extreme precipitation, since models often underestimate the magnitude of extreme precipitation. For example, a 0.25° version of the Community Earth System Model 1.0 showed significant increases in simulated present day extreme daily precipitation over Europe (plus the United States and Australia) compared to lower resolution versions of the same model, though it was noted that biases still remain (Kopparla et al., 2013).

GCMs do not resolve small-scale heavy precipitation and also have deficiencies in representing relevant dynamical features such as blocking [29]. Moving on to consider downscaled GCM simulations, Europe is well represented by RCM simulations and an assessment of the ENSEMBLES project (van der Linden and Mitchell, 2009) RCMs looked at projections of a set of basic precipitation indices (including wet-day frequency, intensity and percentile exceedance) as well as generalized extreme value (GEV) theory return periods of up to 100 years (Rajczak et al., 2013). Projections showed increases in mean

[29] Blocks are large-scale high pressure patterns in the atmosphere that are nearly stationary, which 'block' the movement of cyclonic weather systems, resulting in the same kind of weather for extended periods. They can remain in place for days, or even weeks.

precipitation and wet-day frequency in northern Europe, with the opposite pattern in southern Europe. A similar pattern is seen in extreme events, but increases in heavy events reach further south.

The Spanish project ESCENA used a set of five high resolution (25km) RCMs to examine precipitation and extremes over the Iberian Peninsula (Dominguez et al., 2013). It was found that several models underestimated the amount of rain on heavy precipitation days. This aspect of model performance had not improved in comparison with the ENSEMBLES project results though ESCENA covered more emissions scenarios and driving GCMs than ENSEMBLES.

The new high resolution EURO-CORDEX reanalysis driven RCM ensemble (Jacob et al., 2014) has been evaluated against the high resolution European E-OBS observational dataset (Kotlarksi et al., 2014) over the period 1989-2008. The RCMs are able to capture the basic features of European climate, including spatial and temporal variability, but there are some deficiencies with respect to certain metrics, regions and seasons. Precipitation biases are in the ±40% range. Common model biases, such as a cold/wet bias over most parts of Europe, and a warm/dry summer bias in southern Europe are seen. The increase in model spatial resolution from 50km to 12.5km indicates no clear benefit in the representation of seasonal means over large subdomain regions. Comparison with simulations from the ENSEMBLES project based on the older SRES emissions scenarios shows similar large-scale patterns of change between the SRES A1B and RCP scenarios. Projections of precipitation from EURO-CORDEX show a less clear difference between RCP4.5 and RCP8.5 than are apparent for temperature changes (Jacob et al., 2014). It was found that the high resolution RCM simulations show higher daily precipitation intensities compared to the coarser GCM simulations. Also, the projected change in daily precipitation intensity differs from GCMs, which results in a smoother shift from weaker to moderate and higher intensities i.e. GCMs simulate more frequent weaker rainfall events and less frequent high intensity events, whereas RCMs simulate a lower frequency of weaker events but a higher frequency of stronger events relative to GCMs. One current deficiency in the EURO-CORDEX ensemble is that the very wet GCMs from CMIP5 are currently not yet downscaled, although the temperature spread is well covered (Figures 22 and 23).

A comprehensive review of RCM projection studies focusing on hydrology for Europe by Madsen et al. (2014) was prepared as part of COST Action ESO901 (European Procedures for Flood Frequency Estimation) and gives a comprehensive overview of a large number of national and European studies. Most of the studies considered use SRES emissions scenarios. A majority of the studies reviewed find projected increases in extreme precipitation, consistent with the observed trends. 30% increases by 2100 were found in Brussels (Willems and Vrac, 2011; Willems et al., 2012), 30-50% increases in the 50 and 100-year daily precipitation in the Czech Republic (Kysely and Beranová, 2009; Kysely et al., 2011; Hanel et al., 2011), and small increases in maximum daily precipitation in Cyprus by 2050 (Hadjinicolaou et al., 2011). Studies for Denmark found projected increases in daily extremes (Sunyer et al., 2012), and a national study found increases in 1-24 hour intensities of 10-50% over the next 100 years (Anrbjerg-Nielsen, 2012). Short duration precipitation extremes are also found to increase at locations in Sweden (Olsson et al., 2009; Olsson et al., 2012).

Kendon et al. (2014) have performed the first climate change experiments at 1.5km grid spacing, using a model more typically used for weather forecasts with explicit convection. The simulations were focused on the UK and show that the model is able to simulate realistic hourly rainfall, with better representation of the duration and spatial extent compared with a coarser resolution 12km version of the same RCM using parameterized convection (Kendon et al., 2012). Increases in hourly rainfall intensity in winter were found, and also intensification of short duration rainfall during summer.

Figure 22: Jacob et al., 2014, projected seasonal changes of heavy precipitation (%) based on the RCP4.5 scenario for 2071–2100 compared to 1971–2000. Hatched areas indicate regions with robust and/or statistical significant change. Heavy precipitation is defined as the 95th percentile of daily precipitation (only days with precipitation 1 mm/day are considered).

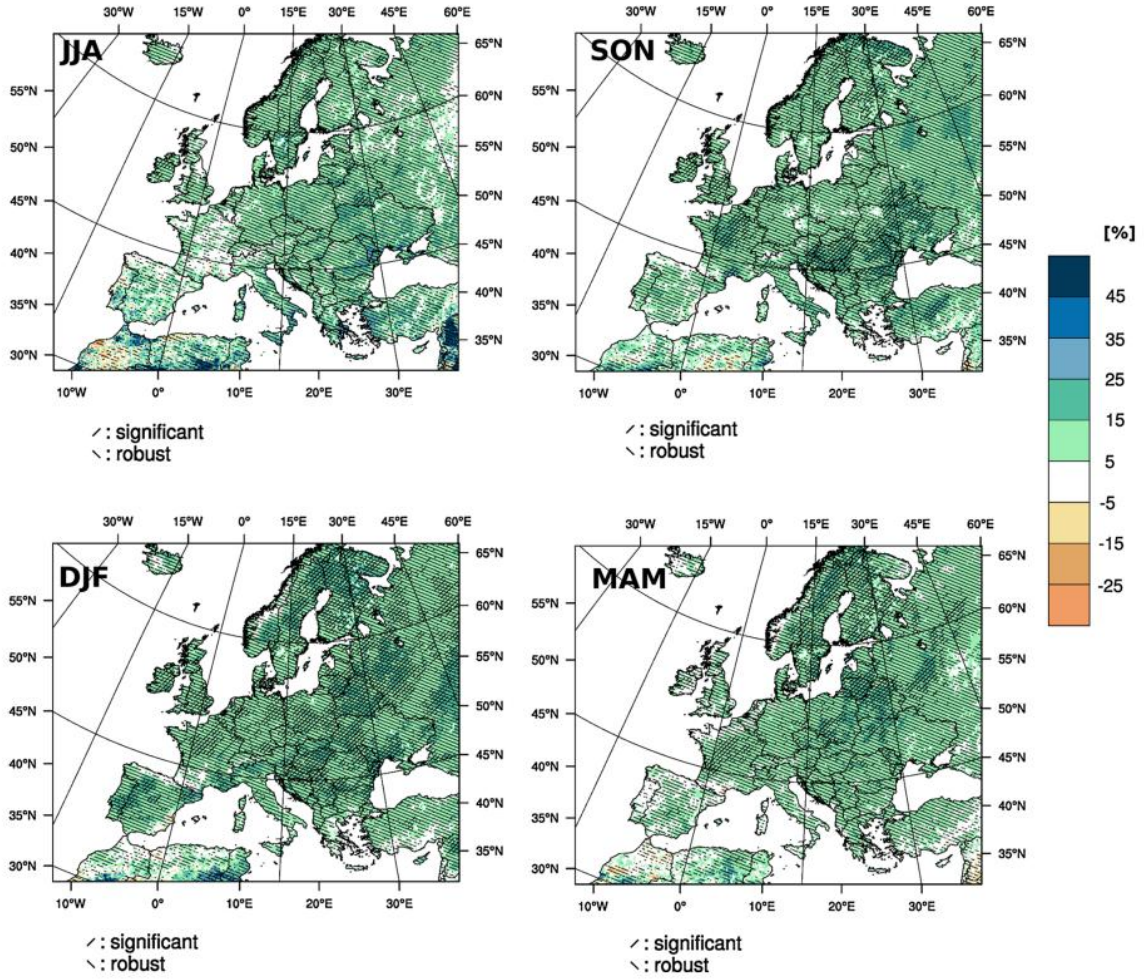

Related work by Chan et al. (2013) found that an increase in resolution improved the representation of orographic precipitation and this was evident over the mountains of Wales, where a 50km resolution simulation underestimated mean precipitation and event intensity was too weak. In contrast, over southeast England where extremes are largely convective during summer, increasing the resolution did not necessarily lead to an improvement at the daily timescale. Chan et al. (2014a) also showed that UK summer 1-hourly precipitation increases by around 10% across a range of return periods at 1.5km resolution whereas a 12km RCM showed decreases at shorter return periods of less than 5 years but strong increases above 20 year return period events. Using extreme value theory to investigate sub-daily extremes, Chan et al. (2014b) found that the 1.5km model was more successful at representing multi-hourly summer 'very extreme' events than the 12km model. Moving towards daily scales brings the 12km results more into agreement with the 1.5km results and the observations. Again, both the 1.5km and 12km simulations have comparable winter extremes, though generally weaker than summer at daily or shorter timescales. 'Gridpoint storms' were found to be one cause of unrealistic very extreme events at the 12km resolution.

Figure 23: Jacob et al., 2014, projected seasonal changes of heavy precipitation (%) based on the RCP8.5 scenario for 2071–2100 compared to 1971–2000. Hatched areas indicate regions with robust and/or statistical significant change. Heavy precipitation is defined as the 95th percentile of daily precipitation (only days with precipitation 1 mm/day are considered).

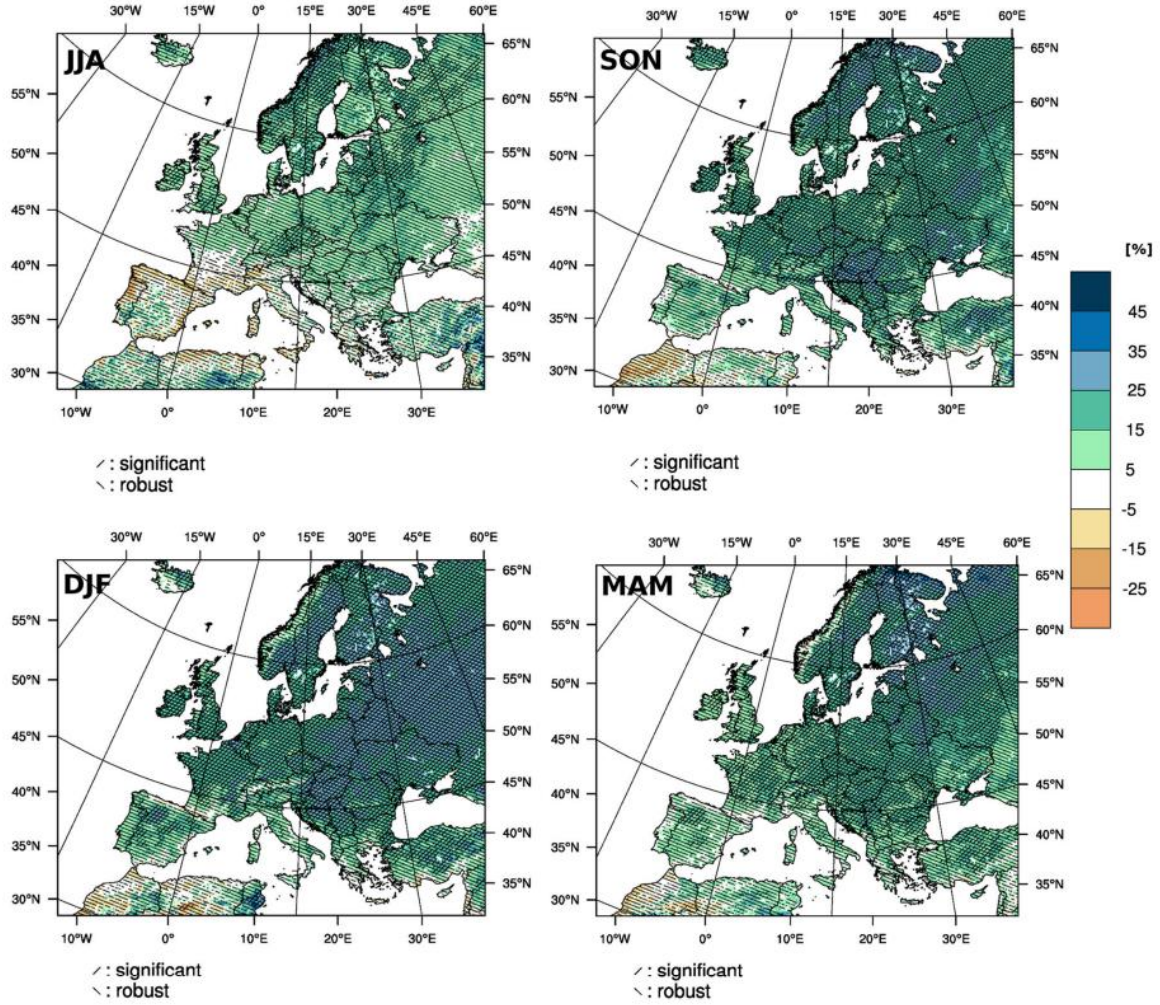

There is increasing evidence that atmospheric temperatures can lead to more extreme rainfall over short time scales (up to a few hours) (Westra et al., 2014). UK extreme summer hourly precipitation intensities have been found to be linked to temperature (Blenkinsop et al., 2015), hence a warming atmosphere is a potential mechanism for increased summer rainfall intensities. Chan et al. (in prep) show, for the southern UK, a shift towards a more anticyclonic regime, which produces more days with strong daytime heating, but within an environment unfavourable to convective storms. This suggests that future precipitation intensities cannot simply be extrapolated from present-day temperature scaling and demonstrate the pitfalls of using regional temperature alone as a scaling variable.

Other regional climate models have also been run at very high resolutions. Kücken et al. (2013) ran a 2.8km version of the COSMO model for central Europe for the year 2003 and found that the simulated drought and heat waves of summer 2003 showed good agreement with observations. Feldmann et al. (2013) used the COSMO-CLM RCM to assess near future (2011-2040) changes in mean and extreme precipitation in Central Europe, but forced with different GCMs (ECHAM5 and HadCM3). The horizontal resolution of the versions of the RCM used varies from about 18km to 7km. The projections showed an increase in extreme precipitation in both winter and summer, but in winter this was proportional to the increase in total precipitation, whereas in summer it was a result of a broadening of

the precipitation distribution. More recently Ban et al. (2015) have run a 2.2km resolution convection-resolving model across a region including the Alps from northern Italy to northern Germany under RCP8.5. They found a decrease in summer mean precipitation, but that extreme daily and hourly events increased consistently at 6-7% per degree of warming (i.e. the Clausius-Clapeyron scaling). In contrast with other studies, they did not find a more rapid increase in the intensity of extreme events which might suggest that a simple scaling relationship could be used as a tool for climate change adaptation for heavy precipitation, despite, in this case, the presence of complex topography.

These studies indicate that the benefit of higher spatial resolution in climate models is more apparent when precipitation is being considered, and particularly for more extreme metrics and more localised events. As discussed for the very high resolution simulations of Kendon et al. (2015) and Chan et al. (2014), there may be benefits associated with a move to a convection-resolving model, though even in this case the benefits are not clear for all metrics. Vautard et al. (2013) note that 'although local-scale feedbacks should be better represented at high resolution, combinations of parameterizations have to be improved or adapted accordingly'. One view is that high resolution simulations may be most valuable over regions where orographic rainfall is particularly influential (e.g. the Alpine ridge), and may add less value to projections over flatter regions (e.g. northern Germany) (Prein et al., 2015, submitted). However, convection-permitting simulations have been found to be valuable in convective regimes and seasons where orography is less influential (Kendon et al., 2014). The number of very high resolution climate model simulations available featuring explicit convection is currently limited, and therefore it remains difficult to draw broad conclusions about how sub daily rainfall might change in the future. However, this is expected to improve as more of these studies become available (Westra et al., 2014).

The contrast in precipitation between wet and dry regions and between wet and dry seasons is forecast to increase, with regional exceptions. These changes in precipitation will have different effects in southern and northern Europe, generally increasing in the North, particularly in winter, and decreasing in the South with a higher risk of longer dry spells, and an increase in arid and semi-arid areas. Greater inter-annual and seasonal variability is expected, winter & spring getting wetter, while summer and autumn will be drier.

A majority of recent studies using RCMs produce consistent trends towards more extreme rainfall events over many parts of Europe, consistent with trends in observations. A key research gap that is beginning to be more widely addressed is the introduction and evaluation of high spatial resolution convection resolving models which should have a significant impact on the simulated representation of high frequency extreme rainfall events.

3.3 Hail

Key Messages

- There are few ground based hail observation networks, with satellite cloud temperature data and numerical models used to identify hail producing convective or frontal instability.
- Most extreme hail events occur in the summer over Central Europe where convective energy is greatest.
- Hail occurs most frequently in mountainous areas, especially the Alps, due to moisture convergence and upward forcing, but is less frequent over the central Alps due to reduced uplift. Satellite data show a higher incidence of hail in elevated regions, for example Northern Italy and Southern Germany.
- Intense hail events are associated with increases in Convective Available Potential Energy (CAPE) observed over the 30 year period 1978-2009 in Europe, attributed to increased temperatures, evaporation and low level moisture. A north-to-south gradient (and weaker east-to-west gradient) of increasing CAPE has been identified in central Europe. The atmosphere has become more unstable over the last two to three decades over Central Europe, consistent with the observed increase in CAPE.
- Hailstorm projection studies, although limited to France, Northern Italy and Germany, show increases in the convective conditions that lead to hail and in some areas an increase in damage days. The studies are not always consistent and demonstrate changes which are not very large and lack statistical significance.

This section explores the intensity and frequency of hail storms, methods of classification, mechanisms of hail formation, and the compilation of a catalogue of European hail events. It reviews research on the occurrence of extreme hail in different geographic and meteorological contexts (e.g. mountain areas and low moisture levels) and work associating extreme hail with atmospheric convection. It also examines observational studies based on hail sensors, satellite data and ground based reports of hailstone size which are collected by the European Severe Weather Database initiative. The section also reviews research on modelling hail.

Hail can be responsible for significant damage to buildings, crops, automobiles and infrastructure. Hailstorms are most common in mid-latitudes where surface temperatures and moisture contents of the air are high enough to promote the instability associated with strong thunderstorms, but the upper atmosphere is cool enough to support ice formation processes. Hail with diameter 10 cm or larger occurs most frequently during the summer months, in several European regions, with increased hailstorm frequency often found downstream of hills and mountains.

Significant hail events in Europe have been recorded in southern Germany in July 1984, June 2006, July 2013; south-west France in 2013 (Berthet et al. 2013); Spain in 2013 (Merino et al. 2013), and Sofia (Bulgaria) in 2013 (Papagianuki 2013) and 2014. These events were caused by summer supercell thunderstorms and caused significant economic damage. Two supercells moving over central and southern Germany on 27 and 28 July 2013 caused economic losses of €2.8 billion, which represent the highest insured loss by natural hazard in Germany so far, with extensive damage to cars, solar panels, greenhouses and other infrastructure, (Greiser et al., 2015)[30] and (Punge presentation, Expert Workshop, 2015).

[30] http://www.oeschger.unibe.ch/events/conferences/ekas/index.php?id=view&absid=79

3.3.1 Observations and data – hail

Datasets

Hail forms within deep convective clouds with observations recorded only by ground-based hail pad networks. Proxies for hail events can be also derived from satellite temperature imagery and radar reflectivity. These are supplemented with eye witness and media reports which are collected by organisations such as the Tornado and Storm Research organisation (TORRO), the European Severe Storm Laboratory (ESSL) which maintains the European Severe Weather Database (ESWD), and Schweizer Hagel (an agricultural cooperative). These databases provide information about the spatial distribution and the frequency of severe convection. However, observational databases are limited in spatial or temporal extent and biased towards population centres where there are more observers.

Hail is commonly classified according to diameter of the hailstones; the ESWD, for example, only reports hail >=2cm diameter. Another hail classification scheme is the TORRO Hailstorm intensity scale (Webb 1986) which classifies hail on a scale from H0, being hard hail with diameter 5 mm causing nil damage to H10, being super hailstorms with diameter >100 mm and causing extensive structural damage with risk of severe or fatal injuries to people (Table 4).

Table 4: TORRO hail classification scale[31]

Intensity Class	Intensity Category	Typical Hail Diameter (mm)*	Probable Kinetic Energy, J-m2	Typical Damage Impacts
H0	Hard Hail	5	0-20	No damage
H1	Potentially Damaging	5-15	>20	Slight general damage to plants, crops
H2	Significant	10-20	>100	Significant damage to fruit, crops, vegetation
H3	Severe	20-30	>300	Severe damage to fruit and crops, damage to glass and plastic structures, paint and wood scored
H4	Severe	25-40	>500	Widespread glass damage, vehicle bodywork damage
H5	Destructive	30-50	>800	Wholesale destruction of glass, damage to tiled roofs, significant risk of injuries
H6	Destructive	40-60		Bodywork of grounded aircraft dented, brick walls pitted
H7	Destructive	50-75		Severe roof damage, risk of serious injuries
H8	Destructive	60-90		(Severest recorded in the British Isles) Severe damage to aircraft bodywork
H9	Super Hailstorms	75-100		Extensive structural damage. Risk of severe or even fatal injuries to persons caught in the open
H10	Super Hailstorms	>100		Extensive structural damage. Risk of severe or even fatal injuries to persons caught in the open

Other classifications use statistical techniques to identify hail producing synoptic conditions. In one such classification Aran et al. (2011) demonstrated the dominance of synoptic features in generating

[31] http://www.torro.org.uk/hscale.php

extreme hail events on the Iberian Lleida plain, while Kapsch et al. (2012) related large-scale weather patterns to damaging hail events for Germany.

European hail frequency research has been carried out in various countries using data from weather stations, hail pads or radar. Regional to National level climatological studies exist for Germany (Kunz and Kugel, 2015), Finland (Tuovinen et al., 2009), UK (Sanderson et al., 2015,), the Netherlands (Groenemeijer and Delden, 2007), south-eastern Romania (Paraschivescu et al., 2011), Bulgaria (Simeonov, 1996), Greece (Sioutas et al., 2009, Papagiannaki at al., 2013), Cyprus (Nicolaides at al., 2009), and the Crimea & North Caucasus (Zharashuev, 2012).

For the assessment of hail probability across Europe, satellite data is a key data source because of the continuous availability over a large region. Infrared sensors are used to detect overshooting tops (OT) of deep convective clouds which penetrate through the warmer tropopause into the stratosphere. A difference in cloud top temperature of 6 K identifies overshooting tops (OT) which are an important indicator of severe weather, thus hail.

Figure 24 shows a close correlation between the overshooting tops based climatology and model derived hail day density (Punge, 2015), showing the increased likelihood of hail in elevated regions of northern Italy and southern Germany. It also demonstrates the usefulness of this satellite based remote sensing technology for idenitfying hail risk.

Research predicts an increase in the frequency and magnitude of severe hail events in future. The case study (section 5.3) demonstates the benefits of PHI and OT to improve the identification and quantification of extreme hail events, enabling measures to be taken to mitigate their impact and reduce costs associated with hail damage.

Punge at al. (2014) developed a catalogue of hail events in Europe based on nearly 40,000 OT signatures derived from European MSG (SEVIRI) satellite data and hail reports from the European Severe Weather Database (ESWD). The results show high variability in the density of events with the highest density occurring over northern Italy, the Pyrenees, the Appenines, northern Switzerland, southern Germany, the Dinaric Alps, Transylvania and the Massif Central. Regional maxima were observed in northern Turkey, northern England, eastern Scotland and north-west Norway, while lower densities occurred over northern and north western parts of Europe. The distribution, which is mapped in Figure 25, shows good agreement with the seasonal distribution of ESWD hail reports.

Figure 24: Comparison between (a) OT-based climatology (occurences per year and 100 km² and (b) Hail day density (Hand and Cappelutti, 2011).

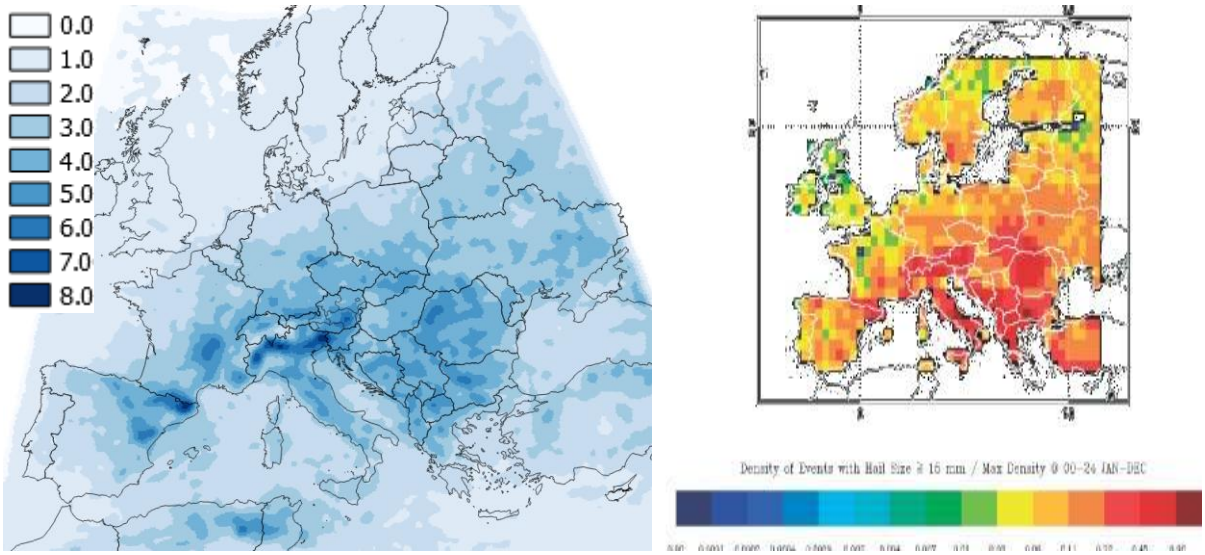

Figure 25: Spatial distribution of OT observations detected in MSG-SEVIRI IRW-channel temperatures for the period 2004–2011 (>0.69 cm on a 0.1° grid) Punge at al., 2014.

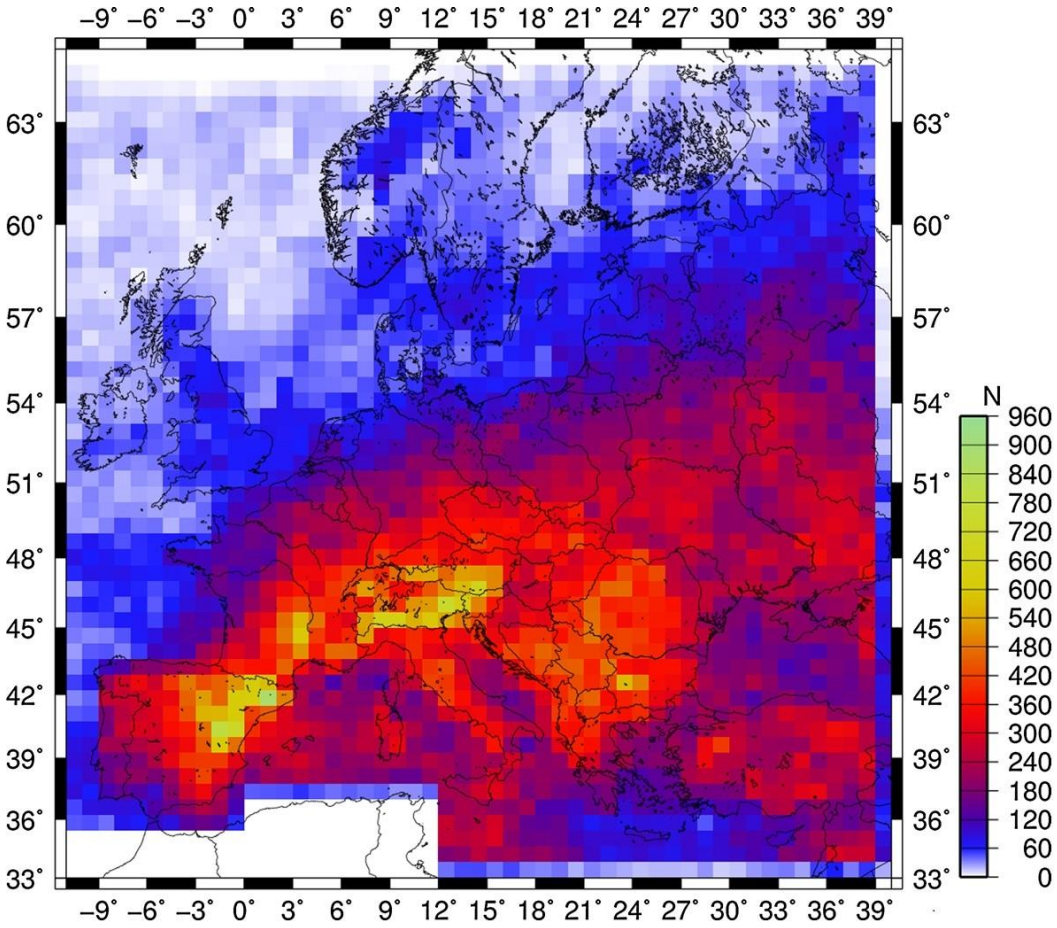

Hail occurrences are also closely related to specific lightning signals (Changon 1992) with lightning detection data available from different sources (EUCLID or LINET). Radar data is another important proxy for hail events with a very high temporal and spatial resolution. Radar reflectivity is available since the mid 2000s or even earlier in many European countries. Several studies demonstrated the capability of radar reflectivity to identify hail signals using two and three dimensional reflectivity or combined with other information from radio soundings or satellite (see, for example, Holleman et al., 2000 or Kunz and Kugel, 2015 for a review). It has the advantage of producing a 3D profile through a hail storm and 2D representation of hail intensity. For example KNMI (Royal Netherlands Meteorological Institute) and RMI (Royal Meteorological Institute of Belgium) derive the probability of hail from the height of the freezing level and the 45-dBZ radar echo top height (method of Waldvogel et al., 1979; DeLobbe and Holleman, 2006). Puskeiler (2013) used the same technique for Germany (Figure 26), but in combination with lightning and insurance loss data for mapping potential hail days. Recent developments in polarimetric methods provide better quality hail detection, measurement and location above ground (Ryzhkov 2010, Heinselman and Ryzhkov 2006); however, records are currently limited for these radars in Europe, radar coverage is limited to major population centres in some regions, and they are subject to technical limitations in mountainous terrain.

Figure 26: Number of days (2005-2011), on which the hail-criterion (vertical extension between 0°C and a specific radar reflectivity >3.5 km) was reached over Germany (Puskeiler, 2013).

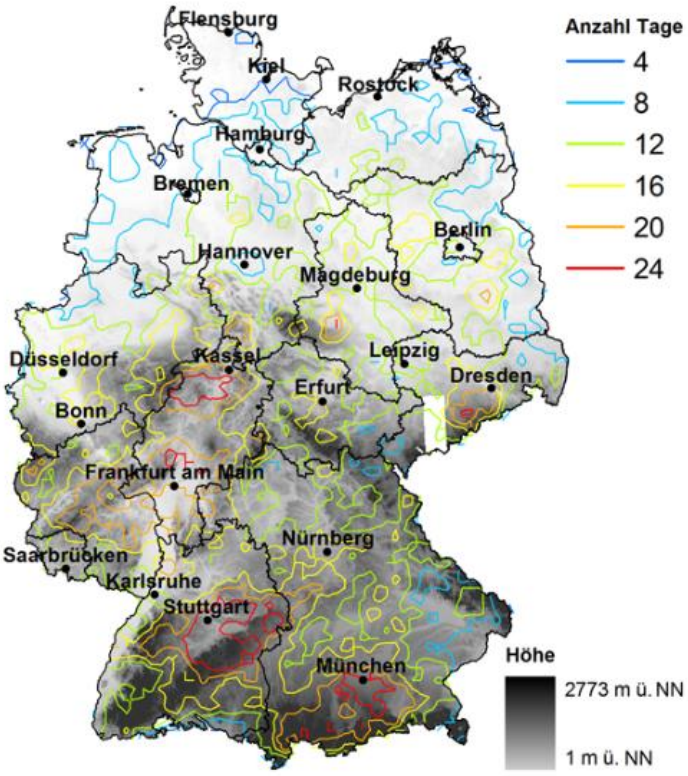

Reanalysis was used to develop a global hail climatology using the UK Met Office's convective diagnosis procedure (CDP) (Hand and Capellutti, 2011). This quantified general thunderstorm and hail day frequency using NWP data to demonstrate the high frequency of hail days in areas of high orography. The CDP models the mean potential temperature and humidity mixing ratio to simulate the

adiabatic lifting and the convective condensation level. The map (Figure 27) shows the increased density of hail days over mountain regions, albeit at relatively low global model resolution. The method was found to overestimate hail occurrence to some degree by underestimating the dampening effect of maritime climate on the formation of strong convection (Punge et al., 2014).

Figure 27: Annual density of hail days (hail >=15mm) over Europe from the CDP. The expected annual number of hail days in each 1° × 1° square can be obtained by multiplying the density by 22. (Hand & Capelutti, 2011)

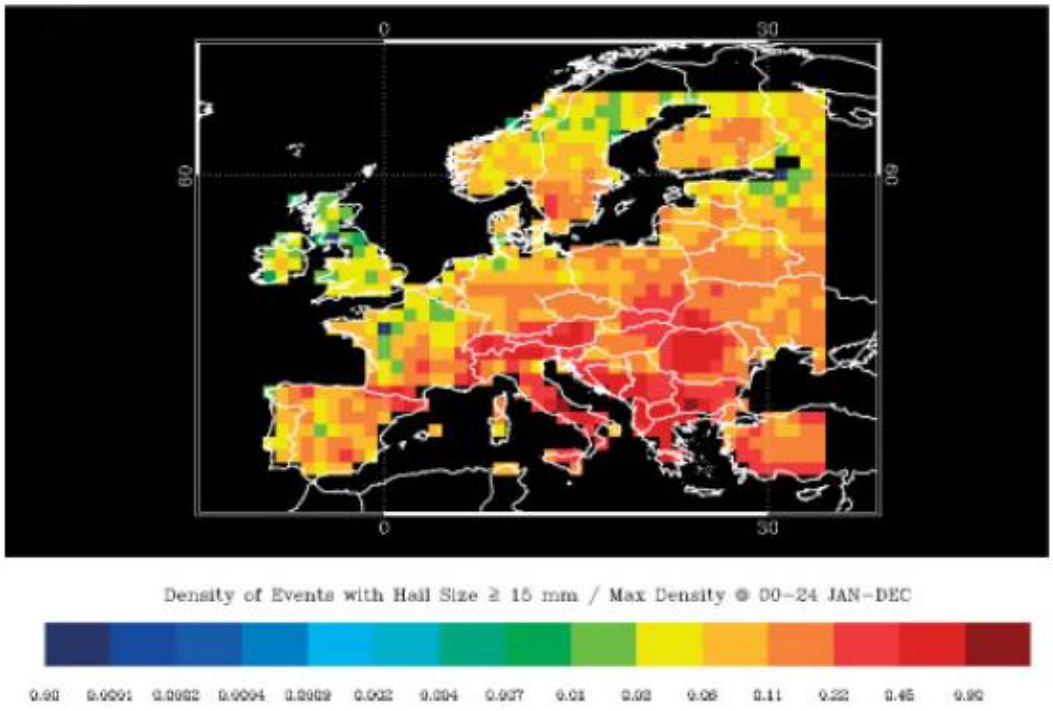

Another method was applied by Mohr (2013), who combined different meteorological parameters relevant for hailstorm formation using a logistic (multivariate regression) model. Applied to different reanalysis data sets, the logistic model estimates the number of days with an increased potential of hail occurrence, denoted to as potential hail index (PHI; Figures 27 and 28). The results confirm a positive trend for the period 1971–2000 (Mohr et al., 2015a).

Data sets of hail damages produced by models, e.g. *HailCalc*[32], are widely used to assess impacts from past hail events in Europe. The *HailCalc* hail hazard model is based on Europe-wide hail hazard event data set of radar derived hail kinetic energy which can be directly related to the intensity and extent of hail damage. The dataset includes nearly 2,000 historical hailstorms which are combined with additional climatological and meteorological data to generate an event set of approximately 15,000 events on a 3 km grid. The database also includes vulnerability functions developed in partnership with re-insurance companies. The recent *Willis* European Hail Model is based on OT data provided by Punge et al. (2014), but used in the current version additional filtering of meteorological data sets using ERA Interim reanalysis.

[32] Originally developed by ETH Zurich & Swiss Re, Hailcalc Europe and acquired by RMS (www.rms.com)

The occurrence of hail is related to atmospheric instability so its likelihood is related indices such as the convective instability index (CI) and the Showalter index which is used to predict storms in Europe (Showalter, 1953, quoted in Merino at al. 2014). These indices are usually considered in combination with mesoscale factors such as wind flow, specific humidity and water vapour flux.

3.3.2 Observed trends and variability - hail

The occurrence of hail over Europe is not uniform as most hail events occur in the summer over Central Europe where convective energy is greatest. Trends in hail observations are sometimes made by using damage as a proxy (e.g., Kunz et al., 2009), although damage is also a function of hail type (size, density, accompanying horizontal wind speed and kinetic energy) and vulnerability of the impacted area to damage.

A study of convective parameters for the 30 year period 1978-2009 in Germany and Europe identified increasing Convective Available Potential Energy (CAPE) attributed to increased moisture at low levels, in turn due to rising temperatures and increased evaporation (Mohr and Kunz, 2013). A north-to-south gradient (and weaker east-to-west gradient) of increasing CAPE in Germany and Europe was identified. The results agreed well with OT detections and lightning detection data. It was demonstrated that the atmosphere has become more unstable over the last two to three decades over Central Europe, consistent with the observed increase in higher convective potential.

Results of the Logistic Hail Model from Mohr (2013) to produce the hail climatology for the period 1951-2000, however, do not reveal significant trends over the past, mainly due to the high annual variability of the potential hail days (Mohr et al., 2015). Figure 28 (a) shows concentrations in the mean potential hail index mainly north and south of the Alpine regions and in the Iberian Peninsula over the period. Figure 28 (b) shows increasing hail trends in southern France and Spain based on the logistic hail model, and decreases mainly over eastern Europe. Figure 29 shows the potential hail index from 1951 to 2010 at five European locations. Of the five cities considered, Milan in Italy is most hail prone, being affected on average 40 days per year, and Lleida in Spain is least prone, affected on average 12 days per year.

Berthet et al. (2011) found no changes in the number of hail events, but identified an increase in hail size related to increasing temperatures for hail-prone Pyrenean and Mediterranean regions of France based on hail pad measurements over a 22-year period (1989-2009).

Figure 28: (a) Mean Hail Index 1951-2000 from downscaled reanalysis NCEP=NCAR (JJA) and (b) Modified Logistic Hail Model (Mohr et al., 2015a)

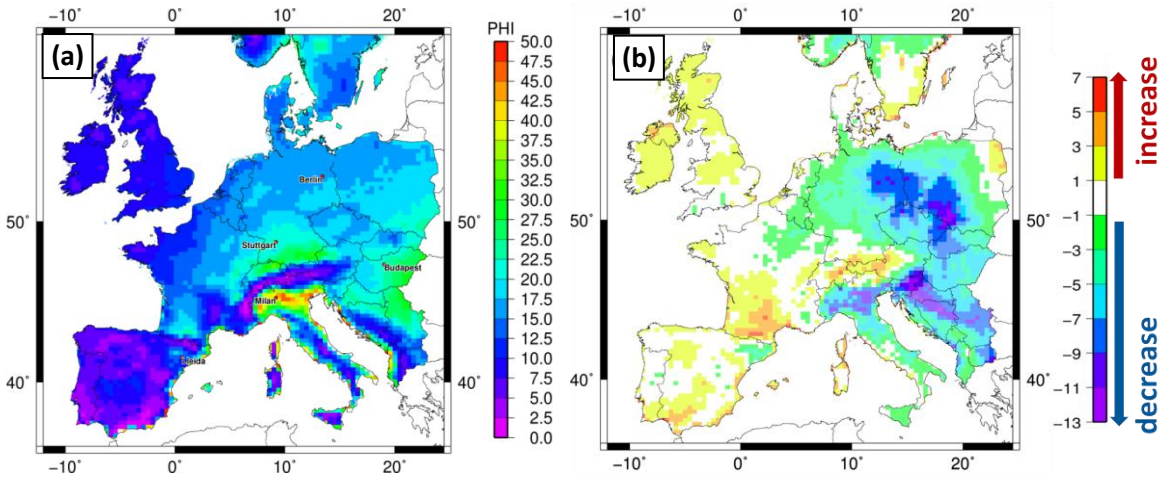

Figure 29: Potential Hail Index 1955-2010 in days per year (Mohr et al., 2015b)

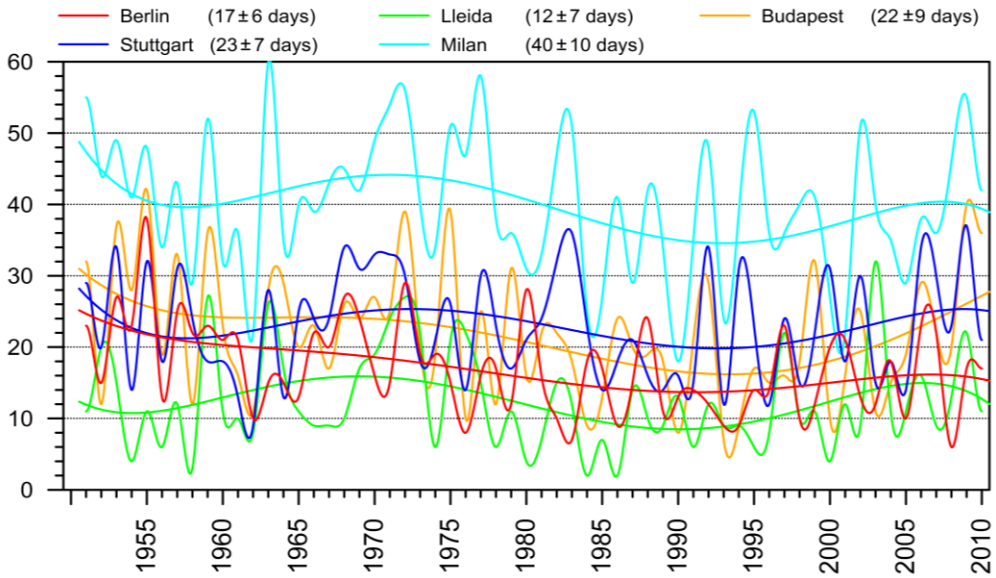

Baldi et al. (2014) studied hailstorm intensity in Italy by using observational data sets and a statistic model. They identified areas of greatest intensity in the NW Alpine region, generally leeward of the Alps, and in an area in the South West. The results of the statistical approach estimated maximum hail occurrences in north-west Italy and south Tuscany with values ranging between 1.5 and 2 annual events, but less probability for the hot spots in the northern parts. According to this approach, the southern region is more prone to intense events (H2 intensity, table 4). However, the analysis was limited in scope by the lack of a national hail monitoring network (Figure 30).

Figure 30: Distribution of hail events: a) decadal distribution at municipality scale; b) yearly distribution at provincial scale (Baldi et al., 2014).

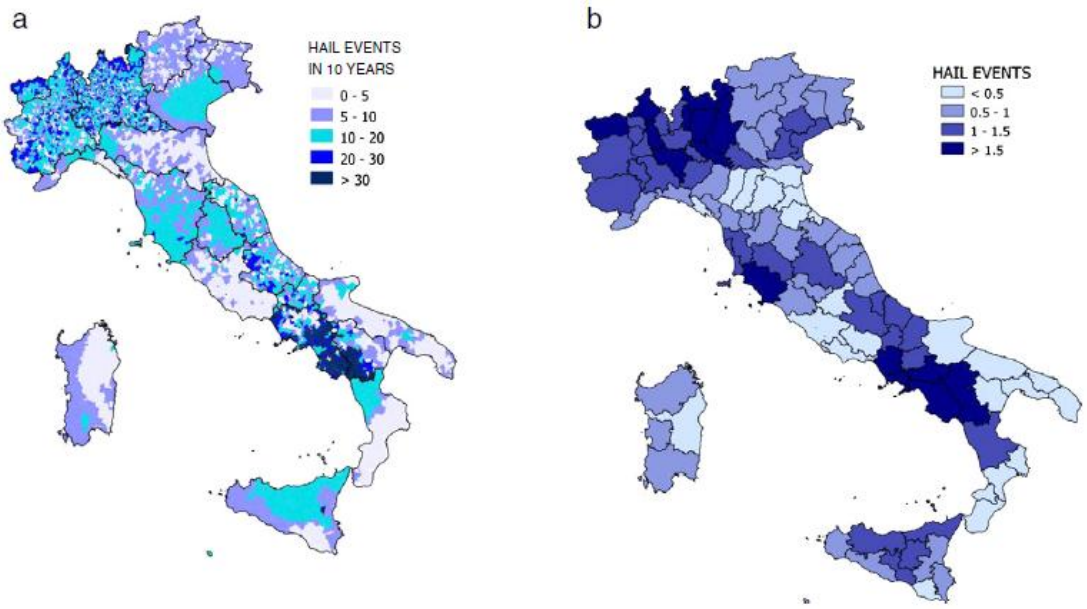

Caution is recommended in using the observational record as evidence of climate change in terms of severe thunderstorms due to the large interannual variability in thunderstorm favouring conditions and occurrences of severe events.

3.3.3 Projections

Much of the published work relevant to future hail projections is based upon developing the relationships between large-scale atmospheric environments and small scale severe weather events, such as severe thunderstorms, though some work has explicitly considered hail storms. While there have been several publications on expected changes in severe convective storms for the United States (US), only a few studies are available European countries.

Brooks (2013) considered the possible impacts of climate change on severe thunderstorms, which are more likely to form in environments with large values of CAPE along with high wind shear. Climate model simulations for the US point towards increases in CAPE and decreases in wind shear in the future.

A majority of previous work on convective modelling has been focused on the United States, but studies have found differences in the qualitative relationship between CAPE and wind shear over the US and Europe (Brooks, 2009; Grunwald and Brooks, 2011). For Europe it has been shown that GCMs can produce reasonable spatial patterns of severe thunderstorms, though with less certainty over the reproduction of the magnitude of events (Marsh et al., 2007; 2009).

Data from an ensemble of different RCMs were used to estimate changes in large-scale weather patterns that were identify to be related to severe hailstorms in Germany (Kapsch et al. 2012). Using a Bayesian model, the study project an increase in hailstorm frequency in Germany, for example between 7 and 15% for the period 2031-2045 compared to 1971-2000. Mohr et al. (2015a), by applying the logistic hail model to an ensemble of seven high-resolution (7 km) RCM realizations, found an increase in the potential for hail events in the future (2021–2050) compared to the past (1971–2000). Changes, however, were statistically significant in the northwest and south of Germany only (Figure 31).

RCM data at 25 km for the UK have been used to drive a simple model of hailstone formation to project changes in hailstorms numbers and hailstone sizes during the 21st century (Sanderson et al., 2015). Model validation showed reasonable agreement with observations, and climate change projections based on the SRES A1B scenario show a downward trend in damaging hailstorms (with hailstones of greater than 15mm diameter). Statistically significant downward trends were found for hailstones with diameters between 21 and 50 mm, and melting made little difference to the projected changes. The results are subject to large uncertainties, in part due to the convective parameterisations used in the model, and by considering only one model run and not an ensemble.

To conclude, the limited number of studies that have investigated projections of hailstorms appear to be inconsistent and demonstrate changes which are not very large and often lacking statistical significance. Therefore, future projections of hailstorms feature a high level of uncertainty. Furthermore, several scientific questions are still unanswered, for example, how the weather systems will change in the future, the conditions for the most severe hailstorms, and the relationship between changes in the meteorological parameters and cloud microphysics, or to changes in aerosol distributions.

Figure 31: Overview of changes in the Probability Hail Index (PHI) for Germany: Increased hail risk based on a model mini-ensemble for 7 regional climate simulations (a) number of runs showing an increase and (b) changes when at least five of the seven runs show a significant increase according to the Wilcoxon rank-sum test. between 2021–2050 and 1971–2000 represented by an ensemble of seven climate simulations.

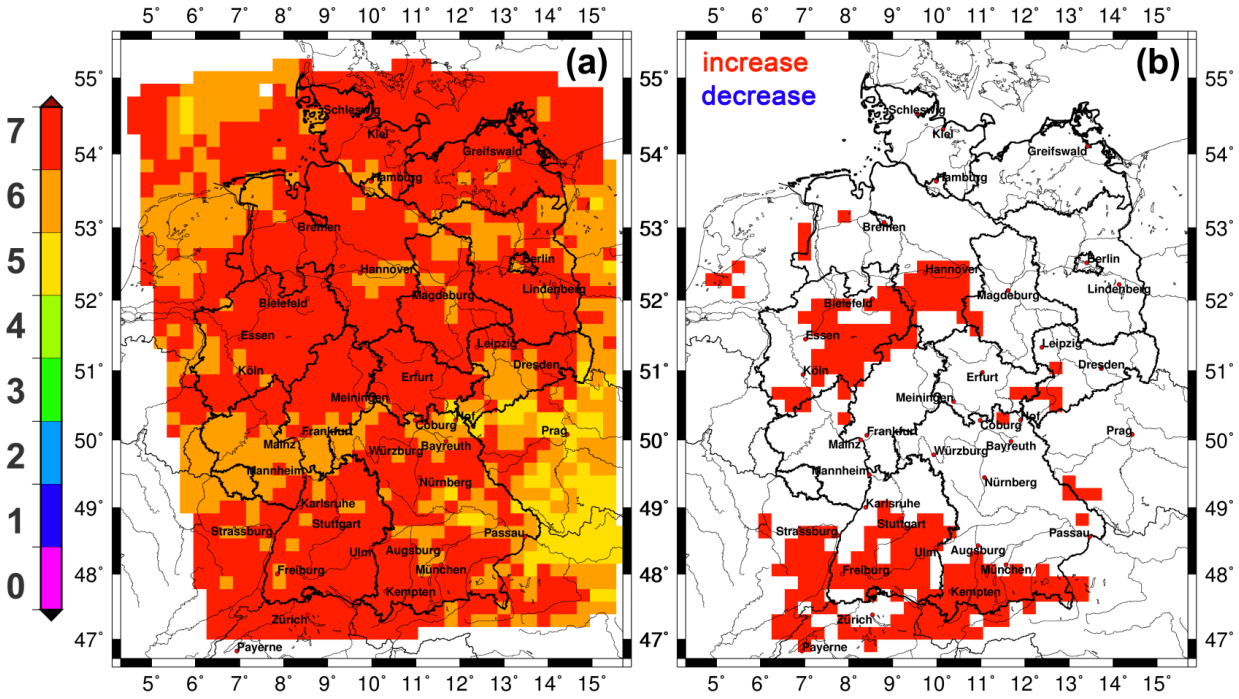

3.4 Drought

Key Messages

- Drought can have a significant impact by reducing the availability of surface and groundwater resources. Drought is a cumulative event and recent severe droughts include Italy (1997-2002), the Baltic countries 2005-2009, the European heatwave of summer 2003, and the widespread European drought of 2011.
- The 1950s were prone to long, intense, Europe-wide meteorological and hydrological droughts. In Northern and Eastern Europe the highest drought frequency and severity was from the early 1950s to the mid-1970s. Southern and western Europe (in particular the Mediterranean) show the highest drought frequency and severity from 1990. There has been a small but continuous increase of the European areas prone to drought from the 1980s to the early 2010s.
- Both the Palmer and Thornthwaite drought severity indices show little evidence of more severe global drought over the last 60 years. The use of combined indices e.g. combined SPI, SPEI and RDI can improve on single indicators to identify extreme droughts.
- Drought studies have identified drought hotspots in the Mediterranean and southern Europe, the Carpathians and the Balkans.
- Drought frequency increased slightly during the decade 2001–2010, during which four significant drought events occurred.
- Regional climate models for Europe project a decrease in summer precipitation until 2100 of 17% on average, and by 30% in June for the period of 2071-2100. Dry periods are expected to occur 3 times more often at the end of the current century and to last longer by 1 to 3 days compared to the period of 1971-2000. Future inclusion of evapotranspiration in Earth system models will affect these projections.
- There is significant uncertainty associated with future projections of drought, climate variability being the dominant source of uncertainty in both observed and projected soil moisture drought.

Droughts have a significant impact on agriculture, causing reduced yields and economic losses. Droughts also affect water resources reducing the availability of surface and groundwater resources. The European drought of 2011 for example affected several European countries including Germany, the Netherlands, Slovakia and the Czech Republic. River levels were below average in large parts of central and eastern Europe, affecting navigability for example on the Rivers Rhine and Danube. Low reservoir levels affected electricity production in Serbia, Bosnia and Herzegovina experienced drinking water shortages, and winter crop production was reduced in Romania, Bulgaria, Hungary and the Ukraine, where winter grain yields were estimated to be 30 percent below average. Unusually dry conditions also triggered forest fires in several countries including Germany (Upper Bavaria), the Ukraine, Moldova and Slovakia (see case study Section 5.2).

Drought is a cumulative event, often difficult to define and involving wide-reaching consequences for agriculture, ecosystems, water availability, and society. Understanding how the occurrence of drought may change in the future and which sources of uncertainty are dominant can inform appropriate decisions to guide drought impacts assessments.

This section explores meteorological, soil moisture (agricultural) and hydrological droughts. Drought is defined as “a sustained and regionally extensive occurrence of below average natural water availability,

and can thus be characterized as a deviation from normal conditions of variables such as precipitation, soil moisture, groundwater and streamflow" (Tallaksen and Van Lanen, 2004) or by the IPCC's 4th Assessment Report as a 'prolonged absence or marked deficiency of precipitation that results in water shortage for some activity or for some group', or a 'period of abnormally dry weather sufficiently prolonged for the lack of precipitation to cause a serious hydrological imbalance'. Fuller definitions of drought include the duration, intensity and spatial impacts on water storage, supply and demand which can only be neglected for purely meteorological drought (Lloyd-Hughes, 2012, 2013).

A persistent drought propagates from meteorological to soil moisture (agricultural) drought affecting plant and crop growth, or into a hydrological drought affecting watercourses, water resources (groundwater and surface water) and natural ecosystems (Figure 32). Drought is therefore often defined in terms of its impacts on agriculture and water availability. For example, the 2005 drought event in Spain led to a 49% loss of cereal production and estimated losses for non-irrigated crop and pasture of €2,500 million (Sepulchre-Canto et al, 2012). Persistent droughts can have significant social and economic impacts in terms of water resources shortages for drinking water and plant growth. Significant droughts have occurred in 2010, 2011 and 2015 (Appendix 2). The drought of 2011 is featured as a case study in Section 5.

Figure 32: Drought drivers: As well as temperature, several factors affect the development of droughts. These should all be taken into account for assessing historical drought trends and the contribution of anthropogenic climate change to recent drought events. Red arrows indicate factors that contribute to drought, and blue arrows show factors that counteract it. (Seneviratne, 2012)

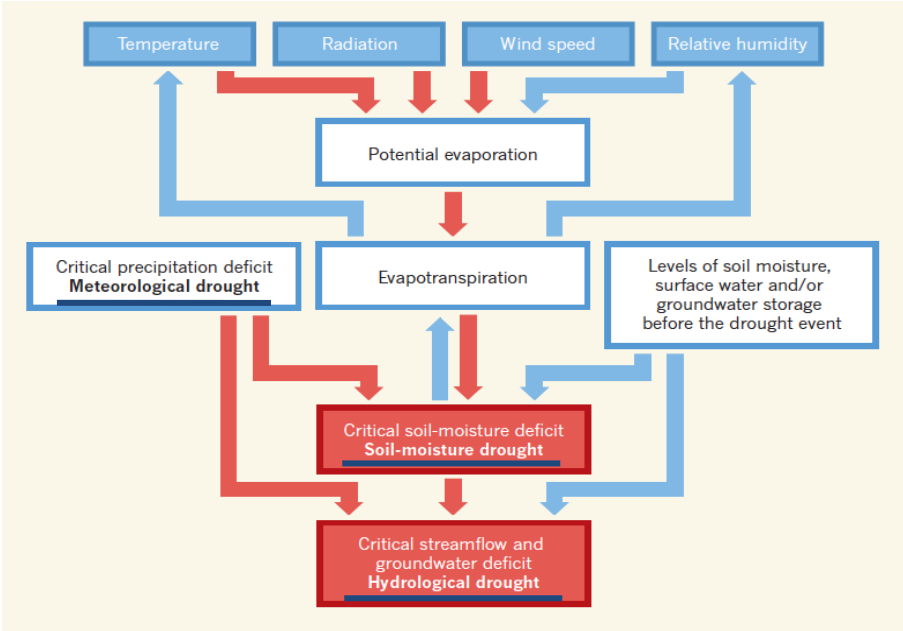

Recently, the EU-FP7 DROUGHT-R&SPI (Rainfall & Standardised Precipitation Index) provided a wider view of drought impacts, vulnerability and risks at the pan-European scale (e.g. Blauhut et al., 2015; De Stefano et al., 2015). Maps for Europe showing likelihood of drought impact occurrence are given for agriculture, energy production, public water supply and water quality, as well as maps for several vulnerability factors. The European climatology of the three main types of drought are explored in the sections below (3.4.1 to 3.4.3).

Current drought information is available from the European Drought Observatory (EDO) shown in Figure 33 for the droughts of, and regional centres such as DMCSEE for south-eastern Europe. Global drought monitoring systems include the SPEI Global Drought Monitor and the Global Integrated Drought Monitoring and Prediction System.

Figure 33(a) Current drought situation June 2015 and (b) first 10-days of June 2011 (EDO).

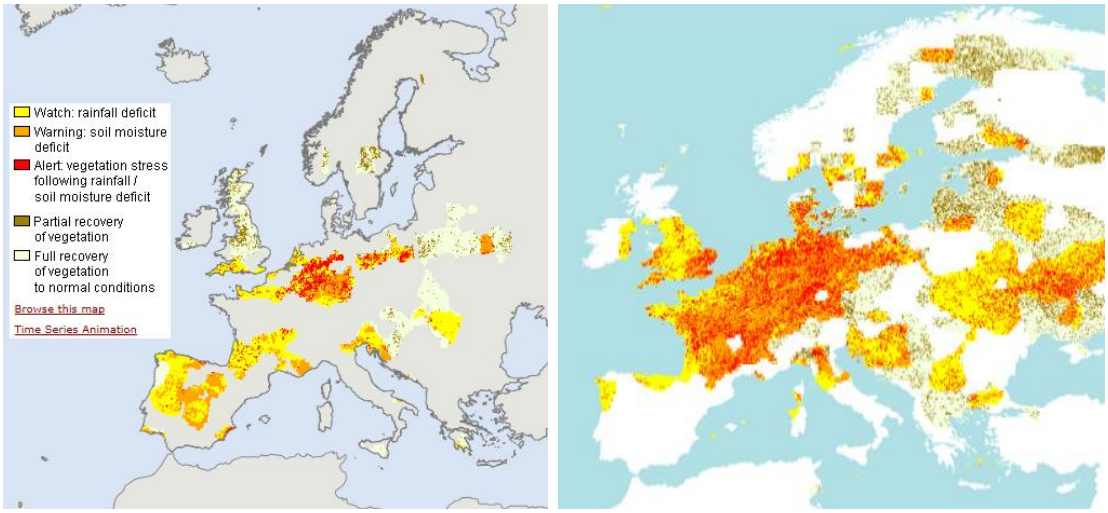

(a) (b)

Historical drought information is available from the European Drought Centre which hosts the European Drought Reference (EDR) and currently classifies 11 major drought events based on SPI from daily to 6-monthly timescales (Stagge 2013), and the European Drought Impact Report Inventory (EDII), both compiled as part of the EU-FP7 funded DROUGHT R&SPI Project. The EDII now contains close to 5000 impact reports from 33 countries. These reports stem from a variety of sources that reflect availability and reporting traditions across Europe. The impact reports span the period 1900 to date, but most entries relate to impacts that occurred since the 1970s with an increasing trend. The UK Drought Portal classifies droughts from 1961-2012 based on the standardized precipitation index (SPI) for periods of 1-24 months. The German Drought Monitor classifies soil drought on the standardized soil moisture index (SMI) based on data from 1953-2014. Other significant research projects include WATCH, DEWFORA, DROUGHT_CH, and DrIVER.

New European drought datasets are becoming available from EDO/JRC-IES)/ETH including SPI, the Standardized Precipitation Evapotranspiration index (SPEI) for the period 1950-2013 based on the E-OBS dataset (Haylock et al. 2008), a standardised runoff index (SRI) (Gudmundsson and Seneviratne, 2015), and a soil moisture product based on calibrated simple model for 1984-2013 (Orth and Seneviratne, 2015, submitted to ERL).

3.4.1 Meteorological Drought

3.4.1.1 Observations - meteorological drought

Meteorological drought is defined in terms of absolute rainfall or period of rainfall deficiency based on rainfall accumulation periods representing drought duration, from days or weeks for a meteorological drought, to months or seasons for a soil moisture or hydrological drought. Common drought indices include those based only on precipitation, for example SPI (Standardized Precipitation Index) and CDD (Consecutive Dry Days); those based on temperature, e.g. the warm spell duration index (WSDI); and those which include evapotranspiration like the SPEI and the Palmer Drought Severity Index (PDSI) (Gudmensson 2015, Seneviratne et al. 2012, Heim and Brewer, 2012), Table 5.

Table 5: List of Drought indices described in section 3.4

Drought Index	Ref	Notes
The Standardized Precipitation Index (SPI)	McKee et al. 1993	A probability index which uses a standardized scales showing negative for drought, and positive for wet conditions. Originally developed for US 1889-1991.
Standardised Precipitation Evapotranspiration Index (SPEI)	Vicente-Serrano et al. 2010	A multi-scalar drought index based on climatic data used for determining the onset, duration and magnitude of drought conditions in a variety of natural and managed systems. Originally developed for Iberia 1961-2011.
Consecutive Wet/Dry Days, Wet/Dry Spells Index CWD, CDD	ETCCDI see Appendix 4.2	A period of consecutive wet or dry days when precipitation is above or below a 1mm threshold (ETCCDI).
Palmer Drought Intensity Index (PDSI)	Sheffield et al. 2012, Palmer W. C., 1965	Precipitation and temperature analyzed in a water balance model; comparison of meteorological and hydrological drought across space and time. See also Palmer Hydrological Drought Index (PHDI).
Self-calibrating PDSI (scPDSI)	Antofie 2015, Van der Schrier 2014, Wells & Goddard 2004	Improves on PDSI by changing the (US based) standardization and measures the departure of soil moisture from the normal conditions, using a hydrological accounting system.
Reconnaissance Drought Indicator(RDI)	Spinoni 2015, Antofie 2015	The ratio of rainfall to PET.
Palfai Drought Index (PADI)	Antofie 2015, Palfai 1990	The ratio of the mean temperatures from April to August and the monthly precipitation from October to August.
Soil Water Index	Copernicus	METOP ASCAT satellite product Global, 0.1° and continents at various depths http://land.copernicus.eu/global/products/swi
Crop moisture index	Heim 2002, Bradford 2000, Palmer W C., 1968	Derived from the PDSI, the CMI estimates short-term crop moisture and drought for US crop-producing regions. https://www.drought.gov/drought/
Surface Water Supply Index (SWSI)	Heim 2002, Bradford, 2000, Shafer and Dezman, 1982.	Developed in the US (Colorado) to complement PDSI in managed catchments.

Standardised precipitation indices (SPI & SPEI) show a tendency to wetter conditions throughout the 20th century in Europe, while seasonal analyses show an increase in mean precipitation in winter, and decreases over much of Europe in summer (IPCC, 2014). The SPI is suitable for short timescales when it is closely related to soil moisture, to longer timescales when it can be related to groundwater and reservoir storage. In their drought analysis for Calabria in southern Italy, Buttafuoco et al. (2014) evaluated SPI to identify the area with extreme dry conditions over 1916-2006. The analysis identified

several droughts in the region and suggested a trend towards drier conditions for the period, although not persistent throughout the series length.

The SPEI calculates PET from measured climate variables (wind speed, surface humidity and solar radiation) and is a better indicator of drought than just rainfall. For example, the use of PET data showed clearly the drought signal for the 2003 summer drought in Central Europe (Teuling et al. 2013). SPEI data are available from NCAR-UCAR[33] for 1901-2011 based on modelled input data[34] and the Penman-Monteith method. A Thornthwaite SPEI product is available from CSIC[35].

The widely used Palmer Drought Severity Index (PDSI) uses temperature, precipitation, PET and antecedent wetness (prior month) to estimate relative dryness. It is effective in determining long-term drought, but is not as comparable across regions as SPI, although improved by the self-calibrating PDSI (Antofie, 2015).

PDSI values are sensitive to the method of calculating PET. Penman Monteith generates higher values of PDSI in recent decades, and a lower percentage area in drought compared with the temperature-only Thornthwaite method (Figure 34). Both methods show little evidence of more severe global drought over the last 60 years, contradicting previous studies (Seneviratne 2012). However PDSI but can be reformulated to show an increase in droughts over the same period (Sheffield et al. 2012).

Figure 34: Impact of parameterization of potential evaporation (Blue PDSI_Th, Red PDSI_PM) (Sheffield et al., 2012)

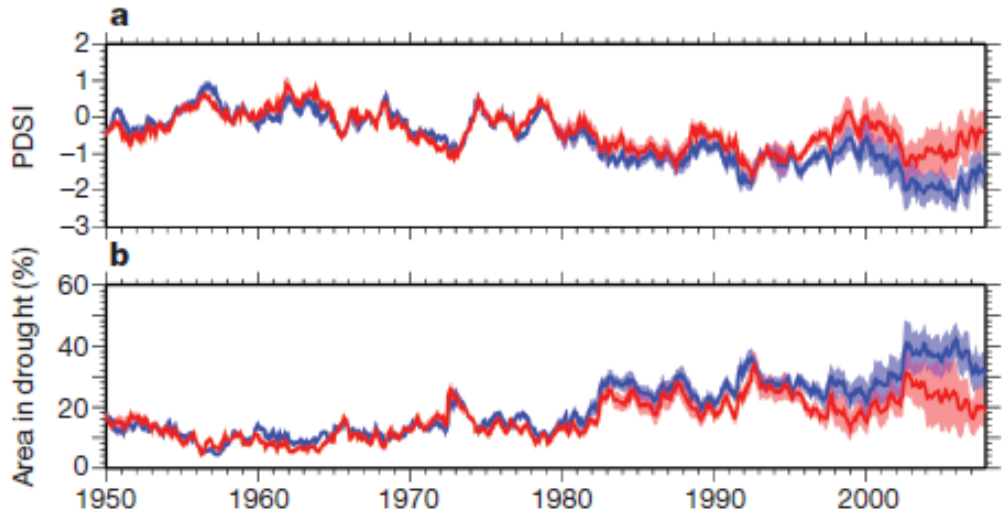

Hence some studies have produced apparently conflicting results of how drought is changing over time, attributed to the formulation of the PDSI and the reduction in the number of observations stations in the underlying datasets (Trenberth, 2014).

Accurate attribution of the causes of drought needs to account for natural variability, and teleconnections with global phenomena such as El Niño (drier over land) and La Niña (wetter over

[33] National Center for Atmospheric Research (NCAR), University Corporation for Atmospheric Research (UCAR) https://climatedataguide.ucar.edu/climate-data

[34] CRU TS3.2 dataset: http: //badc.nerc.ac.uk/view/badc.nerc.ac.uk__ATOM__ACTIVITY_0c08abfc-f2d5-11e2-a948-00163e251233 ; doi: 10.5285/D0E1585D-3417-485F-87AE-4FCECF10A992

[35] Consejo Superior de Investigaciones Científicas http://sac.csic.es/spei/database.html

land) events. Increased heating from global warming may not cause droughts, but it is expected that when droughts occur they are likely to set in quicker and be more intense. There appears to be evidence of a "dry gets drier, wet gets wetter" tendency on European if not global scale. In addition to the limitations of estimating PET (above), the use of temperature as a driver for drought overlooks the fact that, in dry conditions, the causal link is often reversed, that is, drought itself induces hot temperatures when the lack of soil moisture leads to a suppression of evaporative cooling (Seneviratne, 2015).

The use of combined indices can improve on single indicators to isolate the drought signal. Spinoni et al. (2015) combined SPI, SPEI and RDI, (the ratio of rainfall to PET) in a combined drought indicator to identify the most severe droughts in northern, central and southern Europe 1950-2012 (Figure 35).

Figure 35a: Northern Europe country drought series for the period 1950–2012 according to the indicator X-12 for some selected countries (drought events are marked in red). X-12 represents an index based on the average of values for SPI, SPEI and RDI accumulated over 12-months.

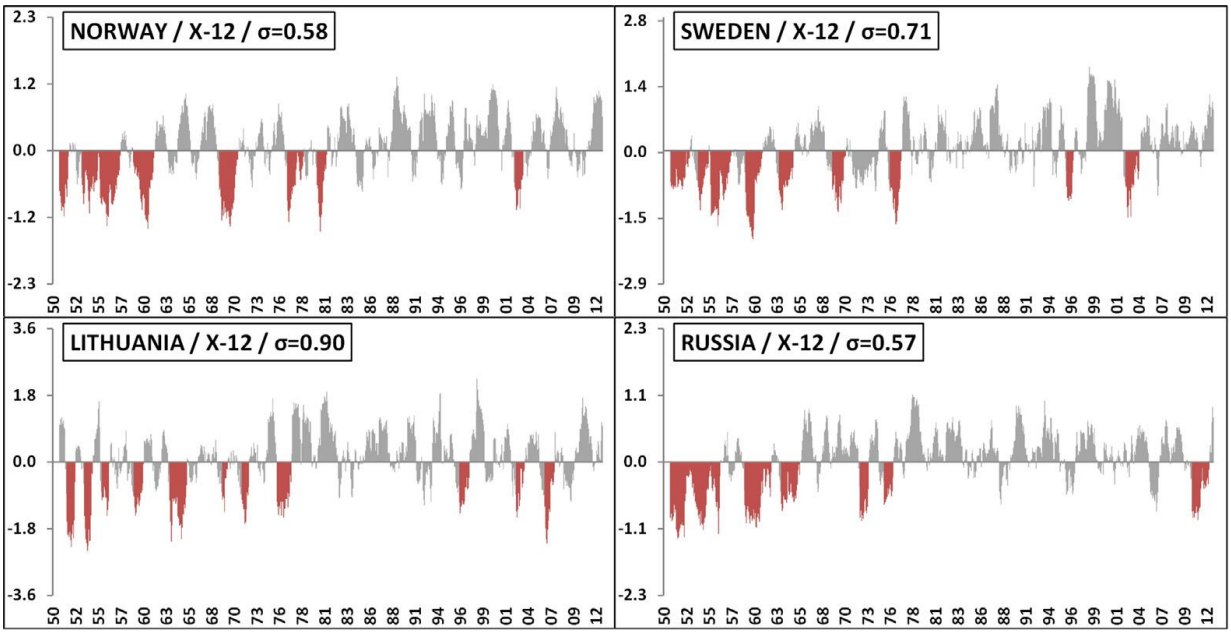

Figure 35b: Central Europe country drought series for the period 1950–2012 according to the indicator X-12 for some selected countries.

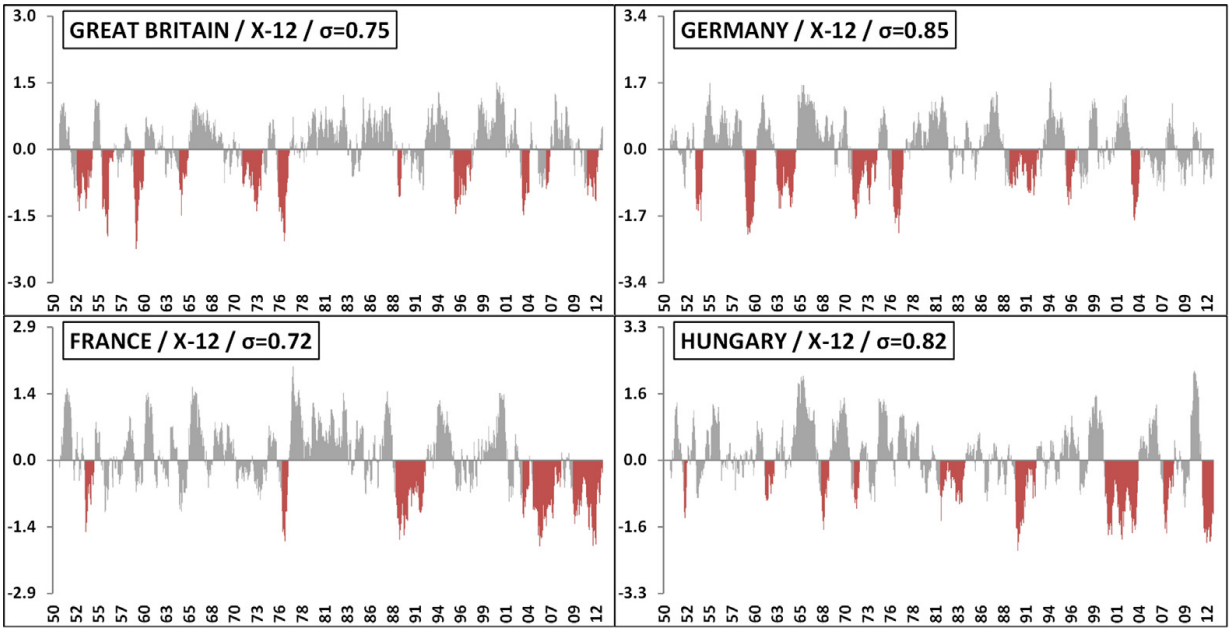

Figure 35c: Southern Europe country drought series for the period 1950–2012 according to the indicator X-12 for some selected countries.

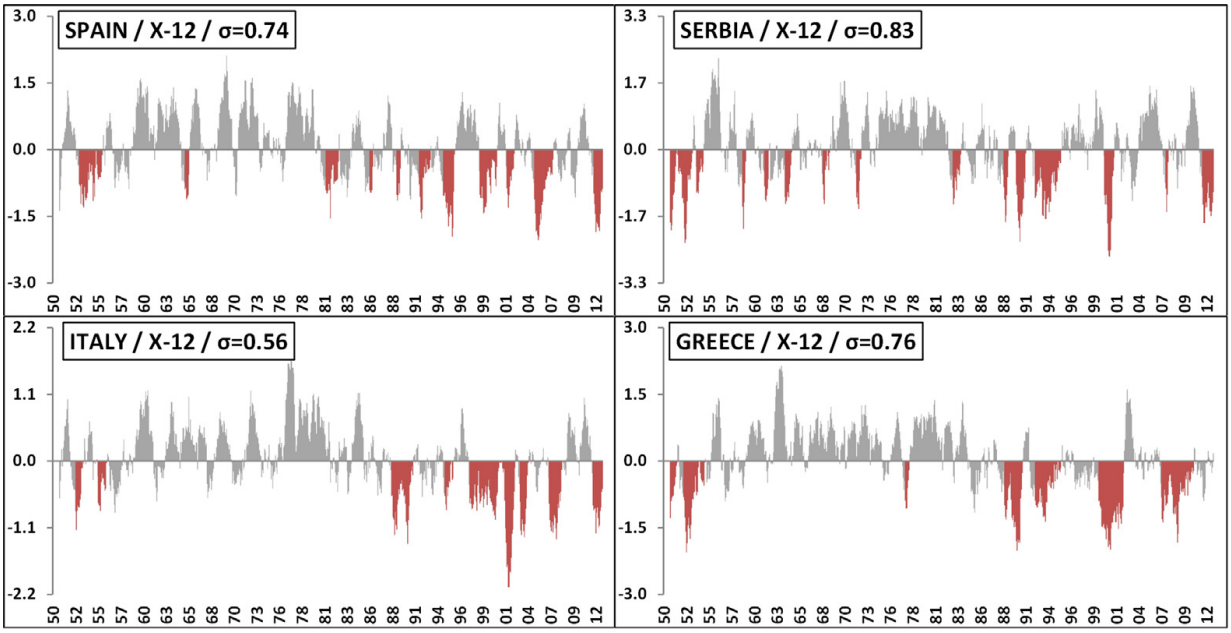

Recent severe droughts include Italy (1997-2002), the Baltic countries 2005-2009, the European heat wave of Summer 2003, and the widespread European drought of 2011, (see the case study below). Drought hot-spots were identified in S=southern Europe e.g. south-west Germany, the Carpathians, and the Balkans (e.g. Romania 2007). The highest drought frequency and severity in northern and eastern Europe has been shown to be from the early 1950s to the mid-1970s. The 1950s were most prone to long, intense, Europe-wide meteorological and hydrological droughts, of which two (1951–52, 1953–54) involved half of Europe. Southern and western Europe (in particular the Mediterranean) showed the

highest drought frequency and severity since 1990. There has been a small but continuous increase of the European areas prone to drought from the 1980s to the early 2010s.

Further analysis identified thirteen droughts in the Carpathian region over the period 1961–2010 based on four daily drought indicators (RDI, SPEI, SPI, and the Palfai Aridity/Drought Index or PADI), and two climate indicators (the Köppen-Geiger climate classification and the FAO-UNEP aridity index). The most intense droughts occurred in 1990, 2000, and 2003, and the wettest years were 2005 and 2010. A study of the most severe drought events confirmed that, in general, the drought frequency increased slightly during the decade 2001–2010, during which four out of the thirteen drought events occurred. The Carpathians are not classified as an arid area according to the FAO-UNEP aridity index, but they form an orographic barrier between mild oceanic (South and West) and continental (North and East) climates. A shift from oceanic to continental climate has been observed over the last 20 years, especially in the Romania Carpathians, and on the country borders between Serbia and Hungary (Spinoni et al., 2013).

Sepulchre-Cento et al., (2012) developed a drought indicator to detect agricultural drought which combines the 3-month Standardized Precipitation Index (SPI-3), soil moisture and the fraction of Absorbed Photosynthetically Active Radiation (fAPAR). In a study of European drought episodes 2000-2011, the indicator discriminated successfully between areas affected by agricultural drought, and it has been adopted by EDO for European-wide drought maps . The indicator could be also used with shorter term indicators such as SPI-1 to identify relatively short intense droughts e.g. Romania 2007.

Drought studies have identified drought hotspots in the Mediterranean and southern Europe, with higher rainfall in the high northern latitudes. A study of the Iberian peninsula by Vicente-Serrano et al. (2014) found evidence of increasing drought severity caused by temperature rise in southern Europe (Figure 36). Both SPI and SPEI showed increased drought frequency and an increase in drought area over the period 1961-2011, with the SPEI indicating more intense droughts than SPI over the last two decades.

Greve at al. (2014) analyzed more than 300 combinations of various data sets of historical land dryness changes from 1948 to 2005 to test whether dry regions are drying out further, and wetter regions are becoming wetter as the climate warms. Significant changes were found in transitional regions, generally towards drier conditions, including for example, the western Mediterranean. Only 11% of the global land area showed a robust ‘dry gets drier, wet gets wetter’ pattern, compared to 9.5% of global land area with the opposite pattern, that is, dry gets wetter, and wet gets drier. This single study suggests that aridity changes over land do not follow a simple intensification of existing patterns.

Drought severity climatology has been produced for the Carpathian region using the self-calibrating PDSI for the period 1961-2010 (Antofie et al. 2015) including the amount of water needed for drought recovery and the climatological probability of receiving that amount of water for the Carpathian region.

Recent new datasets provide retrospective estimates of precipitation, soil moisture, and streamflow deficits in Europe. The drying tendency seen in recent decades in the Mediterranean region is consistent with modelled climate projections.

Figure 36: (a) Changes in the SPI; (b) Changes in SPEI at 54 stations for the period 1961–2011; (c) Changes in the monthly difference between the SPEI and the SPI estimated using least squares regression (Vicente-Serrano et al., 2014).

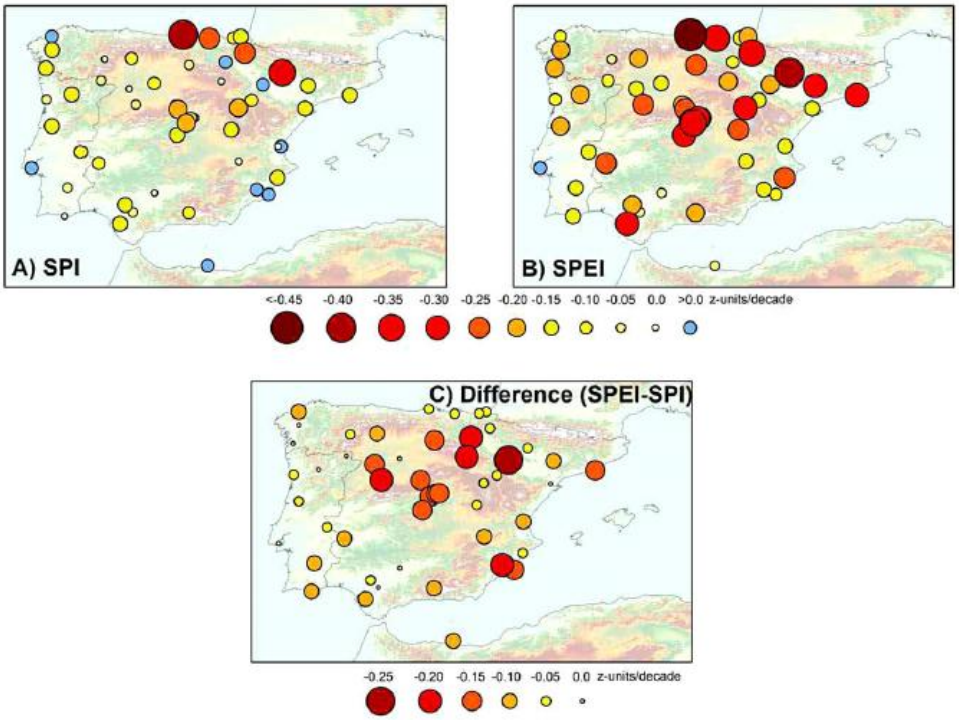

Impacts

The impacts of drought include reduced soil moisture, reduced streamflows and reduced water availability for water supply and irrigation. Secondary impacts include reduced crop yields, especially if occurring in the growing cycle, and adverse impacts on natural ecosystems and habitats. Extremes of heat and drought are also correlated with wildfires, for example those in summer 2013 in southern Greece (Sarris et al. 2013).

Increased temperatures due to global warming may not cause droughts but it is expected that when droughts occur they are likely to set in quicker and become more intense, (Trenberth 2014). Drought indices can therefore be useful as a potential predictor of fire (or burned area), and of impacts on the water environment (reduced hydropower, habitat stress, power station cooling, environmental low flows etc.).

The Drought:R&SPI project reproduced maps of a Europe wide standardised drought vulnerability index based on diverse variables (Figure 37). These include freshwater abstraction, a water exploitation index, water body status, population density, etc. and shows elevated vulnerability in the Iberian Peninsula, Italy and parts of northern Europe.

Figure 37: The vulnerability indices of sensitivity (left) and adaptive capacity (right), NUTS-combo scale (Blauhut & Stahl, 2015 from De Stefano et al. 2015).

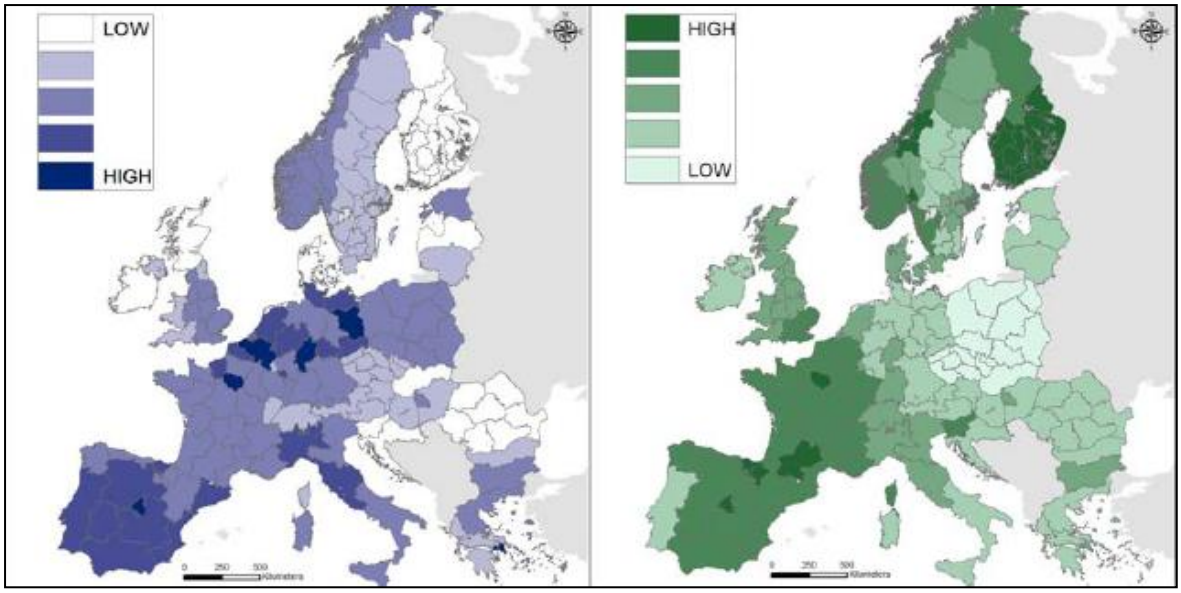

3.4.1.2 Projections – meteorological drought

There is a degree of consistency in model projections which indicate drier and warmer Mediterranean regions, and a northward shift of climatic regimes in Europe (Van Loon, 2015). Previous studies of drought have identified hotspots, particularly in the Mediterranean and eastern Europe (Blenkinsop and Fowler, 2007; Dai, 2013; Giorgi and Lionello, 2008; Orlowsky and Seneviratne, 2013), but they have sometimes produced inconsistent results regarding the future severity of droughts, which may in part be due to the coarse resolution of the global climate models or, in the cases where RCMs have been used, the application of regional averaging, which can both act to smooth extremes.

An assessment of European dry spells projected for the mid-21st century from the ENSEMBLES RCMs considered indices such as the SPI, Palmer Z-Index and PDSI (Heinrich and Gobiet, 2012). In common with other studies, drier conditions were projected for southern European sub-regions, along with increases to event length, magnitude and area. The recent study by Spinoni et al., (2015) looked at drought projections under the SRES A1B scenario for 2041-70 and 2071-2100 and found higher increases in southern Europe. Similarly Jacob et al. (2014) found increases in the length of dry spells in the future, particularly over southern Europe (Figure 38).

Buttstaedt & Schneider (2014) use regional climate projections (A1B scenario) of the statistical downscaling models STARII and WETTREG and the dynamical climate models REMO and COSMO-CLM for the city of Aachen, Germany. The model outputs are compared with the 30-year baseline period of 1971-2000 in order to assess future precipitation patterns for the summer months of June, July and August. Climate projections for the city indicate a decrease in precipitation in summer until 2100 with -17% on average. The highest decrease is shown by COSMO-CLM with -30% rainfall in June for the period of 2071-2100. Dry periods are expected to occur 3 times more often at the end of the current century and to last longer by 1 day (COSMO-CLM) to 3 days (WETTREG) compared to the period of 1971-2000.

Recent studies, (Orlowsky & Seneviratne, 2012) considered seasonal as well as regional drought for IPCC SREX. Projected changes in precipitation and dryness extremes were more ambiguous than those of temperature extremes, despite clear features showing increasing dryness over the Mediterranean and

increasing heavy precipitation over the northern high latitudes. The assessment of projected changes in dryness was sensitive to the choice of index, and models showed less agreement regarding changes in soil moisture than in the commonly used CDD index, which is based on precipitation data only.

Figure 38: Jacob et al. 2014. Projected changes in the 95th percentile of the length of dry spells (days) for 2021–2050 compared to 1971-2000 (a, c, e) and 2071–2100 compared to 1971–2000 (b, d, f) for A1B (a, b), RCP8.5 (c, d) and RCP4.5 (e, f) scenarios. Hatched areas indicate regions with robust and/or statistical significant changes.

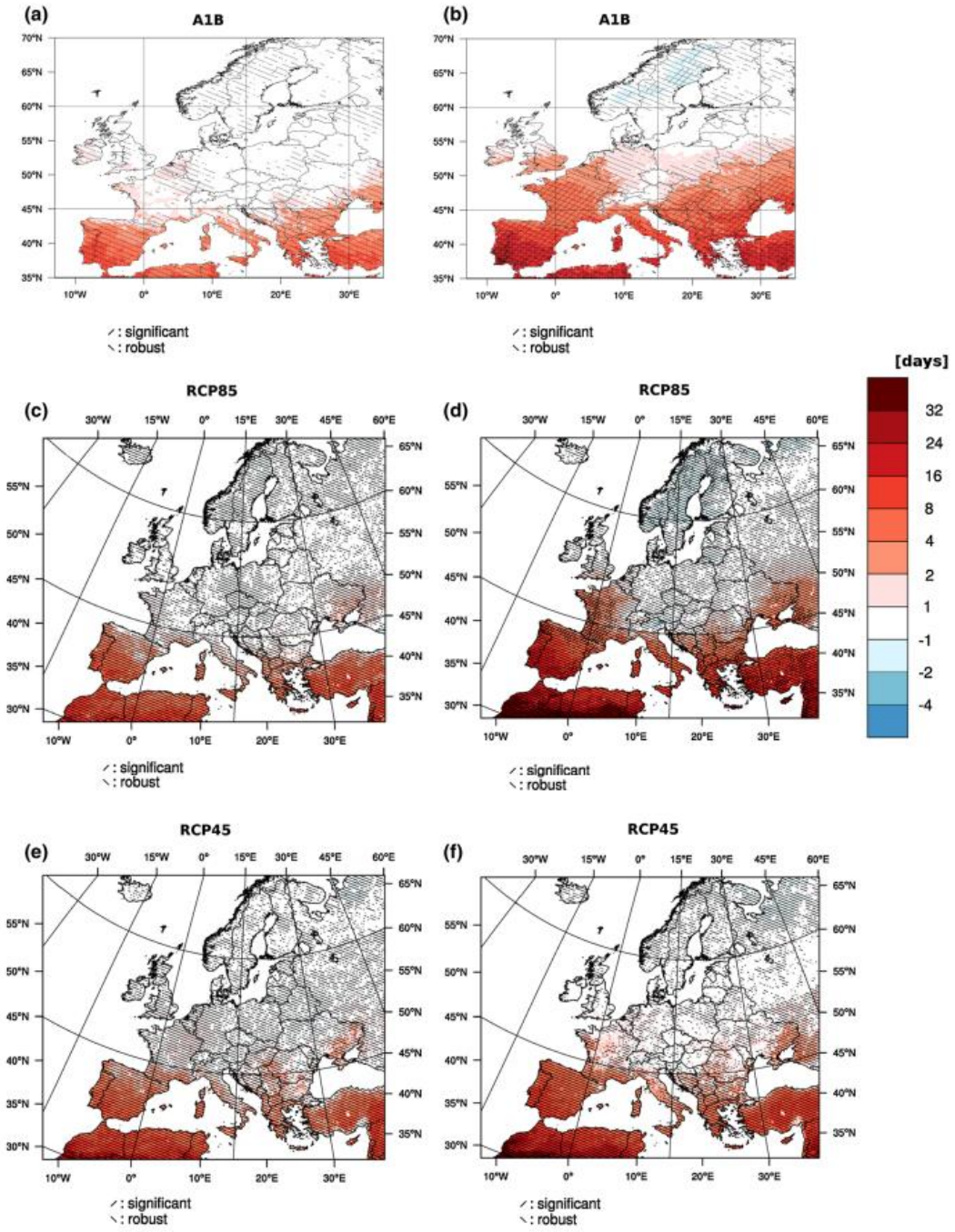

The DROUGHT-R&SPI project (Stagge et al., 2015) found significant increases in drought frequency and severity in the Mediterranean region, in addition to the Atlantic coast and south-eastern Europe. Most of northern Europe is projected to have fewer precipitation based droughts due to increasing

rainfall over these regions. The results were considered to be robust with good agreement between the suite of GCM and RCM model projections.

The inclusion of evapotranspiration could alter projections based solely on precipitation metrics, and since evapotranspiration is largely driven by radiation and surface temperatures, future projections using the SPEI could be more severe than projections based on SPI alone (Stagge et al., 2015).

3.4.2 Hydrological drought

3.4.2.1 Observations - Hydrological drought

Hydrological drought is an outcome of meteorological and soil moisture drought, and is assessed in terms of river or stream flow, and surface water or groundwater storage, at timescales which reflect catchment characteristics. (Tallaksen and Van Lanen, 2004; Van Loon & Van Lanen, 2012). Less responsive groundwater-dominated or larger catchments are sensitive to rainfall deficits over longer multi-year timescales, but in responsive catchments, single season droughts can develop rapidly as a result of rainfall deficiencies over 3-6 months. The assessment of climate induced runoff is complicated due to its very high variability (Van Huijgevoort et al., 2012), with zero flows for much of the year in drier regions, and scarcity of data in some regions, especially southern Europe (Stahl et al., 2014). Specialized statistical distributions are needed to describe a large proportion of very low or zero summer flows (Stahl at al 2010 & 2012).

Vicente-Serrano et al. (2012a, 2014) assessed the magnitude of streamflow droughts in the Iberian peninsula over the period 1961-2009 in terms of the Standardised Streamflow Index (SSI). Figure 39(a) shows an increasingly negative change in the streamflow/precipitation ratio with annual streamflow (Blue: natural basins; yellow: regulated basins; red: highly regulated basins). Figure 39(b) shows the Pearson's r correlation between the annual streamflow/ precipitation ratio and evapotranspiration (ET_0), dotted lines indicating the limits of significance. Figure 39(c) and (d) show the spatial distribution of the magnitude and the correlation respectively.

Hydrological drought is commonly assessed in relation to a threshold, which is useful for water management where the onset, duration and termination of a deficit below a threshold are of interest for operational water management decisions. The variable threshold method (Zelenhasić & Salvai 1987) which is best applicable in regions with non-zero runoff most of the time, calculates the deficit over an extended time period time to identify seasonal trends and features. It identifies deficit periods relative to a daily, monthly or seasonally varying threshold, allowing droughts to be compared between different locations and seasons. A range of different thresholds have been used in applications of the variable threshold method (e.g. Q70, Q80, Q90, Q95), preference depending on location, catchment characteristics, etc. A regional variant of the variable threshold method, the Regional Deficiency Index (RDI; Stahl & Demuth 1999), was used to identify and characterise major pan-European drought events (Parry et al., 2012) and analyse their spatial coherence in Europe over the 1961-2005 period (Hannaford et al., 2011).

Other hydrological indices include the base flow index which is the ratio of base flow to total flow, and recession indices which express the rate of streamflow decay during low rainfall periods, and indices based on water balance calculations (Figure 40, Stahl et al., 2012).

Figure 39: (a) Magnitude of change in the streamflow/precipitation ratio for Iberian peninsula, 1961-2009 (Vicente-Serrano et al., 2014). (b) shows the Pearson's r correlation between the annual streamflow/ precipitation ratio and evapotranspiration (ET_0), dotted lines indicating the limits of significance. (c) and (d) show the spatial distribution of the magnitude and the correlation respectively.

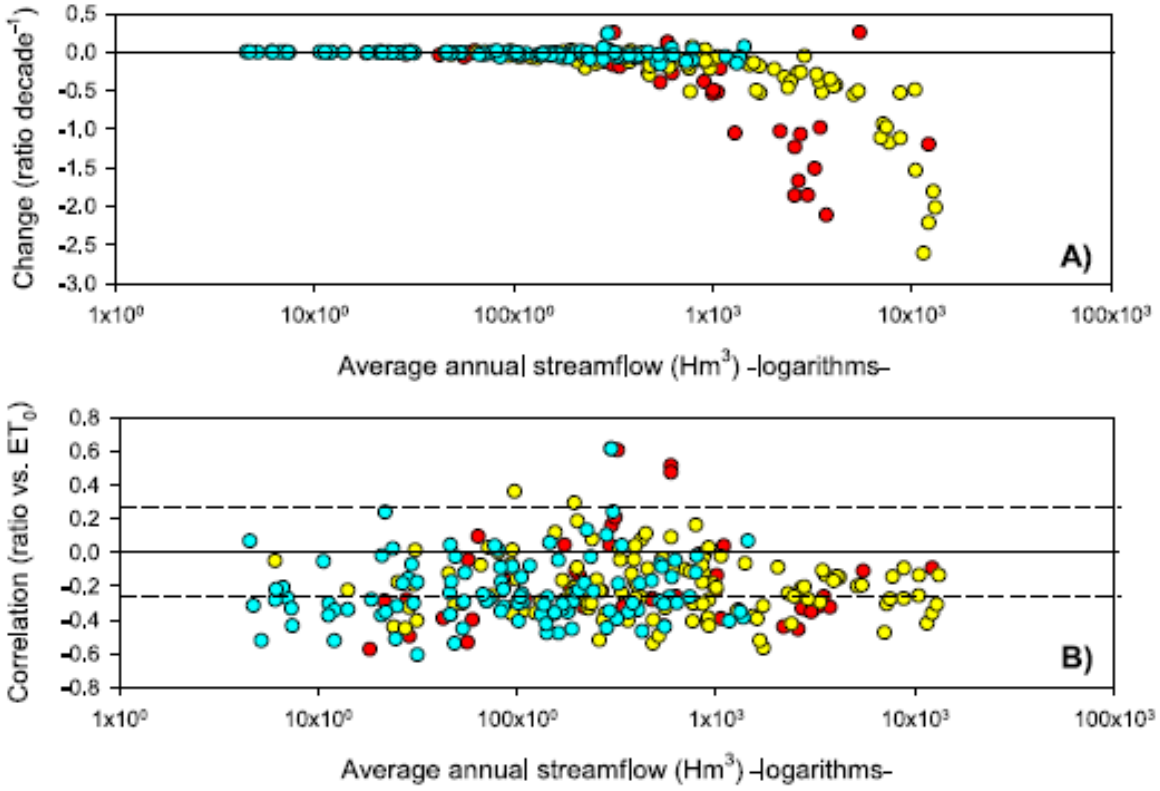

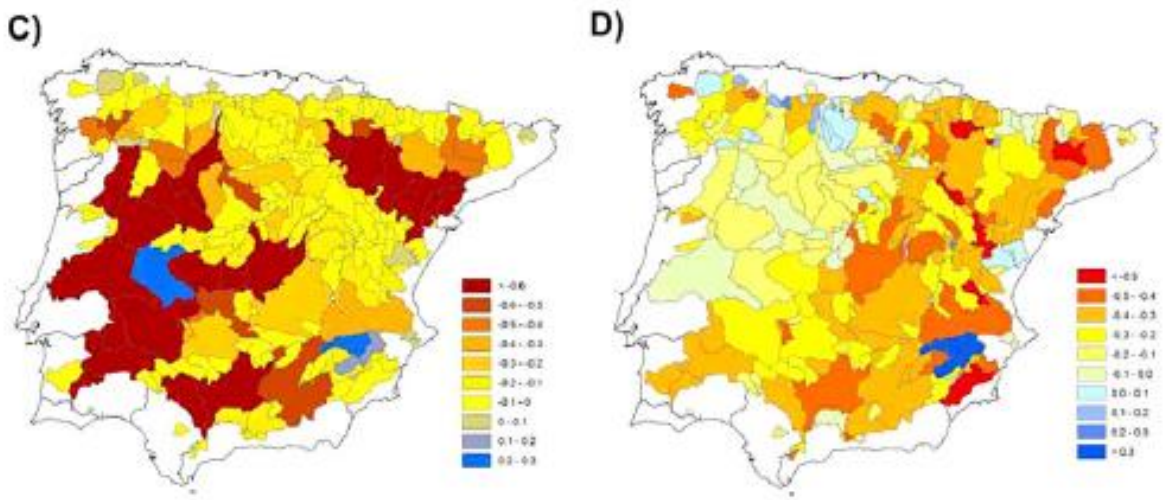

Figure 40: European Drought Trends in simulated August flow 1963-2001 (Stahl et al., 2012). Negative (more severe) drought shown red, positive (less severe) drought shown blue.

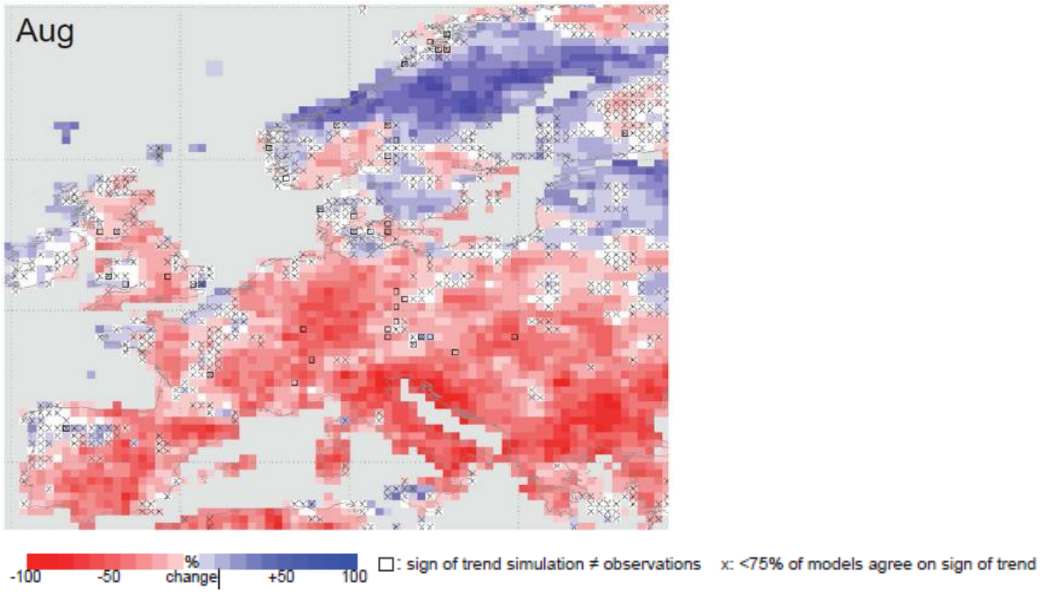

A global drought study by Van Huijgevoort et al. (2012) combined the characteristics of the variable threshold level and the consecutive dry days (CDD) methods to identify hydrological drought events which occur during positive and zero runoff periods. For drier regions, the method better estimated drought duration compared with the CCD method alone which does not identify droughts during periods of runoff. It was used to identify droughts from discharge observations of four major rivers situated in different climate regions, and from the simulated runoff of five land surface models. The new method was shown to more consistently identify regional droughts.

Applications of the threshold level method considers the end of drought to be the instantaneous point in time at which flows rise above the threshold. This understates the often significant transitions between drought and 'normal' conditions at the end of a drought. An alternative approach was developed which defines drought termination as the end of a period of consecutive above-threshold anomalies (i.e. a site-specific criterion), which can be characterised with metrics including duration and rate of change (Parry et al. 2015). This approach was used to produce a chronology of historic drought termination in the Thames catchment in the UK, and to place contemporary events and their characteristics into a long-term historic context. Such an approach has also been applied throughout the UK and could potentially be applied across Europe to better characterise the variability of drought termination at a continental scale, as well as helping to investigate the drivers and impacts of such events.

A reliable forecast of seasonal droughts is important as summer droughts that continue into winter, and winter droughts that continue into summer can both have impacts on water resources replenishment. Drought conditions at the onset of the dry season in warm seasonal climates and at the beginning of winter in cold seasonal climates, is the most reliable predictor of the drought situation during and at the end of the dry winter season (Van Loon at al., 2014). For the prediction of hydrological droughts in seasonal climates, both precipitation forecasts and information about the seasonal cycle of temperature and precipitation are required. Including this knowledge in hydrological drought forecasting could increase forecasting skill considerably, as it makes the forecast less dependent on the forecast skill of actual precipitation and temperature. The study identified seasonality effects for soil moisture and discharge drought characteristics which cannot be explained by meteorological processes alone.

Meteorology-based drought indices (e.g. SPI, PDSI) are used as indicators of hydrological drought but do not account for the effects of seasonality on climate, for example, high evapotranspiration or snowpack. Due to the nonlinear response of soil moisture, groundwater, and streamflow to the meteorological situation in climates with strong seasonality, hydrological drought characteristics cannot be derived straightforwardly from meteorological drought characteristics (Van Loon & Van Lanen 2012, Van Lanen et al., 2013; Van Loon et al., 2014 & 2015).

There is no clear agreement on the choice of scale for quantifying drought magnitude as it has a significant impact on the extreme, with selection depending on spatial and temporal scales of application. The DrIVER (Drought Impacts: Vulnerability thresholds in monitoring and Early-warning Research) project tested nine key distributions for appropriateness with SPI and SSI and found the Tweedie distribution was to be best for UK. Catchment control (van Lanen et al., 2013) is the effect of hydrological scale on catchment characteristics which determine the lags between meteorological drought and hydrological drought. For catchments in the UK, the strongest correlations between accumulation periods of SPI and SSI vary depending on catchment characteristics (Barker et al., 2015).

There are a number of projects aimed at improving understanding of drought, developing indices, and mapping drought risk. The Water and Global Change (WATCH) project combined ERA 14 model reanalysis with a soil moisture indicator (Weedon et al., 2011). The DrIVER project used standardised drought indices (SPI, SPEI and SSI) to improve drought monitoring and early warning systems in three continents through an understanding of how drought indicators link to drought impacts to reduce vulnerability. For example, Blauhut and Stahl (2015) used SPI and SPEI derived from E-OBS data to map drought risk for the period 1970-2012 in terms of its impact on water quality, agriculture, and industry for the Drought: R&SPI project.

3.4.2.2 Projections - hydrological drought

A majority of studies of trends in future drought occurrence have tended to focus on meteorological and soil moisture drought (van Loon, 2015) but there have been a number which focus on hydrological drought.

Forzieri et al. (2014) simulate increasing severity and frequency of European stream flow drought due to climate change by coupling a hydrological model with an ensemble of bias corrected climate simulations based on the SRES A1B scenario (Figure 41). The analysis showed that streamflow droughts will become more severe and persistent in many parts of Europe, except in northern and north-eastern parts of Europe. In particular, southern regions will face strong reductions in low flows. Future water use will aggravate the situation by 10-30% in southern Europe, whereas in some sub-regions in western, central and eastern Europe a climate driven signal of reduced droughts may be reversed due to intensive water use.

Studies have shown that assessed trends in streamflow may not necessarily be representative of longer term changes as a result of interdecadal variability (Hannaford et al., 2013). Uncertainties in hydrological drought projections can stem from different representation of terrestrial water-cycle processes in hydrological models (Prudhomme et al., 2013). To overcome this, Van Huijgevoort et al. (2014) suggested selecting combinations of climate and hydrological models which performed best during the control period.

Figure 41: Ensemble-average change in the 20 year return level minimum flow (left) and deficit volumes (right) due to only climate change between the corresponding time slices and the control period (1961–1990). Fig 8 from Forzieri et al., 2014.

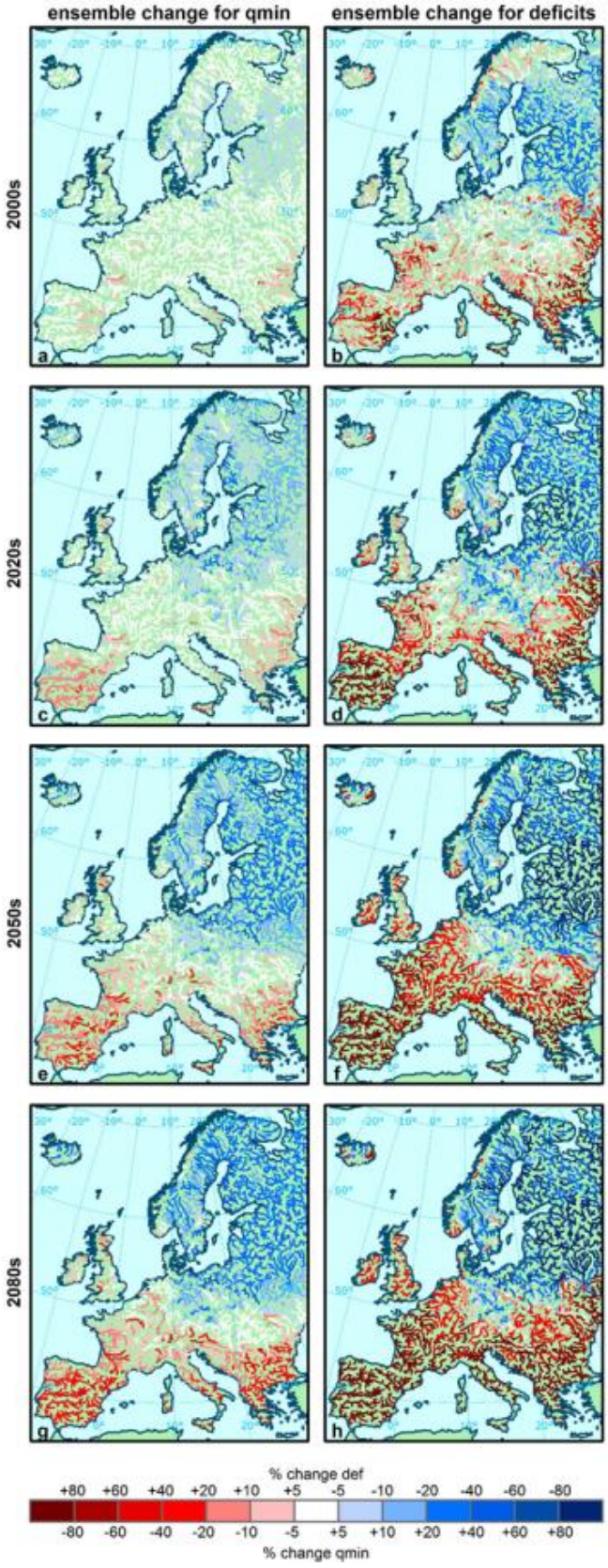

Some studies indicate a move towards probabilistic and ensemble based studies of drought. Taylor et al. (2013) utilised four drought indices in order to assess a range of categories of drought: the SPI, Soil Moisture Anomaly (SMA), the PDSI and the Standardised Runoff Index (SRI). These were calculated for the SRES A1B and RCP2.6 from monthly model output from a 57-member perturbed parameter ensemble (PPE) of the HadCM3C model. Although patterns of drought globally were comparable between the A1B and RCP2.6 scenarios, the RCP2.6 scenario (which represents climate mitigation) tended to reduce future changes in drought. In general, climate mitigation reduced the area over which there was a significant increase in drought but had little impact on the area over which there was a significant decrease in time spent in drought.

Wanders et al. (2015a & 2015b) quantified the impact of climate change on future low flows and associated hydrological drought characteristics on a global scale using an alternative drought identification approach that considers adaptation to future changes in hydrological regime. They assessed a fixed versus varying threshold approach in order to account for potential adaptation, effectively basing the threshold definition on a moving average and assuming the populations will make progress towards adapting to these changes over time. They found that there was a significant negative trend in the low flow regime over the 21st century over certain regions, which included the Mediterranean. They concluded that using an approach that accounts for adaptation could have a substantial influence on future hydrological drought characteristics. Vidal et al. (2012) also considered adaptation but distinguished between 'retrospective adaptation' and 'prospective adaptation' and also concluded that adaptation reduces the expected changes in drought severity. A global scale study by Prudhomme et al. (2014) found that including plant response to increased CO2 levels predicted little or no increase in streamflow drought frequency in the future, in contrast to other models.

3.4.3 Soil moisture drought

3.4.3.1 Observations - soil moisture drought

Soil moisture drought occurs when there is a deficit of soil moisture in the plant rooting zone causing moisture stress and reductions in growth. A persistent soil moisture drought may develop into to a hydrological drought affecting streamflow, groundwater resources and water sensitive ecosystems. Indices of soil moisture drought include the Palmer Drought Severity Index (PDSI) and soil moisture anomaly (SMA) defined in Appendix A.1. A key study based on PDSI (Sheffield, 2012) showed little change in global drought over the past 60 years. However, previous assessments of changes in drought over the last 115 years indicate an increase in the severity and frequency of drought may be happening globally. In particular, calculations based on the Palmer Drought Severity Index (PDSI) show a decrease in moisture globally since the 1970s with a corresponding increase in the area in drought, due in part to surface warming (Dai et al., 2004, Briffa et al., 2009 cited in Trenberth 2014). A number of recent studies have produced inconsistent results of how drought is changing under climate change which could be due to the formulation of the PDSI and the datasets used to determine the evapotranspiration component (Trenberth et al., 2014). Additional investigation shows that assessing how precipitation has changed is a factor.

Maps of soil moisture, CDD precipitation anomaly are available for significant events from the EDO based on comparison with the base period 1961-1990. For example maps for autumn 2011 are shown in Figures 42-44: (EURO4 CIB[36]).

[36] http://cib.knmi.nl/mediawiki/index.php/European_Drought_in_November_2011

Figure 42: Precipitation anomaly in percentage of the 1961-1990 climatology. The Danube catchment is included for illustrative purposes. Left: Autumn 2011, right: November 2011.

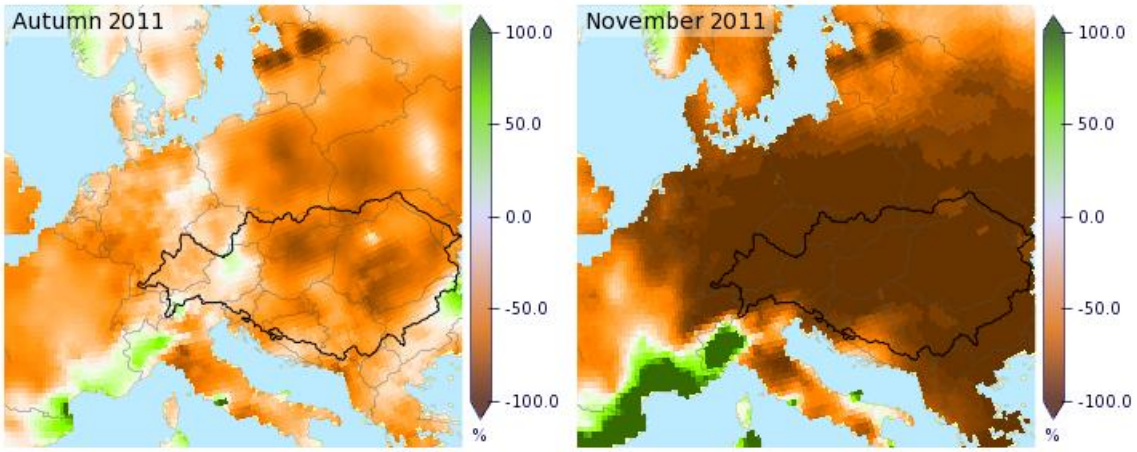

Figure 43: Consecutive number of dry days for stations throughout central Europe. Left: November climatology 1961-1990, right: November 2011 (EDO).

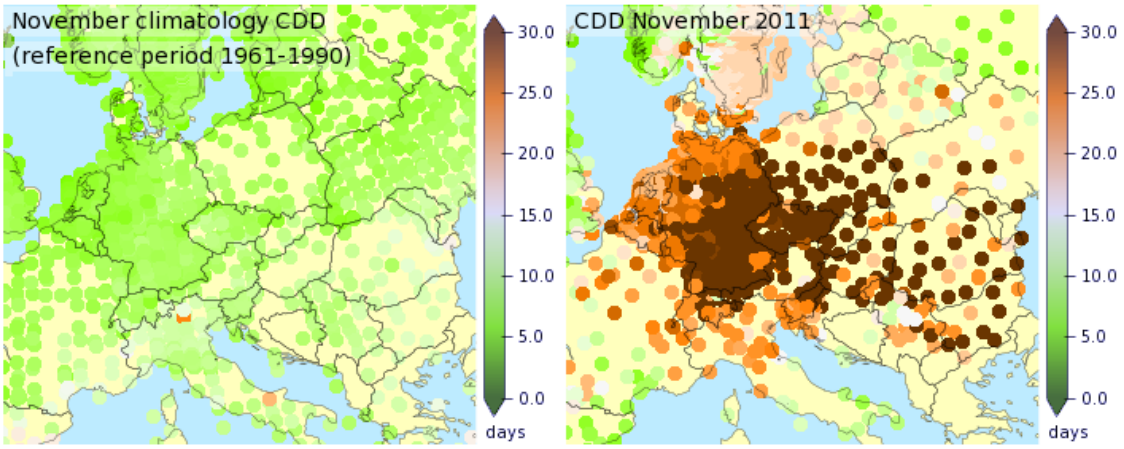

Figure 44: ESA soil moisture map for November 2011 in m^3/m^3. Note that the areas in the Netherlands, northern Germany and Denmark with high soil moisture content are areas where groundwater levels are regulated. The satellite registers the soil moisture content of the upper ~2 cm of the soils. With a value of 0.10 m^3/m^3 soil moisture, this corresponds to storage of approximately 100 mm water in 1 m^3 soil or 1 mm in the top cm.

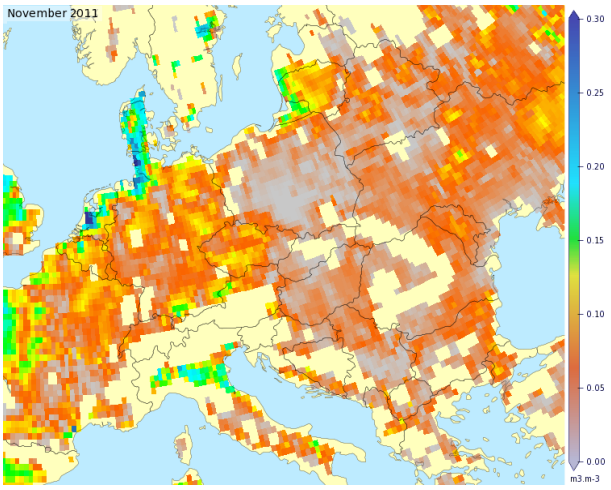

Using the PDSI and its intermediate Z-index product for the Mediterranean region, Dubrovsky et al. (2014) discovered a significant decrease in soil moisture in all seasons, with the most significant decrease occurring in summer. The displayed changes exhibit high inter-model agreement. A stochastic daily weather generator, calibrated with the modelled daily data, indicated a trend toward more extreme weather in the Mediterranean. Temperature maxima will increase not only because of an overall rise in temperature means, but partly (in some areas) because of increases in temperature variability and daily temperature range. Increased mean daily precipitation sums on wet days occurring in some seasons, and some parts of the Mediterranean may imply higher daily precipitation extremes, and decreased probability of wet day occurrence will imply longer drought spells all across the Mediterranean.

Figure 45 shows changes in summer soil moisture between the periods 1961 to 1990 (baseline) and 2021 to 2050 (scenario). At the pan-European scale, soil moisture content has not changed significantly since the 1950s (Kurnik et al., 2014b). At the sub-continental scale, however, significant trends in summer soil moisture content can be observed. In parts of northern Europe soil moisture content increased; these increases are likely due to increases in precipitation amounts. In the Mediterranean region decreases in soil moisture were observed, particularly large changes being recorded in south-eastern Europe, south-western Europe, and southern France. However, limited availability of climate data in the region affects confidence in of the modelled trends.

Figure 45: Projected changes in summer soil moisture between the periods 1961 to 1990 (baseline) and 2021 to 2050 (scenario)[37]

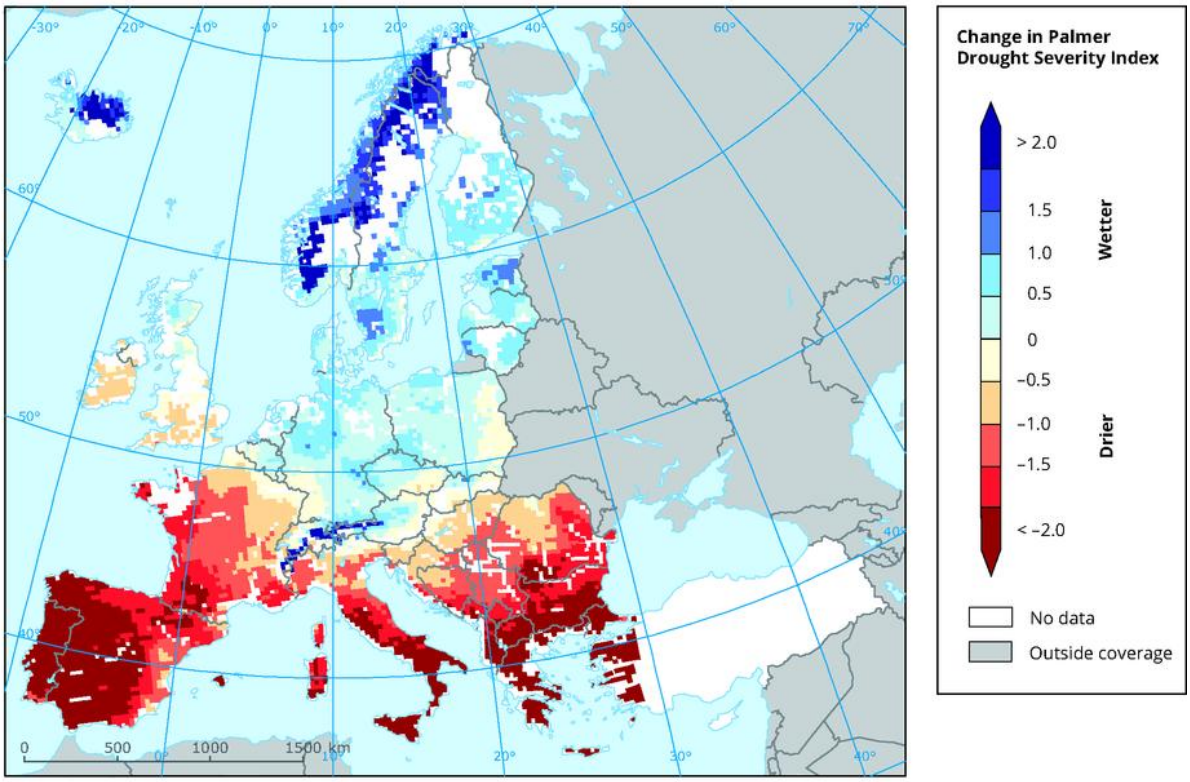

[37] http://www.eea.europa.eu/data-and-maps/indicators/water-retention-3/assessment

3.4.3.2 Projections - soil moisture drought

The greatest difference in future drought predictions between future scenarios is given by the PDSI metric which is strongly influenced by temperature via its impact on evapotranspiration. Climate mitigation (under the RCP2.6 scenario) generally reduced future changes in drought compared to the business as usual scenario (A1B) and had a larger impact on significant increases than decreases in time spent in drought.

There are considerable uncertainties in future projections. Drought thresholds have been found to have relatively little effect on the proportion of time spent in drought. Higher thresholds generally produced a larger affected land area with a reduced time spent in drought, particularly for SPI. This study showed that the choice of drought index is of less importance than absolute threshold when conducting impacts assessments of changes in future physical drought hazards, although there are inevitably threshold effects when considering socio-economic impacts.

Projections from the Burke et al. (2010) study of drought for the 21st century were estimated by applying non-stationary extreme value theory to monthly drought indices. All drought indices show an overall increase in drought in the future. However, the spread of values is considerable ranging from little change or a slight decrease to a significant increase depending on ensemble member and, to a smaller extent, location. The impacts of these projections are put in the context of the severe UK drought in 1976. This work provides preliminary steps towards a probabilistic assessment of changes in future drought.

Orlowsky and Seneviratne (2013) found that internal climate variability is the dominant source of uncertainty in projections of soil moisture drought and for the far future (end of the 21th century) the differences between climate models become dominant.

Appendices

A.1 Temperature, precipitation, drought and excess heat indices

No.	ID	Definitions of the ETCCDI core indices (1-27) and independent indices (28-44)
1	FD	Number of frost days: Annual count of days when TN (daily minimum temperature) < 0^{o}C. Let TN_{ij} be daily minimum temperature on day i in year j. Count the number of days where: $TN_{ij} < 0^{o}C$.
2	SU	Number of summer days: Annual count of days when TX (daily maximum temperature) > 25^{o}C. Let TX_{ij} be daily maximum temperature on day i in year j. Count the number of days where:$TX_{ij} > 25^{o}C$.
3	ID	Number of icing days: Annual count of days when TX (daily maximum temperature) < 0^{o}C.Let TX_{ij} be daily maximum temperature on day i in year j. Count the number of days where:$TX_{ij} < 0^{o}C$.
4	TR	Number of tropical nights: Annual count of days when TN (daily minimum temperature) > 20^{o}C.Let TN_{ij} be daily minimum temperature on day i in year j. Count the number of days where:$TN_{ij} > 20^{o}C$.
5	GSL	Growing season length: Annual (1st Jan to 31st Dec in Northern Hemisphere (NH), 1st July to 30th June in Southern Hemisphere (SH)) count between first span of at least 6 days with daily mean temperature TG>5^{o}C and first span after July 1st (Jan 1st in SH) of 6 days with TG<5^{o}C.Let TG_{ij} be daily mean temperature on day i in year j. Count the number of days between the first occurrence of at least 6 consecutive days with: $TG_{ij} > 5^{o}C$.and the first occurrence after 1st July (1st Jan. in SH) of at least 6 consecutive days with:$TG_{ij} < 5^{o}C$.
6	TX_x	Monthly maximum value of daily maximum temperature: Let TX_x be the daily maximum temperatures in month k, period j. The maximum daily maximum temperature each month is then: $TX_{x_{kj}} = \max(TX_{x_{kj}})$
7	TN_x	Monthly maximum value of daily minimum temperature: Let TN_x be the daily minimum temperatures in month k, period j. The maximum daily minimum temperature each month is then: $TN_{x_{kj}} = \max(TN_{x_{kj}})$
8	TX_n	Monthly minimum value of daily maximum temperature: Let TX_n be the daily maximum temperatures in month k, period j. The minimum daily maximum temperature each month is then: $TX_{x_{kj}} = \min(TX_{x_{kj}})$
9	TN_n	Monthly minimum value of daily minimum temperature: Let TN_n be the daily minimum temperatures in month k, period j. The minimum daily minimum temperature each month is then: $TN_{x_{kj}} = \min(TN_{x_{kj}})$
10	TN10p	Percentage of days when TN < 10th percentile :Let TN_{ij} be the daily minimum temperature on day i in period j and let $TN_{in}10$ be the calendar day 10th percentile centred on a 5-day window for the base period 1961-1990. The percentage of time for the base period is determined where:$TN_{ij} < TN_{in}10$To avoid possible inhomogeneity across the in-base and out-base periods, the calculation for the base period (1961-1990) requires the use of a bootstrap procedure. Details are described in Zhang et al. (2005).

11	TX10p	Percentage of days when TX < 10th percentile :Let TX_{ij} be the daily maximum temperature on day i in period j and let $TX_{in}10$ be the calendar day 10th percentile centred on a 5-day window for the base period 1961-1990. The percentage of time for the base period is determined where:$TX_{ij} < TX_{in}10$ to avoid possible inhomogeneity across the in-base and out-base periods, the calculation for the base period (1961-1990) requires the use of a bootstrap procedure. Details are described in Zhang et al. (2005).
12	TN90p	Percentage of days when TN > 90th percentile :Let TN_{ij} be the daily minimum temperature on day i in period j and let $TN_{in}90$ be the calendar day 90th percentile centred on a 5-day window for the base period 1961-1990. The percentage of time for the base period is determined where: $TN_{ij} > TN_{in}90$ to avoid possible inhomogeneity across the in-base and out-base periods, the calculation for the base period (1961-1990) requires the use of a bootstrap procedure. Details are described in Zhang et al. (2005).
13	TX90p	Percentage of days when TX > 90th percentile :Let TX_{ij} be the daily maximum temperature on day i in period j and let $TX_{in}90$ be the calendar day 90th percentile centred on a 5-day window for the base period 1961-1990. The percentage of time for the base period is determined where: $TX_{ij} > TX_{in}90$ to avoid possible inhomogeneity across the in-base and out-base periods, the calculation for the base period (1961-1990) requires the use of a bootstrap procedure. Details are described in Zhang et al. (2005).
14	WSDI	Warm spell duration index: Annual count of days with at least 6 consecutive days when TX > 90th percentile. Let TX_{ij} be the daily maximum temperature on day i in period j and let $TX_{in}90$ be the calendar day 90th percentile centred on a 5-day window for the base period 1961-1990. Then the number of days per period is summed where, in intervals of at least 6 consecutive days: $TX_{ij} > TX_{in}90$
15	CSDI	Cold spell duration index: Annual count of days with at least 6 consecutive days when TN < 10th percentile. Let TN_{ij} be the daily maximum temperature on day i in period j and let $TN_{in}10$ be the calendar day 10th percentile centred on a 5-day window for the base period 1961-1990. Then the number of days per period is summed where, in intervals of at least 6 consecutive days:$TN_{ij} < TN_{in}10$
16	DTR	Daily temperature range: Monthly mean difference between TX and TNLet TX_{ij} and TN_{ij} be the daily maximum and minimum temperature respectively on day i in period j. If I represents the number of days in j, then: $$DTR_j = \frac{\sum_{i=1}^{I}(Tx_{ij} - Tn_{ij})}{I}$$
17	Rx1 day	Monthly maximum 1-day precipitation: Let RR_{ij} be the daily precipitation amount on day i in period j. The maximum 1-day value for period j are: $Rx1day_j = max\ (RR_{ij})$
18	Rx5 day	Monthly maximum consecutive 5-day precipitation: Let RR_{kj} be the precipitation amount for the 5-day interval ending k, period j. Then maximum 5-day values for period j are: $Rx5day_j = max\ (RR_{kj})$
19	SDII	Simple precipitation intensity index: Let RR_{wi} be the daily precipitation amount on wet days, w (RR ≥ 1mm) in period j. If W represents number of wet days in j, then: $$SDII_j = \frac{\sum_{w=1}^{W}(RR_{wj})}{W}$$
20	R10 mm	Annual count of days when PRCP≥ 10mm: Let RR_{ij} be the daily precipitation amount on day i in period j. Count the number of days where: $RR_{ij} \geq 10mm$

21	R20 mm	Annual count of days when PRCP≥ 20mm: Let RR_{ij} be the daily precipitation amount on day i in period j. Count the number of days where: $RR_{ij} \geq 20mm$
22	Rnn mm	Annual count of days when PRCP≥ nnmm, nn is a user defined threshold: Let RR_{ij} be the daily precipitation amount on day i in period j. Count the number of days where: $RR_{ij} \geq nnmm$
23	CDD	Maximum length of dry spell, maximum number of consecutive days with RR < 1mm: Let RR_{ij} be the daily precipitation amount on day iin period j. Count the largest number of consecutive days where: $RR_{ij} < 1mm$
24	CWD	Maximum length of wet spell, maximum number of consecutive days with RR ≥ 1mm: Let RR_{ij} be the daily precipitation amount on day in period j. Count the largest number of consecutive days where: $RR_{ij} \geq 1mm$
25	R95p TOT	Annual total PRCP when RR > 95p. Let RR_{wj} be the daily precipitation amount on a wet day w (RR ≥ 1.0mm) in period i and let$RR_{wn}95$ be the 95th percentile of precipitation on wet days in the 1961-1990 period. If W represents the number of wet days in the period, then: $R95p_j = \sum_{w=1}^{W}(RR_{wj})$ where $RR_{wj} > RR_{wn}$ 95
26	R99p TOT	Annual total PRCP when RR > 99p: Let RR_{wj} be the daily precipitation amount on a wet day w (RR ≥ 1.0mm) in period i and let $RR_{wn}99$ be the 99th percentile of precipitation on wet days in the 1961-1990 period. If W represents the number of wet days in the period, then: $R99p_j = \sum_{w=1}^{W}(RR_{wj})$ where $RR_{wj} > RR_{wn}$ 99
27	PRCP TOT	Annual total precipitation in wet days: Let RR_{ij} be the daily precipitation amount on day i in period j. If I represents the number of days in j, then: $PRCPTOT_j = \sum_{i=1}^{I}(RR_{ij})$
		Indices independent of ETCCDI (28-44)
		Precipitation indices
28	S95p TOT	Unlike R95pTOT, which uses a fixed climatological 95th percentile, the S95pTOT assumes a separate 95th percentile for each year based on a Weibull distribution fit to the wet-day precipitation amounts, an analytical expression for S95pTOT is derived. Leander et al, 2014
29	SPI	The Standardized Precipitation Index : A probability index which uses a standardized scales showing negative for drought, and positive for wet conditions. Originally developed for US 1889-1991. McKee et al., 1993
30	SPEI	Standardised Precipitation Evapotranspiration Index: A multi-scalar drought index based on climatic data used for determining the onset, duration and magnitude of drought conditions with respect to normal conditions in a variety of natural and managed systems such as crops, ecosystems, rivers, water resources, etc. Originally developed for Iberia 1961-2011. Vicente-Serrano et al., 2010
31		Threshold based indices : A threshold associated with a significant climatic value or requiring some operational intervention, e.g. flood or drought mitigation.
32	SDII	Simple day (precipitation) intensity index: The ratio of annual or seasonal total rainfall to the number of days during the year or season when rainfall occurred.
33	EPIC	European Precipitation Index based on simulated Climatology: An index based on simulated climatology used as to monitor the European domain for upcoming severe storms possibly leading to flash floods. Originally developed for the simulation period e.g. 1971-2001. Alfieri et al., 2012.
34	CEI	Circulation Extremity Index: An event ranking index based on a 28-member model ensemble. Originally developed for the period 1958-2002. Kaspar & Mueller, 2014

35	mCEI	Modified Circulation Extremity Index: 5-component circulation index incorporating max/min temp, PDSI, number wet/dry days and proportion of heavy rain days, originally developed for the period 1950 to 2012. Gallant et al., 2014.
		Drought indices
36	PDSI	Palmer Drought Intensity Index: Precipitation and temperature analyzed in a water balance model; comparison of meteorological and hydrological drought across space and time. See also Palmer Hydrological Drought Index (PHDI). Sheffield et al. 2012, Palmer W. C., 1965
37	scPDSI	Self-calibrating PDSI: Improves on PDSI by changing the (US based) standardization and measures the departure of soil moisture from the normal conditions, using a hydrological accounting system. Antofie 2015, Van der Schrier 2014, Wells & Goddard 2004
38	RDI	Reconnaissance Drought Indicator The ratio of rainfall to PET. Spinoni 2015, Antofie 2015
39	PADI	Palfai Drought Index : The ratio of the mean temperatures from April to August and the monthly precipitation from October to August. Antofie 2015, Palfai 1990
40	SWI	Soil Water Index: METOP ASCAT satellite product Global, 0.1° and continents at various depths http://land.copernicus.eu/global/products/swi Copernicus
41	CMI	Crop moisture index: Derived from the PDSI, the CMI estimates short-term crop moisture and drought for US crop-producing regions. https://www.drought.gov/drought/ Heim 2002, Bradford 2000, Palmer W C., 1968
42	SWSI	Surface Water Supply Index: Developed in the US (Colorado) to complement PDSI in managed catchments. Heim 2002, Bradford, 2000, Shafer and Dezman, 1982.
		Excess heat indices
43	EHF	Excess heat factor from Perkins & Alexander (2013) and Nairn (2009). $EHI(accl) = ((T_i + T_{i-1} + T_{i-2}) / 3) – ((T_{i-3} + ... + T_{i-31})/30)$ $EHI(sig) = ((T_i + T_{i-1} + T_{i-2}) / 3) – T_{95}$ $EHF = \max(1, EHI(accl)) \times EHI(sig)$ When EHF > 0, then heat wave conditions are present. This index is used for forecasting purposes (BoM) and the UK Met Office Global Hazard Map but also for the impacts studies (e.g. PwC 2011).
44	HWM	Heat Wave Magnitude Index from Russo et al. (2014) The HWMI is defined as the maximum magnitude of the heat waves in a year, where a heat wave is the period >= 3 consecutive days with maximum temperature above the daily threshold for the reference period 1981-2010. This threshold is the 90^{th} percentile of the daily maximum centred on a 31 day window (Russo et al. 2014).

A.2 Case studies

A2.1 Case study: 2010 Russia heat wave

Comprehensive reviews of this extreme event are given by Grumm (2011) and Barriopedro et al. (2011) which show the highest July temperature in the region since records began (WMO, 2010). The event lasted nearly two months without respite, from late June well into August. The high temperatures, which had been preceded by very dry conditions, resulted in widespread wildfires, which, as in Greece in 2007, worsened the impacts of the heat, especially in urban centres (Kovonalov et al., 2011). The excess mortality figures are of a similar magnitude as those from the 2003 event in western Europe (around 55,000 e.g. Matsueda 2011, Barriopedro et al., 2011), and there were substantial economic losses, especially in agriculture (Coumou & Rahmstorf 2012). The spatial extent of this event was greater than that of the previous significant event, in 2003 (Barriopedro et al., 2011). A number of studies have connected the events in Russia with the extreme flooding event in Pakistan which occurred roughly at the same time (Lau & Kim, 2010, Trenberth & Fasullo, 2012, Galarneau et al., 2012). Otomi et al. (2012) suggest that a reversal of the Arctic Oscillation early in the summer drove the high temperatures seen in Europe, but also Japan, as well as the preceding cold winter. In determining to what extent this event is attributable to anthropogenic climate change two apparently opposing results were obtained (Dole et al., 2011, Rahmstorf & Coumou 2011). However, Otto et al. (2012) have reconciled these two studies by finding that the magnitude (intensity) of the heat wave was possible without human influences, but that its probability of occurring has increased as a result of anthropogenic emissions.

This event can be represented in a number of different ways. Using an individual station from HadISD (Dunn et al., 2012), the daily timeseries can show clearly the duration of the event and its intensity. Figure 46 shows the daily average temperature in 2010 for the station in the Moscow Botanic Gardens, compared to the average and expected range. By integrating these excess degrees over time for each station, maps of a combined duration and intensity show the extent of the heat wave (Figure 46 left). Showing the same event using one of the indices suggested in Perkins & Alexander (2013), the Excess Heat Factor (EHF, Nairn et al., 2009) has a much wider extent (Figure 46 right). For the ETCCDI percentile based indices, again there are subtle differences depending which dataset it used. Figure 47 (Donat et al., 2013a) shows the overall characteristics of this heat wave are very similar, with high numbers of warm days and warm nights in July and August.

Figure 46: The year of 2010 for the station in Moscow Botanic Gardens (lat=55.8, lon=37.6) is shown in green from HadISD (Dunn et al., 2012). The climatological mean calculated over 1975-2005 and smoothed by a 21-point binomial filter is shown by the black curve. The 5th and 95th percentiles are shown by the red lines, with yellow shading in between. The area highlighted in red is what is measured by the integrated degree days index in Figure 47.

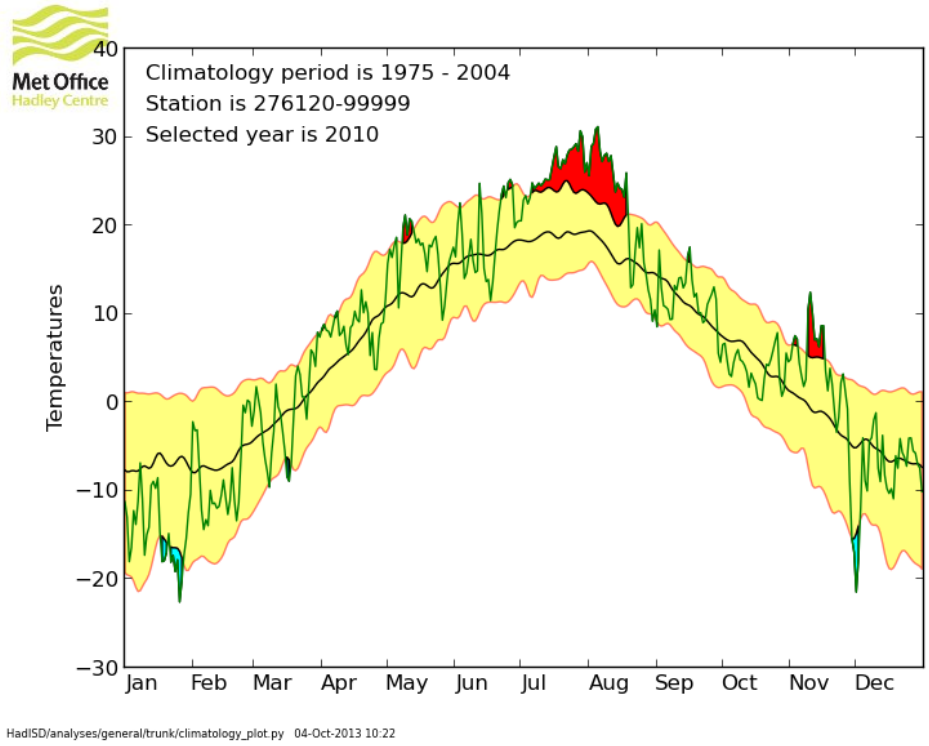

Figure 47: (left) the integrated degree days and (right) the integrated EHF calculated from HadISD for July and August 2010.

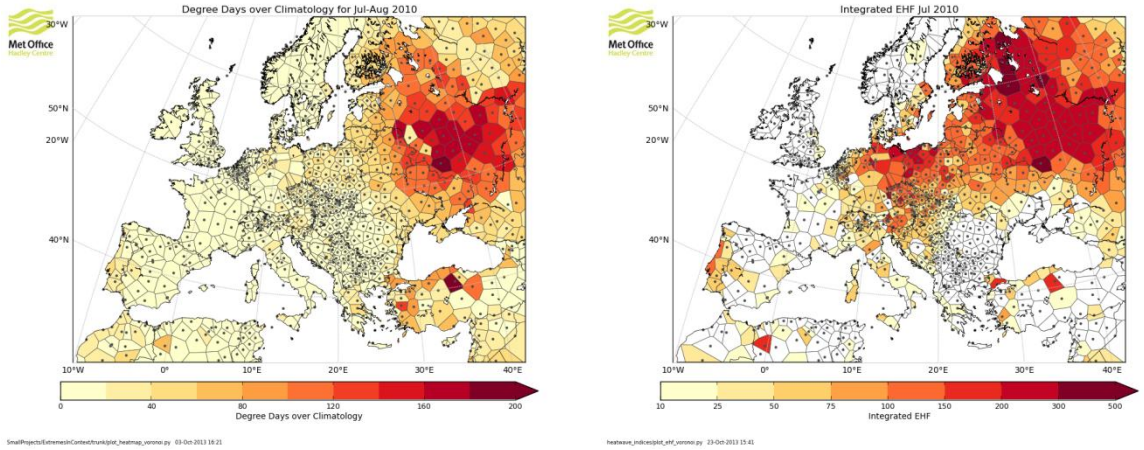

Figure 48: the TN90p (left) and the TX90p (right) indices from HadEX2 (Donat et al., 2013a) for July and August 2010. In a normal month, the expectation would be for around 3 days to be above the 90th percentile when using the TX90p and TN90p measures.

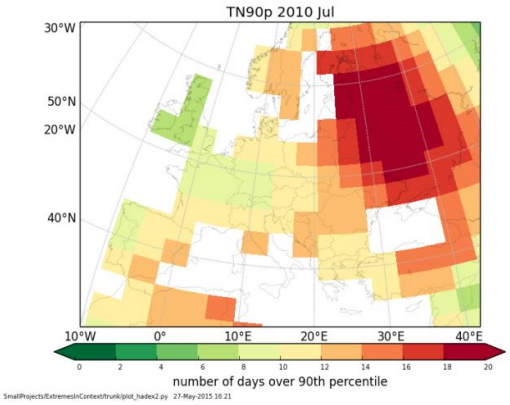
TN90p 2010 Jul
30°W
50°N
20°W
40°N
10°W
0°
10°E
20°E
30°E
40°E
0 2 4 6 8 10 12 14 16 18 20
number of days over 90th percentile
SmallProjects/ExtremesInContext/trunk/plot_hadex2.py 27-May-2015 16:21

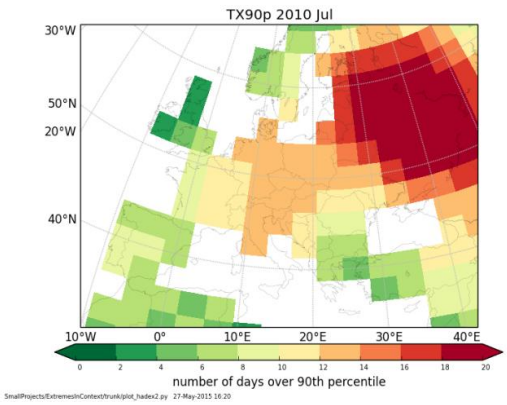
TX90p 2010 Jul
30°W
50°N
20°W
40°N
10°W
0°
10°E
20°E
30°E
40°E
0 2 4 6 8 10 12 14 16 18 20
number of days over 90th percentile
SmallProjects/ExtremesInContext/trunk/plot_hadex2.py 27-May-2015 16:20

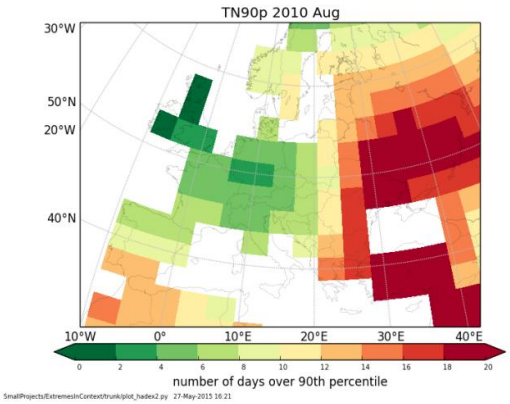
TN90p 2010 Aug
30°W
50°N
20°W
40°N
10°W
0°
10°E
20°E
30°E
40°E
0 2 4 6 8 10 12 14 16 18 20
number of days over 90th percentile
SmallProjects/ExtremesInContext/trunk/plot_hadex2.py 27-May-2015 16:21

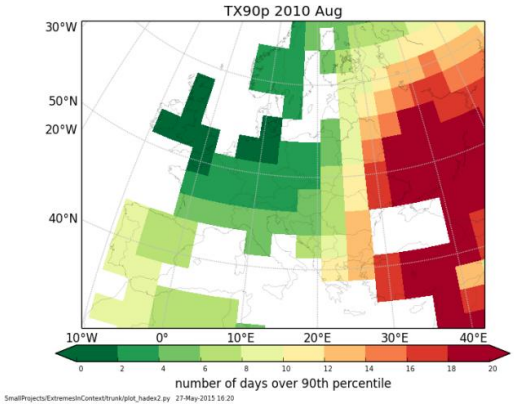
TX90p 2010 Aug
30°W
50°N
20°W
40°N
10°W
0°
10°E
20°E
30°E
40°E
0 2 4 6 8 10 12 14 16 18 20
number of days over 90th percentile
SmallProjects/ExtremesInContext/trunk/plot_hadex2.py 27-May-2015 16:20

A3.2 Case study: 2002 and 2013 extreme precipitation

ECA&D data have been analysed by KNMI for two noteworthy Central European heavy precipitation events of 11 and 12 August 2002 and 30 May-2 June 2013. Precipitation amounts exceeded 100mm during late May /early June 2013 over a sizeable area of Switzerland, Austria, southern and eastern Germany and Czech Republic (Figure 49. Some stations recorded over 200mm, close to the average monthly precipitation amount. Figure 50 shows precipitation anomalies for the two events compared with the 1981-2010 baseline.

Figure 49: Total observed precipitation for the events of 11-12 August 2002 (left) and 30 May - 2 June 2013[38].

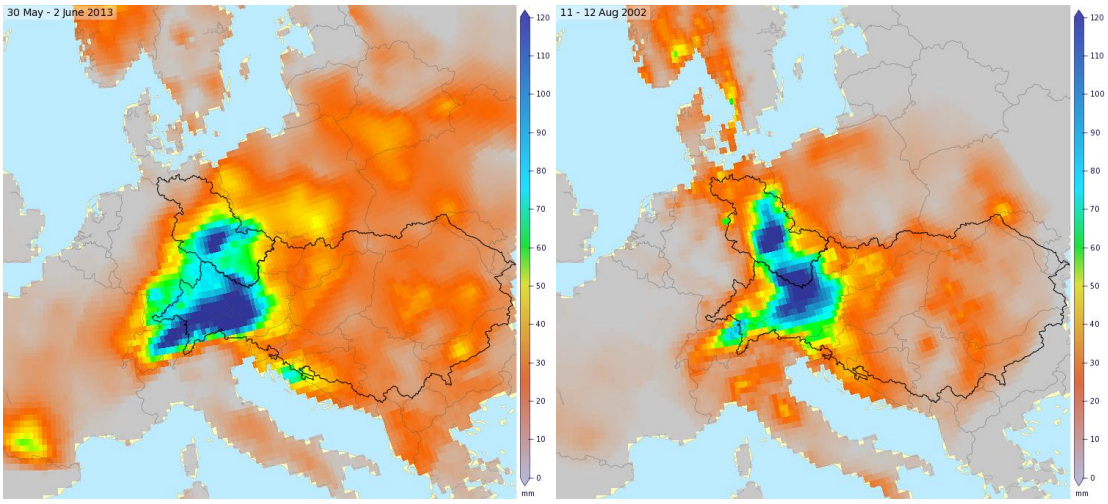

Figure 50: Precipitation anomaly in percentage for July 2002 (left) and May 2013 (right) with respect to the normal amount over the period 1981-2010 (source: E-OBS).

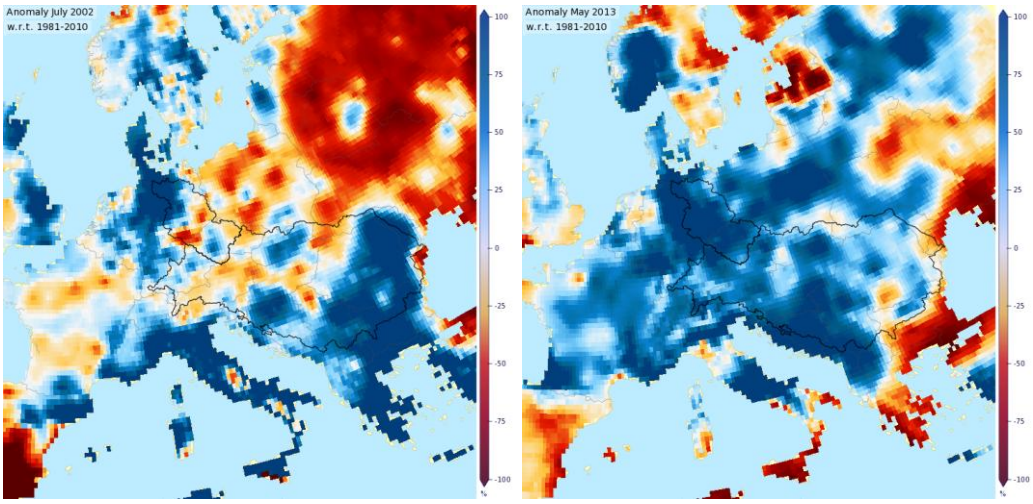

Although generally similar, the events differ in terms intensity, duration and antecedent conditions and generated very different impact in terms of flooding. The 2002 event was a high intensity short duration event concentrated over the Elbe basin. The 2013 event was less intense but followed a wetter than average month with record high soil moisture values in a large part of Germany. Examination of historic ECA&D data for 1951- 2012 did not indicate any significant trend in extreme precipitation.

[38] http://cib.knmi.nl/mediawiki/index.php/Central_European_flooding_2013

Figure 51 suggests a trend towards more heavy precipitation days in May, and the opposite in June, but the differences are generally not significant (green circles). A seasonal analysis indicates a significant shift towards wetter winters.

Figure 51: Trend in very heavy (>20mm) precipitation days 1951-2012 for May (left) and June (right) (source: E-OBS).

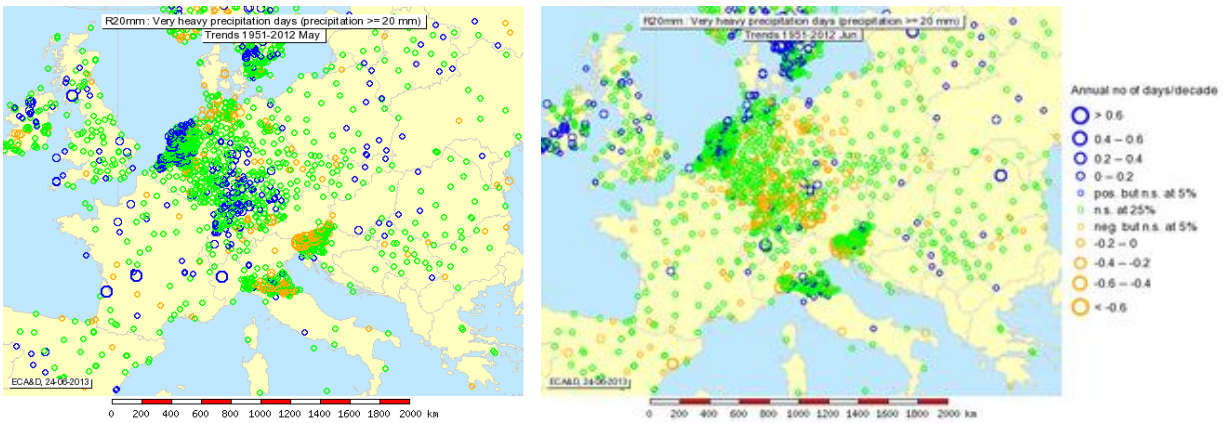

The study concludes that there is no convincing evidence of a tendency towards more extreme precipitation events in this region during the warm season. However, the frequency of weather patterns associated with heavy rainfall event has increased, and heavy precipitation events are projected to increase in frequency, intensity and/or amount under global warming (Hirabayashi et al., 2013). The study also highlights the influence of high sea surface temperatures in the eastern Mediterranean and especially the Black Sea, and persistence of the low pressure system due to meanders in the Northern Hemisphere jet stream[39] on the heavy precipitation events.

Scientific Issues

Data are required at a resolution sufficient to quantify intensity and location of heavy and extreme rainfall. Rain gauge data are available over land only, and are sparse in some places. Satellite data provides greater coverage, and radar data provides high resolution data in certain areas. There are a number of merged synoptic and radar/satellite data, but they combine data from different sources and methodologies.

Gauge records are of variable length and there may be discontinuities when they are moved or replaced. Satellite data are available for at most 30 years, and may contain several updates to instruments and processing algorithms resulting in temporal discontinuities. The use of different datasets by country or region can result in spatial discontinuities at national borders.

A2.3 Case study: Drought in 2011 in Europe

A study[40] of the European drought of 2011 found the autumn was dry over most of Europe, when several European countries including Germany, the Netherlands, Slovakia and the Czech Republic

[39] The jet stream is a narrow band of fast flowing air at high altitudes generally flowing from the west to east over the mid-latitudes and are caused by a combination of the planet's rotation on its axis and atmospheric heating (by solar radiation).
[40] http://cib.knmi.nl/mediawiki/index.php/European_Drought_in_November_2011

reported the lowest recorded precipitation in November. River levels were below average in large parts of central and eastern Europe, affecting navigability for example on the Rivers Rhine and Danube. Low reservoir levels affected electricity production in Serbia, Bosnia experienced drinking water shortages, and winter crop production was reduced in Romania, Bulgaria, Hungary and the Ukraine, where winter grain yields were estimated to be 30 percent below average. Unusually dry conditions also triggered forest fires in several countries including Germany (Upper Bavaria), the Ukraine, Moldova and Slovakia.

An analysis of EC&D station data for 200 stations showed that November 2011 was the driest November since 1920 and autumn 2011 was the sixth driest autumn since 1920. An analysis of three indices, the total precipitation amount, the number of consecutive dry days (CDD) and the monthly maximum consecutive 5-day precipitation amount (RX5d), showed an increasing trend in autumn (SON) precipitation over this period, although parts of Europe showed the opposite - a reduction in November precipitation (Klein Tank et al., 2009). The study showed a reduction in the number of consecutive dry days in autumn, while a general increase, especially in eastern Europe, was observed in November although the pattern is noisy. For the month of November in the study period, eastern Europe showed a drying trend while western Europe is observed to get wetter. The extensive drought of November 2011 and the dry conditions during the whole autumn season are not consistent with the long-term trends observed.

The analysis of the 2011 European drought[3] included an analysis of long term trends in terms of precipitation anomaly, CDD and SPI. Only stations for which the trend is significant at the 25% level are shown. Hence, November 2011 drought and the dry conditions during the whole autumn season, are not consistent with the long-term trends as observed in a large number of stations (Figures 52 and 53, van den Besselaar).

2011 was the mid-point of a significant multi-year drought in the UK from 2010 to 2012 (Kendon et al., 2013). In terms of rainfall accumulations over 12–24 months, the drought was in the top ten most significant events across England and Wales in the last 100 years in lowland regions. Reduced spring rainfall impacted severely on water resources, streamflows and agriculture causing environmental stress, and loss of amenities. From early April 2012, there was an abrupt change in the jet stream position and UK weather patterns which transformed the hydrological situation. Exceptional rainfall terminated the drought abruptly, avoiding the anticipated economic, social and environmental impact, and concern turned to flooding (Marsh et al., 2013).

Figure 52: Trend over the period 1951-2012 when the trend is significant at 25% or higher. Stations for which the trend is not significant at 25% are not shown. Top left: Precipitation in autumn, top right: precipitation in November, middle left: consecutive dry days in autumn, middle right: consecutive dry days in November, bottom left: Maximum 5-day precipitation amount in autumn, bottom right: Maximum 5-day precipitation amount in November. Note that the erratic nature of precipitation adds to the noisy character of the trends in precipitation amount and maximum 5-day precipitation amount.

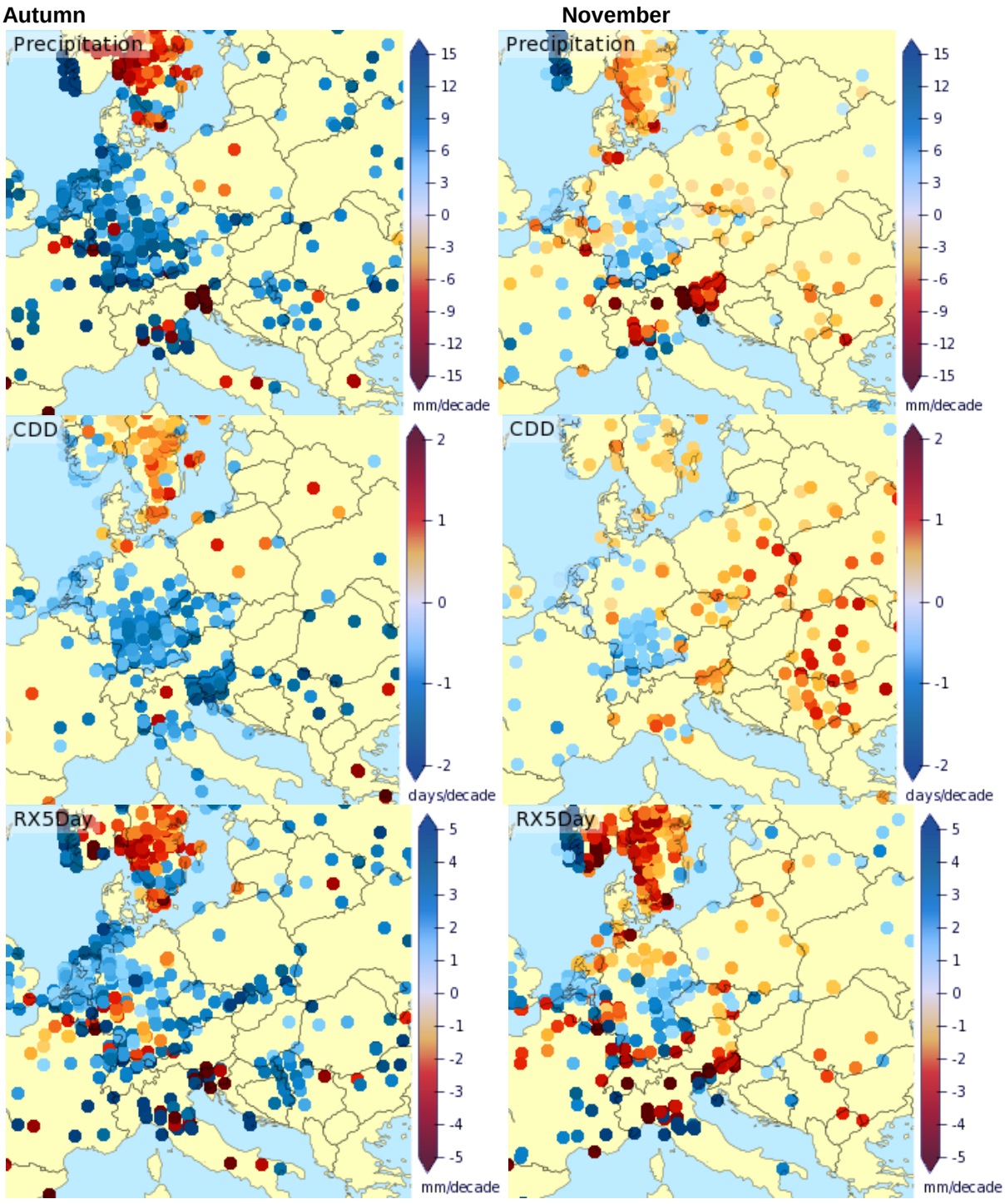

Figure 53: 20-year return values of consecutive dry days in November determined over the period 1991-2010.

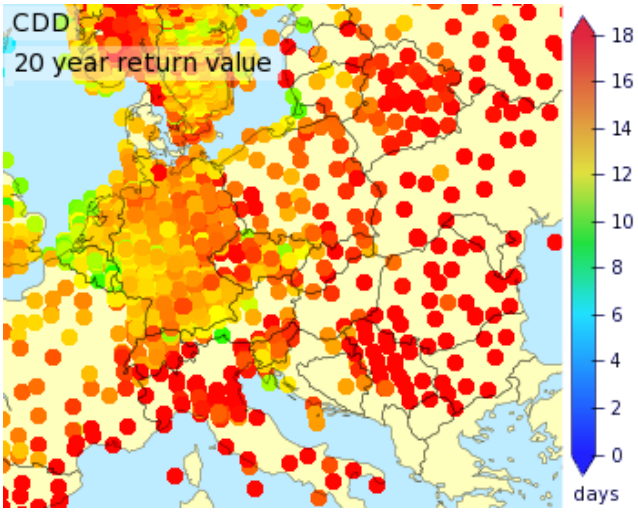

A2.4 Case Study Hail

Following a heat wave in late July 2013 with temperatures in excess of 35 °C, weather front Andreas affected large parts of Central Europe. Severe hailstorms occurred in two regions in Germany, the first around Hannover and Wolfsburg on 27th July; the second was in the Baden-Württemberg region of southern Germany, where golf-ball sized hail stones caused major damage to roofs, windows, solar panels and other installations the cities of Rotenberg, Tuebingen und Reutlingen[41] (Figure 54). Total losses for the insurance industry are estimated to be €4.2 billion including insured losses of €3.2 bn (Munich Re).

Figure 54: Images of hail damage and largest hailstone on 6 August 2013, Swabian Jura

Radar-based hail hazard assessment reveals a large-scale increase in hail probabilty from northern-to-southern Germany, as well as local-scale hot spots due to flow modifications by orography. Statistical models indicate an increase in hail coccurence in past decade and an increased hail potential in the future due to increased convective energy caused by an increase in low-level moisture.

The southern event occurred on the Swabian Jura, a high plateau extending 220 km from south west (at the foot of the Black Forest) to northeast, and approximately 50 km wide. Research shows that hail storms are related to orography, often occurring leeward of elevated terrain (Baldi et al., 2014).

Figure 55 (a) shows hail size and location in Germany 27th July-6th August 2013, with larger hail stones exceeding 8cm. Figure 56 shows the number of hail days per 1 x 1 km² in which hail signals were detected in DWD radar data between 2005 and 2013 . Distincy clusters can be seen in southern and central Germany.

[41] http://www.swissre.com/media/news_releases/nr_20130923_hailstorms.html

Figure 55: (a) Hail size and location in Germany 27th July-6th August 2013 (b) Number of hail days per 1 x 1 km² in which hail signals were detected in DWD radar data between 2005 and 2013. Source: Karlsruher Insitut für Technologie (KIT).

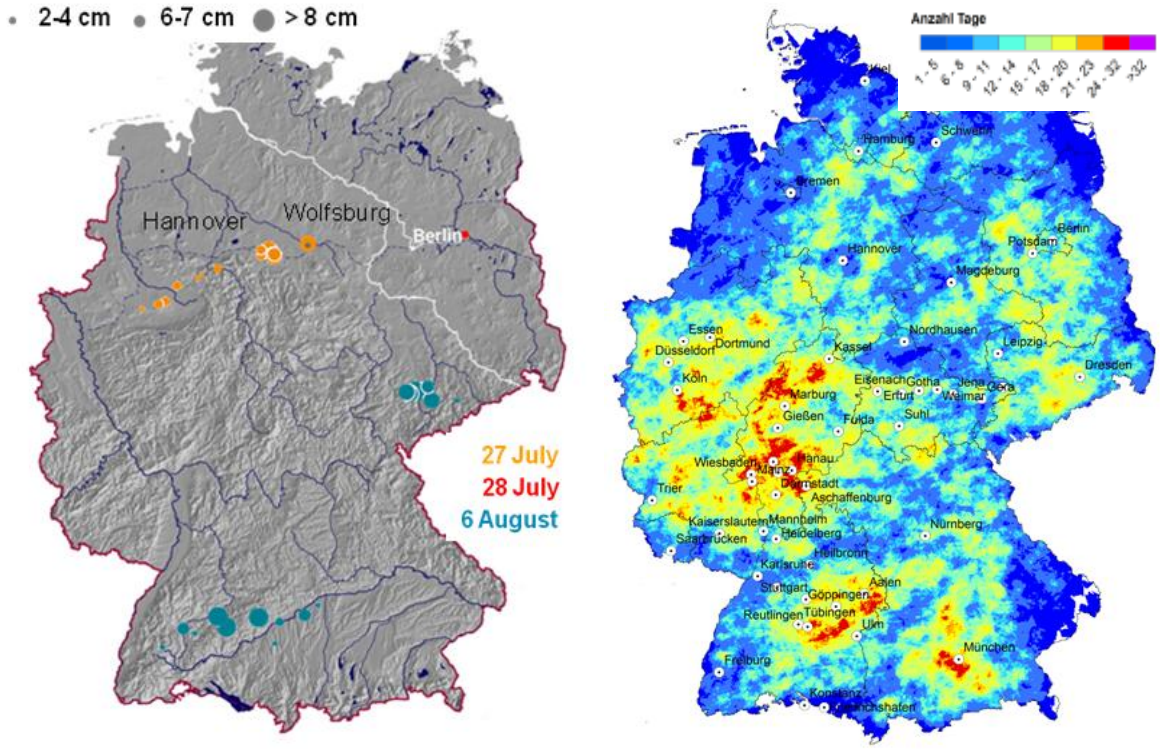

Figure 56 shows a close correlation between the Overshooting Tops (OT) based climatology and model derived hail day density (Punge et al., 2014), showing the increased likelihood of hail in elevated regions of northern Italy and southern Germany. It also demonstrates the usefulness of this satellite based remote sensing technology for estimating hail risk.

Figure 56: Comparison between (a) OT-based climatology (occurences per year and 100 km²) and (b) Hail day density (Hand and Cappelutti, 2011).

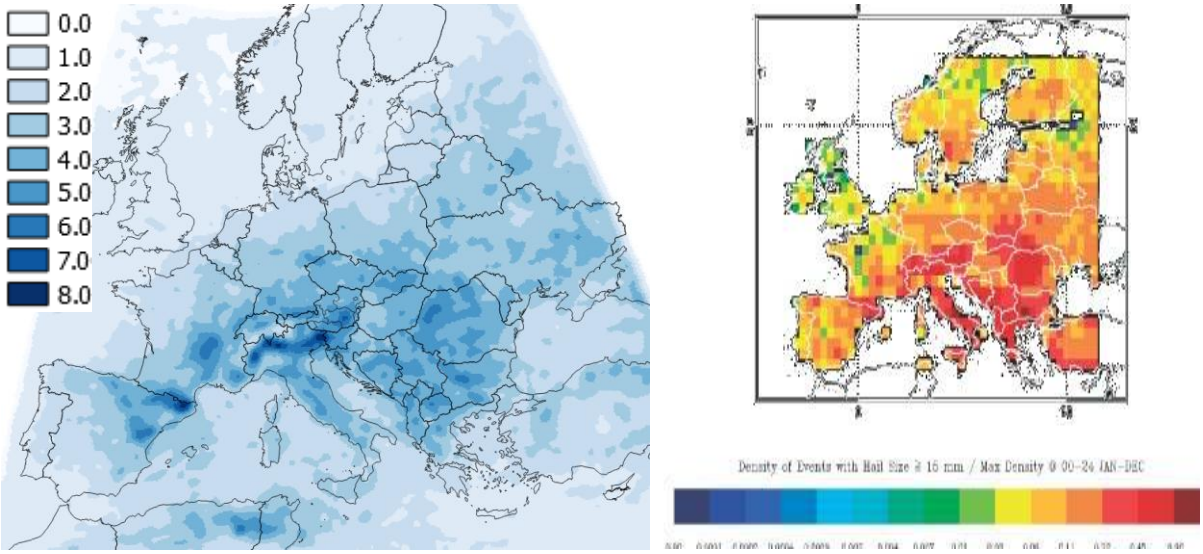

Research predicts an increase in the frequency and magnitude of severe hail events in future. This case study demonstates the benefits of PHI and OT to improve the identification and quantification of

extreme hail events, enabling measures to be taken to mitigate their impact and reduce costs associated with hail damage.

The July 2013 event was joint first largest on record along with the event in 1984 which affected Munich. Flooding occurred in southern and eastern Germany in June, then large parts of Central Europe experienced a heat wave with temperatures peaking far beyond 35 °C in late July – the highest temperature in Germany was recorded in Rheinfelden (Baden) at 38.6 °C. The storms developed in the coastal regions of southern France, in the zone between warm sub-tropical air and cool Atlantic air, developing into a mesoscale convective complex (MCC). A hail bearing weather front crossed large parts of Central Europe between 26 and 30 July, and in Germany, a region 5 km by 27 km south of Stuttgart on the borders of the Swabian Alb, and a zone northeast of the Ruhr up to Wolfsburg, were severely affected. At €2.8 billion, the hailstone damage was the most expensive hailstorm in Germany's history and the world's most expensive event for the insurance industry in 2013[42].

[42] http://www.genre.com/knowledge/publications/iipc1404-en.html

References

Alexander L.V., Zhang X., Peterson T.C., Caesar J., Gleason B., Klein Tank A.M.G, Haylock M., Collins D., Trewin B., Rahimzadeh F., Tagipour A., Rupa Kumar K., Revadekar J., Griffiths G., Vincent L., Stephenson B., Burn J., Aguilar E., Brunet M., Taylor M., New M., Zhai P., Rusticucci M., and Vazquez-Aguirre J.L., 2006, Global observed changes in daily climate extremes of temperature and precipitation, JOURNAL OF GEOPHYSICAL RESEARCH, VOL. 111, D05109, doi:10.1029/2005JD006290, 2006

Alfieri L., Burek P., Feyen L., Forzieri G., 2015 Global warming increases the frequency of river floods in Europe European Commission – Joint Research Centre, Ispra,

Alfieri, L. , Thielen, J., 2012, A European precipitation index for extreme rain-storm and flash flood early warning, Met Apps, Special Issue: Rainfall: high-resolution observation and prediction. Guest editors: C. Charlton-Perez, H. L. Cloke and A. Ghelli

Antofie T, Naumann, Spinoni J, and Vogt J, Estimating the water needed to end the drought or reduce the drought severity in the Carpathian region, Hydrology and Earth System Sciences (Impact Factor: 3.64). 01/2015; 19:177-193. DOI: 10.5194/hess-19-177-2015

Aran M., J.C. Pena, M. Torà, Atmospheric circulation patterns associated with hail events in Lleida (Catalonia), Atmospheric Research 100 (2011) 428–438.

Arblaster, J. M., & Alexander, L. V. (2012). The impact of the El Niño-Southern Oscillation on maximum temperature extremes. Geophysical Research Letters, 39(20).

Avila, F. B., Dogn, S., Menang, K. P. Rajczak, J.,Renom, M., Donat, M.G., Alexander, L.V. (2015) Systematic investigation of gridding-related scaling effects on annual statistics of daily temperature and precipitation maxima: a case study for south-east Australia, Weather and Climate Extremes, submitted

Bachmair,S., Svensson,C., Hannaford,J., Barker,L.J., and Stahl,K.: A quantitative analysis to objectively appraise drought indicators and model drought impacts, Hydrol. Earth Syst. Sci. Discuss., 12, 9437-9488, doi:10.5194/hessd-12-9437-2015, 2015

Baldi, M., Ciardini, V., Dalu, J.D., De Filippis, T., Maracchi, G., Dalu, G., Hail occurrence in Italy: Towards a national database and climatology Atmospheric Research, Volume 138, 1 March 2014, Pages 268-277

Ballesteros,M., Gonzales-Tanago, I., Urquijo, J., De Stefano, L., Vulnerability to drought: Mapping underlying factors across Europe, (in the book Drought: Research and Science-Policy Interfacing, eds. Joaquin Andreu, Abel Solera, Javier Paredes-Arquiola, David Haro-Monteagudo, Henny van Lanen, CRC Press, 2015).

Ban, N., Schmidli, J., Schär, C., 2015, Heavy precipitation in a changing climate: Does short-term summer precipitation increase faster?. GRL, 42, 1165-1172.

Barker, L.J., Hannaford, J., Svensson, C., Tanguy, M. (2015). A preliminary assessment of meteorological and hydrological drought indicators for application to catchments across the UK. Proceedings of the International Conference on Drought: Research and Science-Policy Interfacing, Valencia, Spain, 10-13 March 2015 – Andreu et al. (Eds) © 2015 Taylor & Francis Group, London, ISBN 978-1-138-02779-4

Barriopedro, D., Fischer, E.M., Luterbacher, J., Trigo, R.M., García-Herrera, R., (2011), The hot summer of 2010: redrawing the temperature record map of Europe, Science, 332(6026), 220-224

Beniston, M., 2004, The 2003 heat wave in Europe: A shape of things to come? An analysis based on Swiss climatological data and model simulations, Geophys. Res. Lett., 31, L02202.

Berthet, C., Dessens, J., Sanchez, J.L, Regional and yearly variations of hail frequency and intensity in France, 2011, Atmospheric Research, Volume 100, Issue 4, June 2011, Pages 391–400

Berthet, C., Wesolek, E., Dessens, J., Extreme hail day climatology in Southwestern France, 2011, Atmospheric Research. VOL. 123, pp. 139–150 2013, 6th European Conference on Severe Storms, Palma de Mallorca, Spain

Black, E., Blackburn, M., Harrison, G., Hoskins, B., & Methven, J. (2004). Factors contributing to the summer 2003 European heat wave. Weather, 59(8), 217-223

Blauhut. V., Stahl. K., 2015, DROUGHT:R&SPI Technical Report #27 from De Stefano et al., 2015.

Blauhut, V., Gudmundsson, L., Stahl, K. (2015): Towards pan-European drought risk maps: quantifying the link between drought indices and reported drought impacts, Environ. Res. Lett. 10, 014008, doi:10.1088/1748-9326/10/1/014008

Blenkinsop, S., Fowler, H.J., 2007, Changes in European drought characteristics projected by the PRUDENCE regional climate models." International Journal of Climatology 27(12): 1595-1610

Blenkinsop, S., Chan S.C., Kendon E.J., Fowler H.J., (2015), Temperature influences on intense UK hourly precipitationand dependency on large-scale circulation, Environmental Research Letters 2015, 10(5), 054021

Blunden, J. and Arndt, D. S., 2015: State of the Climate in 2014. Bull. Amer. Meteor. Soc., 96, ES1–ES32. doi: http://dx.doi.org/10.1175/2015BAMSStateoftheClimate.1

Bradford, R.B., Drought Events in Europe, in Vogt J.V., & Somma F., (eds.), Drought and Drought Mitigation in Europe, 2000

Briffa, K. R., van der Schrier, G., Jones, P. D., 2009, Wet and dry summers in Europe since 1750: evidence of increasing drought. Int. J. Climatol. 29, 1894–1905

Brooks, H. E., 2009, Proximity soundings for severe convection for Europe and the United States from reanalysis data, Atmospheric Research 93(1-3): 546-553

Brooks, H.E., Severe thunderstorms and climate change, Atmospheric Research, Volume 123, 1 April 2013, 129-138, http://dx.doi.org/10.1016/j.atmosres.2012.04.002

Burke, E. J., R. H. J. Perry, et al. (2010). "An extreme value analysis of UK drought and projections of change in the future." Journal of Hydrology 388(1-2): 131-143

Busuioc, A., Dumitrescu, A., Soare, E., & Orzan, A. (2007). Summer anomalies in 2007 in the context of extremely hot and dry summers in Romania. Romanian Journal of Meteorology, 9(1-2), 1-17

Buttafuoco, G.; Caloiero, T.; Coscarelli, R. Analyses of Drought Events in Calabria (southern Italy) Using Standardized Precipitation Index, WATER RESOURCES MANAGEMENT, Volume:29, Issue:2, Pages:557-573, Special Issue: SI, DOI: 10.1007/s11269-014-0842-5, Published:JAN 2015

Buttstaedt, M; Schneider, C, Climate change signal of future climate projections for Aachen, Germany, in terms of temperature and precipitation , METEOROLOGISCHE ZEITSCHRIFT Volume: 23 Issue: 1 Pages: 63-74 Published: JUN 2014

Caesar, J., L. Alexander, and R. Vose (2006), Large-scale changes in observed daily maximum and minimum temperatures: Creation and analysis of a new gridded data set, J. Geophys. Res., 111, D05101, doi:10.1029/2005JD006280

Casanueva, A., Rodríguez-Puebla, C., Frías, M.D., González-Reviriego, N., Variability of extreme precipitation over Europe and its relationships with teleconnection patterns, Hydrol. Earth Syst. Sci., 18, 709–725, 2014 www.hydrol-earth-syst-sci.net/18/709/2014

Cattiaux, J., Douville, H., Schoetter, R., Parey, S., & Yiou, P., 2015, Projected increase in diurnal and inter-diurnal variations of European summer temperatures. Geophysical Research Letters

Cattiaux, J., Vautard, R., Cassou, C., Yiou, P., Masson-Delmotte, V., & Codron, F. (2010). Winter 2010 in Europe: a cold extreme in a warming climate. Geophysical Research Letters, 37(20)

Cattiaux, J., Yiou, P., & Vautard, R. (2012). Dynamics of future seasonal temperature trends and extremes in Europe: a multi-model analysis from CMIP3. Climate dynamics, 38(9-10), 1949-1964

Chan, S. C., E. J. Kendon, et al. (2013). "Does increasing the spatial resolution of a regional climate model improve the simulated daily precipitation?" Climate Dynamics 41(5-6): 1475-1495.

Chan, S.C., E J Kendon, NM Roberts, HJ Fowler, & S Blenkinsop, Temperature constraints on UK precipitation do not extend to future hottest days, February 2015 submitted to Nature Geoscience

Chan S.C., E J Kendon, H J Fowler, S Blenkinsop and N M Roberts, (2014) Projected increases in summer and winter UK sub-daily precipitation extremes from high resolution regional climate models. Environ. Res. Lett. 9, 084019

Chan S.C., Kendon E.J., Fowler H.J., Blenkinsop S. and Roberts N.M., Ferro C.A.T., (2014), The value of high-resolution Met Office regional climate models in the simulations of multi-hourly precipitation extremes. J Climate, 27, 16, 6155-6174, doi 10.1175/JCLIM-13-00723.1

Christidis N., Jones G.S., Stott P.A., (2015), Dramatically increasing chance of extremely hot summers since the 2003 European heat wave, Nature Climate Change, 5, 46–50 (2015) doi:10.1038/nclimate2468

Christidis N., Stott P. A., Brown S. J. (2011). The role of human activity in the recent warming of extremely warm daytime temperatures. Journal of Climate, 24(7), 1922-1930.

Christidis N., Stott P. A., Brown S., Hegerl, G. C., Caesar J. (2005). Detection of changes in temperature extremes during the second half of the 20th century. Geophysical Research Letters, 32(20).

Chrysanthou A., Schrier, G., Besselaar E.J.M., Klein-Tank, A.M.G., Brandsma T., (2014). The effects of urbanization on the rise of the European temperature since 1960. Geophysical Research Letters, 41(21), 7716-7722.

Ciais P., Reichstein M., Viovy N., Granier A., Ogée J., Allard V., Valentini R. (2005). Europe-wide reduction in primary productivity caused by the heat and drought in 2003. Nature, 437(7058), 529-533.

Clark R.T, Brown S.J, Murphy J.M (2006) Modeling Northern Hemisphere summer heat extreme changes and their uncertainties using a physics ensemble of climate sensitivity experiments, J. Clim., 19, 4418–4435

Collins, M., R. Knutti, J. Arblaster, J.-L. Dufresne, T. Fichefet, P. Friedlingstein, X. Gao, W.J. Gutowski, T. Johns, G.Krinner, M. Shongwe, C. Tebaldi, A.J. Weaver and M. Wehner, 2013: Long-term Climate Change: Projections, Commitments and Irreversibility. In: Climate Change 2013: The Physical Science Basis. Contribution of Working Group I to the Fifth Assessment Report of the Intergovernmental Panel on Climate Change [Stocker, T.F., D. Qin, G.-K.Plattner, M. Tignor, S.K. Allen, J. Boschung, A. Nauels, Y. Xia, V. Bex and P.M. Midgley (eds.)]. Cambridge University Press, Cambridge, United Kingdom and New York, NY, USA.

Coumou, D., & Rahmstorf, S. (2012). A decade of weather extremes. Nature Climate Change, 2(7), 491-496.

Coumou, D., & Robinson, A. (2013). Historic and future increase in the global land area affected by monthly heat extremes. Environmental Research Letters, 8(3), 034018

Coumou, D., Lehmann, J., & Beckmann, J. (2015). The weakening summer circulation in the Northern Hemisphere mid-latitudes. Science, 1261768.

Cowtan, K., & Way, R. G. (2014). Coverage bias in the HadCRUT4 temperature series and its impact on recent temperature trends. Quarterly Journal of the Royal Meteorological Society, 140(683), 1935-1944.

Dai, A., Trenberth, K. E. & Qian, T. A global data set of Palmer Drought Severity Index for 1870–2002: relationship with soil moisture and effects of surface warming. J. Hydrometeorol. 5, 1117–1130 (2004)

De Lima, M., Isabel, P.; Santo, Fatima Espirito; Ramos, Alexandre M.; Trigo, Ricardo M. Trends and correlations in annual extreme precipitation indices for mainland Portugal, 1941-2007, 2015, THEORETICAL AND APPLIED CLIMATOLOGY, Volume:119, Issue:1-2, Pages:55-75, DOI: 10.1007/s00704-013-1079-6, Published:JAN 2015, 10.1007/s00704-013-1079-6.

De Stefano, L., González Tánago, I., Ballesteros, M., Urquijo, J., Blauhut, V., Stagge, J.H. & Stahl, K. (2015): Methodological approach considering different factors influencing vulnerability - pan-European scale. DROUGHT-R-SPI Technical Report no. 26, 121 pg., Madrid, Spain (http://www.eu-drought.org/technicalreports/2).

Dole R, Hoerling M, Perlwitz J, Eischeid J, Pegion P, Zhang T, Quan X-W, Xu T, Murray D (2011) Was there a basis for anticipating the 2010 Russian heat wave? Geophys. Res. Lett., 38, L06702, doi: 10.1029/2010GL046582.

Dominguez, M., R. Romera, et al. (2013). "Present-climate precipitation and temperature extremes over Spain from a set of high resolution RCMs." Climate Research 58(2): 149-164.

Donat, M. G., and L. V. Alexander (2012), The shifting probability distribution of global daytime and night-time temperatures, Geophys. Res. Lett., 39, L14707, doi:10.1029/2012GL052459.

Donat M.G, Alexander L.V, Yang H, Durre I, Vose R, Dunn R.J.H, Willett K.M, Aguilar E, Brunet M, Caesar J, Hewitson B, Jack C, Klein Tank A.M.G, Kruger A.C, Marengo J, Peterson T.C, Renom M, Oria Rojas C, Rusticucci M, Salinger J, Elrayah A.S, Sekele S.S, Srivastava A.K, Trewin B, Villarroel C, Vincent L.A, Zhai P, Zhang X, Kitching S, (2013a), Updated analyses of temperature and precipitation extreme indices since the beginning of the twentieth century: The HadEX2 dataset, J. Geophys. Res. Atmos., 118, 2098–2118 doi:10.1002/jgrd.50150

Donat, M. G., King, A. D., Overpeck, J. T., Alexander, L. V., Durre, I., & Karoly, D. J. (2015). Extraordinary heat during the 1930s US Dust Bowl and associated large-scale conditions. Climate Dynamics, 1-14.

Donat, M.G., L.V. Alexander, H. Yang, I. Durre, R. Vose, J. Caesar. 2013b. Global Land-Based Datasets for Monitoring Climatic Extremes. Bull. Amer. Meteor. Soc., 94, 997–1006, http://dx.doi.org/10.1175/BAMS-D-12-00109.1.

Dosio, A., P. Paruolo, and R. Rojas (2012), Bias correction of the ENSEMBLES high resolution climate change projections for use by impact models: Analysis of the climate change signal, J. Geophys. Res., 117, D17110,doi:10.1029/2012JD017968.

DROUGHT:R&SPI project Cooperation Work Programme 2011, Theme 6: Environment (including Climate Change, ENV.2011.1.3.2-2: Vulnerability and increased drought risk in Europe (Grant agreement no: 282769), Reports http://www.eu-drought.org/

Dubrovsky, Martin; Hayes, Michael; Duce, Pierpaolo; et al. Multi-GCM projections of future drought and climate variability indicators for the Mediterranean region , REGIONAL ENVIRONMENTAL CHANGE Volume: 14 Issue: 5 Special Issue: SI Pages: 1907-1919 Published: OCT 2014

Dunn, R. J. H., Donat, M. G., and Alexander, L. V.: Investigating uncertainties in global gridded datasets of climate extremes, Clim. Past, 10, 2171-2199, doi:10.5194/cp-10-2171-2014, 2014.

Dunn, R. J. H., Willett, K. M., Thorne, P. W., Woolley, E. V., Durre, I., Dai, A., ... & Vose, R. S. (2012). HadISD: a quality controlled global synoptic report database for selected variables at long-term stations from 1973-2010. Climate of the Past, 8, 1763-1833.

Durack, P. J.,Wijels, S. E. & Matear, R. J. Ocean salinities reveal strong global water cycle intensification during 1950 to 2000. Science 336, 455_458 (2012).

Easterling, D. R., Horton, B., Jones, P. D., Peterson, T. C., Karl, T. R., Parker, D. E., ... & Folland, C. K. (1997). Maximum and minimum temperature trends for the globe. Science, 277(5324), 364-367.

Ehret, U., Zehe, E., Wulfmeyer, V., Warrach-Sagi, K., and Liebert, J.: HESS Opinions "Should we apply bias correction to global and regional climate model data?", Hydrol. Earth Syst. Sci., 16, 3391-3404, doi:10.5194/hess-16-3391-2012, 2012.

European Commission, Disaster Risk Reduction Increasing resilience by reducing disaster risk in humanitarian action, DG ECHO Thematic Policy Document no. 5. September 2013.

European Environment Agency, Climate Change, Impacts & Vulnerabilty in Europe 2012, An indicator based report, EEA Report No. 12, 2012, ISNN 1725-9177 (http://www.eea.europa.eu/publications/climate-impacts-and-vulnerability-2012)

Explaining Extreme Events of 2013 from a Climate Perspective: http://www2.ametsoc.org/ams/index.cfm/publications/bulletin-of-the-american-meteorological-society-bams/explaining-extreme-events-of-2013-from-a-climate-perspective/

Extreme Weather Events in Europe: http://www.easac.eu/fileadmin/PDF_s/reports_statements/Extreme_Weather/Extreme_Weather_full_version_EASAC-EWWG_final_low_resolution_Oct_2013f.pdf

Ferrari, T., Ijjaali E.,, Jabrane M., Van Lanen, H.A.J., and Huang, Y., IAHS Publ. No. 340, 77–85, 2010.

Feldmann, H., G. Schadler, et al. (2013). "Near future changes of extreme precipitation over complex terrain in Central Europe derived from high resolution RCM ensemble simulations." International Journal of Climatology **33**(8): 1964-1977.

Fischer, E. M. (2014). Climate science: Autopsy of two mega-heat waves. Nature Geoscience, 7(5), 332-333.

Fischer, E. M., & Knutti, R. (2014). Detection of spatially aggregated changes in temperature and precipitation extremes. Geophysical Research Letters, 41(2), 547-554.

Fischer, E. M., & Knutti, R. (2015). Anthropogenic contribution to global occurrence of heavy-precipitation and high-temperature extremes. Nature Climate Change. http://dx.doi.org/10.1038/nclimate2617Fischer, E. M., K. W. Oleson, and D. M. Lawrence (2012), Contrasting urban and rural heat stress responses to climate change, Geophys. Res. Lett., 39, L03705, doi:10.1029/2011GL050576.

Fischer, E. M., & Schär, C. (2009). Future changes in daily summer temperature variability: driving processes and role for temperature extremes. Climate Dynamics, 33(7-8), 917-935.

Fischer, E.M., C. Schär, 2010: Consistent geographical patterns of changes in high-impact European heat waves, Nature Geoscience, doi: 10.1038/NGEO866

Fischer, E. M.; Sedlacek, J.; Hawkins, E.; et al., Models agree on forced response pattern of precipitation and temperature extremes , GEOPHYSICAL RESEARCH LETTERS Volume: 41 Issue: 23 Pages: 8554-8562 Published: DEC 16 2014

Fischer, E. M., Seneviratne, S. I., Vidale, P. L., Lüthi, D., & Schär, C. (2007). Soil moisture-atmosphere interactions during the 2003 European summer heat wave. Journal of Climate, 20(20), 5081-5099.

Fischer, E.M., and R. Knutti, 2013: Robust joint projections for humidity and temperature extremes, Nature Climate Change, 3, 120-126, doi:10.1038/nclimate1682Fischer, E.M., K.W. Oleson, and D.M. Lawrence,

2012: Contrasting urban and rural heat stress responses to climate change, Geophys. Res. Lett., 39, doi:10.1029/2011GL050576

Forzieri, G. L. Feyen, R. Rojas, M. Flörke, F.Wimmer, A. Bianchi, Ensemble projections of future streamflow droughts in Europe Hydrol. Earth Syst. Sci., 18, 85–108, 2014 www.hydrol-earth-syst-sci.net/18/85/2014/ doi:10.5194/hess-18-85-2014

Fouillet, A., Rey, G., Laurent, F., et al., (2006). Excess mortality related to the August 2003 heat wave in France. Int. Arch. Occup. Environ. Health, 80, 16–24.

Founda, D., & Giannakopoulos, C. (2009). The exceptionally hot summer of 2007 in Athens, Greece—A typical summer in the future climate?. Global and planetary change, 67(3), 227-236.

Frich P, Alexander LV, Della-Marta P, Gleason B, Haylock M, Klein Tank AMG, Peterson T (2002) Observed coherent changes in climatic extremes during the second half of the twentieth century. Clim Res 19:193–212. doi:10.3354/cr019193

Galarneau Jr, T. J., Hamill, T. M., Dole, R. M., & Perlwitz, J. (2012). A multiscale analysis of the extreme weather events over western Russia and northern Pakistan during July 2010. Monthly Weather Review, 140(5), 1639-1664.

Gallant, Ailie J. E.; Karoly, David J.; Gleason, Karin L., Consistent Trends in a Modified Climate Extremes Index in the United States, Europe, and Australia, JOURNAL OF CLIMATE Volume: 27 Issue: 4 Pages: 1379-1394 Published: FEB 2014

García-Herrera, R., Díaz, J., Trigo, R. M., Luterbacher, J., & Fischer, E. M. (2010). A review of the European summer heat wave of 2003. Critical Reviews in Environmental Science and Technology, 40(4), 267-306.

García-Ortega, E., Fita, L., Romero, R., López, L., Ramis, C., Sánchez, J.L., 2007. Numerical simulation and sensitivity study of a severe hailstorm in northeast Spain. Atmospheric Research 83, 225 – 241

Garssen, J., Harmsen, C., and de Beer, J. (2005). The effect of the summer 2003 heat wave on mortality in The Netherlands. Available at: http://www.eurosurveillance.org/em/v10n07/1007-227.asp

Gervais, M., Tremblay, L. B., Gyakum, J. R., & Atallah, E. (2014). Representing extremes in a daily gridded precipitation analysis over the United States: Impacts of station density, resolution, and gridding methods. Journal of Climate, 27(14), 5201-5218

Giaiotti, D., Nordio, S., Stel, F., 2003. The climatology of hail in the plain of friuli venezia giulia. Atmospheric Research 67-68, 247–259

Giorgi, F. and P. Lionello, 2008, Climate change projections for the Mediterranean region, Global and Planetary Change 63(2-3): 90-104.

Giorgi, F. and E. Coppola, 2010, Does the model regional bias affect the projected regional climate change? An analysis of global model projections, Climatic Change, 100(3-4): 787-795.

Golding BW, 1998: Nimrod: A system for generating automated very short range forecasts Meteorological Applications / Volume 5 / Issue 01 / March 1998, pp 1-16 1998 Meteorological Society

Gornall, J., Betts, R., Burke, E., Clark, R., Camp, J., Willett, K., & Wiltshire, A. (2010). Implications of climate change for agricultural productivity in the early twenty-first century. Philosophical Transactions of the Royal Society B: Biological Sciences, 365(1554), 2973-2989.

Greiser J, Marescot, L., Smith, M., Lai, M., Estimating Hail Insured Loss from Radar Images – Application to the 2013 Events in Germany, 2015, Risk Management Solutions (RMD) UK & Switzerland

Greve, P., Gudmundsson, L., Orlowsky, B., Seneviratne, S.I., 2015, Introducing a probabilistic Budyko framework Geophysical Research Letters, 42, 2261-2269, doi:10.1002/2015GL063449.

Greve, P., Orlowsky, B., Mueller, B., Sheffield, J., Reichstein, M., Seneviratne, S., 2014, Global assessment of trends in wetting and drying over land Nature Geoscience, http://dx.doi.org/10.1038/ngeo2247

Greve, P., Seneviratne, S.I., 2015, Assessment of future changes in water availability and aridity, *Geophys. Res. Lett.*, *42*, 5493–5499,

Grumm, R.H., 2011, The central European and Russian heat event of July-August 2010. Bull. Amer. Meteor. Soc., 92, 1285–1296 doi: http://dx.doi.org/10.1175/2011BAMS3174.1

Grunwald, S., Brooks, H.E., 2011, Relationship between sounding derived parameters and the strength of tornadoes in Europe and the USA from reanalysis data, Atmospheric Research, 100(4): 479-488.

Gudmundsson L. and Seneviratne S., 2015 A comprehensive drought climatology for Europe (1950 -2013), Proceedings of: Drought: Research and Science-Policy Interfacing ; 31-37 ; 978-1-315-68722-3 ; CRC Press

Hadjinicolaou, P., C. Giannakopoulos, et al. ,2011, Mid-21st century climate and weather extremes in Cyprus as projected by six regional climate models,Regional Environmental Change, 11(3): 441-457.

Hagemann, S., Chen, C., Haerter, J.O., Heinke, J., Gerten, D., Piani, C., 2011. Impact of a statistical bias correction on the projected hydrological changes obtained from three GCMs and two hydrology models. J. Hydrometeorol. 12. http://dx.doi.org/10.1175/2011JHM1336.1: 556-578

Hand W H, Cappelluti G, A global hail climatology using the UK Met Office convection diagnosis procedure (CDP) and model analyses Meteorological Applications, Volume 18, Issue 4, pages 446–458, December 2011, DOI: 10.1002/met.236

Hanel M, Adri Buishand T, and Ferro C A T, A non-stationary index flood model for precipitation extremes in transient regional climate model simulations, JOURNAL OF GEOPHYSICAL RESEARCH, VOL. 114, D15107, doi:10.1029/2009JD011712, 2009

Hanlon, H. M., Morak, S., & Hegerl, G. C. (2013). Detection and prediction of mean and extreme European summer temperatures with a multimodel ensemble. Journal of Geophysical Research: Atmospheres, 118(17), 9631-9641.

Hannaford, J.; Lloyd-Hughes, B.; Keef, C.; Parry, S.; Prudhomme, C.. 2011 Examining the large-scale spatial coherence of European drought using regional indicators of rainfall and streamflow deficit. *Hydrological Processes*, 25 (7). 1146-1162. 10.1002/hyp.7644

Hannaford, J., G. Buys, et al. (2013). "The influence of decadal-scale variability on trends in long European streamflow records." Hydrology and Earth System Sciences **17**(7): 2717-2733.

Hannah D.M, Demuth S, Van Lanen H.A.J, Looser U, Prudhomme.C, Rees G, Stahl K and Tallaksen L.M, Large-scale river flow archives: importance, current status and future needs, Hydrological Processes, Volume 25, Issue 7, pages 1191–1200, 30 March 2011

Hansen, J., Ruedy, R., Sato, M., & Lo, K. (2010). Global surface temperature change. Reviews of Geophysics, 48(4)

Hay, L. E., R. J. L. Wilby, et al. (2000). "A comparison of delta change and downscaled GCM scenarios for three mountainous basins in the United States." Journal of the American Water Resources Association **36**(2): 387-397.

Haylock, M., Goodess, C., Haylock, M. and Goddess, C. (2004). Interannual variability of European extreme winter rainfall and links with mean large-scale circulation. International Journal of Climatology 24, 759–776.

Haylock, M.R., Hofstra N, Klein-Tank A.M.G, Klok E.J, Jones P.D, New M (2008), A European daily high resolution gridded data set of surface temperature and precipitation for 1950–2006, J. Geophys. Res., 113, D20119, doi:10.1029/2008JD010201.

Heim R.R, A Review of Twentieth-Century Drought Indices Used in the United States BAMS, 2002

Heim R.R, Brewer M.J, 2012, The Global Drought Monitor Portal: The Foundation for a Global Drought Information System Earth Interactions 12/2012; 16(15):1-28. DOI:10.1175/2012EI000446.1

Heinrich G. and Gobiet, A. (2012) The future of dry and wet spells in Europe: a comprehensive study based on the ENSEMBLES regional climate models, Int. J. Climatol. 32: 1951–1970

Heinselman, P., and A. Ryzhkov, 2006: Validation of polarimetric hail detection. Wea. Forecasting, 21, 839 – 850.

Hermida L., Sánchez J L., López L.,1 Berthet C., Dessens J., García-Ortega E., Merino A., 2013, Climatic Trends in Hail Precipitation in France: Spatial, Altitudinal, and Temporal Variability, Hindawi Publishing Corporation The ScientificWorld Journal, Volume 2013, Article ID 494971, 10 pages http://dx.doi.org/10.1155/2013/494971Hirschi M, Seneviratne S, Alexandrov V, Boberg F, Boroneant C, Christensen O.B, Formayer H, Orlowsky B, Stepanek P (2010) Observational evidence for soil-moisture impact on hot extremes in southeastern Europe, Nature Geoscience 4, 17-21, doi:10.1038/ngeo1032.

Holleman, I.,Wessels, H.R.A., Onvlee, J.R.A., Barlag, S.J.M., 2000. Development of a hail-detection-product. Phys. Chem. Earth B 25, 1293–1297

Horton, D. E., Johnson, N. C., Singh, D., Swain, D. L., Rajaratnam, B., & Diffenbaugh, N. S. (2015). Contribution of changes in atmospheric circulation patterns to extreme temperature trends. Nature, 522(7557), 465-469.

IPCC, 2007. Climate Change 2007: Impacts, Adaptation and Vulnerability. Seneviratne, S.I., T. Corti, E.L. Davin, M. Hirschi, E.B. Jaeger, I. Lehner, B. Orlowsky, and A.J. Teuling (2010) Investigating soil moisture-

climate interactions in a changing climate: A review. Earth-Science Reviews 99(3-4), 125-161, doi:10.1016/j.earscirev.2010.02.004.

EEA (2012) Climate change, impacts and vulnerability in Europe 2012 (EEA Report No 12/2012). European Environment Agency, Copenhagen, accessed 30 June 2014.

IPCC WG2 report, pp503, Section7.3.3.2.2

IPCC, 2013: Summary for Policymakers. In: Climate Change 2013: The Physical Science Basis. Contribution of Working Group I to the Fifth Assessment Report of the Intergovernmental Panel on Climate Change [Stocker, T.F., D. Qin, G.-K. Plattner, M. Tignor, S. K. Allen, J. Boschung, A. Nauels, Y. Xia, V. Bex and P.M. Midgley (eds.)]. Cambridge University Press, Cambridge, United Kingdom and New York, NY, USA

Jacob, D.; Petersen, J.; Eggert, B.; Alias, A.; Christensen, O. B.; Bouwer, L.; Braun, A.; Colette, A.; Déqué, M.; Georgievski, G.; Georgopoulou, E.; Gobiet, A.; Menut, L.; Nikulin, G.; Haensler, A.; Hempelmann, N.; Jones, C.; Keuler, K.; Kovats, S.; Kröner, N.; Kotlarski, S.; Kriegsmann, A.; Martin, E.; Meijgaard, E.; Moseley, C.; Pfeifer, S.; Preuschmann, S.; Radermacher, C.; Radtke, K.; Rechid, D.; Rounsevell, M.; Samuelsson, P.; Somot, S.; Soussana, J.-F.; Teichmann, C.; Valentini, R.; Vautard, R.; Weber, B. & Yiou, P. EURO-CORDEX: new high-resolution climate change projections for European impact research Regional Environmental Change, Springer Berlin Heidelberg, 2013, 1-16.

Jaeger, E. B., & Seneviratne, S. I. (2011). Impact of soil moisture–atmosphere coupling on European climate extremes and trends in a regional climate model. Climate Dynamics, 36(9-10), 1919-1939.Jendritzky, G., de Dear, R., & Havenith, G. (2012). UTCI—Why another thermal index?. International journal of biometeorology, 56(3), 421-428.Johnson, H., Cook, L., and Rooney, C. (2004). Mortality during the heat wave of August 2003 in England and Wales and the use of rapid weekly estimates.WHOFIC/04.081.

Jones, C., F. Giorgi, and G. Asrar, 2011: The Coordinated Regional Downscaling Experiment: CORDEX; An international downscaling link to CMIP5. CLIVAR Exchanges, No. 56, International CLIVAR Project Office, Southampton, United Kingdom, 34–40.

Kapsch M.L., Kunz M., Vitolo R., Economou T., Long-term trends of hail-related weather types in an ensemble of regional climate models using a Bayesian approach, JOURNAL OF GEOPHYSICAL RESEARCH, VOL. 117, D15107, doi:10.1029/2011JD017185, 2012

Karl, TR, Knight, RW, Gallo, KP, Peterson, TC, Jones, PD, Kukla, G, Plummer, N, Razuvayev, V, Lindseay, J and Charlson, RJ (1993) A new perspective on recent global warming: Asymmetric trends of daily maximum and minimum temperature. Bulletin of the American Meteorological Society, 74 (6). pp. 1007-1023. ISSN 0003-0007 (R) *Karl, T.R., N. Nicholls, and A. Ghazi, 1999: CLIVAR/GCOS/WMO workshop on indices and indicators for climate extremes: Workshop summary. Climatic Change, 42, 3-7.*

Karl, T.R., Arguez, A., Huang, B., Lawrimore, J.H., McMahon, J. R., Menne, M. J., & Zhang, H.M. (2015). Possible artifacts of data biases in the recent global surface warming hiatus. Science, 348(6242), 1469-1472.

Kaspar, M.; Mueller, M. Combinations of large-scale circulation anomalies conducive to precipitation extremes in the Czech Republic, ATMOSPHERIC RESEARCH Volume: 138 Pages: 205-212 Published: MAR 1 2014

Kendon E.J, Ban N, Roberts M.J, Roberts N.M , Chan S.C , Fowler H.J , Evans J.P, 2015, Using new high resolution models to assess the reliability of regional climate projections (submitted to J Climate).

Kendon E.J, Roberts N.M , Senior C.A, and Roberts M.J, 2012: Realism of Rainfall in a Very High-Resolution Regional Climate Model. J. Climate, 25, 5791–5806. doi: http://dx.doi.org/10.1175/JCLI-D-11-00562.1.

Kendon E.J, Roberts N.M, Fowler, H.J, Roberts M.J, Chan S.C, and Fowler, C.A (2014), Heavier summer downpours with climate change revealed by weather forecast resolution model , Nature Climate Change, 4, 570-576 doi: 10.1038/NCLIMATE2258

Kendon M., Marsh T., Parry S., 2013: The 2010-2012 drought in England and Wales. *Weather*, 68: 88-95 doi: 10.1002/wea.2101

Kenyon, J.,and Hegerl, G. C., 2008: Influence of Modes of Climate Variability on Global Temperature Extremes. J. Climate, 21, 3872–3889. doi: http://dx.doi.org/10.1175/2008JCLI2125.1

Kharin, V. V., Zwiers, F. W., Zhang, X., & Wehner, M. (2013). Changes in temperature and precipitation extremes in the CMIP5 ensemble. Climatic Change, 119(2), 345-357

Kiktev, D.B., Caesar, J., and Alexander, L. (2009) Temperature and Precipitation Extremes in the Second Half of the Twentieth Century from Numerical Modeling Results and Observational Data. Izvestiya, Atmospheric and Oceanic Physics, Vol. 45, No. 3, pp. 284-293

Klein Tank, A.M.G., F. Zwiers and X. Zhang (2009) Guidelines on Analysis of extremes in a changing climate in support of informed decisions for adaptation. WMO/TD-1500, Climate Data and Monitoring WCDMP-No. 72. World Meteorological Organization, Geneva, Switzerland

Knutti, R. and J. Sedlacek, 2013, Robustness and uncertainties in the new CMIP5 climate model projections." Nature Climate Change 3(4): 369-373

Kopparla, P., E. M. Fischer, et al., 2013, Improved simulation of extreme precipitation in a high-resolution atmosphere model, Geophysical Research Letters,40(21): 5803-5808

Kriegler, E., J. Edmonds, et al., 2014, A new scenario framework for climate change research: the concept of shared climate policy assumptions, Climatic Change 122(3): 401-414

Kriegler E, O'Neill BC, Hallegatte S, Kram T, Lempert R, Moss R, Wilbanks T (2012) The need for and use of socio-economic scenarios for climate change analysis: a new approach based on shared socio-economic pathways. Global Environmental Change 22:807–822

Krueger, O., Hegerl, G. C., Tett, S. F., 2015, Evaluation of mechanisms of hot and cold days in climate models over Central Europe. Environmental Research Letters, 10(1), 014002

Kuglitsch, F. G., Toreti, A., Xoplaki, E., Della-Marta, P. M., Zerefos, C. S., Türkeş, M., & Luterbacher, J. (2010). Heat wave changes in the eastern Mediterranean since 1960. Geophysical Research Letters, 37(4).

Kundzewicz, Zbigniew W.; Kanae, Shinjiro; Seneviratne, Sonia I.; et al. Flood risk and climate change: global and regional perspectives , HYDROLOGICAL SCIENCES JOURNAL-JOURNAL DES SCIENCES HYDROLOGIQUES Volume: 59 Issue: 1 Pages: 1-28 Published: JAN 2 2014

Kunz, M., Puskeiler, M., 2010. High-resolution assessment of the hail hazard over complex terrain from radar and insurance data. Meteorologische Zeitschrift 19, 427–439

Kunz, M., Sander, J, Kottmeier, Ch., 2009: Recent trends of thunderstorm and hailstorm frequency and their relation to atmospheric characteristics in southwest Germany. International Journal of Climatology, 29, 2283-2297

Kurnik, B., Kajfež-Bogataj, L. and Horion, S. (2014b) An assessment of actual evapotranspiration and soil water deficit in agricultural regions in Europe, to be published in *International Journal of Climatology*. doi: 10.1002/joc.4154

Kysely, J., Beranova, R., 2009, Climate-change effects on extreme precipitation in central Europe: uncertainties of scenarios based on regional climate models." Theoretical and Applied Climatology 95(3-4): 361-374

Kysely, J., L. Gaal, et al., 2011, Climate change scenarios of precipitation extremes in Central Europe from ENSEMBLES regional climate models." Theoretical and Applied Climatology 104(3-4): 529-542

Lau W.K.M, Kim K.M, 2012, The 2010 Pakistan flood and Russian heat wave: Teleconnection of hydrometeorological extremes, J. Hydrometeor, 13, 392–403, doi: http://dx.doi.org/10.1175/JHM-D-11-016.1

Lavers, D. A., and G. Villarini (2013), The nexus between atmospheric rivers and extreme precipitation across Europe, Geophys. Res. Lett., 40, 3259–3264, doi:10.1002/grl.50636

Leander, R.; Buishand, T.A.; Klein-Tank, A.M.G, An Alternative Index for the Contribution of Precipitation on Very Wet Days to the Total Precipitation, JOURNAL OF CLIMATE Volume: 27 Issue: 4 Pages: 1365-1378 Published: FEB 2014

Lhotka, O. and Kyselý, J. (2015), Hot Central-European summer of 2013 in a long-term context. Int. J. Climatol.. doi: 10.1002/joc.4277

Lloyd-Hughes B, 2012, A spatio-temporal structure-based approach to drought characterisation (http://onlinelibrary.wiley.com/doi/10.1002/joc.2280/abstract)

Lloyd-Hughes B, 2013, The impracticality of a universal drought definition, Theoretical & Applied Climatology, 117 (3-4), pp 607-611. ISSN 1434-4483 doi:10.1007/s00704-013-1025-7. Available at http://centaur.reading.ac.uk/35085/

Lorenz, R., Jaeger, E. B., & Seneviratne, S. I. (2010). Persistence of heat waves and its link to soil moisture memory. Geophysical Research Letters, 37(9)

Lott, J.N., R.S. Vose, S.A. Del Greco, T.R. Ross, S. Worley, and J.L. Comeaux, 2008: The integrated surface database: Partnerships and progress. 24th Conference on Interactive Information Processing Systems for Meteorology, Oceanography, and Hydrology (IIPS), New Orleans, LA, American Meteorological Society, Paper 131387

Lustenberger, A.; Knutti, R.; Fischer, E. M.Sensitivity of European extreme daily temperature return levels to projected changes in mean and variance , JOURNAL OF GEOPHYSICAL RESEARCH-ATMOSPHERES Volume: 119 Issue: 6 Pages: 3032-3044 Published: MAR 27 2014

Luterbacher, J., Dietrich, D., Xoplaki, E., Grosjean, M., Wanner, H. (2004) European seasonal and annual temperature variability, trends and extremes since 1500, Science, 303, 1499–1503, doi: 10.1126/science.1093877

Lung, T., Lavalle, C., Hiederer, R., Dosio, A. and Bouwer, L.M. (2013) A multi-hazard regional level impact assessment for Europe combining indicators of climatic and non-climatic change, Global Environmental Change, 23, 522-536

Madsen, H.; Lawrence, D.; Lang, M.; Martinkova, M; Kjeldsen, T. R., Review of trend analysis and climate change projections of extreme precipitation and floods in Europe, JOURNAL OF HYDROLOGY Volume: 519 Pages: 3634-3650 Part: D Published: NOV 27 2014

Mahlstein, I., Knutti, R., Solomon, S., & Portmann, R. W. (2011). Early onset of significant local warming in low latitude countries. Environmental Research Letters, 6(3), 034009

Marsh, P. T., H. E. Brooks, et al. (2007). "Assessment of the severe weather environment in North America simulated by a global climate model." Atmospheric Science Letters **8**(4): 100-106

Marsh, P. T., H. E. Brooks, et al. (2009). "Preliminary investigation into the severe thunderstorm environment of Europe simulated by the Community Climate System Model 3." Atmospheric Research **93**(1-3): 607-618.

Marsh T.J., Kendon M.C., Hannaford J., 2013, The 2010-12 drought and subsequent extensive flooding a remarkable hydrological transformation, Centre for Ecology & Hydrology

Martínez, F., Simon-Soria, F., and Lo´pez-Abente, G. (2004). Valoraci´on del impacto de la ola de calor del verano de 2003 sobre la mortalidad. Gac. Sanit., 18, 250–258.

Masterton J.M., Richardson F.A. (1979), Humidex, a method of quantifying human discomfort due to excessive heat and humidity, CLI, 1-79, Environment Canada, Atmos. Environ. Serv., Downsview, Ontario.

Matsueda, M. (2011) Predictability of Euro-Russian blocking in summer of 2010, Geophys. Res. Lett., 38, L06801, doi:10.1029/2010GL046557

Meehl, G. A., & Tebaldi, C. (2004). More intense, more frequent, and longer lasting heat waves in the 21st century. Science, 305(5686), 994-997

Menne, M.J., I. Durre, R.S. Vose, B.E. Gleason, and T.G. Houston, 2012: An overview of the Global Historical Climatology Network-Daily Database. Journal of Atmospheric and Oceanic Technology, 29, 897-910, doi:10.1175/JTECH-D-11-00103.1

Menne, M. J., C. N. Williams, and R. S. Vose (2009), The United States Historical Climatology Network Monthly Temperature Data - Version 2, *Bull. Am. Meteorol. Soc.*, **90**, 993–1007, doi:10.1175/2008BAMS2613.1.

Merino, A., Wu, X., Gascón, E., Berthet C., García-Ortega, E., Dessens, J., 2014, Hailstorms in southwestern France: Incidence and atmospheric characterization, Atmospheric Research 140–141 (2014) 61–75,

Micu D.M., Dumitrescu, A, Cheval, S, Birson M-V., 2015, Changing Climate Extremes in the Last Five Decades (1961-2010) In "Climate of the Romanian Carpathians: Variability and Trends", 2015, Springer Atmospheric Sciences, auths: Micu DM, Dumitrescu, A, Cheval, S, Birson M-V.

Miralles, D. G., Teuling, A. J., van Heerwaarden, C. C., & de Arellano, J. V. G. (2014). Mega-heat wave temperatures due to combined soil desiccation and atmospheric heat accumulation. Nature Geoscience, 7(5), 345-349.

Mishra, V., Ganguly, A. R., Nijssen, B., & Lettenmaier, D. P. (2015). Changes in observed climate extremes in global urban areas. Environmental Research Letters, 10(2), 024005

Mohr, S., Kunz, M., 2014, Changes in Hail Potential Over Past and Future Decades, presentation (http://www.oeschger.unibe.ch/events/conferences/hail/presentations/24_Mohr.pdf)

Mohr, S. Kunz M.,Recent trends and variabilities of convective parameters relevant for hail events in Germany and Europe, Atmospheric Research, Volume 123, 1 April 2013, Pages 211-228

Mohr, S., Kunz, M. and Geyer, B. (2014b): Hail Potential in Europe based on a regional climate model hindcast. Geophys. Res. Lett. (In preparation)

Mohr, S., Kunz, M. and Keuler, K. (2014a): Changes in the Hail Potential Over Past and Future Decades: Using a Logistic Hail Model. J. Geophys. Res. (Submitted)

Mohr, S., Kunz, M., Keuler, K., 2015: Development and application of a logisticmodel to estimate the past and future hail potential in Germany. Journal of Geophysical Research, 120, doi:10.1002/2014JD022959

Morak, S., Hegerl, G. C., & Kenyon, J. (2011). Detectable regional changes in the number of warm nights. Geophysical Research Letters, 38(17)

Morice, C. P., Kennedy, J. J., Rayner, N. A., & Jones, P. D. (2012). Quantifying uncertainties in global and regional temperature change using an ensemble of observational estimates: The HadCRUT4 data set. Journal of Geophysical Research: Atmospheres (1984–2012), 117(D8)

Moss RH, Edmonds JA, Hibbard KA, Manning MR, Rose SK, van Vuuren DP, Carter TR, Emori S, Kainuma M, Kram T, MeehlGA, Mitchell JFB, Nakicenovic N, Riahi K, Smith SJ, StoufferRJ, Thomson AM, Weyant JP, Wilbanks TJ (2010) The next generation of scenarios for climate change research and assessment. Nature 463:747–756. doi:10.1038/nature08823

Mueller, B., & Seneviratne, S. I. (2012). Hot days induced by precipitation deficits at the global scale. Proceedings of the national academy of sciences, 109(31), 12398-12403

Nairn J, Fawcett R, Ray D (2009) Defining and predicting excessive heat events: A national system, CAWCR Tech. Rep. 017, 83–86

Nanding, N., Rico-Ramirez, M.A., Han, D., Comparison of different radar-raingauge rainfall merging techniques Journal of Hydroinformatics Vol 17 No 3 pp 422–445, 2015, doi:10.2166/hydro.2015.001

NAS and NMI (2013) Extreme Weather Events in Europe: Preparing for Climate Change Adaptation. Oslo: Norwegian Academy of Science and Letters and the Norwegian Meteorological Institute

Nature News, 2014, http://www.nature.com/news/russian-summer-tops-universal-heat wave-index-1.16250 (accessed 19 May 2015)

Neu, Urs et al., 2013: IMILAST: A Community Effort to Intercompare Extratropical Cyclone Detection and Tracking Algorithms. Bull. Amer.Meteor. Soc., 94, 529–547

Niedzwiedz, Tadeusz; Lupikasza, Ewa; Pinskwar, Iwona; Kundzewicz, Zbigniew W.; Stoffel, Markus; Malarzewski, Lukasz, Variability of high rainfalls and related synoptic situations causing heavy floods at the northern foothills of the Tatra Mountains, THEORETICAL AND APPLIED CLIMATOLOGY, Volume:119, Issue:1-2, Pages:273-284, DOI: 10.1007/s00704-014-1108-0, Published:JAN 2015

Nikulin, G., Kjellström, E., Hansson, U.L.F., Strandberg, G., & Ullerstig, A. (2011). Evaluation and future projections of temperature, precipitation and wind extremes over Europe in an ensemble of regional climate simulations. Tellus A, 63(1), 41-55

Nisi, L., Martius, O., Hering, A., Germann, U., Kunz, M, 2015: Spatial and temporal distribution of hailstorms in the Alpine region: a long-term, high resolution, radar-based analysis. Submitted for publication 2015

Olsson, J., K. Berggren, et al. (2009). "Applying climate model precipitation scenarios for urban hydrological assessment: A case study in Kalmar City, Sweden." Atmospheric Research **92**(3): 364-375

Olsson, J., U. Willen, et al. (2012). "Downscaling extreme short-term regional climate model precipitation for urban hydrological applications." Hydrology Research **43**(4): 341-351.

O'Neill, B. C., E. Kriegler, et al. (2014). "A new scenario framework for climate change research: the concept of shared socioeconomic pathways." http://www.dnva.no/binfil/download.php?tid=58783 **122**(3): 387-400.

Orlowsky B, Seneviratne S.I, Global changes in extreme events: Regional and seasonal dimension in climatic change, February 2012, Volume 110, Issue 3-4, pp 669-696, 2011

Orlowsky B, Seneviratne S.I: 2013, Elusive drought: uncertainty in observed trends and short- and long-term CMIP5 projections, Hydrol. Earth Syst. Sci., 17, 1765-1781, 2013, www.hydrol-earth-syst-sci.net/17/1765/2013/ doi:10.5194/hess-17-1765-2013

Orlowsky, B., Seneviratne S.I, Global changes in extreme events: regional and seasonal dimension (http://dx.doi.org/10.1007/s10584-011-0122-9) Climatic Change February 2012, Volume 110, Issue 3-4, pp 669-696, Date: 22 July

Otomi Y, Tachibana Y, Nakamura T (2013) A possible cause of the AO polarity reversal from winter to summer in 2010 and its relation to hemispheric extreme summer weather, Clim. Dyn., 40, 1939-1947, doi:10.1007/s00382-012-1386-0

Otto F.E.L, Massey N, Van Oldenborgh G.J, Jones R.G, Allen M.R (2012) Reconciling two approaches to attribution of the 2010 Russian heat wave, Geophys. Res. Lett., 39, L04702, doi:10.1029/2011GL050422

Palfai, I., Description and forecasting of droughts in Hungary, in Proceedings 14th International Congress on Irrigation and Drainage, Rio de Janeiro, Brazil.. No. 1-C. International Commission on Irrigation and Drainage, 1990

Palmer, W. C., 1965: Meteorological droughts. U.S. Department of Commerce, Weather Bureau Research Paper 45, 58 pp

Papagiannaki, K., 2013

Pappenburger, Florian, ECMWF, 1 Nov 2013 #10 Seamless forecasting of floods and droughts and other extreme events https://www.youtube.com/watch?v=Xj2aSt1v7O4&x-yt-cl=85027636&x-yt-ts=1422503916

Parker, D. E. (2010), Urban heat island effects on estimates of observed climate change. WIREs Clim Change, 1: 123–133. doi: 10.1002/wcc.21

Parry, Simon; Hannaford, Jamie; Lloyd-Hughes, Ben; Prudhomme, Christel. 2012 Multi-year droughts in Europe: analysis of development and causes. *Hydrology Research*, 43 (5). 689-706. 10.2166/nh.2012.024

Perkins, S. E. (2015). A review on the scientific understanding of heat waves–their measurement, driving mechanisms, and chaFnges at the global scale. Atmospheric Research

Perkins S.E, Alexander LV (2013) On the Measurement of Heat Waves. J. Climate, 26, 4500–4517, doi: http://dx.doi.org/10.1175/JCLI-D-12-00383.1

Perry M, Hollis D, Elms M, 2009: The Generation of Daily Gridded Datasets of Temperature and Rainfall for the UK, National Climate Information Centre Climate Memorandum No 24, Met Office NCIC, June 2009.

Peterson, T.C., and Coauthors: Report on the Activities of the Working Group on Climate Change Detection and Related Rapporteurs 1998-2001. WMO, Rep. WCDMP-47, WMO-TD 1071, Geneve, Switzerland, 143pp. (Available as: wgccd.2001.pdf

Pfahl, S., & Wernli, H. (2012). Quantifying the relevance of atmospheric blocking for co-located temperature extremes in the Northern Hemisphere on (sub-) daily time scales. Geophysical Research Letters, 39(12)

Piani, C., Haerter, J., and Coppola, E.: Statistical bias correction for daily precipitation in regional climate models over Europe, Theor. Appl. Climatol., 99, 187–192, doi:10.1007/s00704-009-0134-9, 2010

Plavcova, Eva, Kysely, Jan, Stepanek, Petr, 2014, Links between circulation types and precipitation in Central Europe in the observed data and regional climate model simulations , INTERNATIONAL JOURNAL OF CLIMATOLOGY Volume: 34 Issue: 9 Pages: 2885-2898

Prein, A. F., W. Langhans, et al., 2015, A review on regional convection-permitting climate modeling: Demonstrations, prospects, and challenges, Reviews of Geophysics 53(2): 323-361.

Prudhomme, Christel, Ignazio Giuntolia, Emma L Robinson, Douglas B. Clark, Nigel W. Arnell, Rutger Dankers, Balázs M. Feketee, Wietse Franssen, Dieter Gerten, Simon N. Gosling, Stefan Hagemann, David M. Hannah, Hyungjun Kim, Yoshimitsu Masaki, Yusuke Satoh, Tobias Stacke, Yoshihide Wadam, Dominik Wissern, 2013, Hydrological droughts in the 21st century, hotspots and uncertainties from a global multimodel ensemble experiment (http://dx.doi.org/10.1073/pnas.1222473110)

Punge H.J., Bedka K.M., Kunz M., Werner A., 2014, A new physically based stochastic event catalog for hail in Europe, Natural Hazards , DIO: 10.1007/s11069-014-1161-0

Puskeiler, M., 2013: Radarbasierte Analyse der Hagelgefährdung in Deutschland. Phd Thesis, Karlsruher Institute of Technology, Karlsruhe, Germany, Wiss,. Ber. Institute of Meteorology and Climate Research 59, KIT Scientific Publishing, 226 pp

PwC (2011) Protecting human health and safety during severe and extreme heat events, a national framework. Report for the Commonwealth Government, PricewaterhouseCoopers Australia, 84 pp. (Available online at http://www.pwc.com.au/industry/government/publications/extreme-heat-events.htm)

Quesada B, Vautard R, Yiou P, Hirschi M, Seneviratne SI (2012) Asymmetric European summer heat predictability from wet and dry southern winters and springs, Nature Climate Change, 2(10), 736-741, doi:10.1038/nclimate1536

DROUGHT-R&SPI (Fostering European Drought Research and Science-Policy Interfacing), FP7 Cooperation Work Programme 2011, Theme 6: Environment (including Climate Change, ENV.2011.1.3.2-2: Vulnerability and increased drought risk in Europe (Grant agreement no: 282769), Reports http://www.eu-drought.org/

Rahmstorf, S., &Coumou, D., 2011, Increase of extreme events in a warming world. Proceedings of the National Academy of Sciences, 108, 44

Rajczak J., P. Pall, P., Schär, C., 2013, Projections of extreme precipitation events in regional climate simulations for Europe and the Alpine Region, Journal of Geophysical Research: Atmospheres, Volume 118, Issue 9, pages 3610–3626

Rebetez, M., Dupont, O., & Giroud, M., 2009, An analysis of the July 2006 heat wave extent in Europe compared to the record year of 2003. Theoretical and Applied Climatology, 95(1-2), 1-7

Riediger, U., Gratzki, A., 2014, Future weather types and their influence on mean and extreme climate indices for precipitation and temperature in Central Europe, METEOROLOGISCHE ZEITSCHRIFT Volume: 23 Issue: 3 Pages: 231-252

Rogelj, J., M. Meinshausen, et al., 2012, Global warming under old an new scenarios using IPCC climate sensitivity range estimates, Nature Climate Change 2(4): 248-253

Rohde, R., Muller, R. A. et al. (2013) A New Estimate of the Average Earth Surface Land Temperature Spanning 1753 to 2011. Geoinfor Geostat: An Overview 1:1.. doi:10.4172/gigs.1000101

Rojas, R., 2012, Assessment of future flood hazard in Europe using a large ensemble of bias-corrected regional climate simulations. Journal of Geophysical Research (Atmospheres). VOL. 117

Rojas, R., 2011, Improving pan-European hydrological simulation of extreme events through statistical bias correction of RCM-driven climate simulations. Hydrology and Earth System Sciences. VOL. 15 NO. 8, 2011

Rojas, R,. Feyen, L,. Bianchi, A., Dosio, A., 2012, Assessment of future flood hazard in Europe using a large ensemble of bias-corrected regional climate simulations Journal of Geophysical Research: Atmospheres (1984–2012) VOL 117, Issue D17

Rothfusz, L. P., Headquarters, N.S.R., 1990, The heat index equation (or, more than you ever wanted to know about heat index), Fort Worth, Texas: National Oceanic and Atmospheric Administration, National Weather Service, Office of Meteorology, 90-23

Ruiz-Labourdette, D.; Genova, M.; Schmitz, M. F.; et al. Summer rainfall variability in European Mediterranean mountains from the sixteenth to the twentieth century reconstructed from tree rings , INTERNATIONAL JOURNAL OF BIOMETEOROLOGY Volume: 58 Issue: 7 Pages: 1627-1639 Published: SEP 2014

Russo, S A Dosio, R G Graversen, J Sillmann, H Carrao, M B Dunbar, A Singleton, P Montagna, P Barbola, J V Vogt, 2014, Magnitude of extreme heat waves in present climate and their projection in a warming world Journal of Geophysical Research: Atmospheres, Volume 119, Issue 22, pages 12,500–12,512, 2014, DOI: 10.1002/2014JD022098

Rutgersson, A.; Jaagus, J.; Schenk, F.; et al., Observed changes and variability of atmospheric parameters in the Baltic Sea region during the last 200 years , CLIMATE RESEARCH Volume: 61 Issue: 2 Pages: 177-190 Published: SEP 2014

Ryzkhov A, 2010, DIscrimnation between large and small hail size, Final Report for NSSL/Lincoln Laboratory;

Salinas, J. L.; Castellarin, A.; Kohnova, S.; et al. Regional parent flood frequency distributions in Europe - Part 2: Climate and scale controls, HYDROLOGY AND EARTH SYSTEM SCIENCES Volume: 18 Issue: 11 Pages: 4391-4401 Published: 2014

Samaniego, L., Kumar R.,Zink M.,2013, Implications of Parameter Uncertaintyon Soil Moisture Drought Analysis in Germany, J. Hydrometeor., 14, 47-68, doi:http://dx.doi.org/10.1175/JHM-D-12-075.1

Sanderson M.G., W. H. Hand, P. Groenemeijer, P. M. Boorman, J. D. C. Webb, and L. J. McColl, 2014, Projected changes in hailstorms during the 21st century over the UK, Int. J. Climatol.

Sanderson, M. G., W. H. Hand, et al. (2015). "Projected changes in hailstorms during the 21st century over the UK." International Journal of Climatology **35**(1): 15-24.

Sarris, Dimitrios; Christopoulou, Anastasia; Angelonidi, Eleni; et al.Increasing extremes of heat and drought associated with recent severe wildfires in southern Greece , REGIONAL ENVIRONMENTAL CHANGE Volume: 14 Issue: 3 Special Issue: SI Pages: 1257-1268 Published: JUN 2014

Schaller, N., Otto, F.E.L, van Oldenborgh, G.J., Massey, N.R., Sparrow, S., and Allen, M.R., in Explaining Extreme Events of 2013 From A Climate Perspective, Chapter 20 of the Special Supplement to the Bulletin of the American Meteorological Society Vol. 95, No. 9, September 2014.

Schär C., Vidale P.L., Lüthi D., Frei C., Häberli C., Liniger M.A., Appenzeller C (2004) The role of increasing temperature variability in European summer heat waves, Nature, 427, 332–336, doi:10.1038/nature02300.

Schär et al, 2004, The role of increasing temperature variability in European summer heat waves, Nature 427

Schoetter, R., Cattiaux, J., & Douville, H. (2014). Changes of western European heat wave characteristics projected by the CMIP5 ensemble. Climate Dynamics, 1-16.

Schrier, G.v.d., Besselaar, E. J., Klein-Tank, A. M. G., & Verver, G. (2013). Monitoring European average temperature based on the E-OBS gridded data set. Journal of Geophysical Research: Atmospheres, 118(11), 5120-5135.

Seneviratne S.I., 2012, Climate science: Historical drought trends revisited, Nature 491, 338–339, 2012, doi:10.1038/491338a

Seneviratne, S. I. et al. Investigating soil moisture-climate interactions in a changing climate: A review. Earth-Sci. Rev. 99, 125_161 (2010)

Seneviratne, S. I. et al. Managing the risks of extreme events and disasters to advance climate change adaptation in Managing the Risks of Extreme Events and Disasters to Advance Climate Change Adaptation. A Special Report of Working Groups I and II of the Intergovernmental Panel on Climate Change (eds Field, C. B. et al.) 109–230 (Cambridge Univ. Press, 2012)

Seneviratne, S. I., Donat, M. G., Mueller, B., & Alexander, L. V., 2014, No pause in the increase of hot temperature extremes. Nature Climate Change, 4(3), 161-163

Sepulcre-Canto, G. S. Horion, A. Singleton, H. Carrao, and J. Vogt, 2012 Development of a Combined Drought Indicator to detect agricultural drought in Europe (http://dx.doi.org/10.5194/nhess-12-3519-2012)

Serra, C., Martinez, M. D., Lana, X. et al. European dry spell regimes (1951-2000): Clustering process and time trends, ATMOSPHERIC RESEARCH Volume: 144 Special Issue: SI Pages: 151-174 Published: JUL 1 2014

Seubert, Stefanie, Fernandez-Montes, Sonia, Philipp, Andreas, et al. Mediterranean climate extremes in synoptic downscaling assessments, THEORETICAL AND APPLIED CLIMATOLOGY Volume: 117 Issue: 1-2 Pages: 257-275 Published: JUL 2014

Sheffield J, Wood E F, Roderick M L, Little change in global drought over the past 60 years, Nature 491, 435–438 (2012) doi: 10.1038/nature11575

Shepard, D,. 1968, A two-dimensional interpolation function for irregularly-spaced data. In Proc. Jan. 1968 23rd ACM national conf., pp. 517-524, ACM.

Shi, L., Kloog., I, Zanobetti, A., Liu, P., Schwartz, J., (2015) Impacts of temperature and its variability on mortality in New England, Nature Climate Change, doi:10.1038/nclimate2704

Sideris V., Gabella, M., Erdin, R., Germann, U., 2014, Real-time radar–rain-gauge merging using spatio-temporal co-kriging with external drift in the alpine terrain of Switzerland, Quarterly Journal of the Royal Meteorological Society Volume 140, Issue 680, pages 1097–1111, DOI: 10.1002/qj.2188

Sillmann, J.V.V., Kharin, X., Zhang, F.W., Zwiers, D., Bronaugh Climate extremes indices in the CMIP5 multi-model ensemble: Part 1. Model evaluation in the present climate, Journal of Geophysical Research (Atmospheres), 118, 4

Sillmann, J. V. V. Kharin,.F. W. Zwiers,.X. Zhang, D. Bronaugh, 2013, Climate extremes indices in the CMIP5 multimodel ensemble: Part 2. Future climate projections, Journal of Geophysical Research: Atmospheres Volume 118, Issue 6, pages 2473–2493, 27 March 2013, DOI: 10.1002/jgrd.50188 Sillmann, J., Kharin, V. V., Zhang, X., Zwiers, F. W., & Bronaugh, D. (2013a). Climate extremes indices in the CMIP5 multimodel ensemble: Part 1. Model evaluation in the present climate. Journal of Geophysical Research: Atmospheres, 118(4), 1716-1733

Sillmann, J., Kharin, V.V., et al. (2014). "Short Communication Evaluating model-simulated variability in temperature extremes using modified percentile indices." International Journal of Climatology **34**(11): 3304-3311.

Simmons, A. J., & Poli, P. (2014). Arctic warming in ERA-Interim and other analyses. Quarterly Journal of the Royal Meteorological Society., 141, 689, 1147, doi: 10.1002/qj.2422

Sippel, Sebastian; Otto, Friederike E. L., 2014, Beyond climatological extremes - assessing how the odds of hydrometeorological extreme events in South-East Europe change in a warming climate , CLIMATIC CHANGE Volume: 125 Issue: 3-4 Pages: 381-398

Smith, T. M., Reynolds, R. W., Peterson, T. C., & Lawrimore, J. (2008). Improvements to NOAA's historical merged land-ocean surface temperature analysis (1880-2006). Journal of Climate, 21(10), 2283-2296

Spinoni, J., Antofie, T., Barbosa, R., Bihari, Z., Lakatos, M., Szalai, S., Szentimrey, T., Vogt, J., An overview of drought events in the Carpathian Region in 1961–2010, Adv. Sci. Res., 10, 21–32, 2013 www.adv-sci-res.net/10/21/2013/ doi:10.5194/asr-10-21-2013 © Author(s) 2013. CC Attribution (see also Antofie 2015)

Spinoni, J., Lakatos, M., Szentimrey, T., Bihari, Z., Szalai, S., Vogt, J. and Antofie, T. (2015), Heat and cold waves trends in the Carpathian Region from 1961 to 2010. Int. J. Climatol.. doi: 10.1002/joc.4279

Stagge et al. (2015), Future Meteorological Drought: Projections of Regional Climate Models of Europe,Drought:R&SPI Technical report #25 http://www.eu-drought.org/technicalreports

Stagge, J. H.; Tallaksen, L. M.; Gudmundsson, L. ; Van Loon, A. F. & Stahl, K. Candidate Distributions for Climatological Drought Indices (SPI and SPEI) International Journal of Climatology, 2015, published online, doi: 10.1002/joc.4267. (software)

Stahl, K., Hisdal, H., Hannaford, J., Tallaksen, L.M., Van Lanen, H.A.J., Sauquet, E., Demuth, S., Fendekova, M., and J´odar, J.: Streamflow trends in Europe: evidence from a dataset of near natural catchments, Hydrol. Earth Syst. Sci., 14, 2367–2382, doi: 10.5194/hess-14-2367-2010,2010

Stahl K, Tallaksen L.M , Hannaford J, and Van Lanen H.A.J, Filling the white space on maps of European runoff trends: estimates from a multi-model ensemble Hydrol. Earth Syst. Sci., 16, 2035–2047, 2012.

Stahl, K.; Stagge, J. H.; Bachmair, S.; Blauhut, V.; Rego, F. C.; Stefano, L. D.; Dias, S.; Gudmundsson, L.; Gunst, L.; Kohn, I.; Lanen, H. A. V.; Reguera, J. U. & Tallaksen, L. M., Recommendations for indicators for monitoring and early-warning considering different sensitivities: pan-European scale DROUGHT-R&SPI Technical Report, 2015, 28

Stampoulis D, Anagnostou E.N., (2012) Evaluation of Global Satellite Rainfall Products over Continental Europe. J Hydrometeor 13 588–603, doi: http://dx.doi.org/10.1175/JHM-D-11-086.1

Stampoulis, D., Anagnostou, E.N., Nikolopoulos E.I., 2013, Assessment of high-resolution satellite-based rainfall estimates over the Mediterranean during heavy precipitation events. J. Hydrometeor 14, 1500–1514, doi: http://dx.doi.org/10.1175/JHM-D-12-0167.1

Steadman R.G., 1979, The assessment of sultriness. Part I: A temperature–humidity index based on human physiology and clothing science. J. Appl. Meteor., 18, 861–873.

Steadman, R.G., 1984, A universal scale of apparent temperature. Journal of Climate and Applied Meteorology, 23(12), 1674-1687

Shafer, B. A., L. E. Dezman, 1982, Development of a surface water supply index (SWSI) to assess the severity of drought conditions in snowpack runoff areas. Proceedings of the Western Snow Conference, 164-175

Stone, B., 2007, Urban and rural temperature trends in proximity to large US cities: 1951–2000. International Journal of Climatology, 27(13), 1801-1807

Stone, B., Hess, J. J., Frumkin, H., 2010, Urban form and extreme heat events: are sprawling cities more vulnerable to climate change than compact cities. Environmental health perspectives, 118(10), 1425-1428

Stott, P.A., Stone, D.A., Allen, M.R. , 2004, Human contribution to the European heat wave of 2003, Nature, 432, 610–614, doi:10.1038/nature03089

Stott, P., 2015, Attribution: Weather risks in a warming world. Nature Climate Change, doi: 10.1038/nclimate2640

Stratonovitch, P,. Semenov, M.A., Heat tolerance around flowering in wheat identified as a key trait for increased yield potential in Europe under climate change, J. Exp. Bot. (2015) doi: 10.1093/jxb/erv070

Strupczewski, W.G., Kaczmarek, Z., 2001. Non-stationary approach to at-site flood frequency modelling. Part II. Weighted least squares estimation. J. Hydrol. 248,143–151

Strupczewski, W.G., Singh, V.P., Feluch, W., 2001a. Non-stationary approach to at-site flood frequency modelling. Part I. Maximum likelihood estimation. J.Hydrol. 248, 123–142

Strupczewski, W.G., Singh, V.P., Mitosek, H.T., 2001b. Non-stationary approach to at-site flood-frequency modelling. Terink et al. 2010, Evaluation of a bias correction method applied to downscaled precipitation and temperature reanalysis data for the Rhine basin

Sunyer, M. A., H. Madsen, et al., 2012, A comparison of different regional climate models and statistical downscaling methods for extreme rainfall estimation under climate change, Atmospheric Research 103: 119-128.

Tallaksen, L.M., Van Lanen, H.A.J., 2004, Hydrological Drought, Processes and Estimation Methods for Streamflow and Groundwater, Developments in Water Science no. 48

Tallaksen, L.M., Stagge, J.H., Stahl, K., Gudmundsson, L., Orth R., Seneviratne S.I., Van Loon A.F., Van Lanen H.A.J., Characteristics and drivers of drought in Europe - a summary of the DROUGHT:R&SPI project, in Andreu et al. (eds.), Fostering European Drought Research and Science-Policy Interfacing

Taylor, I. H., Burke, E., McColl, L., Falloon, P. D., Harris, G. R., and McNeall, D.: The impact of climate mitigation on projections of future drought, Hydrol. Earth Syst. Sci., 17, 2339-2358, doi:10.5194/hess-17-2339-2013, 2013.

Taylor, K. E., R. J. Stouffer, and G. A. Meehl, 2012: An Overview of CMIP5 and the experiment design. Bull. Amer. Meteor. Soc., 93, 485–498.

Tebaldi C, Hayhoe K, Arblaster JM, Meehl GA (2006) Going to the extremes—an intercomparison of model-simulated historical and future changes in extreme events. Clim Change 79(3):185–211

Terink, W. R. T. W. L. Hurkmans, P. J. J. F. Torfs, and R. Uijlenhoet www.hydrol-earth-syst-sci-discuss.net/7/221/2010/hessd-7-221-2010.pdf

Teuling A J, Van Loon A F, Seneviratne S I, Lehner I, Aubinet M, Heinesch B, Bernhofer C, Grünwald T, Prasse H, Spank U, Evapotranspiration amplifies European Summer Drought GEOPHYSICAL RESEARCH LETTERS, VOL. 40, 2071–2075, doi:10.1002/grl.50495, 2013

Themessl, M. J., A. Gobiet, et al. (2011). "Empirical-statistical downscaling and error correction of daily precipitation from regional climate models." International Journal of Climatology **31**(10): 1530-1544.

Thober, Stephan; Samaniego, Luis, Robust ensemble selection by multivariate evaluation of extreme precipitation and temperature characteristics, JOURNAL OF GEOPHYSICAL RESEARCH-ATMOSPHERES Volume: 119 Issue: 2 Pages: 594-613 Published: JAN 27 2014

Tolika K, Maheras P, Tegoulias I (2009) Extreme temperatures in Greece during 2007: Could this be a "return to the future"? Geophys. Res. Lett., 36, L10813, doi:10.1029/2009GL038538.

Tosic, Ivana; Unkasevic, Miroslava, Analysis of wet and dry periods in Serbia, INTERNATIONAL JOURNAL OF CLIMATOLOGY Volume: 34 Issue: 5 Pages: 1357-1368 Published: APR 2014

Trenberth, K. E., Fasullo, J. T., & Shepherd, T. G. (2015). Attribution of climate extreme events. Nature Climate Change.

Trenberth K.E, Dai A, van der Schrier G, Jones P.D, Barichivich J, Briffa K.R, Sheffield J, Global warming and changes in drought, Nature Climate Change, 4, 17–22, 2014. doi:10.1038/nclimate2067

Trenberth K.E, Fasullo J.T (2012) Climate extremes and climate change: the Russian heat wave and other climate extremes of 2010. J. Geophys. Res., 117, D17103, doi:10.1029/2012JD018020

Trenberth, K. E. (2011). Changes in precipitation with climate change. Climate Research, 47(1), 123. doi:10.3354/cr00953

Trends in extreme weather events in Europe: implications for national and European Union adaptation strategy: http://www.easac.eu/fileadmin/PDF_s/reports_statements/Easac_Report_Extreme_Weather_Events.pdf

Trigo, R.M., Pereira, J.M.C., Pereira, M.G., Mota, B., Calado, M.T., DaCamara, C.C., and Santo, F.E. (2006). The exceptional fire season of summer 2003 in Portugal. Int. J. Climatol., 26, 1741–1757.

Vallebona, Chiara; Pellegrino, Elisa; Frumento, Paolo; et al.Temporal trends in extreme rainfall intensity and erosivity in the Mediterranean region: a case study in southern Tuscany, Italy, CLIMATIC CHANGE Volume: 128 Issue: 1-2 Pages: 139-151 Published: JAN 2015

Van Delden, A., 2001: The synoptic setting of thunderstorms in Western Europe. Atmospheric Research, 56, 89-110

Van den Besselaar., Klein Tank A M G., Buishand T A.,Trends in European precipitation extremes over 1951–2010 INTERNATIONAL JOURNAL OF CLIMATOLOGY Int. J. Climatol. 33: 2682–2689 (2013) Published online 16 November 2012 in Wiley Online Library (wileyonlinelibrary.com) DOI: 10.1002/joc.3619

Van den Besselaar, E.J.M., Klein-Tank, A.M.G., Schrier, G., & Jones, P.D., (2012), Synoptic messages to extend climate data records. Journal of Geophysical Research: Atmospheres (1984–2012), 117(D7).

Van den Torren S, Suzan F, Medina S, Pascal M, Maulpoix A, Cohen J C., Ledrans M., Mortality in 13 French Cities During the August 2003 Heat Wave. American Journal of Public Health: September 2004, Vol. 94, No. 9, pp. 1518-1520.doi: 10.2105/AJPH.94.9.1518

Van der Linden P, Mitchell JFB (eds) (2009) ENSEMBLES: climate change and its impacts: summary of research and results from ENSEMBLES project. Met Office Hadley Centre, Exeter. http://ensembles-eu.metoffice.com

Van der Schrier G, Barichivich J, Briffa K R and Jones P D, 2013, A scPDSI based global data set of dry and wet spells for 1901–2009 J. Geophys. Res. D 118 1–24

Van Huijgevoort, M.H.J., Hazenberg, P., Van Lanen, H. A. J., and Uijlenhoet, R. (2012). A generic method for hydrological drought identification across different climate regions. Hydrology and Earth System Sciences, 16, 2437-2451, DOI: 10.5194/hess-16-2437-2012

Van Huijgevoort, M.H.J., Van Loon, A. F., Rakovec, O., Haddeland, I., Horáèek, S., and Van Lanen, H. A. J.: Drought assessment using local and large-scale forcing data in small catchments, in: Global Change: Facing Risks and Threats to Water Resources, edited by: Servat, E., Demuth, S., Dezetter, A., Daniell.

Van Lanen, H.A.J., Wanders, N., Tallaksen, L.M., and Van Loon, A.F.: Hydrological drought across the world: impact of hydroclimatology and physical catchment structure, Int. J. Climatol., in review, 2012.

Van Loon, A, Hydrological drought explained WIREs Water 2015. doi: 10.1002/wat2.1085 (overview)

Van Loon, A, Van Lanen H, Kampragou, E, Assimacopoulos, D, Haro Monteagudo, D, Andreu, J, Dias S, Rego F, Gudmundsson, L. & Wolters, W. Evaluation of the potential and limitations of Pan-European analyses of drought as a natural hazard on local and national scales, DROUGHT-R&SPI Technical Report, 2015, 34

Van Loon, A.F. and Van Lanen, H.A.J.: (2012): A process-based typology of hydrological drought, Hydrol. Earth Syst. Sci., 16, 1915–1946, doi:10.5194/hessd-8-11413-2011, 2011

Van Loon, A.F., Tijdeman, E., Wanders, N., Van Lanen, H.A.J., Teuling, A.J., and Uijlenhoet, R. (2014): Seasonality Controls Climate-Dependency of Drought Propagation. J. Geophys.Res. Atmos., 119: 4640–4656, doi:10.1002/2013JD020383

Van Loon, A.F., Ploum, S.W., Parajka, J., Fleig, A.K., Garnier, E., Laaha, G., and Van Lanen, H.A.J. (2015): Hydrological drought typology: temperature-related drought types and associated societal impacts. Hydrol. Earth Syst. Sci., 19, 1993–2016, doi:10.5194/hess-19-1993-2015

Van Ruijven, B. J., M. A. Levy, et al. (2014). "Enhancing the relevance of Shared Socioeconomic Pathways for climate change impacts, adaptation and vulnerability research." Climatic Change **122**(3): 481-494

Van Vuuren, P., Edmonds, J., Kainuma, M., Riahi, K., Thomson, A., Hibbard, K., Hurtt, G., Kram, T., Krey, V., Lamarque, J.-F., Masui, T., Meinshausen, M., Nakicenovic, N., Smith, S.,and Rose, S.: The representative concentration pathways: an overview, Clim. Change, 109, 5–31, doi:10.1007/s10584-011-0148-z, 2011.

Vautard, R., A. Gobiet, et al. (2013). "The simulation of European heat waves from an ensemble of regional climate models within the EURO-CORDEX project." Climate Dynamics **41**(9-10): 2555-2575

Venema, V. K., Mestre, O., Aguilar, E., Auer, I., Guijarro, J. A., Domonkos, P., Brandsma, T., 2012, Benchmarking homogenization algorithms for monthly data. Climate of the Past, 8(1), 89-115

Vicente-Serrano S M , López-Moreno J I, Beguería S; Lorenzo-Lacruz J; Azorin-Molina C; Morán-Tejeda E, Accurate Computation of a Streamflow Drought Index, Journal Hydrological Engineering, 2012a DOI: 10.1061/(asce)he.1943-5584.0000433)

Vicente-Serrano, S.M., Azorin-Molina, C., Sanchez-Lorenzo, A., Morán-Tejeda, E., Lorenzo-Lacruz, J., Revuelto, J., López-Moreno, J.I., Espejo, F., 2014a, Temporal evolution of surface humidity in Spain: recent trends and possible physical mechanisms. *Climate Dynamics* 42, 2655-2674. doi: 10.1007/s0038201318857

Vicente-Serrano, S. M., C. Azorin-Molina, A. Sanchez-Lorenzo, J. Revuelto, E. Moran-Tejeda, J. I. Lopez-Moreno, and F. Espejo (2014), Sensitivity of reference evapotranspiration to changes in meteorological parameters in Spain (1961–2011), Water Resour. Res., 50, 8458–8480, doi:10.1002/2014WR015427

Vicente-Serrano S. M., Beguería, S. and LópezMoreno, J.I., 2010, A multiscalar drought index sensitive to global warming: the standardized precipitation evapotranspiration index—SPEI J. Clim. 23 1696–718

Vicente-Serrano S.M., Zouber, A., Lasanta, T., Pueyo, Y., 2012b, Dryness is accelerating degradation of vulnerable shrublands in semiarid Mediterranean environments Ecol. Monogr. 82 407–28

Vicente-Serrano, S.M., Lopez-Moreno, J.I., Beguería, S., Lorenzo-Lacruz, J., Sanchez-Lorenzo, A., García-Ruiz, J.M., Azorin-Molina, C.,Tejeda-Moran, E., Revuelto, J., Trigo, R., Coelho, F., Espejo, F., 2014, Evidence of increasing drought severity caused by temperature rise in southern Europe Environ. Res. Lett., 9 (4), p. 044001 http://dx.doi.org/10.1088/1748-9326/9/4/044001

Vidal, J.-P.,Wade, S., A multi-model assessment of future climatological droughts in the United Kingdom, International Journal of Climatology, Volume 29, Issue 14, pages 2056–2071, 30 November 2009, DOI: 10.1002/joc.1843

Vidal, J.-P., Martin, E., Kitova, N., Najac, J., and Soubeyroux, J.-M.: Evolution of spatio-temporal drought characteristics: validation, projections and effect of adaptation scenarios, Hydrol. Earth Syst. Sci., 16, 2935-2955, doi:10.5194/hess-16-2935-2012, 2012

Vogt J.V., Somma, F., 2000, Drought and drought mitigation in Europe, edited by, Kluwer Academic Publishers, Dordrecht, 2000. No. of Pages: x+325., ISBN 0-7923-6589-5

Vose, R. S., Arndt, D., Banzon, V. F., Easterling, D. R., Gleason, B., Huang, B., & Wuertz, D. B. (2012). NOAA's merged land-ocean surface temperature analysis. Bulletin of the American Meteorological Society, 93(11), 1677-1685

Wanders, N. & Van Lanen, H.A.J., 2015a, Future discharge drought across climate regions around the world modelled with a synthetic hydrological modelling approach forced by three General Circulation Models. Natural Hazard Earth Syst. Sci., 15, 487–504, doi:10.5194/nhess-15-487-2015.

Wanders, N., Wada, Y., Van Lanen H.A.J 2015b, Global hydrological droughts in the 21st century under a changing hydrological regime Earth Syst. Dynam., 6, 1–15, 2015 www.earth-syst-dynam.net/6/1/2015/ doi:10.5194/esd-6-1-2015

Travis, W., Weather and climate extremes: Pacemakers of adaptation? 2014 Weather and Climate Extremes Volumes 5–6, October 2014, Pages 29–3, http://www.sciencedirect.com/science/article/pii/S2212094714000693

Webb, J.D.C., Elsom, D.M., Meaden, G.T., 1986, The TORRO hailstorm intensity scale, J. Meteorol. 11, 337–339.

Weedon, G P., Gomes, S., Viterbo, P., Shuttleworth, W.J., Blyth, E., österle, H., Adam, J. C., Bellouin, N., NBoucher, O., Best, M., Creation of the WATCH forcing data and its use to assess global and regional reference crop evaporation over land during the Twentieth Century, Journal of Hydrometeorology, 12 (5) 2011. pp. 823-848. ISSN 1525-7541 DOI: 10.1175/2011JHM1369.1

Wergen, G., & Krug, J. (2010). Record-breaking temperatures reveal a warming climate. EPL (Europhysics Letters), 92(3), 30008.

Westra, S., H. J. Fowler, J. P. Evans, L. V. Alexander, P. Berg, F. Johnson, E. J. Kendon, G. Lenderink and N. M. Roberts (2014), Future changes to the intensity and frequency of short-duration extreme rainfall , Rev. Geophys., 52, 522-555, doi:10.1002/2014RG000

Wetter, Oliver; Pfister, Christian; Werner, Johannes P., The year-long unprecedented European heat and drought of 1540-a worst case, CLIMATIC CHANGE Volume: 125 Issue: 3-4 Pages: 349-363 Published: AUG 2014

Wheeler, T. R., Craufurd, P. Q., Ellis, R. H., Porter, J. R., & Prasad, P. V. (2000). Temperature variability and the yield of annual crops. Agriculture, Ecosystems & Environment, 82(1), 159-167

Wilhite, D.A., Hayes, M.J., Knutson, C., Smith, K.H., Planning for drought: moving from crisis to risk management, J. Am. Water Resour. Assoc., 36 (2000), pp. 697–710

Willems, P., K. Arnbjerg-Nielsen, et al. (2012). "Climate change impact assessment on urban rainfall extremes and urban drainage: Methods and shortcomings." Atmospheric Research **103**: 106-118.

Willems, P. and M. Vrac (2011), Statistical precipitation downscaling for small-scale hydrological impact investigations of climate change, Journal of Hydrology **402**(3-4): 193-205.

Williams, C. N., Menne, M. J., & Thorne, P. W. (2012). Benchmarking the performance of pairwise homogenization of surface temperatures in the United States. Journal of Geophysical Research: Atmospheres (1984–2012), 117(D5).

WMO, Unprecedented sequence of extreme weather events, accessed 21/04/2015 http://www.wmo.int/pages/mediacentre/news/extremeweathersequence_2010_en.html

Wollenweber, B., Porter, J. R., & Schellberg, J. (2003). Lack of Interaction between Extreme High-Temperature Events at Vegetative and Reproductive Growth Stages in Wheat. Journal of Agronomy and Crop Science, 189(3), 142-150.

Yaglou, C.P., Minard, D., 1957, Control of heat casualties at military training centers. Am Med Ass Arch Ind Hlth, 16, 302–16.

Yiou, Pascal; Cattiaux, Julien, 2014, Contribution of Atmospheric Circulation to wet southern European winter 2013, Bulletin of American Meteorological Society, Volume: 95 Issue: 9 Supplement: S Pages: S66-S69 Published: SEP 2014

Zampieri, M., D'Andrea, F., Vautard, R., Ciais, P., de Noblet-Ducoudré, N., Yiou, P., 2009, Hot European Summers and the Role of Soil Moisture in the Propagation of Mediterranean Drought. *J. Climate*, **22**, 4747–4758. doi: http://dx.doi.org/10.1175/2009JCLI2568.1

Zander, K. K., Botzen, W. J., Oppermann, E., Kjellstrom, T., Garnett, S. T., 2015, Heat stress causes substantial labour productivity loss in Australia. Nature Climate Change.

Zelenhasić, E., Salvai, A., 1987, A method of streamflow drought analysis, Water Resour. Res., 23(1), 156–168, doi:10.1029/WR023i001p00156

Zhang, X., et al., 2005, Avoiding Inhomogeneity in Percentile-Based Indices of Temperature Extremes. J. Climate, 18, 1641-1651 (Available as: JCLI3366.1.pdf)

Zhang, X., F.W. Zwiers, 2015, Observed and Projected Changes in Temperature and Precipitation Extremes, in Dynamics and predictability of large-scale high-impact weather and climate events, Jianping Li, Richard Swinbank, Hans Volkert and Richard Grotjahn, eds., Cambridge University Press, in press

Zhang, X., Alexander, L., Hegerl, G.C., Jones, P., Klein-Tank, A., Peterson, T.C., Trewin, B., Zwiers, F.W., 2011, Indices for monitoring changes in extremes based on daily temperature and precipitation data, Wiley Interdiscip. Rev. Clim. Change, 2, 851\u2013870, doi:10.1002/wcc.147

Zolina, O., 2014a, Multidecadal trends in the duration of wet spells and associated intensity of precipitation as revealed by a very dense observational German network, ENVIRONMENTAL RESEARCH LETTERS Volume: 9 Issue: 2 Article Number: 025003

Zolina, O., Simmer C., Belyaev K., Gulev SK., Koltermann P., 2012, Changes in the Duration of European Wet and Dry Spells during the Last 60 Years, J Climate, 26, 2022-2047

Zolina, O., C. Simmer, S.K. Gulev, and S. Kollet, 2010: Changing structure of European precipitation: Longer wet periods leading to more abundant rainfalls. *Geophysical Research Letters*, 37, L06704.

Zolina, O., Simmer C., Kapala A., Shabanov P., Becker P., Mächel H., Gulec S., Groisman P., 2014b, Precipitation Variability and Extremes in Central Europe New View from STAMMEX Results, BULLETIN OF THE AMERICAN METEOROLOGICAL SOCIETY Volume: 95 Issue: 7 Pages: 995-+ Published: JUL 2014

Zwiers, F.W, Alexander, L.V, Hegerl, G.C., Knutson, T.R., Kossin, J.P., Naveau, P., Nicholls, N., Schär, C., Seneviratne S.I., and Zhang X, Climate Extremes: Challenges in Estimating and Understanding Recent Changes in the Frequency and Intensity of Extreme Climate and Weather Events, 2013, In (Climate Science for Serving Society: Research, Modelling and Prediction Priorities, G. Asrar and J. Hurrell, eds.), 339-389, doi:10.1007/978-94-007-6692-1 13

Zwiers, F. W., Zhang, X., & Feng, Y., 2011, Anthropogenic influence on long return period daily temperature extremes at regional scales. Journal of Climate, 24(3), 881-892.